DOCTOR OF PHILOSOPHY

Road Pothole Detection Method Using Built-in Sensors In Smartphone

Zhang, Dalong

Award date:
2017

UNIVERSITY OF DUNDEE

Road Pothole Detection Method Using Built-in Sensors In Smartphone

by Dalong Zhang

An initial submission of thesis for examination for the degree of Doctor of Philosophy

Division of Physics
School of Engineering, Physics & Mathematics
University of Dundee

2017

Contents

List of Figures

List of Tables

Abbreviations

GPS	Global Positioning System
VBI	Vehicle-Bridge Interaction
IRI	International Roughness Index
APDS	Automatic Pavement-Distress-Survey System
PCES	Pavement Cracks Evaluation System
DOF	Degrees of Freedom
FFT	Fast Fourier Transform
IIR	Infinite Impulse Response
FIR	Finite Impulse Response
WT	Wavelet Transform
DWT	Discrete Wavelet Transform
PCA	Principal Component Analysis
MEMS	Micro-Electro-Mechanical System
GSM	Global System for Mobile communication
FDMA	Frequency Division Multiple Access
TDMA	Time Division Multiple Access
GPRS	General Packet Radio Service
EDGE	Enhanced Data rates for GSM Evolution
HSPA	High Speed Packet Access
WCDMA	Wideband Code Division Multiple Access
NUC	Next Unit of Computing
SATNAV	Satellite Navigation
VR	Virtual Reality

Acknowledgements

I would never have been able to finish my thesis without the guidance of my PHD supervisors Prof. Allan Gillespie and Dr Charles Main. It has always been a great pleasure to work with them in all the past years.

I would like to thank them for giving me the opportunity to undertake this project and to work in a professional research environment.

Furthermore, I would like to thank my parents, my wife and my daughter for all their support and help.

Finally, I would like to thank all members of the Materials and Photonics Systems (MAPS) group at the University of Dundee for providing welcoming, professional and productive surroundings for the work of this project. In particular, I wish to express my gratitude toward Dr. Fu Yu for searching and applying of my PHD project. I thank you all who have encouraged me in everything I do throughout my time in Dundee.

Declaration of authorship

I declare that the thesis entitled

Road Pothole Detection Method Using Built-in Sensors In Smartphone

and the work presented in it are my own. I confirm that:

- this work was done wholly while in candidature for research degree at this University;
- where any part of this thesis has previously been submitted for a degree or any other qualification at this University or any other institution, this has been clearly stated;
- where I have quoted from the work of others, the source is always given. With the exception of such quotations, this thesis is entirely my own work;
- I have acknowledged all main sources of help;
- where the thesis is based on work done by myself jointly with others, I have made clear exactly what was done by others and what I have contributed myself.

Dalong Zhang

August 2015

Abstract

In this thesis, the smartphone is installed on vehicle as a tool to detect potholes on the road. The data collected and pre-processed by smartphone is then analysed to obtain the result.

The history and status of pothole detection study is firstly discussed. The traditional pothole detection method has two disadvantages: 1, low efficiency; 2, limited detection area.

To work out a new method, the suspension models and tyre models are studied. Also the axis-correction and de-noise in signal process discussed for data analysis. Based on these, the requirement of detection system is analysed, and the features of embedded systems are discussed, which leads to the conclusion that smartphone is the best hardware for pothole detection.

Then the smartphone (3 mobiles are chosen: Samsung Note 1, Nexus 7 and iPhone 5) is fixed on vehicle (Nissan Micra K11 and Saab 93) as experiment platform. The Tay Road Bridge is chosen as experiment road. The software Sensor Insider Pro and Sensor Data are chosen to collect data.

Simulations about vehicle and tyre are done by MATLAB Simulink. From the simulation the relationship between the bouncing height and the speed of vehicle is obtained, and is used as threshold in pothole detection.

The experimental data from acceleration sensor and gyroscope is processed by MATLAB using axis-correction and wavelet transform. Together with velocity data gathered by GPS and threshold (calculated from speed), the position of pothole is obtained. Comparing with road, the detection has good accuracy, which proves the feasibility of this pothole detection method.

At the end of thesis, other potential field of application of smartphone is discussed.

Chapter 1. Introduction

1.1 The research project

This research project puts forward a new method for pothole detection, in which a smart-phone is installed on a running vehicle and the data is collected from smart-phone sensors - such as acceleration sensors or gyroscopes - and the GPS built in the smart-phone. By processing the collected data, the potholes on the road on which the vehicle traverse through can be located.

On the basis of looking back the development of smart-phones, the thesis analyses the feasibility and advantages of pothole detection using smart-phones.

Through simulating the suspension model of vehicles, I find out the relationship between pothole and the output signal of sensors, and then put forward a method to determine pothole by variable threshold value related to the vehicle running speed.

Taking Tay Road Bridge as my experimental subject, I designed and implemented experiment to collect the data, which is then processed through a wavelet-based noise-reduction process and produces the final results.

In addition, I compare and discuss the differences between results of acceleration sensors and that of gyroscopes. At last, I initially discuss other areas that smart-phones may be applicant on, including fault inspection of vehicles and pulse detection of human body, with some case studies included.

1.2 Background

There are two methods to detect road pothole. The first method is public reporting, which is economic in manpower and material resources, because the roads having larger traffic flow may draw more attentions. However there may be misreport. Furthermore, the roads having poor traffic flow may draw a little care and have less information available. The second method is more common, which is to use a special pothole–detection vehicle running on the road to detect pothole and record its location (Lin et al., 2008). This kind of vehicle may record its vertical vibrations when its wheels run through the road, or scan and analyse the road by using a vehicle-mounted laser scanner or an ultrasonic scanner (Huston et al., 2000, Wang et al., 2011), or by using a camera to form images under visible light which is more advanced (Lin and Yayu, 2010). Each of these detection methods has advantages and flaws. Generally speaking, the direct-contact detection method has lower error rate but it works slower so the detection efficient is lower, and it can only detect potholes in the locations where the wheels

contacted. The indirect detection method works faster but its error rate is higher. At present most of the techniques are still in experimental stage or the proof stage.

No matter what kind of detection-vehicle is used, it is demanded that the vehicle traverse through each inch of the road so as to collect and obtain complete data. Moreover, the road pothole varies with time. A complex road network requires a long time to detect, thus only constantly updated data are practical, which is a huge job requiring lots of manpower and materials. Under such conditions it is hard to improve the detection efficiency. Meanwhile, with the development of the road network, more and more roads need to be detected; thus the expenditure on this rises year by year. According to figures, the annual expenditure on road pothole repair is up to $1.3 billion in USA (Cheng et al., 1998). At the same time, the loss caused by pothole is up to $4.8 billion. Therefore a new pothole detection method is in demand, which shall be high-efficient, low cost, reliable and easy to be widely promoted and have precise output results. This is the main direction discussed in this thesis.

It takes time to detect and repair of potholes. Generally, the length of repair time depends on repair device (and its level of automation), manpower and size of pothole. For small potholes, simple repair is enough; however, large pothole may require retreading of a long section of road, which consumes long period of time. The length of detection time, on the other hand, depends on number of detection vehicle and length of road network, increase the number of detection vehicles surely will increase efficiency of detection, unfortunately the increase of length of road - which is always increasing - decrease the efficiency.

1.3 This thesis

The following questions are discussed in this thesis:

1. In which way the traditional methods can be improved? Is there a new method that can exceed the traditional methods?
2. What equipments are required?
3. Which physical measurements should be kept?
4. What algorithm is required to analyse the data and obtain the result?
5. The new method should be proved to meet our goal.

Based on the study of previous work, a method of measuring road pothole based on smartphone built in sensor is proposed in this thesis. The smartphone is fixed inside the

vehicle, and the vibration data of the car body is obtained and processed by collecting the data of the built-in accelerator. The noise data and baseline drift are removed by signal processing of the vibration data, and the signals caused by road pothole are reserved. The vehicle body and tyre modules are designed and simulated, and the relationship between vehicle speed, pothole width and vibration amplitude is obtained, and the dynamic threshold based on the speed is proposed. Dundee Tay Road Bridge is used to simulate pothole on expansion joint. The experimental results show high accuracy and little misjudgement.

The following is the structure of the paper:

Chapter 1 is this chapter.

Chapter 2 summarizes and analyzes the previous work.

Chapter 3 studied the data acquisition equipment, and designed the experimental method.

Chapter 4 and 5 establish the dynamic model of the common vehicle suspension and tyre, and give the simulation results.

Chapter 6 designs the methods and steps of data processing.

Chapter 7 data on the experiment are processed, and the results are discussed.

Chapter 8 discusses the previous work and describe the future work on real pothole detection methods.

Chapter 2. Literature review

In Chapter 1, five questions are brought out for my aid of study. First question: In which way the traditional methods can be improved? Is there a new method that can exceed the traditional methods? This question is answered in Section 2.1 with a browse of previous work of pothole detection methods. With the method chosen, the question two: equipment is discussed in Section 2.2 including various vehicle models. At last in Section 2.3, literatures about the question three and four are surveyed. The question five is not in the scope of this chapter and will be discussed in Chapter 7.

2.1 Pothole detection method

2.1.1 Contact measurement

In the contact measurement, the sensor directly contacts the road, or is installed on another device that has direct contact with the road.

The International Roughness Index is a standard roughness test index defined by The World Bank (Sayers, 1998). The standard calculating program of IRI was published in its No.46 report, 1982, in which a one-fourth simulation (similar to a single-wheel trailer) is used. During the mobile is driving on the known section with the speed of 80km/h, the accumulated displacement of suspension system within a certain distance is calculated.

Then after the standard deviation of the flatness measurement device is determined by the continuum flatness instrument, the standard deviation of flatness in every 100 meters is calculated from the displacement of every 10 centimetres.

The existing test methods are mainly special instruments or testing vehicles. The most typical one is the flat monitor assembled with test vehicle (Lin et al., 2008). A 1/4 model is used by IRI for the measurement, in which the vehicle runs with speed of 80km/s and the cumulative vertical displacement of suspension is kept as output.

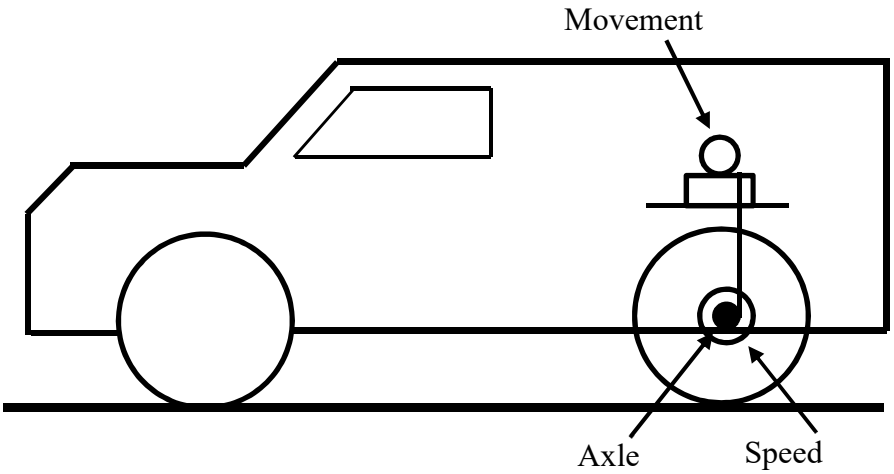

Figure 2-1 Accumulation test vehicle

Table 2-1 Comparison of road test methods

Type	Complexity	Continuous or Intermittent	Efficiency	Measurement Index
3-meter ruler	simple	intermittent	low	Maximum clearance section
Continuous flatness tester	relatively complex	continuous	high	Standard differential cross section
Accumulation tester	relatively complex	continuous	high	VBI
Pavement inspection car	complex	continuous	high	IRI

Smart-phones, i.e. mobile phones with modern intelligent operating system, appear in recent ten years (such as the first one, Moto A6188 in 1999), while the smart-phones having built-in sensors such as acceleration sensors appears much later, such as Sony ERSSION W580C in 2007. Therefore the idea to detect pothole with smart-phones emerges in recent years. In 2008, researchers of MIT (Eriksson et al., 2008) detect road

potholes by adopting special equipment: P2, which includes a GPS and a three-axis acceleration sensor set on a vehicle to collect signals. In 2009, Swin adopted wavelet analysis to process the flatness data of road. In the same year, Spanish researchers used a mobile sensor to record the data of the vehicle so as to implement detection in the site of the accident (Cadenas et al., 2009). In this project, the researchers simulated an Android mobile phone which can automatically contact with the emergency call centre using webservice when an accident occurs. In 2011, Latvia's researchers announced a method to implement real-time detection of pothole with Android smart-phones with built-in acceleration sensors (Mednis et al., 2011, Strazdins et al., 2011). The searchers used four kinds of smart-phones including Samsung and HTC to carry out the experiment, gathering Z-axis data and obtaining results with the correct rate of 90%. In the same year, Italian researchers (Bujari et al., 2012) announced a method to implement road crossing recognition by using three-axis acceleration data of smart-phones with high-pass filtering and pattern recognition. In 2012, Indian researchers installed Android smart-phone Google Nexus S and HTC Wildfire on the Suzuki Access 125 vehicle to obtain brake data so as to evaluate the road traffic condition (Bhoraskar et al., 2012). In addition, researchers of Taiwan also installed a HTC Diamond mobile phone (Windows Mobile operating system) and an external GPS on a motorcycle to inspect the road flatness (IRI) with a three-axis acceleration sensor (Tai et al., 2010). Similarly, the researchers of Microsoft Research India installed a HP iPAQ hw6965 mobile phone (Windows Mobile operating system) and an external three-axis acceleration sensor on the model vehicle to inspect brake, whistle and bump (Mohan et al., 2008).

All those work indicate that using built-in sensors of smart-phones to detect potholes is feasible. However, limited by the age, (no gyroscope is used in any of above researches, only acceleration sensor and GPS (Mathur et al., 2010)) almost all of the above-mentioned methods adopted three-axis acceleration sensors (built-in or external) in the testing platform. In addition, only several papers involved simple high-pass filtering in noise-reduction process of the data (Promwongsa et al., 2014), and other papers involved nothing about this. Thus, the inspection results were not ideal. Moreover, there is no analysis on vehicle characteristics in any research, while the relationship between feature of road surface and built-in sensor can only be obtained by analysing the vehicle characteristics, which means that the data process lacks theory support and can only be done on experimental level. Furthermore, no research considers the difference in result

brought by difference of vehicles. The applicability of these methods is not wide enough. There will be better results if researchers go into a further research.

2.1.2 Non-contact measurement

In the contact measurement method, the contact measurement method can only provide information of part of road contacted with the tire. To obtain the data of whole road, the detection vehicle has to run repeatedly on the same road.

The non-contact measurement method uses imaging technology to complete testing. There are two sub-systems: Image acquisition subsystem and Image processing subsystem. The Image acquisition subsystem captures the image of road by using video cameras fixed on testing vehicles, and then transform the image to digital data and store it (Lin and Yayu, 2010). The Image processing subsystem analyse the digital data by manual identity or machine vision recognition and get position of potholes, and stores the result (Georgopoulos et al., 1995).

The image of road is normally obtained by visible light cameras (Nejad et al., 2011). However ultrasonic, infrared or laser scanning technology may also be used (Huston et al., 2000, Wang et al., 2011). In general, the grey-scale of image is kept and used for analysis (Acosta et al., 1992), because the change of light source may also change the colour of images and finally affect the analysis result if colour of image is kept. To maintain the stability of the light into the camera, an active light source is commonly installed on the testing vehicle (Perttunen et al., 2011).

The Image processing can be divided to several modules such as pre-processing, segmentation, feature extraction, classification, decision making and evaluation (Hou et al., 2007). The purpose of pre-processing is to identify and normalise areas of different brightness. The feature extraction obtains the geometry and statistical parameters of the image, or identify the feature of the image by image transformation. Image classification divides the image categories and provides service for decision making and evaluation.

To detect minor changes on the road, the camera should have high enough resolution, and fast enough imaging speed. At the same time, the speed of vehicle cannot be too high, otherwise it is a great challenge to the image acquisition and storage system.

The French road management department LCPC developed the road surface damaged Dolly (GERPHO) in early 1970. The GERPHO works at night with special lighting system to take photograph of road, so that it can avoid the effects of the environment

light source. The cost of GERPHO photography is high. In addition, it requires operators to interactively work together and cannot process detection work automatically.

Another non-contact measurement system, which is called Automatic Pavement-Distress-Survey System (APDS), was released in 1990 by Fukuhara in Japan (Fukuhara et al., 1990). It works at night with laser scanning technology, with the maximum detection speed is 10 km/h. APDS stores data on tapes, and processes data with 512 MC86020 microprocessors. The disadvantage of this system is that it is too big and complex, and can only work at night.

Association of MHM in United States developed the automated road image analysis (ARIATM) in the late 1980's. ARIATM uses 2 cameras to obtain image of road surface. It takes 15 minutes to process 1.609 km road (Mohajeri et al., 1991).

Between late 1980's and early 90's, the evaluation system of pavement cracks (PCES) was developed by United States Earth Technology Corporation. This non-contact measurement system uses line-scan camera which is more advanced than the traditional surface-scan to gain road data, but requires special data acquisition card and high intensity lighting. Due to the immature image processing technique and high cost of data acquisition card and data processing software, no funding was provided to further this study.

In 1995, a detection system named Large-Area Laser Scanner with Holographic Detector Optics for Real-Time Recognition of Cracks in Road Surfaces (CREHOS) was published by Dr. Max Monti of tress analysis laboratory (IMAC) of Swiss Federal Institute of technology (EPFL). CREHOS scans road with a laser beam, and collects and pre-processes analog data (Monti et al., 1995).

In late 1990's the automatic road analyser ARAN was developed by Canadian Roadware Company. Its camera has high intensity, high speed flash, which frees the quality of video from effect of environment brightness, shadows of trees or the position of the sun. According to the introduction of the company, it is the only commercially available automatic road analyser in the world. But in fact ARAN is not fully automatic, and still requires manual intervention to work.

2.1.3 Sub-conclusion

Both contact and non-contact measurement methods have advantages and disadvantages. Contact measurement method has high accuracy and stability, and is

suitable for all kinds of terrain and conditions. But its measuring field is very narrow, which makes it inefficient.

Non-contact measurement method can scan a large area at a time by using image processing method, thus it is faster. But it has higher error rate. Plus it is easily influenced by the illumination of the surrounding environment and is not so stable. The accuracy of non-contact measurement method is very difficult to be increased, unless a revolutionary new algorithm appears.

However, it is possible to keep the advantage of contact measurement method and increase its efficiency by using new measurement technologies. Therefore in this study, the contact measurement method is used. The new measurement technology is described in Chapter 3.

2.2 Modelling

2.2.1 Vehicle modelling

When the vehicle is running on the road, the vibration caused by the unevenness of the road, pothole and speed bump will spread innerly to the vehicle through wheels, suspension and vehicle body. In the experimental scheme, as the smart-phone with built-in sensor is fixed in the centre of the vehicle, the acceleration shown on sensor is considered as the acceleration of the vehicle. Assuming that the vehicle is running forward at a constant speed, the measured value in the vertical direction of the acceleration sensor shall have a certain relationship with roughness degree of the road, which is determined by the response characteristics of the structure of the vehicle. Therefore to research the vibration of the vehicle when it traverses through the pothole, the structure of the vehicle shall be analysed (Dupont et al., 2008). Meanwhile, in regard to signal processing, the vehicle can be regarded as a system and the road condition is an input signal for the system, so the vibration detected by the smartphone actually is a response of the vehicle system to signals of pothole on the road which is an output signal (Li et al, 2008).

Further, as a whole system, the vehicle is made up of various subsystems such as tyres (Elmadany, 2012), suspension system, damper, steering system, engine/power transmission system and vehicle body (as shown in the Table 2-2) (Wu et al., 2013, Xie et al., 2009). Each subsystem is approximate to having no internal relative motion and they are connected with hinges, springs, dampers or rubber elements (Hunt, 1991). In modelling procedure, to research the integrity property of the vehicle system, each

subsystem is studied first, so that models for subsystems are established with range of their physical parameters estimated. At the same time, subsystems that are non-relative to the project are ignored. In addition, subsystems that have no relative motion (or no significant motion) are combined together as one bigger subsystem to improve the efficiency and accuracy of model (Lu et al., 2013). On the other hand, simplify some less important subsystems and combine multiple subsystems between which there is no relative motion or the relative motion is not important to improve the processing efficiency, in the meantime cutting the loss of accuracy.

Table 2-2 Subsystems of the vehicle with their elements

Engine	Cylinder block, crankshaft connecting rod mechanism, air valve, intake system, exhaust system, fuel supply system, ignition system, cooling system, lubricating system, starting system	
Chassis	Transmission system	clutch, transmission, drive shaft, drive axle
	Driving system	frame, front axle, drive axle, wheel housing (including steering wheels and driving wheels), suspension
	Steering system	steering and steering mechanism
	Brake device	power supply device, control device, transmission device and brake
car body	Front sheet metal parts, cab, car carriage	
Electrical equipment	Battery, engine starting system, ignition system, lighting system and signal device	

Actually, for this research project, the core study object is the interaction force between vehicle and road. So adopt the most typical digital simulation method which is establishing digital vehicle simulation model, to get numerical results of interaction force between vehicle and road via simulation analysis with regard to the signal output of pothole on the road.

Degrees of freedom (DOF) is the number of independent parameters that define vehicle's configuration. It is the number of parameters that determine the state of the vehicle system (Zhang, 2010).

2.2.1.1 2-DOFs suspension system of 1/4 vehicle

This model focuses on the degree of freedom of vertical motion of sprung mass and un-sprung mass. It studies the effect of stiffness and damping of suspension and tires (Yan and Zhou, 2011, Aleksander and Iljoong, 1992).

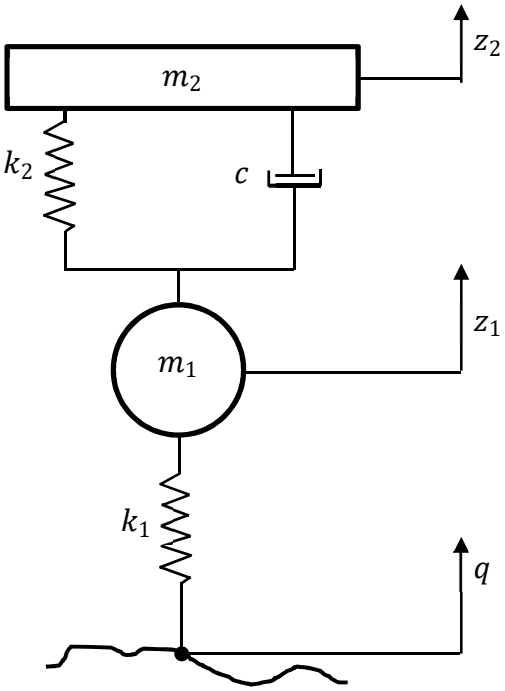

Figure 2-2 2-DOFs suspension system of 1/4 vehicle

Based on the Lagrangian formula, the summary of pressure on tyre from vehicle and gravity of tyre should balance the support from ground on tyre; at the same time, the gravity of vehicle should balance with support from suspension and spring. Corresponding dynamics equation is as followed:

$$\begin{cases} m_1 z_1 + c(z_1 - z_2) + k_2(z_1 - z_2) + k_1(z_1 - q) = 0 \\ m_2 z_2 + c(z_2 - z_1) + k_2(z_2 - z_1) = 0 \end{cases} \tag{2.1}$$

In which m_1 is mass of tire, m_2 is mass of 1/4 vehicle body, k_1 is rigidity of tire, k_2 is rigidity of suspension spring, c is damp of suspension, z_1 is vertical displacement of tire, z_2 is vertical displacement of vehicle body, q is vertical displacement of ground.

With only two degrees of freedom, the 1/4 vehicle model can only show the vertical motion of one tire. A more complex model is needed, which should contain at least one front tire and one rear tire. So it is necessary to study the 1/2 vehicle model which has four degrees of freedom.

2.2.1.2 4-DOFs suspension system of 1/2 vehicle

As there are two front tires and two rear tires on each vehicle, there are two types of 1/2 vehicle model: front/rear model - which is also known as Pitch model, and left/right model – which is also known as Roll model (Gao et al., 2007).

First, the Pitch model is analysed. The force analysis of Pitch model is shown in the following diagram (Chen et al., 2012):

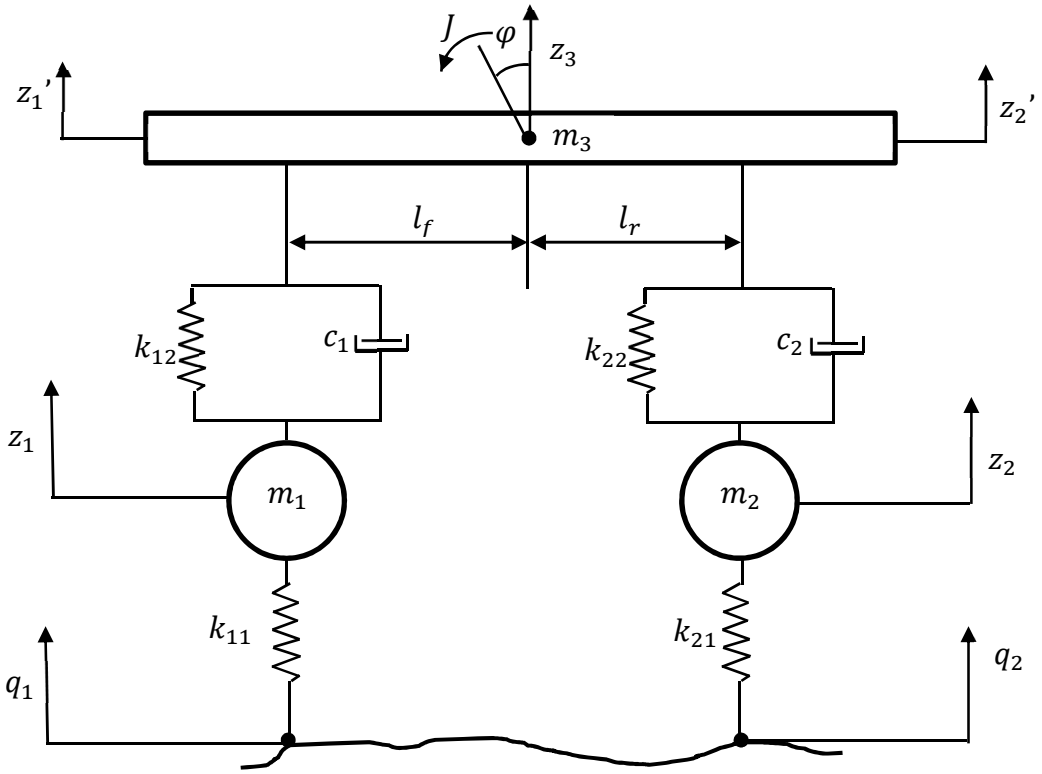

Figure 2-3 4-DOFs suspension system of 1/2 vehicle (pitch model)

Thus the dynamic equation of 1/2 vehicle can be derived as follows:

$$\begin{cases} m_1 z_1 = k_{11}(z_1 - q_1) + k_{12}(z_1' - z_1) + c_1(z_1' - z_1) \\ m_2 z_2 = k_{21}(z_2 - q_2) + k_{22}(z_2' - z_2) + c_2(z_2' - z_2) \\ m_3 z_3 = k_{12}(z_1 - z_1') + k_{22}(z_2 - z_2') + c_1(z_1 - z_1') + c_2(z_2 - z_2') \\ J\phi = -\left[k_{12}(z_1 - z_1') + c_1(z_1 - z_1')\right] l_f + \left[k_{22}(z_2 - z_2') + c_2(z_2 - z_2')\right] l_r \end{cases} \tag{2.2}$$

In which m_1, m_2 are mass of tire, m_3 is mass of 1/2 vehicle body, k_{11}, k_{21} are rigidity of tire, k_{12}, k_{22} are rigidity of suspension spring, c_1, c_2 are damp of suspension. z_1, z_2 are vertical displacement of tire, z_1', z_2' are vertical displacement of vehicle body, J is moment of inertia of 1/2 vehicle body, φ is the rotary angle of vehicle body at the centre of gravity, q_1, q_2 are vertical displacement of ground, l_f, l_r are the distances of the suspension locations, with reference to the centre of gravity of the vehicle body.

The Roll model of 1/2 vehicle is similar with the Pitch model. The force analysis is shown in the following diagram:

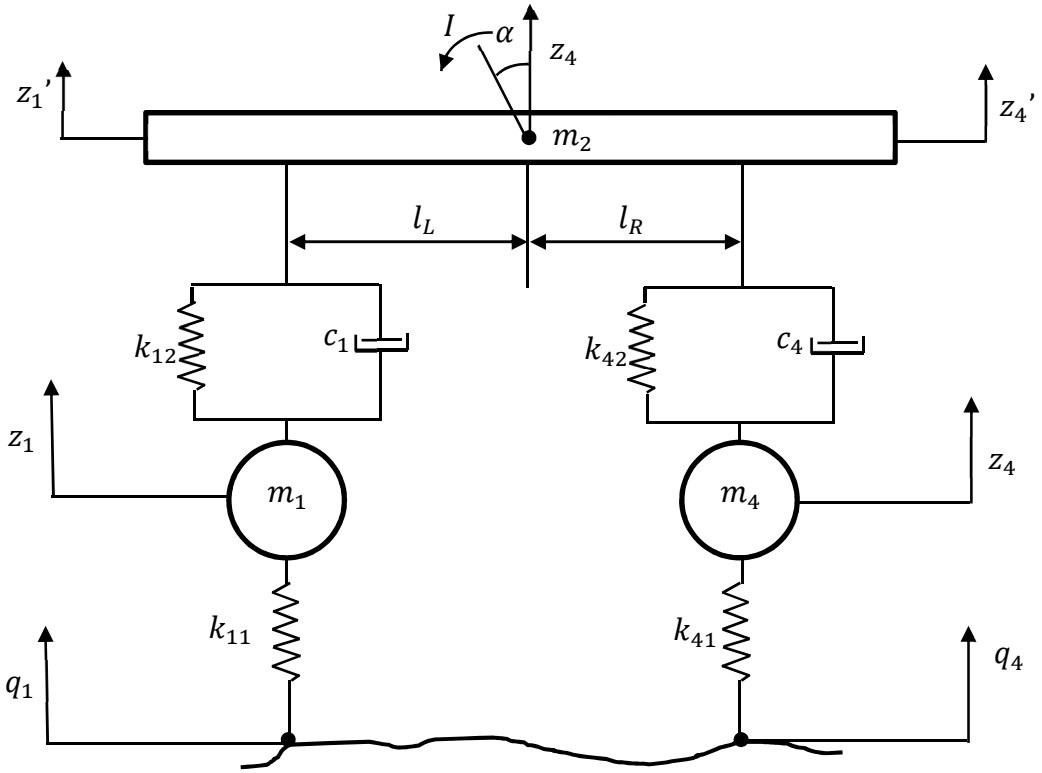

Figure 2-4 4-DOFs suspension system of 1/2 vehicle (roll model)

So the dynamics equation is:

$$\begin{cases} m_1 z_1 = k_{11}(z_1 - q_1) + k_{12}(z_1' - z_1) + c_1(z_1' - z_1) \\ m_4 z_4 = k_{41}(z_4 - q_4) + k_{42}(z_4' - z_4) + c_4(z_4' - z_4) \\ m_2 z_2 = k_{12}(z_1 - z_1') + k_{42}(z_4 - z_4') + c_1(z_1 - z_1') + c_4(z_4 - z_4') \\ I\alpha = -\left[k_{12}(z_1 - z_1') + c_1(z_1 - z_1')\right] l_L + \left[k_{42}(z_4 - z_4') + c_4(z_4 - z_4')\right] l_R \end{cases} \tag{2.3}$$

In which m_1, m_4 are mass of tire, m_2 is mass of 1/2 vehicle body, k_{11}, k_{41} are rigidity of tire, k_{12}, k_{42} are rigidity of suspension spring, c_1, c_4 are damp of suspension. z_1, z_4 are vertical displacement of tire, z_1', z_4' are vertical displacement of vehicle body, I is moment of inertia of 1/2 vehicle body, α is the rotary angle of vehicle body at the centre of gravity, q_1, q_4 are vertical displacement of ground, l_L, l_R are the distances of the suspension locations, with reference to the centre of gravity of the vehicle body.

In the research project, the two front wheels are assumed to traverse through the pothole simultaneously, and so are the two rear wheels, which doesn't cause the vehicle to swing left and right. Thus my study focuses on the analysis of the pitch angle of the

vehicle. So the Pitch model of 1/2 vehicle is used in my study, no swing is considered. Moreover, in real life, the vehicle may be bounced up from road, which means the displacement of vehicle in the vertical direction should be considered.

In the contact measurement, when the vehicle passes through the pothole, from the side direction view, the tyres firstly contact with the falling edge of pothole, and then contact with the rising edge of pothole, as shown in figure 5-14. This is exactly the same as the processing of the vehicle passing through the expansion joint of bridge, and can be analysed using the dynamic response of the 1/2 vehicle model. Therefore, in the experiment in this thesis, the expansion joints on Dundee Tay Road Bridge are used as the experimental object.

2.2.1.3 7-DOFs suspension system of the whole vehicle

The force analysis of the whole vehicle is shown in Figure 2-5 (Guan et al., 2010):

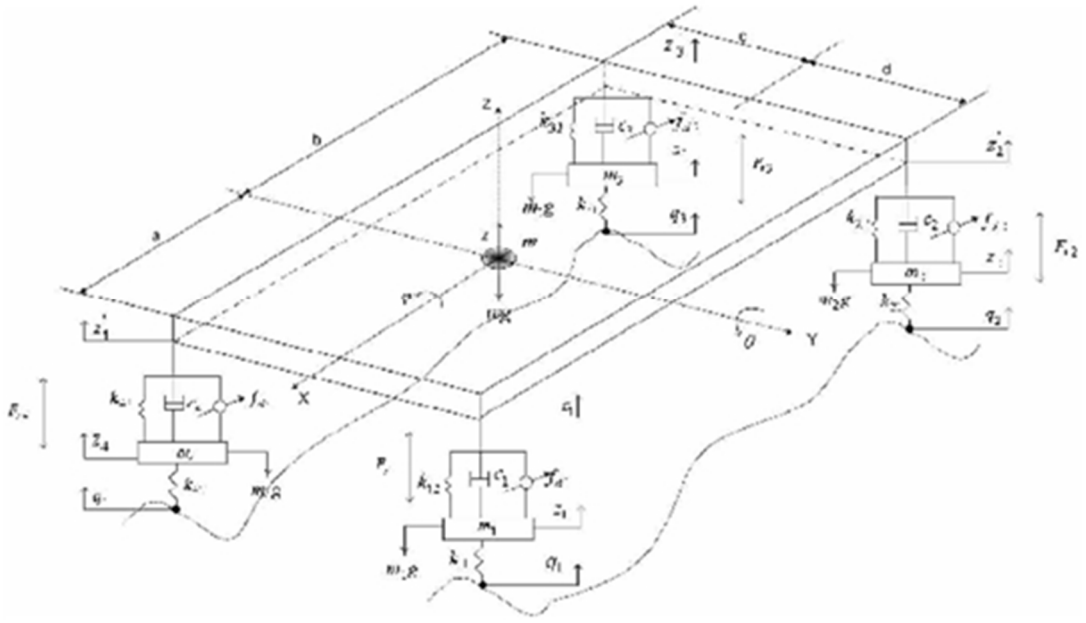

Figure 2-5 7-DOFs suspension system of the whole vehicle

The dynamic equation is as follows (Fan et al., 2007):

$$
\begin{cases}
m_1 z_1 = k_{11}(q_1 - z_1) + k_{12}(z_1' - z_1) + c_1(z_1' - z_1) \\
m_2 z_2 = k_{21}(q_2 - z_2) + k_{22}(z_2' - z_2) + c_2(z_2' - z_2) \\
m_3 z_3 = k_{31}(q_3 - z_3) + k_{32}(z_3' - z_3) + c_3(z_3' - z_3) \\
m_4 z_4 = k_{41}(q_4 - z_4) + k_{42}(z_4' - z_4) + c_4(z_4' - z_4) \\
mz = k_{12}(z_1 - z_1') + k_{22}(z_2 - z_2') + k_{32}(z_3 - z_3') + k_{42}(z_4 - z_4') \\
\qquad + c_1(z_1 - z_1') + c_2(z_2 - z_2') + c_3(z_3 - z_3') + c_4(z_4 - z_4') \\
J_x\phi = -\left[k_{32}(z_3 - z_3') + c_3(z_3 - z_3') + k_{42}(z_4 - z_4') + c_4(z_4 - z_4')\right]c \\
\qquad + \left[k_{12}(z_1 - z_1') + c_1(z_1 - z_1') + k_{22}(z_2 - z_2') + c_2(z_2 - z_2')\right]d \\
\qquad - (f_{d3} + f_{d4})c + (F_{r3} + F_{r4})c + (f_{d1} + f_{d2})d - (F_{r1} + F_{r2})d \\
J_y\theta = -\left[k_{12}(z_1 - z_1') + c_1(z_1 - z_1') + k_{42}(z_4 - z_4') + c_4(z_4 - z_4')\right]a \\
\qquad + \left[k_{22}(z_2 - z_2') + c_2(z_2 - z_2') + k_{32}(z_3 - z_3') + c_3(z_3 - z_3')\right]b \\
\qquad - (f_{d1} + f_{d1})a + (F_{r3} + F_{r4})a + (f_{d2} + f_{d3})b - (F_{r2} + F_{r3})b
\end{cases}
\tag{2.4}
$$

All the parameters in the equation have the same meaning as in chapter 2.2.1.2.

For this research project, the whole vehicle model is much more complex than 1/2 vehicle model without any improvement. So the 1/2 vehicle Pitch model is chosen for this study.

2.2.2 Tyre modelling

As the part of a vehicle that has direct contact with roads, tyres not only support vehicle weight, but also work as a cushion against the impact which is caused when the vehicle travels on surface of roads, provide sufficient adhesion for driving and braking, and brings adequate steering and directional stability. Apart from the aerodynamic force and gravity, near all the other forces and torques are generated by the rolling of tyre on the surface of ground. Therefore, it is necessary to research the mechanical characteristics of tyres.

The movement of a vehicle depends on the tyre force, such as longitudinal braking force and the driving force, lateral force and external tilt force, back to the positive torque and rolling torque etc., all these forces are functions of slip rate, sideslip angle, camber angle, vertical load, road friction coefficient and vehicle velocity (Furuichi and Hideo, 1978). Therefore, the establishment of accurate mathematical model of tire mechanics, in essence, is how to express the functions' relationship.

2.2.2.1 General theoretical model of tyre dynamic

In 1940, Fromn derived the tyre cornering model for the first time by simplifying the tyre as “beam”. In this way the relationship between steady state sideslip angle and lateral force is explained by the lateral deformation of the crown of tyre.

Fiala improved the tyre cornering model in 1954. He assumed that the beam layer or buffer layer was lateral translation deformation and bending deformation with effect of lateral force. By simplifying the beam layer or buffer layer as a elastic supporting "beam" affected by lateral concentration force, the relationship among lateral force, aligning torque, slip angle and camber angle were obtained (Barone, 1977). Experiments proved that Fiala’s model is more precise with lateral force, while larger error is with aligning torque.

In 1966 Pacejka studied the static and dynamic mechanism of tyre and introduced the string model of finite width provided with tread elements, in which the tyre was considered as many flexible supported stretched parallel strings joined together by lateral cord (Pacejka, 1979).

Sharp brought out spoke type model in the middle 80s. He considered the tyre as identical radial spokes which were flexible and were connected with the hub. The regular deformation of spokes leaded to hysteresis losses. Assume there is no slippage，the circumferential and lateral deformation of spokes when entering the area touching with ground can be calculated using kinematics. The force upon the spoke and force behind the spoke can then be calculated with elastic property of spokes. Finally the total force and torque can be calculated by summarising all the forces and torques inside the area touching with ground. The feature of this model is less number of parameters but less preciseness (Takayama et al., 1983).

2.2.2.2 Semi-empirical model of tyre dynamic

Major error is likely to happen when pure theoretical model of tyre is used to simulate the dynamic of whole vehicle (Scavuzzo et al., 1993). It is convenient to use experimental data, however, due to the variety of the road, the limited number of experiments cannot cover the dynamic of tyre on all roads with various vertical load. Thus the semi-empirical model is brought out to resolve the problem.

Fiala derived the dimensionless equation from Fromn’s simplified tyre model in 1954.

In 1988 Zeostal et al. describe semi-empirical model in the following form:

$$F = \mu F_Z \frac{a_1\alpha^3 + a_2\alpha^2 + \dfrac{C\alpha}{\mu F_Z}}{a_1\alpha^3 + a_3\alpha^2 + a_4\alpha + 1} \tag{2.5}$$

In the equation, C stands for the cornering stiffness of tyre, which is the slope of the curve at the origin of the lateral force. The drawback of this model is the number of variable is too large.

In 1987, Pacejka et al. established the Magic formula based on large number of experiments (Bakker et al., 1987). The Magic formula can describe the feature of forces and torques on tyre under pure slip, pure cornering or pure brake, pure drive conditions with preciseness and convenience. It is a practical model. The equation is:

$$Y(X) = D\sin\{C\arctan[BX - E(BX - \arctan(BX))]\} \tag{2.6}$$

In which X represents the slip angle and Y represents side force; or X represents longitudinal slip and Y represents longitudinal force (in this equation one symbol may represent various physical quantities). C governs the shape of the curve (shape factor), D is peak factor, and E is curvature factor.

Generally, the tyre model is the combination of experimental value of variables and theoretical calculations. Each model has its own application scope. If a model is used for an impropriate condition, the preciseness of calculation can be greatly reduced. In this study, the hitting between the tyre and the edge of pothole is too strong, and may be out of range of most models. Thus the model must be carefully chosen so that it can provide enough accuracy.

This project only study the uniform linear motion of the vehicle. Therefore, this paper focuses on the pressure and the supporting force in the vertical direction.

2.3 Signal Processing

The output of sensor is normally a weak analogue signal, which requires amplification, filtering, A/D convention before being process by computers. The purpose of signal processing is to filter the redundant content of signal, especially noise and interfere, and to transform the signal to a form that is easy for analysis.

The study of signal processing started in 60s of 20th century. The simulation of circuit and filter designing done by Bell Laboratory and MIT laid the foundation of digital filter. In the middle 60s, the Fast Fourier Transform (FFT) is invented to increase the speed of spectral decomposition to more than 100 times, which enabled the PC to do

spectral decomposition. Thus it is practical to process signal with digital filtering and Fast Fourier Transform, which becomes the core of digital signal processing. The term 'Digital Signal Processing' began to be used in scientific and technology fields.

2.3.1 Coordinate axis transformation

The coordinate axis transformation is an operation that transfer the signal from one coordinate system to another, which can be done by general transformations such as translation, rotation or scaling, or mapping from one system such as Cartesian coordinates to another, such as polar coordinates (Jiali et al., 2008). The mapping relation needs to be predetermined, otherwise the mapping cannot be processed. However, in this project, the relation between the local coordinate system of the sensor and the global coordinate system may change at any time. Because there are relative movement (and relative rotation) among the ground, the vehicle and detection sensor, three coordinate systems are required. The movement and rotation is represented as transformations from one coordinate to another. Therefore the mapping relation cannot be predetermined. A statistics method is used to determine the mapping relation between sensor coordinate system and global coordinate system.

2.3.2 De-noise

The digital signal filter is a discrete time system that processing digital signals in order to obtain expecting response characteristic. It process the digital signal transferred from analog signal.

Theoretically the digital signal filter can implement any filtering that can be represented by mathematical algorithm. The two main limitation of digital signal filer is its processing speed and cost. The digital signal filter cannot run faster than its internal circuit. But as the cost of IC continue to decrease, the digital signal filter becomes more and more common and an important part of everyday life as radios, mobile phones and stereo.

The digital signal filter is assembled by basic digital circuits such as register, time, adder and multiplier. With the development of integrated circuits, its performance continues to increase and cost continues to decrease. Therefore the application of the digital signal filter is wilder. According to the characteristic of digital filter, it can be classified to linear and non-linear, causal and non-causal, infinite impulse response (IIR) and finite impulse response (FIR) and so on. Among all the digital signal filters, the linear time invariant digital filter is the most basic type.

Because the digital filter can make use of time delay unit, so it can introduce a degree of non-causality and become more flexible and powerful than traditional digital filters. Comparing with IIR filer, FIR filter has the advantage of easy implementation and system stability, it has been widely used (Huan, 2005).

2.3.2.1 Kalman filter

Kalman filter is an effective recursive filter (autoregression filter). It can estimate the dynamic of a system from incomplete and noisy measurements.

An example of Kalman filter is to predict the position and velocity of the object from a set of limited observations (possibly biased) of the object including noise. It can be found in many engineering applications, such as radar and computer vision. Meanwhile, Kalman filter is also an important topic in control theory and control engineering.

For the radar, people are interested in its ability to track targets. However, the measurements of position, velocity and acceleration may contain noise at any time. Kalman filter can obtain a good estimation of position of target by de-noise with dynamic of target. This estimation can be the estimation of current quantities (filtering), of future quantities (forcasting), or of past quantities (interpolation or smooth).

This filtering method is named after its inventor Rudolph E. Kalman. But actually Peter Swerling proposed a similar algorithm earlier.

Kalman filter is firstly implemented by Stanley Schmidt. Kalman found out that his filter is useful to predict the orbit in Project Apollo when he visited NASA's Ames Research Centre. Later, the guidance computer on Apollo used Kalman filter. Papers about Kalman filter is written by Swerling (1958), Kalman (1960) and Kalman and Bucy (1961).

Kalman filter now has many different implementations. The form proposed by Kalman is called simple Kalman filer. Apart from it, there are variants such as Schmidt's extended filter, information filter and the square root filter which is developed by Bierman Thornton. The most common application of Kalman filter is phase-locked loop, which exists in radars, computers and any video or communication equipment (Gao et al., 2004).

2.3.2.2 FFT filter

Fast Fourier Transform (FFT) is the fast algorithm of discrete Fourier transform. The FFT can also be used to compute the inverse transform of the discrete Fourier transform.

FFT has a wide range of applications, such as digital signal processing, computing the multiplication of large integers, solving partial differential equations, and so on.

The most common FFT algorithm is Cooley-Tukey algorithm. Using divide and conquer (D&C), this approach recursively breaks the discrete Fourier transform of length N=N1N2 down to a sequence of smaller discrete Fourier transforms, in which the number of smaller transforms is N2 and length of each smaller transform is N1.

This method is well known after published in an algorithm for the machine calculation of complex Fourier series (J. W. Cooley and J. W. Tukey, 1965). However, later it is found out that these two authors just re-invented the algorithm brought out by Carl Friedrich Gauss in 1805. Actually this algorithm was brought out for several times with various forms in history.

The most common application of Cooley-Tukey algorithm is to break down a DFT with length of N to two DFT with length of N/2. This application is usable only for DFT with length of power of 2, thus it is called radix-2 decimation-in-time (DIT) FFT. As indicated by Causs, Cooley and Tukey, Cooley-Tukey algorithm can be used for not only DFT of any length (mixed-radix FFT), but also other variants such as the split-radix FFT. Although the Cooley-Tukey algorithm is a recursive method, in many traditional implementations it is rewritten in a non-recursive form. Besides, because Cooley-Tukey algorithm breaks a DFT to several smaller DFTs, it can be combined with any other DFT algorithm.

2.3.2.3 Wavelet

Wavelet analysis is also called wavelet transform (WT). The wavelet analysis is a fast developing branch of applied mathematics based on the foundation work done by Y. Meyer, S. Mallat and I. Daubechies. The appearance of wavelet analysis is a milestone in history of signal analysis development, and is being wildly used in multiple field, including molecular dynamics, ab initio calculations, astrophysics, density-matrix localization, geophysics, optics, turbulence and quantum mechanics. DWT (Discrete Wavelet Transform) is also used in many other area such as image processing, blood pressure, heart rate and ECG analysis, DNA analysis, protein analysis, meteorology, General signal processing, speech recognition, computer graphics and multifractal analysis. Theoretically wavelet analysis can be used instead of Fourier Transform. In this section, the history and development of wavelet analysis is discussed.

The Fourier analysis is one of the most widely used mathematical analysis methods

since the analysis theory of heat conduction was published by Fourier in 1822. The Fourier analysis is a spectral analysis, which can reveal the spectrum of a signal. But the Fourier analysis has its own disadvantage. The Fourier coefficient is the weighted average of signal $f(x)$ on the whole time-domain, with which is impossible to represent the local feature of $f(x)$ on time-domain. However the local feature of $f(x)$ on time-domain is important in both theoretical and practical application.

The idea of scaling and translation was firstly used to compose wavelet orthogonal basis by Alfred Haar, who gave out the construction of the Harr wavelet in 1910. The 70's is important for the development of the wavelet analysis, when the birth of wavelet analysis was prepared by the establishment of Calderon-type reproducing formula, the atomic decomposition for Hardy spaces and study of unconditional basis. In 1982, a basis is firstly constructed by J. O. Stormberg, which is similar with modern wavelet basis.

The first real wavelet basis was constructed by Y. Meyer in 1986. After that Lemarie and Battle independently constructed wavelet function with exponential decay. S. Mallat introduced the concept of multi-resolution analysis (MRA), with which the previously proposed wavelet functions were uniformed. In 1988 orthogonal wavelet basis with limited subset was constructed by Daubechies. The single orthogonal wavelet was constructed based on spline function by Jintai Cui and Jianzhong Wang in 1990. They also discussed the best localization properties of scaling function and wavelet function. In 1994, multi-wavelet theory was founded by Goodman based on MRA. He also gave out the sample of construction of multi-resolution wavelet. In recent years, the high-resolution wavelet theory has been attracting the attention of researchers, with many of its topic being studied (Hesami et al., 2009, Yang et al., 2007).

In my study, the wavelet analysis is used in two aspects:

1 – To separate the data to the summation of a group of signals, in which I may find the key feature signal;

2 – To filter the noise and enhance the useful signal.

2.4 Conclusion

Based on discussions in this chapter, the contact measurement is chosen as my pothole detection method, which will be analysed in detail in Chapter 3 and carried out in Chapter 4. The 4-DOFs suspension system of 1/2 vehicle is chosen as the suspension model in my study, and energy conservation will be used in tyre model. Both

suspension model and tyre model will be discussed in Chapter 5. For the collected data, the principal component analysis (PCA) is chosen to process axis-correction, and wavelet analysis is chosen to process de-noised. The data process is discussed in Chapter 6.

Chapter 3. Detection system design

Based on the discussion of the Chapter 2, the contact measurement method is chosen to be used in my study.

In this chapter, considering the disadvantage of traditional contact measurement methods, a new contact measurement method is proposed. Firstly the requirement feature of each module is analysed in Section 3.1, and then the detection method - especially how it overcomes the disadvantage of traditional contact measurement methods – is brought out in Section 3.2. In Section 3.3, the hardware requirement is discussed based on Section 3.1 and 3.2. At last the data collection is designed to be carried out in Chapter 4.

3.1 Detection method requirement analysis

In my design, the measurement device should be deployed and applicable in large scale, so that it can be used by different owners and therefore can be used to detect the same road repeatedly. In this way the disadvantage that can only cover a small part of road is resolved. Secondly, to improve the efficiency of the whole detecting system, the device should be able to easily store and send data to a server. To reduce the workload of the server, this front-end device should have capacity of data pre-processing. At last, it should be universally, so that it is stable and can be used on different types of road.

3.2 Detection method

The objective of this project is to design or search for a device that is fixed on the vehicle, and the device is mounted as many vehicles as possible.

When the vehicle traverses through a pothole, the vibrations caused by the pothole will spread to the vehicle body through wheels, dampers and suspension and lead to the vibration of the vehicle body. When a device with built-in acceleration sensors is fixed on the vehicle, (The ‘fixed’ here means to install device firmly on equipment such as mobile holder, so that the vibration of device is synchronised with vehicle.) the vibration of the device can be considered as a synchronization vibration. Thus when vibration of device is detected through its acceleration sensors or other sensors, the vibration of the vehicle can be obtained, which means the pothole is detected. Combining with the GPS built-in the device, the location of the vehicle can be determined, which means that the location of the pothole is determined.

The device may store the data from the sensors in its internal storage or send the data to the system data server via wireless network. The system reads and processes the data

from the device. Combining with the GPS built-in the device, the location of the vehicle can be determined, which means that the location of the pothole is determined. The process can be fulfilled with computing capability of the device or other calculating devices (e.g. a work station connected with the data server). Although the real-time calculation by device can reduce data flow and calculation workload on the work station, the power dissipation and power consumption of the device will increase, which reduces its stand-by time. Thus the work station is the better device with respect to the measurement of pothole.

When a lot of vehicles with devices run on the road to collect data and send the collected data to the central terminal, the operation efficiency of the whole system will be greatly increased because each vehicle can be considered as a detection vehicle, which means that there are lots of inspecting vehicles involved. With plenty of vehicles installed the detection device, at any time there are some of the vehicles testing and sending data on the road. As long as there are such kind of vehicles running on the road, the data of that road is always being collected. The efficiency of running many vehicles (with detection device) on the road is much higher than single detection vehicle.

The advantage of running many vehicles with detection device is not only higher efficiency. Due to the noise of the road and vehicle body, the contact measurement method can only detect the part of road that has contact with tyre of vehicle, every single detection device may bring errors in measurements. However by revising the information of multiple detection vehicles, more precise information can be obtained. Thus it can improve the accuracy of detection.

The collection devices will be installed in the vehicle and as predicted, it requires many devices to meet the needs in the future. And the specific demands are as follows:

1. Intelligent system: OS shall be of sufficient intelligence and openness; there is mature development tool to develop and debug the application software needed conveniently;
2. Well-established hardware: the hardware shall include CPU, mainboard, storage, battery, communication interface and sensor, constituting a complete embedded system;
3. Low cost: it has large quantity demand and it is needed to control the cost within acceptable and reasonable range.

The detection device can detect the displacement of the vehicle vertical direction, in order to infer pothole. That is to say the sensor in the detection device should includes a module to digitise and record distance data. For example, distance data can be converted to voltage or current, then the voltage or current can be converted to digital

signal by A/D converter. In this way the distance is digitised. This job should be applied to acceleration or gyroscope type sensor. The detection device collects data from front-end sensors, then pre-processes and packages as local data, then waits to send to server to process or sends real-time data to server if there is wireless fidelity (Wi-Fi) connection. The server collects data from all the detection devices, analyses and presents result to users.

3.3 Demand analysis of each module

In the Section 3.3, development, feature and requirements of each module of detection device is discussed.

3.3.1 CPU

The work of CPU is to assign work load to modules of detection device, and do calculation for data pre-processing. Hence the CPU should satisfy following requirements:

1 the processing speed of CPU should be high enough to pre-process the collected data when the vehicle is running with a reasonable speed;

2 the power consumption of CPU should be in proper range, so that the detection device can keep working whenever the vehicle is on the road;

3 the cost of CPU should be low enough so that CPU can be large-scale deployed.

3.3.2 Sensor

By using flexural electrodes and circuit, the acceleration sensor can measure acceleration and convert linear acceleration signals to electrical signals as output (Ravi et al., 2005). For example, some laptops have built-in acceleration sensors to monitor whether the notebook is dropped. And if that happens, the laptop automatically turns off hard disks to prevent serious damage.

Accelerometers measure the information of the transformation motion in three directions, which is its linear acceleration (Xiaoya et al., 2010); Gyroscopes, however, measure the information of its rotating movement, which is its angular motion.

Gyroscopes also able to measure the flatness of the road. When vehicles travels on the road and encounters a pothole, the tilt between four tires will cause the rotation of the vehicle body, which will have a response on the gyroscope. In this way the gyroscope can be used to measure the flatness of the road information.

Gyroscopes are not sensitive on vehicle noise (for example, noise from the engine). Engine noise may cause the vehicle body to shake, and the acceleration sensor is unable to distinguish the difference between the vibrations caused by the roads and the vibration caused by engine noise. Thus the rate of miscarriage by acceleration sensor is increased. But the engine noise has none or a minimal impact on the rotation motion of vehicle body, so that the gyroscope may have more accuracy measurements of the flatness of the road.

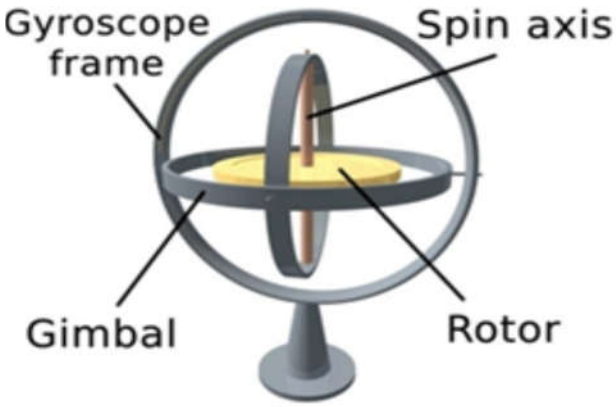

Figure 3-1 Typical gyroscope

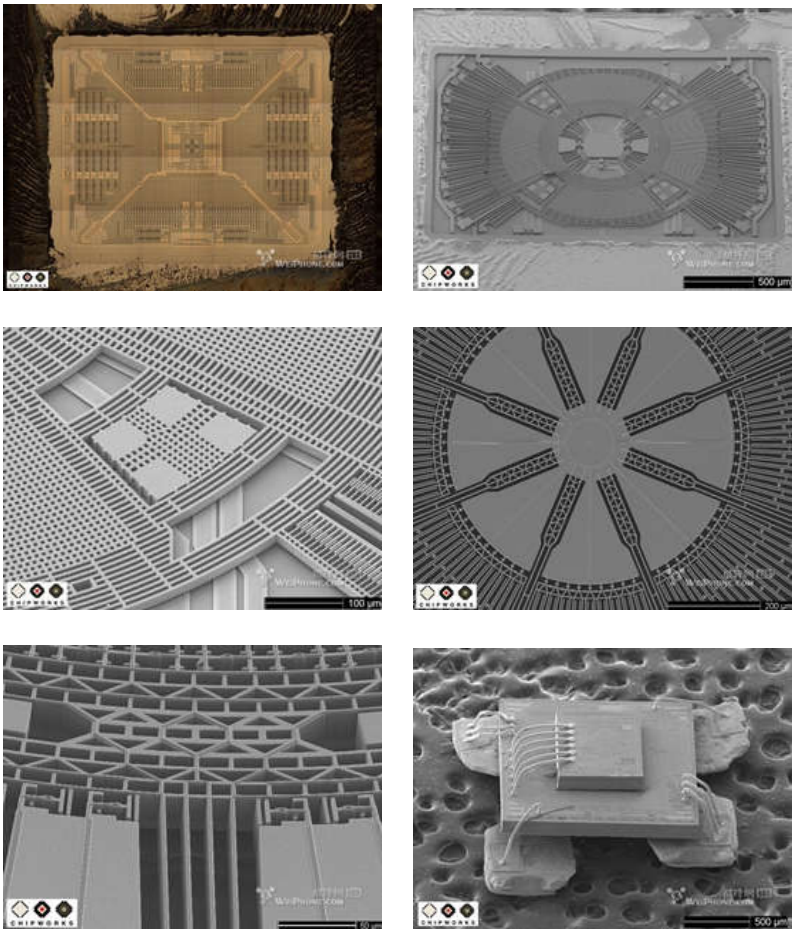

Figure 3-2 Microstructure of gyroscope chips based on MEMS (Micro-electromechanical Systems, is a mini system that integrates optical systems, drive components, mechanical components and electronic control system in a single unit) technology

With lower cost, higher sensitivity, higher accuracy volume miniaturization but lower power consumption, the accelerometer and gyroscope is more and more popular, and applications continue to appear. For instance, a new application: Apple will use microphone and accelerometer to reduce vibration noise of iPhone (United States patent publication number US20120286943 A1, http://appft1.uspto.gov/netacgi/nph-Parser?Sect1=PTO2&Sect2=HITOFF&u=%2Fnetahtml%2FPTO%2Fsearch-adv.html&r=17&p=1&f=G&l=50&d=PG01&S1=(apple.AS.+AND+20121115.PD.)&OS=an/apple+and+pd/11/15/2012&RS=(AN/apple+AND+PD/20121115)).

3.3.3 Memory

Memory stores software and data for the detection device. First of all, enough memory supports the detection device to work normally; secondly, the access speed of memory should be fast enough, so that the overall speed of the system will not be slowed down; third, the power consumption of the memory should not too high, otherwise it will

shorten the working time of the detection device as a battery-powered system; finally, same as CPU, the memory should have a low enough cost to be large-scale deployed.

3.3.4 Network

The network of detection device refers to the communication module that connects to wireless network. Strictly speaking, the network itself is not a part of the data processing system. However in Section 3.3.4 the wireless wide area network development and situation are discussed, because one of the requirements of the detection device is that it can real-time sends collected data to server through wireless network (Wi-Fi), it is a necessary part of the detection device.

Table 3-1 Technology and the highest speed of various types of network

	Type	Major Tech	Max download speed	Max upload speed
1G	analog	FDMA	/	/
2G	digital	TDMA (GSM)	GSM: 14.4Kbit/s GPRS: 53.6 Kbit/s EDGE: 217.6 Kbit/s	GSM: 14.4 Kbit/s GPRS: 26.8 Kbit/s EDGE: 108.8 Kbit/s
3G	digital	UMTS (WCDMA/TD-SCDMA/CDMA2000)	UMTS: 384 Kbit/s HSPA: 7.2 Mbit/s HSPA+: 14.4 - 168.8Mbit/s	UMTS: 128Kbit/s HSPA: 3.6Mbit/s HSPA+: 5.76 – 23.0Mbit/s
4G	digital	WiMAX/LTE	LTE: 100Mbit/s LTE-A: 1Gbit/s	LTE: 50Mbit/s LTE-A: 500Mbit/s

Network is becoming more and more important for people's daily life. According to a survey made by O2 and Samsung together shows that nowadays people spend about 2 hours in average to use mobile phones every day. Half of this time is spent to access the Internet, play music and play games, and only 12 minutes are used to make phone calls. (http://www.telegraph.co.uk/technology/mobile-phones/9365085/Smartphones-hardly-used-for-calls.html)

In UK, 4G license is far cheaper than 3G license (as shown in Table 3-1). In 2000 the United Kingdom finance obtained 22.5 billion pounds from the spectrum auction, while the price in 2012 is only 1.3 billion pounds. This suggests that the 4G technique costs less to get start with, which makes it easier to spread. This means that in the future, the spreading speed of 4G is probably faster than 3G.

Therefore a conclusion can be reached: High speed, stable, affordable wireless network has been laying the communication transmission basis for distributed data collection.

3.3.5 Battery

Generally the power consumption of built-in gyroscope is higher than the accelerometer. The typical current consumption of accelerometer is 0.25mA for k3dh (An accelerometer sensor IC comes from STMicroelectronics corporation, used in many smart mobilephones such as Samsung I9100), and the typical current consumption of gyroscope is 6.1mA for k3g (A gyroscope sensor IC comes from STMicroelectronics corporation). However, they are almost negligible compared to the whole machine power consumption. According to the energy consumption of the whole system, the energy consumer includes CPU, sensor, memory, network modules, as well as other captive hardware. The battery should have high energy density, can be repeatedly charge and discharge, and can keep safety under impact.

3.3.6 UI

Some embedded systems have user interface (UI) and some do not. Whether an embedded system has UI depends on the requirements of the system. If the UI is necessary, it should provide clear instruction for user, so that even those who have never used the system can easily learn to use it. The UI should also be hard to crash.

3.3.7 Size

Internal space of vehicle is precious. A large number of vehicles have a long design period in order to have a large internal space. Therefore, as an on-board, the detection device should have a minimal size and weight. The universal adaptability of the detection device should also be taken into account. It may take a wide range of research and experiments to get good results.

3.3.8 Conclusion

In summary, the requirements of the detection device is: it should be an embedded system, which is made up of CPU, sensors, memory, network module, battery etc. On this embedded system, software can be run to complete assigned work.

3.4 Classification and evaluation of embedded systems

3.4.1 Sun SPOT

At initial stage, the project planned to use Sun SPOT, an embedded system with various kinds of sensors mounted inside (three-axis acceleration sensor, temperature sensor and light-sensation sensor) which was promoted by Sun Company in 2008. It includes ARM 920T CPU with 180MHz, 512KB RAM and 4MB Flash on-board memory, USB interface and 2.4GHz IEEE 802.15.4 wireless interface for communication as well as 750mAh rechargeable built-in battery.

Sun SPOT is developed by Sun Company and it certainly adopts Java as development environment, which guarantees the high efficiency of development and easy operation. In addition, Sun Company provides a large quantity of technical support.

However this embedded system has disadvantages as well. The price of Sun SPOT reaches $400 per set. Due to such high cost, it is only used for prototype verification and difficult for wide-scale promotion. Besides, it has poor universality. 180MHz CPU (upgraded to 400MHz then), with low performance, cannot conduct data processing and calculation with high requirement. It is not provided with long-distance wireless data transmission module (such as GPRS or 3G module). And with 4MB Flash memory, it cannot conduct continuous data collection for a long term with high sampling frequency (such as 100Hz), which restricts its application to most extent.

3.4.2 Raspberry Pi

During this experiment, Raspberry Pi is newly promoted with support of Raspberry Pi Foundation in 2012., With the dimension (67.6*30 mm) larger than Sun SPOT (includes BCM2836 CPU with 700MHz (ARM architecture as well), 256MB or 512MB memory, SD card for extension and I/O such as Ethernet, USB, HDMI, RCA. For OS, adopt Linux developed by Open Source (other OS is available for operation as well)), the Raspberry Pi has more mature and richer development tools and supporting software than those of Sun SPOT. What's more, the hardware configuration is higher than that of Sun SPOT (the hardware has been improved much only with four years) and it can even run programs designed for PC with high performance graphic processing unit. In addition, its price is only $25/35 (Raspberry Pi has two versions, the difference is that the latter one has more USB and Ethernet interface).

The mainboard of Raspberry Pi itself does not include the sensor, battery or wireless communication module. In fact, it is much more similar to the host of a PC. And its standard USB interface and Linux OS contributes to easy extension.
However, if Raspberry Pi is applied in the project, it is needed to add the sensor, battery and long-distance wireless data transmission module (such as GPRS or 3G module), which will produce some expense. Even so, Raspberry Pi still has the cost performance much higher than Sun SPOT developed four years ago.

3.4.3 NUC

What's more, the companies such as Intel have been promoting mini computers, namely NUC (next unit of computing) in recent years. Strictly speaking, NUC is not an embedded system. It has good versatility, and it can be used instead of embedded system under most conditions. Therefore it is discussed together with other embedded systems in this thesis. NUC is a host with dimension only 10*10*5cm internally mounted with ultra-low voltage CPU ranging from Celeron to i5, mainboard, memory, 2.5 inch hard disk (notepad mechanical or SSD hard disk) or mSATA interface SSD hard disk, integrated display card and other general devices. And it provides such common interfaces as mini PCI-E, USB, HDMI, Wi-Fi and Bluetooth as well. As it is a platform of x86 and operates windows operating systems (other operating systems are available as well), it has advantages such as universality to operate most kinds of Win-Tel software, small dimension and low power consumption (to tens of watts). However, it is not popularized currently mainly because of the high price: the price of CPU and mainboard is 100-300 pound; in addition the internal storage and hard disk shall be purchased; if this system is used for this project, modules such as sensor and 3G are needed to be purchased as well.

3.4.4 Mobile phone

There are a number of manufacturers and a variety of types of mobile phone. To understand the feature of mobile phone, one has to know about their history and development.

3.4.4.1 The development history of mobile phone

3.4.4.1.1 The development of mobile phone network: from 1G to 4G

In 1999, Internet was rapidly popularizing around the whole world, so more and more users generated the demand for mobile network. Under such circumstances, the

shortcomings of 2G network (including GPRS (so-called 2.5G) and EDGE (so-called 2.75G)), such as slow network speed, unstable connection and lost connection when change service zone, are exposed. Therefore, it is a milestone of the development of mobile communication network that 3G network such as CDMA2000, WCDMA and TD-SCDMA are approved in the same year.

3G network witnesses an extremely rapid development. Under differences of application environment, the actual access speed of 3G network varies from 300k to 2Mbps. The more advanced technology, HSDPA, or so-called 3.5G network, have theoretical download speed of 14Mbps and upload speed of 5.8Mbps, which is a huge improvement comparing with the speed of 2G network (dozens kbps to over 100 kbps). As a result the market and users have higher requirements to the performance of the mobile phone itself.

3.4.4.1.2 Development of hardware of smart-phone

The hardware has experienced a rapid development along with OS and software.

1. CPU: In early days the mobile phones are mainly used for voice communication and do not have much additional functions, therefore the design of mobile phones does not focus on the computing speed but how to reduce the power dissipation as much as possible so as to extend the stand-by time, which requires the assistance of better battery processing technologies and power management program. However, under the same technological level and the same architecture, the higher processing speed means higher frequency of system clock, which means that the increase of power dissipation is inevitable. At that time, a reasonable reduce of the processing speed of CPU is acceptable in order to reduce the power dissipation and extend stand-by time.

However, with the arrival of 3G era, the users need a stronger CPU to process more powerful programs, which immensely promote and propel the development of CPU. Based on the research experience on desktop CPU, the CPU clock of smart-phones rapidly increases to GHz from dozens of MHz, with the number of core increases from one to two, four and even eight. Meanwhile, the GPU responsible for graphics acceleration has been developed. One thing should be noted that so far the CPU for the majority of the smart-phones is the SoC (System on Chip) architecture based on ARM. Compared to the desktop CPU (Typical Intel x86 series), smart-phone CPU requires lower power dissipation, lower cost and is more compact, which is more suitable for the embedded system.

Although the CPU of embedded system varies from the architecture of x86, we still can roughly compare their performances. In consideration of the development area of desktop CPU in recent years, Moore's Law (the observation that : when the price does not change, the number of transistors in an integrated circuit doubles approximately every 18 months as well as the performance. In other words, the computer performance that can be bought with each dollar doubles every 18 months. The Law reveals the development speed of the information technology) is not as sure as it was in the past, and it shows the trend of declining, while the development of embedded CPU is still rapid.

2. User interface (UI): The earliest mobile phones had small screens that can only display monochrome. Those mobile phones before Moto GC87C in 1998 even adopted LED digital tube for display. This is partly limited by the manufacturing technologies, techniques and cost, partly because it is hard to process and display rich colours for the low speed CPU. In fact, the basic function of making calls has no demand for a strong CPU. However, since the beginning of the 3G era, smart-phones have become the personal digital assistant, on which a large number of software requires advanced hardware to support advanced requirements such as high resolution display with large number of colours. On one hand, the UI becomes more and more easy to use with introduction of touch screen and gesture-control; on the other hand, high-quality UI consumes more resources, which promotes the development of hardware. With advanced UI, the smart-phones are easy to use not only by the professional users, but also by the senior, children and less-educated people.

3. Memory: the memory capacity increases to gigabytes from hundreds kilobytes or several megabytes in the early stage. The access speed increases and power dissipation reduced along while the memory capacity increases.

4. Input/output device (I/O): has upgraded from infrared way and series ports to Wi-Fi and USB ports, with the speed increased greatly.

5. Sensors: In early days, microphone is the only sensor on the mobile phone, which is used to receive voice signals. Later, more sensors are added to the mobile phone to support more functionality. The acceleration sensors are used to detect the change of gravity to verify the change of mobile phones' attitude so as to automatically adjust display. Since then the developers have found that the acceleration sensors can be used for more purposes. A typical example is using acceleration sensor to control the data transmission between two mobile phones. For example, in the famous social contact

software Bump, simply by a slight touch of two mobile phones the two owners can mutually link as connections, which is a typical model of using acceleration sensors and GPS Location Based Service. Another example is that, it can be used to control mobile phone games through tilting the devices rightwards or leftwards, which is particularly helpful in racing games. However the acceleration sensors cannot completely determine the gesture of the devices because it cannot measure the angular acceleration. Thus gyroscopes are equipped to some smart-phones to provide more precise output in the combination of the acceleration sensors, and used in more applications.

The development trend of sensors is diversification and high technology. Currently the mainstream smart-phones adopt various sensors such as acceleration sensors and light sensors which can detect the change of illumination intensity and adjust the brightness of screen so as to improve the display performance. Some high-end smart-phones even adopt gyroscopes, temperature meters, barometers which is used to measure altitude, magnetometers, and distance sensors which can automatically shut down the touch screen to avoid mistake-touch when the user makes calls with his face near the touch screen .The trend of research reflects in miniaturization, low power dissipation and high precision. Originally, the built-in acceleration sensors of mobile phones are used for recognizing the gravity direction so as to automatically adjust the screen display direction with the rotation of the mobile phones when the users rotate their phones, which provides convenience for the users. When this function is adopted in the software, the situation is full of variety. A lot of functions can be realized when the acceleration sensors are used to detect device vibration (Xu et al., 2012). A typical example is to use acceleration sensors in many mobile games as one of the input units. Thus the users can control the roles (such as racing bicycles) in the games only by shaking the mobile phone rightwards or leftwards to adjust the mobile phone's relative inclination angle to the ground, which brings more enjoyment of the games. In fact it happens to be one of the most distinctive functions of Nintendo's historical game device, Wii. Besides in games, shaking mobile phone also can be used as one of the input orders for users. Since then adding connections by shaking mobile phones at the same time has appeared in many social contact software. In the past, when two smartphone users stand next to each other, if they hope to add each other to contact list, instead of manually type contact information into phone, which takes time and may contain misspelling words, they can open blue tooth and find each other, then click 'Connect' and input password,

then the match process is completed. Now with built-in sensors, Location Based Service of GPS and Internet data connection, this process is highly simplified: the users just need to stand together, open a social app and then shake smartphone at the same time. In addition, the characteristics of acceleration sensors have been used in other creative functions. For example, if the sensor detects that the mobile phone is picked up and the attitude changed from horizontal to vertical, the incoming call will be answered automatically; and if the sensor detects that the mobile phone is turned to face down, the incoming call will be refused automatically.

Table 3-2 Power Dissipation and Precisions of Acceleration Sensors and Gyroscopes: Samsung Galaxy Note 1 (N-7000) and iPhone 5

	Samsung Note N7000		Apple iPhone 5	
	Accelerometer	Gyroscope	Accelerometer	Gyroscope
Model	ST LIS3DH	ST L3G4200D	ST LIS331DLH	ST L3G4200DH
Measurement range	±2g/±4g/±8g/±16g	±250/±500/±2000 dps	±2g/±4g/±8g	±250/±500/±2000 dps
Frequency range	1Hz - 5kHz	100 - 800Hz	0.5Hz - 1kHz	100 - 800Hz
Precision	16 bit	16 bit	16 bit	16 bit
Minimum operating current	1mA	1.5mA	10mA	1.5mA
size	3x3x1 mm	4x4x1 mm	3x3x1 mm	4x4x1 mm

Accelerometers and gyroscopes are more and more widely used on mobile. The first built-in accelerometer is introduced to iPhone to provide gravity sensor, so that phone can accommodate to different gestures of the users. After that there are more and more applications of accelerometers on mobile, resulting the development of a lot of software. Iphone4 is the first mobile that introduces the gyroscope, which enables mobiles to sense their motion. Since then, an increasing number of mobile phones, including the iPhone series, Samsung's high-end Android phones, and Nokia lumia920 (Windows Mobile series) also have built-in gyroscope. It can be predicted that there will be more mobile phones in the future with built-in gyroscope. The built-in gyroscope is one of the development directions of mobile-built-in sensors in the future.

6. GPS: Strictly speaking, GPS is not a traditional-type sensor, but for the system that calls the GPS, if the GPS is considered as a black box and how it works is not involved, the GPS has no difference with the other sensors such as acceleration sensors and gyroscopes. It can output the information parameters such as three-dimensional coordinate of the current location and the current movement speed, as other sensors output information about acceleration, altitude, temperature etc.

However, the GPS receiver installed inside the smart-phones is only a minor part of the huge system of GPS. Apart from the receiver, the whole GPS system includes 24 GPS satellites (21 main satellites and 3 standby satellites) and maintenance stations on

ground. Whether the GPS receiver can output correct data totally depends on whether the GPS satellite sends correct signals. GPS signals include carrier wave, ranging code and navigation message, based on which the GPS receiver can work out the current location and movement speed. From this point, the actual working mode of the built-in GPS is different from other sensors.

Before the emergence of smart-phones, due to the limitation of algorithm and hardware technologies the main issues for GPS receiver are the large power dissipation, slow computing speed (cold start time can be longer than 1 minute, and the satellite-search speed is slow), high cost and poor precision. The precision of civil communication signals is about 100 meter, which is because of the interference to civil communication signals implemented by American government before the year 2000. A lot of manufacturers produce independent GPS receivers, which works as accessories of smart-phones or PDAs using Bluetooth as communication method. However, the Bluetooth itself consumes so much power that deteriorate the working time of GPS receivers. With the creation of more efficient algorithm and the improvement of processing techniques, the production cost of GPS receiver drops, which enables the GPS to become one of the standard configurations of smart-phones. The precision of GPS receiver is about 10 meter and can totally meet the demand of vehicle navigation. Quite a number of users need smart-phones as their SATNAV (satellite navigation) when they drive on the highways. Therefore for these users a new function to use GPS does not bring more burdens to endurance of the battery (of the smart-phone).

The precision of speed detection of GPS is high. Generally, the precision of GPS to measure geo-location is within 10 meters. If two measurements are taken at regular interval to calculate the speed according to the distance between two points, the error will be rather large. But in fact, the speed detection method of GPS is to detect the Doppler frequency shift of signals, with which the error is generally around 0.5km/h. With such a high precision the requirements for speed detection of vehicles can totally be met.

The combination of Network, PDA and sensors will broaden the applications of smart-phones. It is how to find out new application fields, fully develop the functions of smart-phones and finish the jobs which cannot be realized or need more cost to be realized in the past that will be the research focus in the future.

In conclusion, with the rapid development of technologies in recent years, all conditions necessary for this research project are complete and mature.

Table 3-3 Milestone Events for the Development of Smart-phones

Year	Event	Company/Product
1999	The first smartphone	Motorola A6188
2000	The first 3G smartphone	Panasonic P2101V
2005	The first smartphone with built-in GPS	Mio DigiWalker A700
2007	The first smartphone with built-in acceleration sensor	Sony ERSSION W580C
2008	The first iPhone	Apple iPhone 1
2008	The first Android smartphone	HTC G1
2010	The first 4G smartphone	HTC EVO

Almost all smartphones can be perfectly used as a SATNAV today. More and more navigation software appear, providing many functions that traditional SATNAV cannot, such as display of real-time traffic jam and road condition update.

3.4.4.1.3 Development of Software on Smart-phone

Smart-phones should have a relatively complete OS. In the early stage of the development of PDA, the design of OS stems partly from desktop OS such as Linux and WinCE. This kind of OS has relatively mature architecture. Meanwhile, it makes it easier to transfer the existing desktop software to PDA's OS and at a lower cost. In 2008 the App Store greatly aroused the developers' interest in iOS software programming. In 2009 the emergence of Android reduced the cost of embedding OS in smart-phones for the manufacturers; as a result an increasing number of users can afford their smart-phones

A mature and excellent OS can not only facilitate its users but also give the developers much more facility and activity to develop the corresponding application software in an easy way eagerly. Facility means that an excellent OS should have software developing tools which are mature, powerful and easy to use for developers, such as xcode, jdk/eclipse, Visual Studio; and activity means that the Network & Store/Market-based release mode has changed the software release mode in the past, greatly boosting the developer's positivity of software development.

Table 3-4 Comparison of development platform of three mainstream smartphones

Operation System	Programming Platform	Latest Version	Developer's OS
iOS	xcode	6.0	OS X
Android	jdk/eclipse	4.4	multi-platform
Windows Phone	Visual Studio	2013(12.0)	Windows

Table 3-5 Number of software in App Store of three mainstream smartphones

OS	Name	Quality of software
Android	App Store	1.2 million
iOS	Google Play	1.2 million
Windows Phone	Store	0.3 million

IPhone app store appears and enables any developer to use the development tools provided by Apple to develop and upload his own application to the app store. At the same time, it provides thousands of applications for users to download, no matter where they are or what time it is. This model greatly stimulated the enthusiasm of developers. Up to now, there are more than 1 million applications in the app store. Since then, the similar mode appears on Android and Windows phone platform as well, enables users to find, download and use the software more conveniently.

As shown in the data issued by IDC, the total sales volume of mobile phones globally reached 1,821,800,000 in 2013 including 1,004,200,000 smart phones, increasing by 38.4% compared to the sales volume in 2012. It shows that the smart phones have been replacing traditional functional phones gradually, becoming the useful tools for consumers. Besides, apart from the basic functions of making and receiving phone calls and messages, the phones have three additional functions as powerful processing ability, multi physical-quantity measuring sensors and Internet wireless access whenever and wherever possible, which makes smart phones as the pocket information processing devices unprecedentedly and revolutionarily. Depending on these, an increasing number of innovative functional applications have been designed and realized. And some are applied, increasing work efficiency greatly (such as Bump) and some even make the functions unrealizable in the past possible (such as Nokia Here). Under such condition as perfect and mature hardware, it is how to develop new better functions with more innovation for them that becomes the most urgent problem today.

Table 3-6 Typical software on smartphones making use of sensors/GPS/camera

Name of software	Description	Modules used
Bump	Users only have to collide the mobile phones with each other to exchange contact information, photo and other goals	Acceleration sensor, GPS
VR software and games	virtual reality, enhanced reality and gaming	acceleration sensor, compass, gyroscope, camera
Nokia HERE	Digital map that can provide information such as nearby shops, point of interests and gas station.	acceleration sensor, gyroscope, GPS, compass，camera
Pothole detection software（pothole Hunter/Agent/Detector/Radar/Street Bump）	Detecting potholes in a certain city	acceleration sensor, GPS
MOVES	Keep record of how many kilometres the user walks each day, with how many steps, which transport is used, the position the user stops and so on.	acceleration sensor, GPS
‘Getting taxi’ software	Passengers can release needs of taxi on smartphone and get in touch directly with taxi drivers. The efficiency of taxi is improved.	GPS

3.4.4.2 Features of mobile phone

The first feature of smartphone is strong function of its hardware. Due to the variety of user needs, various hardware are designed to be integrated together, including high-

speed CPU and numerous sensors. The former provides high processing speed, and the latter enables the smartphone to collect data in a variety of ways.

The second feature of smart phone is customised software. All smartphones have a fully functional operating system. On top of the operating system, a variety of development tools can be used to develop software. At the same time, uses of smartphones can choose to install the various software at any time according to their needs. Hence the smartphone is flexible and can perform a variety of tasks under a variety of conditions.

Smartphone has high performance-price ratio. Due to the large user demand, various manufactures are competitive, which leads to the low profitability of the product. Therefore the smartphone can be purchased at low price, which makes smartphone suitable for large-scale deployment.

Generally smartphones are equipped with a large touch screen and easy to use user interface (UI), which is suitable for all types of users, even those who have not previously used smartphone. So that the usage of software on smartphone is easy.

Both the operating system and hardware of smartphone have gone through several generations of development. Hence they are matured with not many bugs on software or hardware, which brings good stability and low failure rate to the smartphone.

Smartphone has been more and more widely used. For example, using smartphones as data acquisition and processing device to treat children amblyopia (Tao Yin, Dalong Zhang, et al. 2017), or using smartphone cameras to take pictures of human faces for fatigue detection (Chen Jia, Dalong Zhang, et al. 2017), have received good effect.

3.5 Conclusion

Mobile phone is the most suitable equipment for the project.

The target of the project is to put the phone inside the vehicle and fix it to the greatest extent; collect data with sensor mounted inside the phone; conduct analysis and process for the data to obtain the information on roads or vehicles.

In order to achieve the above aims, we need to take into the following factors:

1. Realizability: use the smart phone as detection tool and the measurable physical quantities are only those measured and resulted by the sensors mounted inside the phone, just referring to the acceleration sensor, gyroscope and GPS mentioned in last chapter;
2. Easy operation: as a measuring method with final target users being general masses, it shall be operated easily to the greatest extent. It is not needed to conduct much deep specialized training for users who can still learn it quickly and operate it easily. And

the user will not make serious mistake during mistake, resulting in unpredictable result. Take some examples: simplify the operation to such extent as only one start button in software interface for operating or even free from interface as the software can operate automatically for a long term in the background. In addition, simplify the fixation way of phone inside the vehicle for easy operation. For example, consider to fix the phone onto the support above the centre console (as it is the most common position where the phone is placed), or the user even does not need to consider the placing of phone. Either placed in any position inside the vehicle or even put inside the pocket of the user, the phone can work properly and analyse the accurate results.

3. Accuracy: the system shall be able to conclude accurate results as much as possible under different conditions. At early experiment stage, in order to simplify test, remove unnecessary disturbances to the greatest extent. In addition, in order to solve the primary key problem, design an experiment scheme which has removed minor disturbances and improved accuracy.

4. Robustness: the system shall have anti-jamming capability. In case of some minor faults, it shall be provided with some reserved schemes and correction function.

Softwares mentioned in Table 3-6 are tested and show unsatisfying detection rate. It is hard to find exact reason without access of source code of softwares. One possible reason is that the process to sensor data is defective, e.g. Ineffective denoise and baseline drift may affect the accuracy of detection. It reveals that a good data processing algorithm is essential to obtain high accuracy.

Chapter 4. Experiment design

In Chapter 3 the smartphone is chosen to be fixed inside vehicles as the detection device. Then in Chapter 4, the detailed experiment plan is discussed, including which road will be tested, on which vehicle the smartphone will be fixed, with which software to use to collect road data, and which smartphone will be used.

4.1 Introduction to road for experiment

The common motor lanes can be divided into highway and non-highways. The roads inside cities are mostly non-highways with many driving limits that may affect experimental result, such as numerous turns, traffic lights that may cause frequent acceleration and deceleration, more complex surface of road and more up and downs that may bring difficulty to verify early experimental results. Therefore, the flat and straight road sections are selected at early experiment stage, which has low traffic flow, distinct surface features and is easy to be tested repeatedly.

1. Dundee Tay Road Bridge

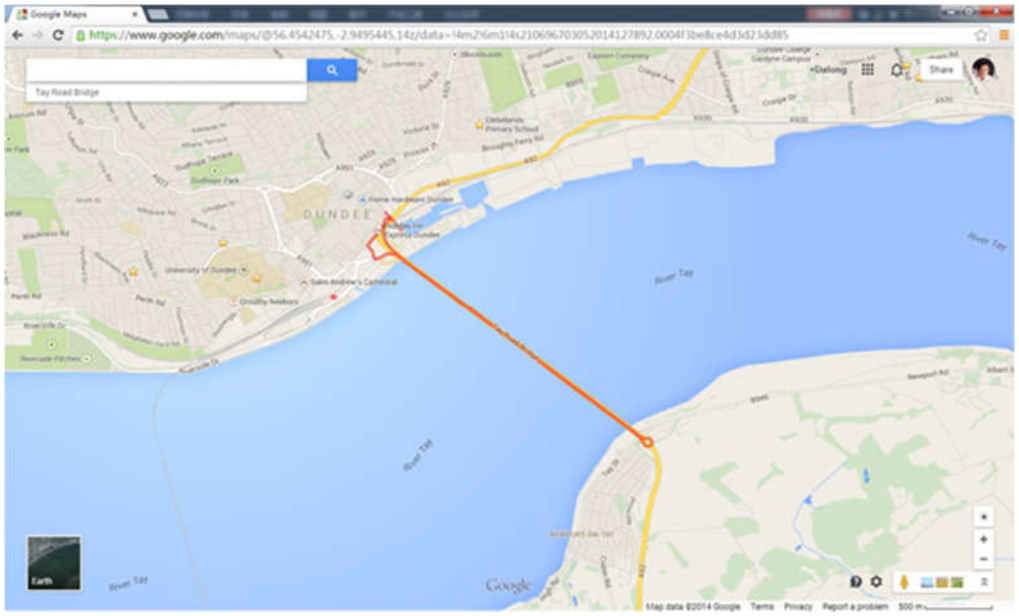

Figure 4-1 Dundee Tay Road Bridge

The Dundee Tay Road Bridge was established in 1966 with total length of 2250 meters. The bridge carries the A92 road across the Firth of Tay from Newport-on-Tay in Fife to Dundee in Scotland. It is one of the longest road bridges in Europe. The bridge consists of 42 spans. It is coloured in orange in Figure 4-1. The Figure 4-1 and Figure 4-2 also show that the main body of bridge is straight. There is no traffic light on the bridge, and from the field survey, it is found out that the sidewalk is paved with cement

boards of length of 2 meters each. The number of cement boards between adjacent expansion joints is used to safely estimate the distance between adjacent expansion joints, which is later used as verification of the detection method of this study. So the expansion joints of the bridge can be considered as the feature of road surface which makes it easy to verify in the experiments (Zhang, 2005).

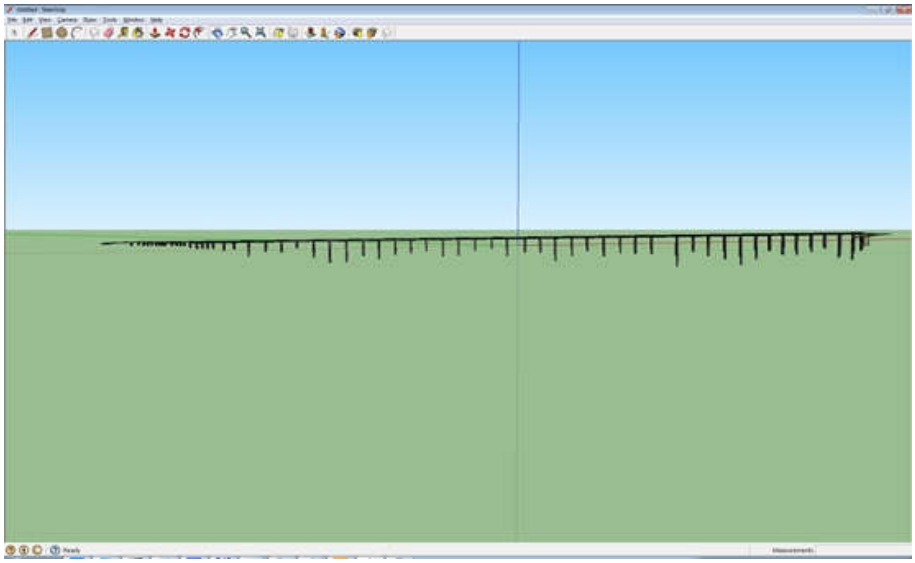

Figure 4-2 3D model of Tay Road Bridge

Typical expansion joint on Tay Road Bridge is shown in Figure 4-3.

Figure 4-3 Typical expansion joint on Tay Road Bridge

2. Edinburgh Forth Road Bridge

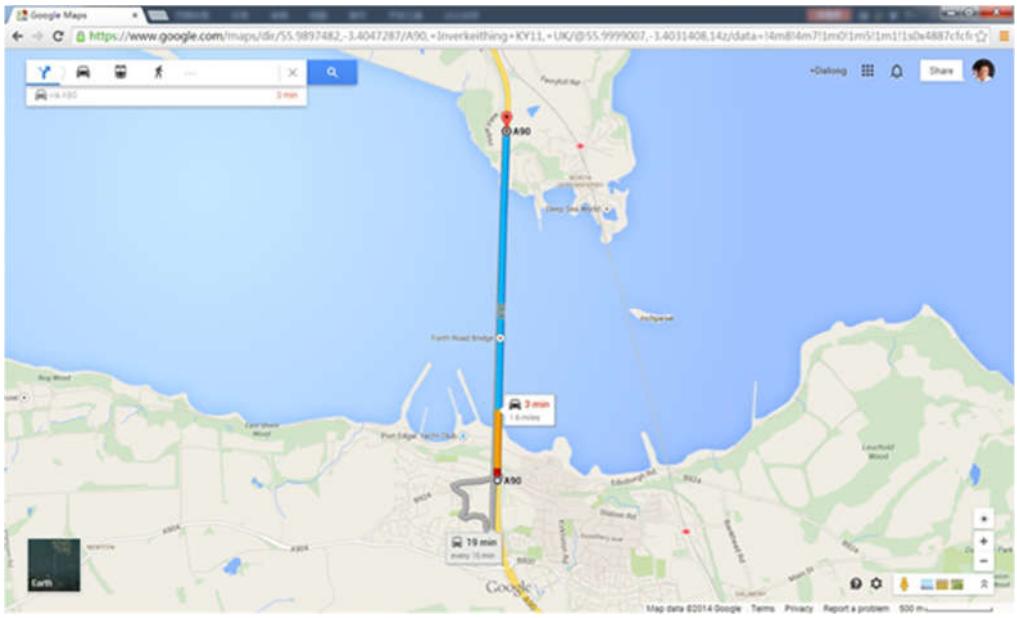

Figure 4-4 Forth Road Bridge

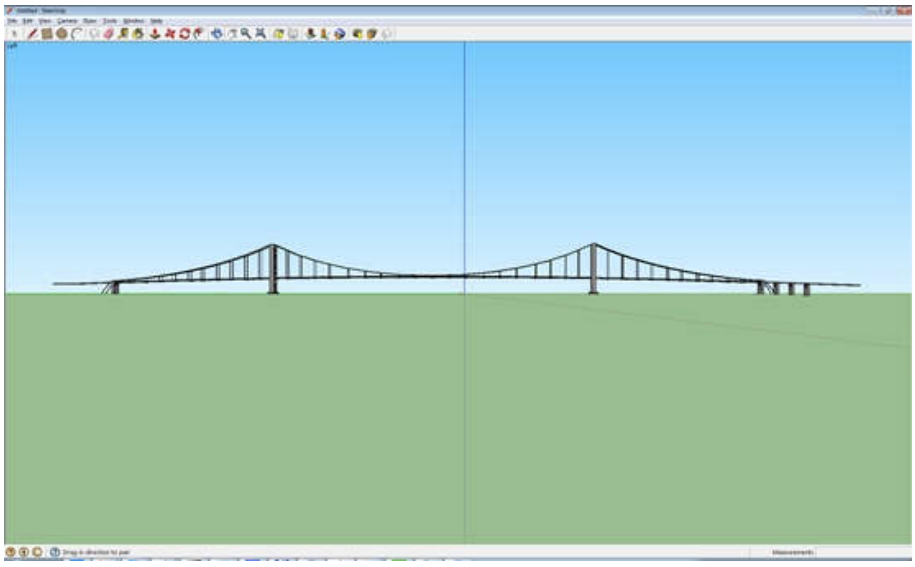

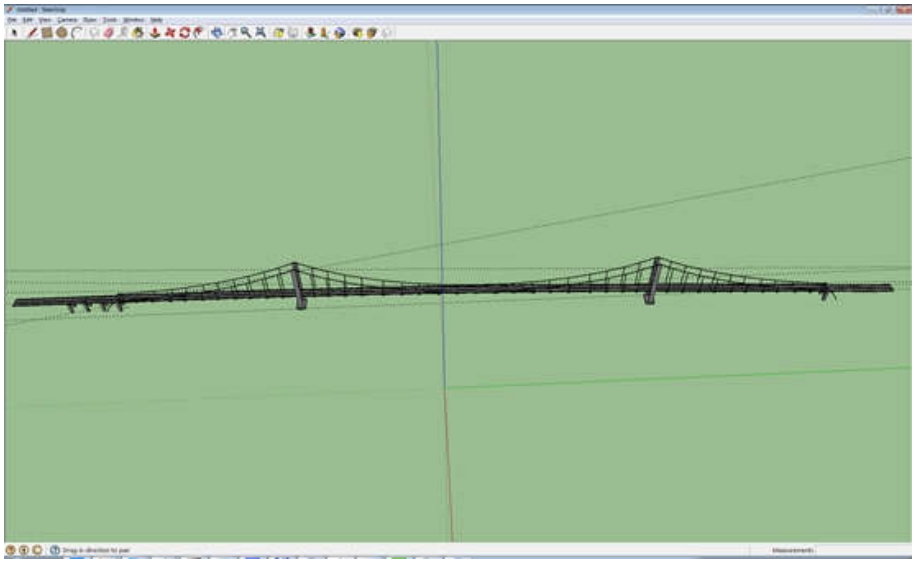

Figure 4-5 3D model of Forth Road Bridge

The Edinburgh Forth Road Bridge (the blue and orange part in Figure 4-4) was established in 1964 with total length of 2512 meters (Andrew et al., 2006). The road is divided into three sections from south to north: S1 (408m), S2 (1006m), S3 (408m) in suspension type. The daily traffic flow in average is about 65000 vehicles (Carter et al., 2009). The speed for the vehicles in the bridge is limited to 50 miles/h lower due to strong wind or other severe weather. Because of the architectural feature of the bridge, the surface of bridge has arc shape instead of complete flatness (Colford, 2008).

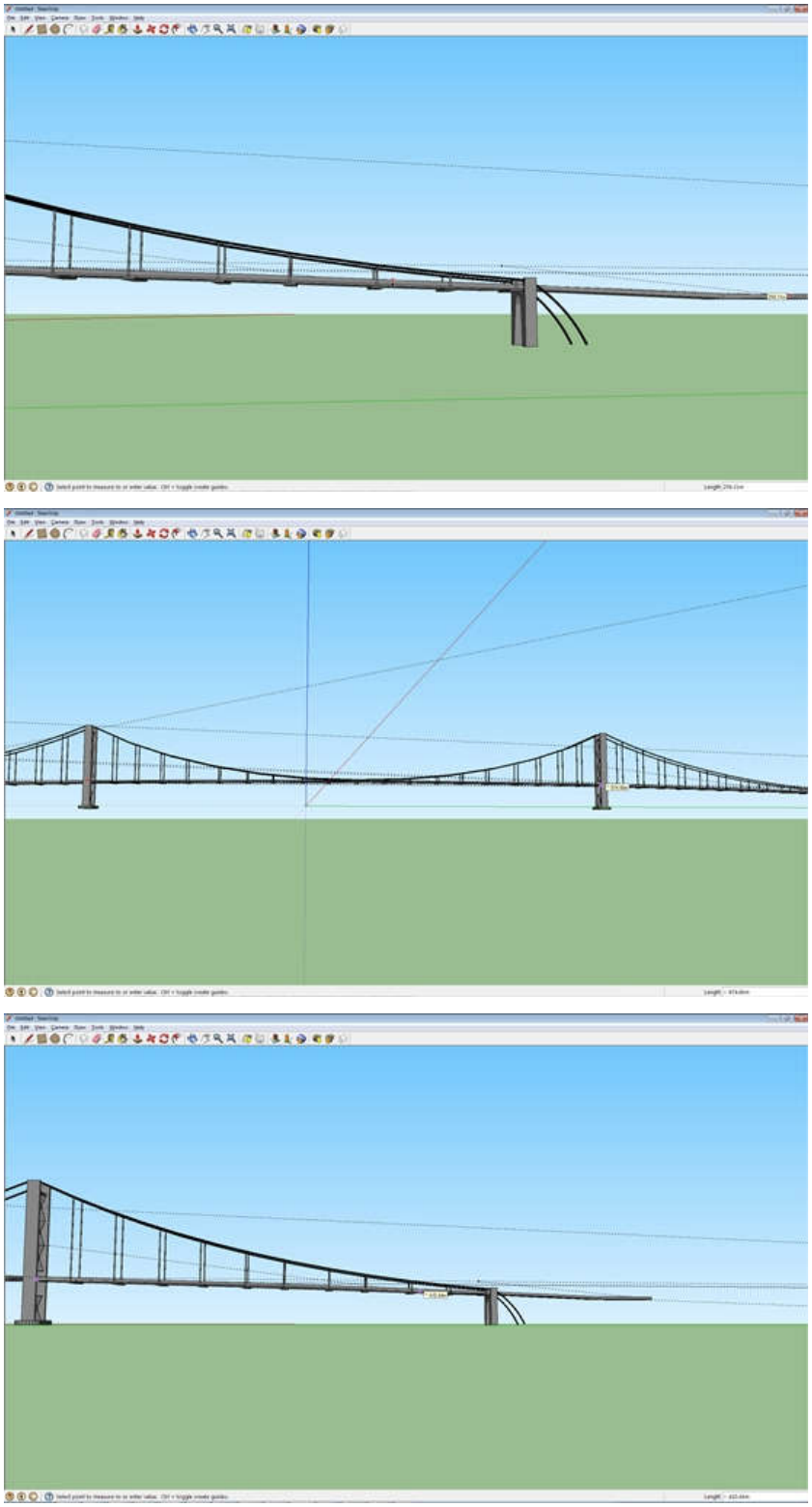

Figure 4-6 Three sections from south to north of Forth Road Bridge: S1 (408m), S2 (1006m) and S3 (408m)

The vehicle was driven at the constant speed of 50miles/h in straight road for several times. In order to keep constant driving speed, select the time ranging from 1:00 to 3:00a.m, when there is smallest traffic flow for measurement.

There are expansion gaps distributed in the bridge floor. When the vehicle passes by, there appears obvious bumping. It is deemed that these gaps represent the potholes with typical sizes on the road. If these expansion gaps can be detected, potholes of size larger than width expansion gap should also be able to be detected.

According to the general driving experience on the road, the expansion gaps on road bridges (including Forth Road Bridge and Tay Road Bridge), have the average width of 2-4cm which may result in obvious bumping of vehicles. Hence, it is considered that the pothole with such size appearing on the road needs to be detected. And if the width of pothole is smaller than that value (for example, the width is 1cm), obviously it is too small which distributes widely on the road. Where it is required to detect such pothole mandatorily, it will need much more calculation resource but with little sense. As a result, it is appropriate to set the width of expansion gap on the road bridge as the lower threshold value (namely, the minimum value) for the width of pothole needing detection.

In further analysis, when the pothole has such narrow width (same with that of the expansion gap), the tire of the vehicle cannot contact the bottom of pothole. And no matter how depth the pothole has, it will bring about the same influence and result.

To sum up, set the lower threshold value as 4cm for the width of pothole and under such width condition, the depth will not be considered.

Hence, the width of expansion gap on the road bridge completely meets the minimum width value requirement of the pothole which can be treated as the experiment subject for the research of potholes. Besides, it is acceptable that the detection sensitivity can be improved without a large increase in calculation quantity.

Features for treating expansion gaps on the road bridge as simulants of potholes:

1. The size value is close to the lower value of pothole. And if the size of pothole similar to that of expansion gap can be detected, the potholes larger than the gap can be certainly detected.

2. The road bridge floor is a straight line so that the project can focus on the detection on the smooth and straight road section with unnecessary disturbances removed;

3. With low traffic flow, it is easy to control the driving speed to prevent the speed-up and down influencing the results. (Detection time is 1:00 – 3:00a.m.).

4. Proper concentration degree: generally, there is one pothole every 20m with corresponding interval time being 3s;

5. It brings about convenience for the in-field investigation, photo taking, result comparison and handling;

6. Same size of all potholes: keep consistency;

7. It is available to conduct experiments for several times within short time to improve the experiment efficiency;

8. It is flat pavement generally except for the expansion gags, which provides easy comparison;

9. The additional uneven areas (small-sized cracks) can provide further comparison details. In conclusion, select the expansion gaps on two sections of bridge as the research subjects.

4.2 Vehicles to be tested

In order to reduce the influence of gear shifting to the minimum, automatic gearshift vehicles are selected. Due to limited conditions and considering the universality and pertinence of application in the future, small and medium-sized domestic vehicles are selected. The two detection vehicles used in experiments are shown in Table 4-1.

Table 4-1 Two detection vehicles used in experiments

Detection Vehicle 1	Detection Vehicle 2
Nissan Micra K11	Saab 9-3 2.0T
Manufacture year: 1996	Manufacture year: 2002
Automatic transmission: continuously variable transmission (CTV)	Automatic transmission
Displacement: 1.0L	Displacement: 1998cc
Three doors and five seats (hatchback)	Four doors and five seats
Front engine and front drive	Front engine and front drive
Dead-weight: about 700kg	Dead-weight: 1500kg
Tire: 155/70R13	Tire: 125/85/16
Length: 3700mm, width: 1600mm, height: 1440mm, wheel tread: 2300mm	Length: 4630mm, width: 1800mm, height: 1440mm, wheel tread: 2675mm

4.3 Collection software

The software Sensor Insider Pro is adopted for Android platform smartphones (Samsung and Nexus 7). Developed by Lucana Tech, Sensor Insider Pro can record all kinds of data collected by built-in sensors with self-defined sampling frequency and four set of output format.

In the experiment, the parameters to be measured include acceleration, rotation, GPS coordinate and GPS speed. In order to meet the accuracy requirement of the experiment, the sampling frequency needs to be set to the highest level. On Samsung Note the sampling frequency is set as 150Hz. All the data is stored in MAT format in the form of (Acc means accelerometer, Gyro means gyroscope, x/y/z means three axes, t means time stamp):

Acc_x = […….];

Acc_y = […….];

Acc_z = [……];

Acc_t = [……];

Gyro_x = [……];

Gyro_y = [……];

Gyro_z = [……];

Gyro_t = [……];

…..

The advantage of this file format lies in that it can be directly imported into Matlab without any modification (as Figure 4-7 shows). Note that the expression of name of parameter such as Location_GPS_Spd()=[……] is illegal in Matlab and result error message in importing process. The solution is to open .MAT file by txt editor (such as notepad++ or ultraedit) and delete the brackets in Location_GPS_Spd()=[……], so that it looks like Location_GPS_Spd=[……].

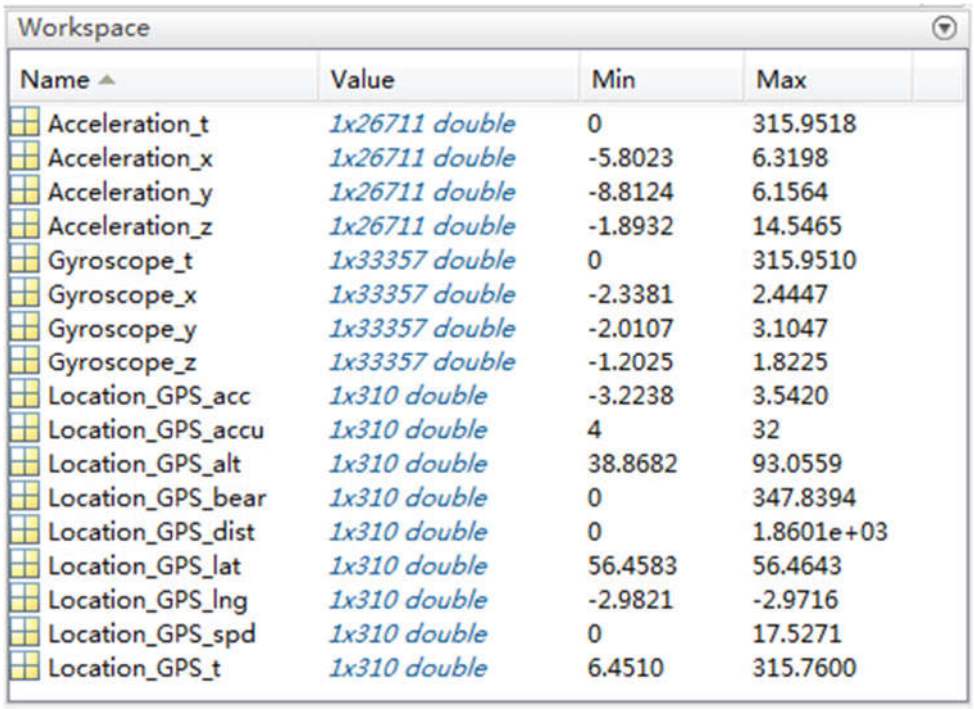

Figure 4-7 Parameters measured and imported into Matlab

The data is stored in a similar way for GPS. Moreover, GPS stores KML files, which makes it easier to load and display the route in Google maps.

The software Sensor Data is used for iOS platform (iPhones). It has similar basic functionality with the Sensor Insider Pro. Both software can access the measurements of built-in sensors and store the data in smartphone memories. The difference is that iOS does not have public file system, the data can only be output by tools as iTunes or iTools. In addition, Sensor Data cannot store data in .MAT format. Instead, the data is saved in .csv format which can also be imported into Matlab.

4.4 Experiment scheme

Samsung Note (GT-N7000), Apple iPhone4 and Google Nexus 7 are chosen as detection devices. The differences between detection devices are shown in Table 4-2.

Table 4-2 Differences between detection devices

Serial	Brand	Model	Operation system	Embedded sensor
1	Samsung	Note (GT-N7000)	Android 4.0.1	acceleration sensor, gyroscope, GPS
2	Apple	iPhone4	iOS 6.3	acceleration sensor, gyroscope, GPS
3	Google	Nexus 7	Android 4.2.2	acceleration sensor, gyroscope, GPS

The data is collected between 1-3am with minimum traffic. The smartphones are fixed inside the locker under the centre console to the most extent, which makes it able to consider the vibration of phone is closely similar to that of vehicle. (Directions of axes defined in Figure 4-8) X-axis of the phone points to the direction of the vehicle's head. Due to the limited conditions, Mobile is fixed with its LCD screen facing up, and its front (y direction in Figure 4-8) facing head of vehicle, and z-direction of mobile forming an angle with horizontal plane so that the driver can see the LCD screen. It is similar to the placement of mobile when mobile equipped SATNAV (satellite navigation system) is used. In this way gravity has components on both z and y directions. And it not only simplifies the experiment but also is featured by some universality.

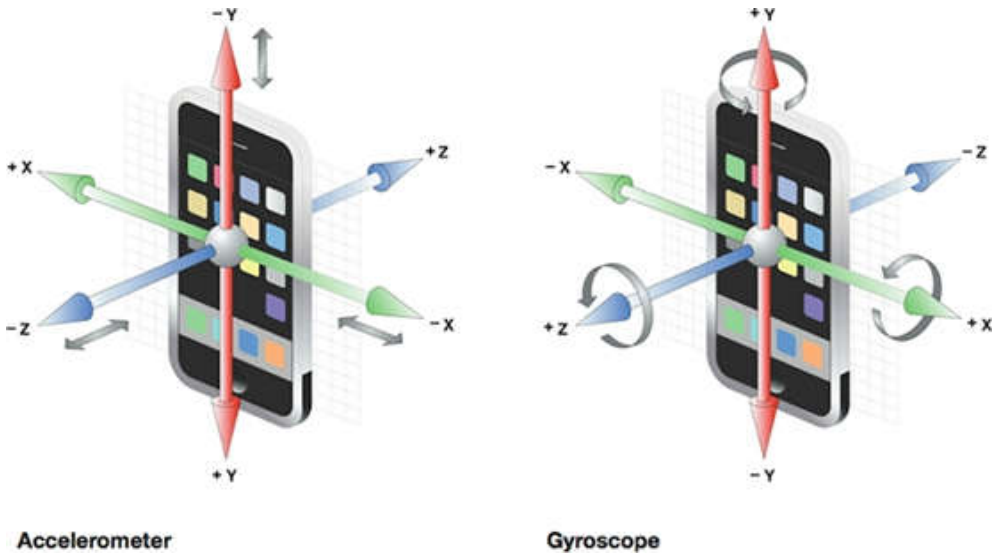

Figure 4-8 Axes direction defined by accelerometer and gyroscope

Keep the vehicle pass by the bridge at a constant speed of 40miles/h (on Tay Road Bridge) or 50miles/h (on Forth Road Bridge) in straight line for several times.

Before measurement, make sure the smartphone has enough storage space left and sufficient battery life. Restart the smartphone without operating any other software, then start the measuring software. Start the vehicle and preheat for 1 minute. It also gives the GPS time to search the satellite, as GPS receiver normally takes tens of seconds to search the satellite and calculate the position (the actual time depends on the number of connectable satellites).

In order to verify the measurement accuracy of built-in sensors (mainly GPS to measure vehicle speed), connect Nissan Micra with OBD II Bluetooth module and adapter to read the speed data from the sensor built inside the vehicle, and then transmit the data to Samsung Note through Bluetooth for storage . The speed data from vehicle sensor and GPS speed data of the smartphone have good quality, which proves that the GPS speed data of the smartphone meets the requirement of the research.

Here are some data example:

Figure 4-9 shows acceleration data collected from road from Dundee to Edinburgh. Note that the curve at the top is acceleration of z-axis direction, which is perpendicular to the ground. Because the gravity acceleration always acts along the z-direction, therefore there is always a direct current (DC) component with the value close to $10m/S^2$.

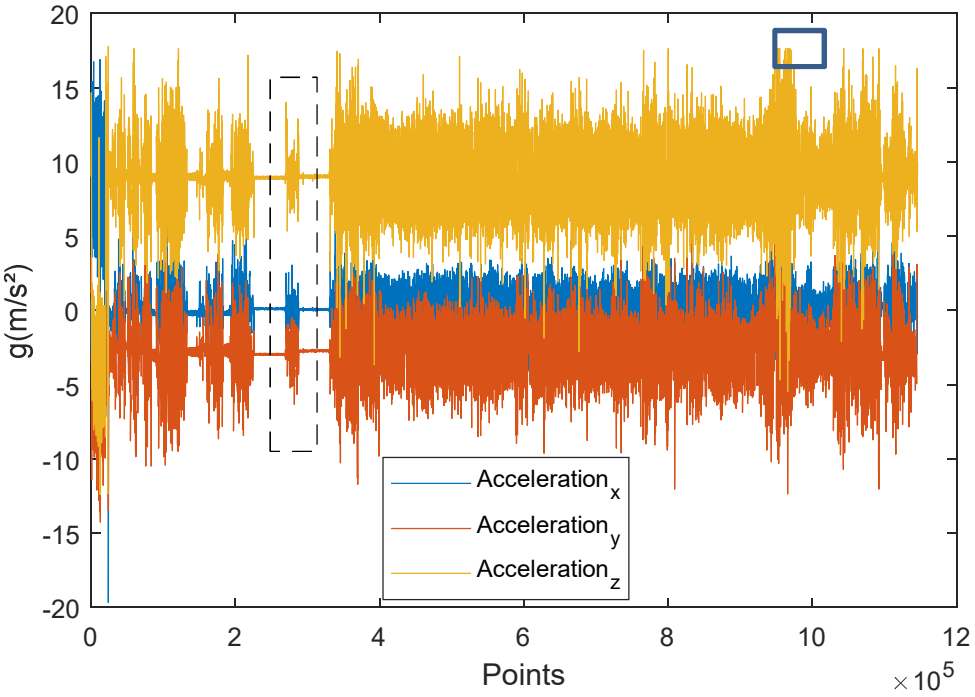

Figure 4-9 1145642 points collected from Dundee to Edinburgh on 24/09/2012 with sample rate of 200Hz. Sample time about 5728 seconds

As can be seen in the Figure 4-9, acceleration data obtained at some points is clipping distorted (clipped signal is shown in the blue box in Figure 4-9). This is because the max range of acceleration in mobile or panel is about 20 m/S^2, which is about 2g. As there is always the gravity acceleration along the z-axis, it can be considered as a numerical 1g DC component. Considering the maximum z-axis acceleration is 2g, the biggest signal along the z-axis is only 1g. If the acceleration is beyond the range, the clipping distortion occurs. However the bumping of vehicles are likely to be greater than 1g. Although the range of built-in accelerometer in mobile or panel may be changed (for example to exceed the range to 6g) by the software to avoid this kind of problem, the accuracy (generally within 2g range the accuracy is between 0.04-0.004 m/S^2) will decrease.

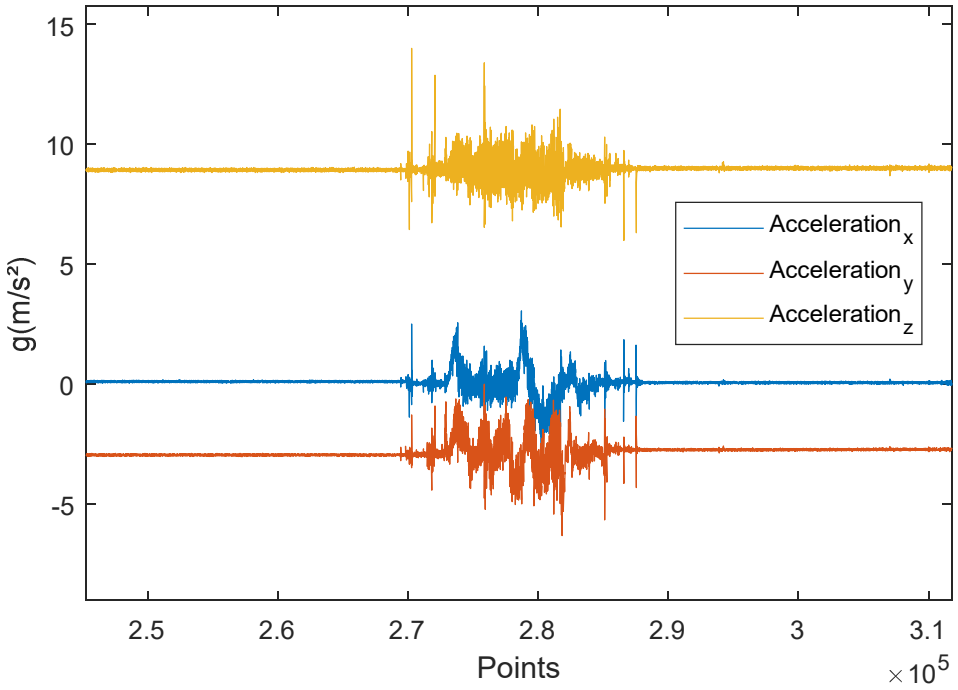

Figure 4-10 Zoom in of previous diagram, containing about 6100 points, sampled in about 30 seconds

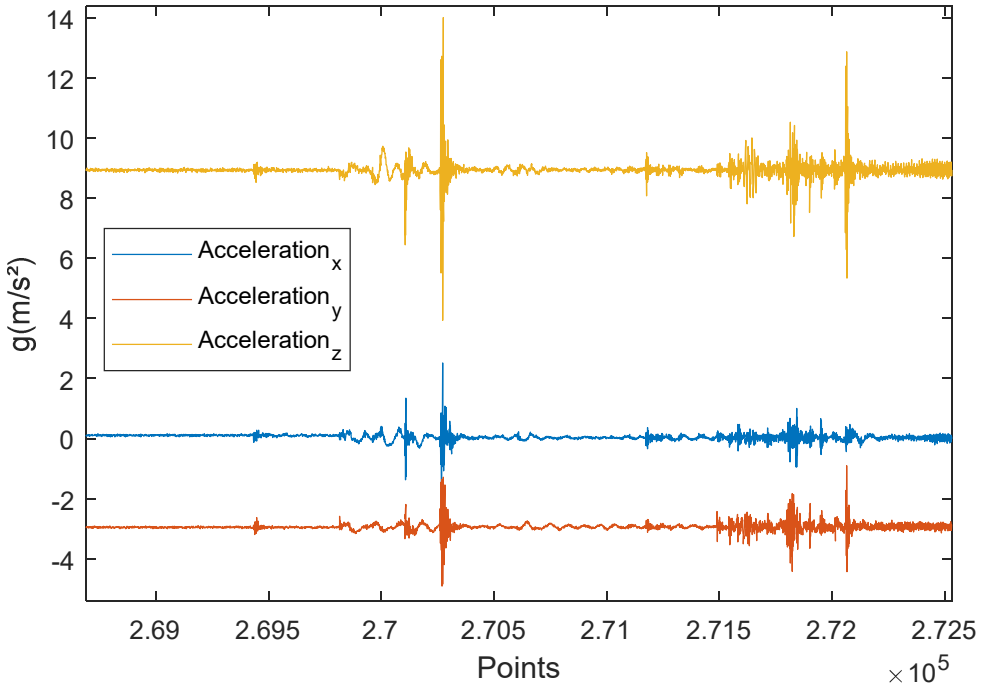

Figure 4-11 Further zoom in of previous diagram. About 3100 points measured in 15 seconds

Gyroscope sensor data shows as Figure 4-8:

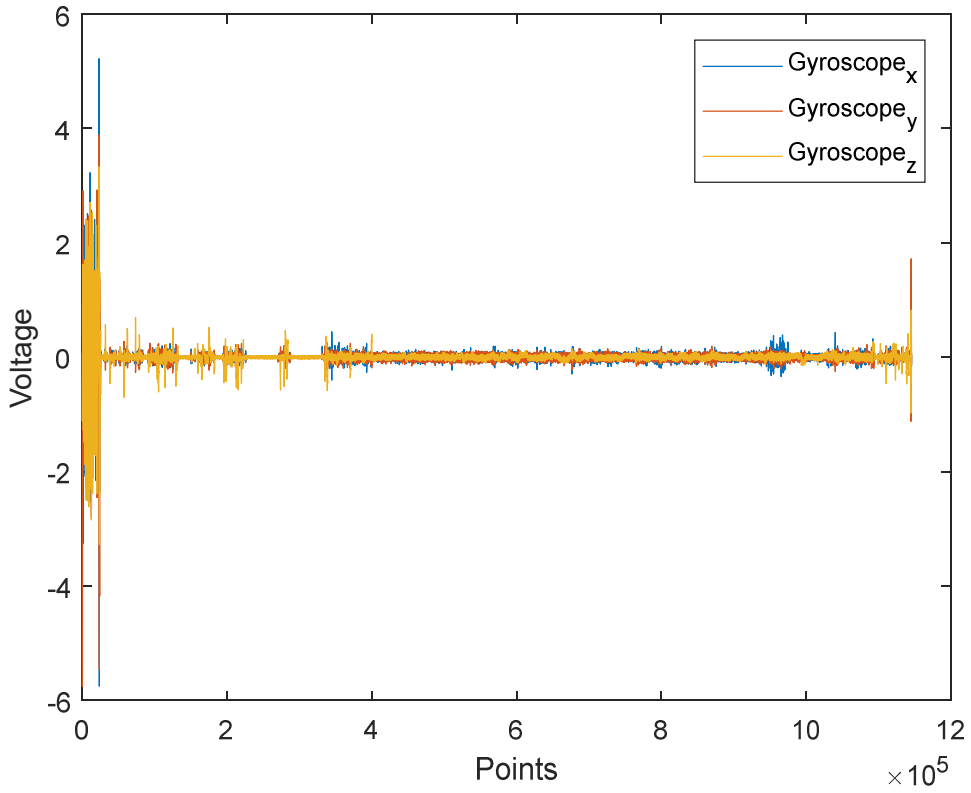

Figure 4-12 1145642 points from Dundee to Edinburgh, measured on 24/09/2012 with sample frequency of 200Hz. Sample time about 5728 seconds

General precision of built-in gyroscope in phone or panel: it is easy to know from the Figure 4-12, that the reading of gyroscopes ranges between -0.5 - +0.5 rad/S (The output value of Gyroscope is measured by voltage. For the same input, various Gyroscope chips may output different values, but the output values are proportional to the angular velocity (measured by radius/second). Therefore for the sensor used in this study, the output data can be considered as being proportional to the angular velocity, which is measured by radius/second). The gyroscope does not produce clipping distortion like accelerometer sensor does, and all the waveforms can be properly recorded. In addition, the precision of gyroscope is normally about 0.0003 per cent, and also better than acceleration sensor.

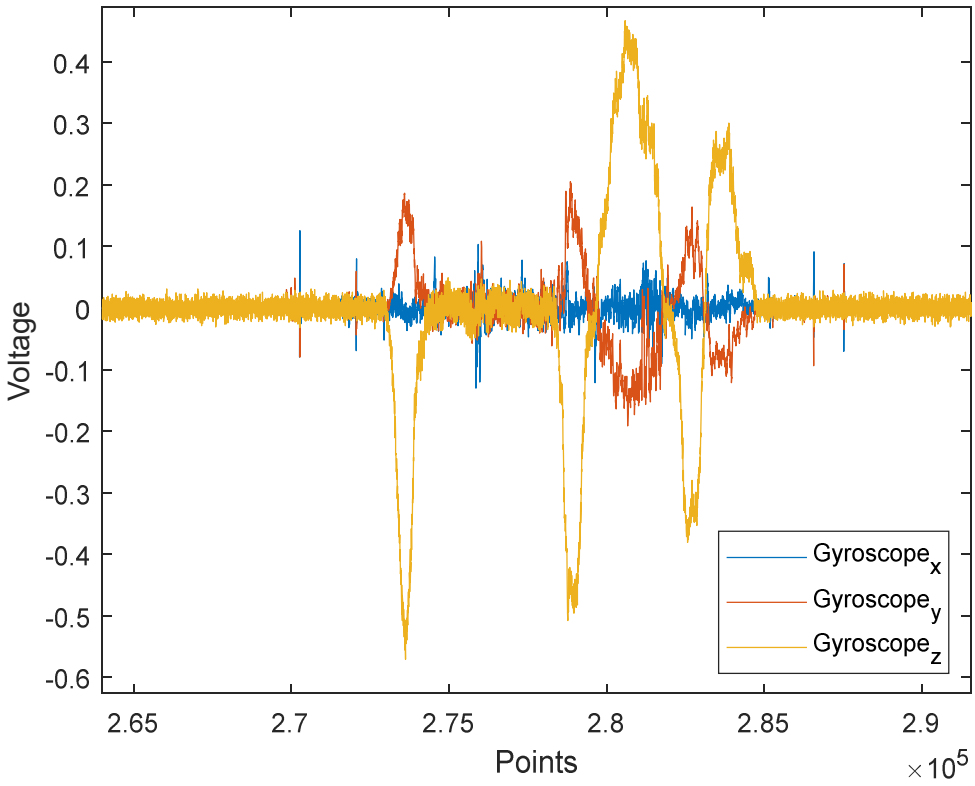

Figure 4-13 Zoom in of 4-5, containing about 25000 points, or 125 seconds

The kml data of GPS can be shown in Google maps, as Figure 4-10 shows:

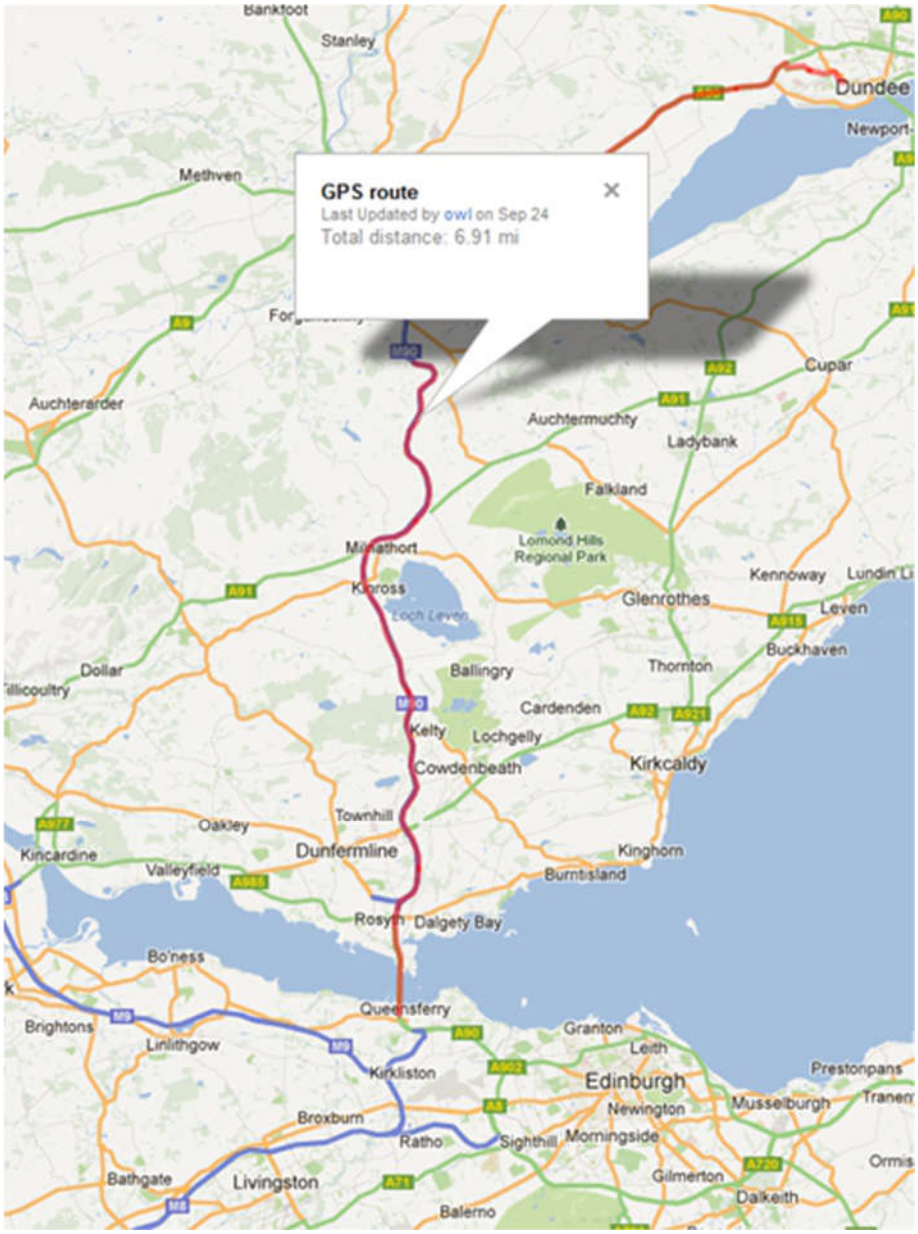

Figure 4-14 Dundee to Edinburgh, 24/09/2012. Google maps can only display a small part of geometry information of kml file, so that the length displayed in this screenshot is 6.91 miles.

Speed data can be obtained by GPS. The positioning information directly measured with GPS is low in precision, generally error in from a few meters to dozens of meters; however the speed information is measured using the Doppler effect and is normally high in precision.

The most direct method to use GPS to measure vehicle speed, is to firstly find current geographic coordinates, and measure the geographic coordinates after a period of time; then calculate the distance traveled from the two coordinates, and divide by the time interval. However, the accuracy of GPS is about 10 meters (for civilian purpose), which brings large error into calculation. Therefore another method is often used by GPS in

real practice, which is based on Doppler Effect. The signal of clock frequency offset is detected to obtain the relative speed between GPS receiver and satellite. As the frequency of the clock signal is very stable, the accuracy of this method is very high, with the error reduced to be within 1km/h. Therefore, the accuracy of the speed measured by a smartphone is within 1km/h.

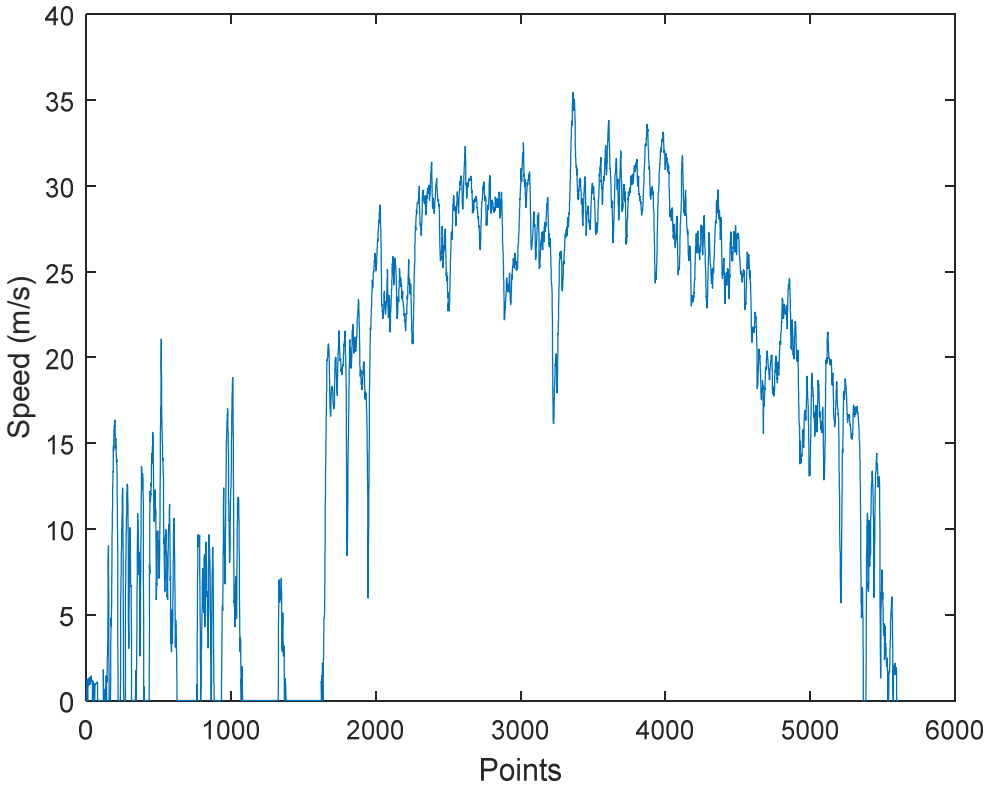

Figure 4-15 Sample of speed data, 5613 points from Dundee to Edinburgh, collected on 24/09/2012

4.5 Summary of chapter

The design of the experiment should follow these conditions:

1. Fix the smartphone inside the vehicle, as discussed in Chapter 3;
2. The vehicle drives straight at constant speed, so the noise can be reduced to minimum;
3. In order to maintain the stability of the speed, the experiment need to be operate between 1:00-3:00 in the midnight, which meets the smallest volume of traffic flow.

After the analysis of the characteristics of data collection devices, the data collection process is presented. And following this process, the real data is collected for further processing and analysis.

Chapter 5. Modelling and simulation

5.1 Simulation of suspension system

In this section, simulation results of the three types of vehicle suspension model in chapter 2 will be discussed.

5.1.1 2-DOFs suspension system of 1/4 vehicle

A simulation model for the suspension system of 1/4 vehicle in line is established with the equation 2.1 in MATLAB/SIMULINK (as the following diagram shows):

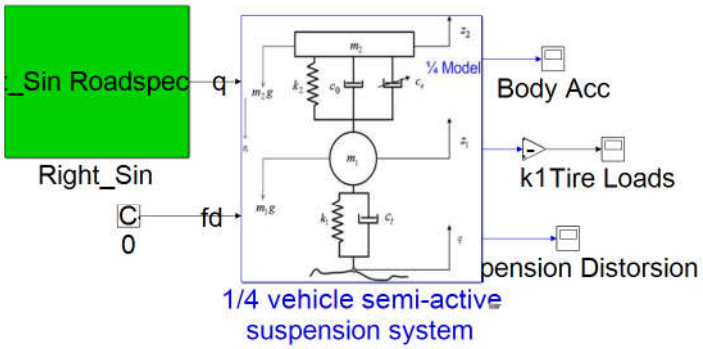

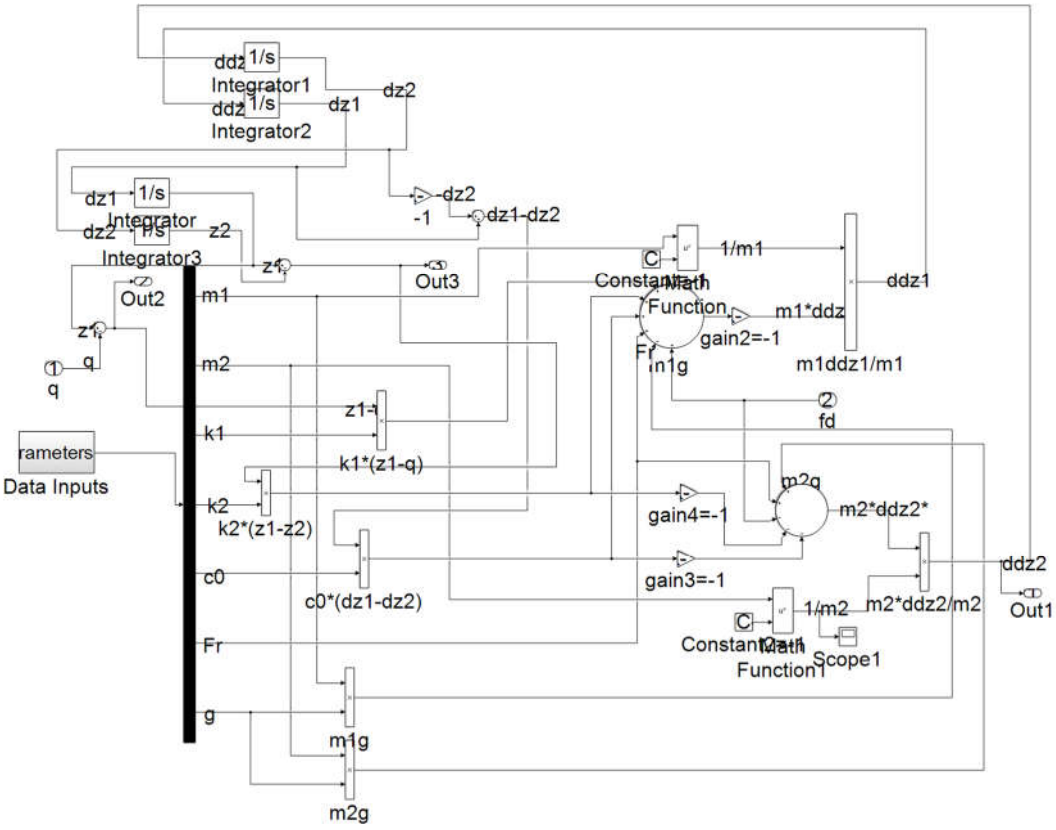

Figure 5-1 2-DOFs simulation model of suspension system of 1/4 vehicle in MATLAB/SIMULINK

When the sine wave is used as the road input excitation:

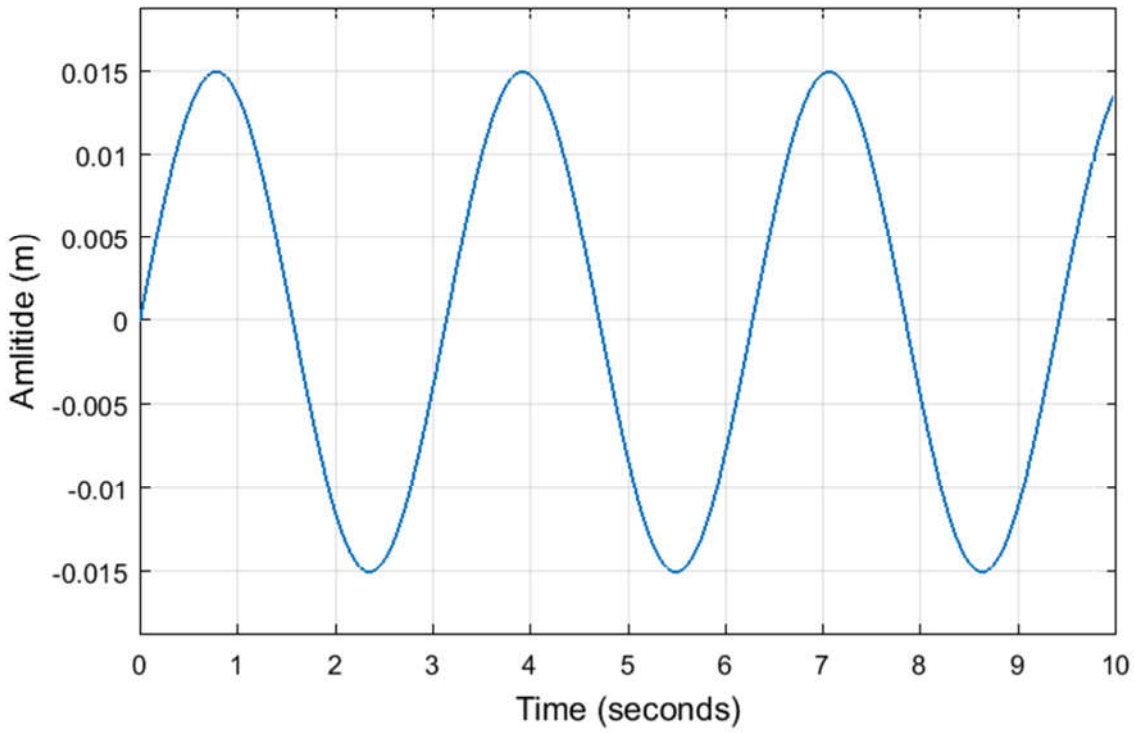

Figure 5-2 Use sine wave as the road input excitation, x-axis represents time (measured by second), and y-axis represents displacement of tyre in the vertical direction (measured by meter).

The output wave is as in the following diagram:

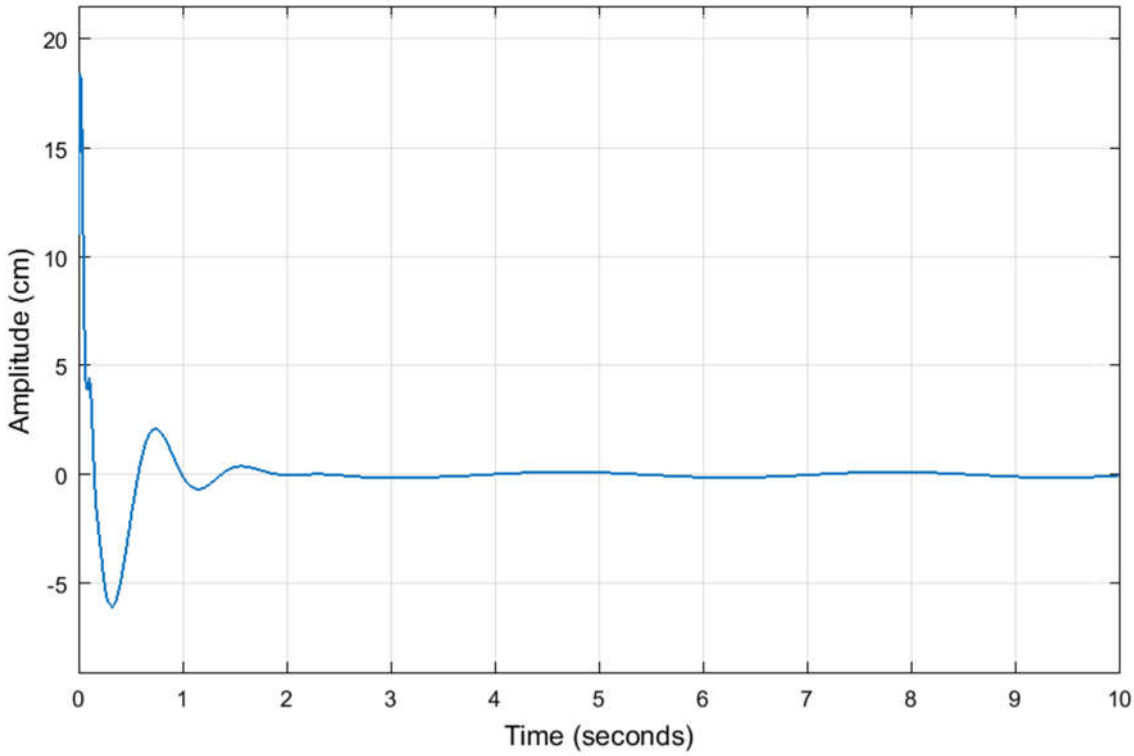

Figure 5-3 Output wave of 2-DOF vehicle model

The above figure shows that the suspension can absorb the energy of the shock, and after a period of time, the magnitude of the shock will become stable on a small value.

5.1.2 4-DOFs suspension system of 1/2 vehicle

In this section, the Pitch model is analysed. Figure 5-4 is the simulation model of 4 DOF 1/2 vehicle designed according to Equation 2.2 using Simulink. Figure (a) is the graphical block diagram of the simulation model, which is formed by a road spectrum generator, a model parameter input module, and a 4 DOF 1/2 vehicle model and result output module. The road spectrum generator is the input for the 4 DOF 1/2 vehicle model, and it represents the feature of the road surface (Guanqiang and Fang, 2007). In this study the sine wave is used. Other input, such as white noise, can be used to replace this part to study various types of road surfaces. Figure (b) shows the detail of the grey block of Figure (a), in which result is shown as waveform by oscilloscope. The result is also saved in files for further analysis. Figure (c) shows the detail of the yellow block of Figure (a), which is the implementation of Equation 2-2 by modules such as differentiator, summator and multiplicator.

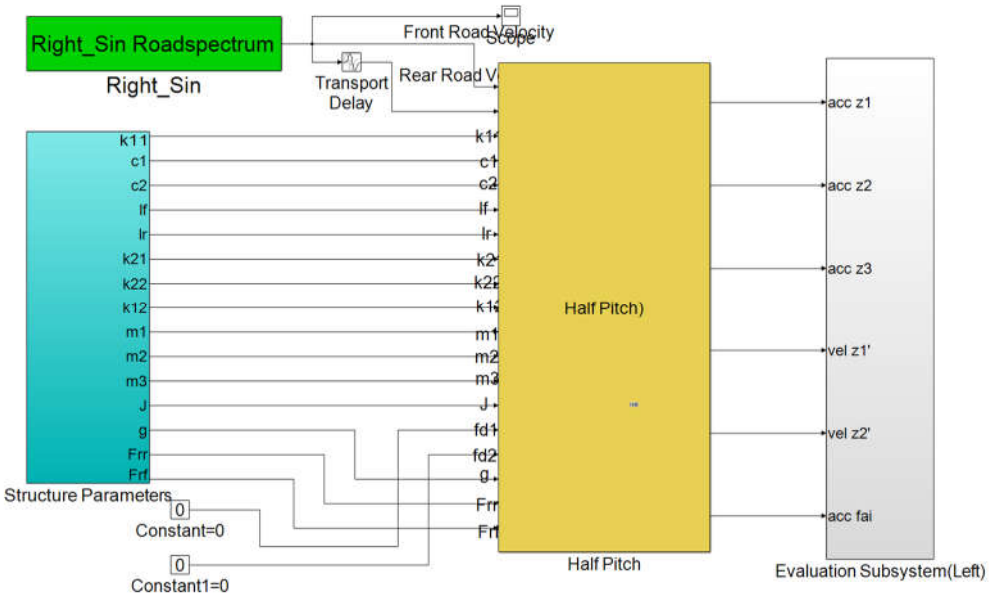

(a)

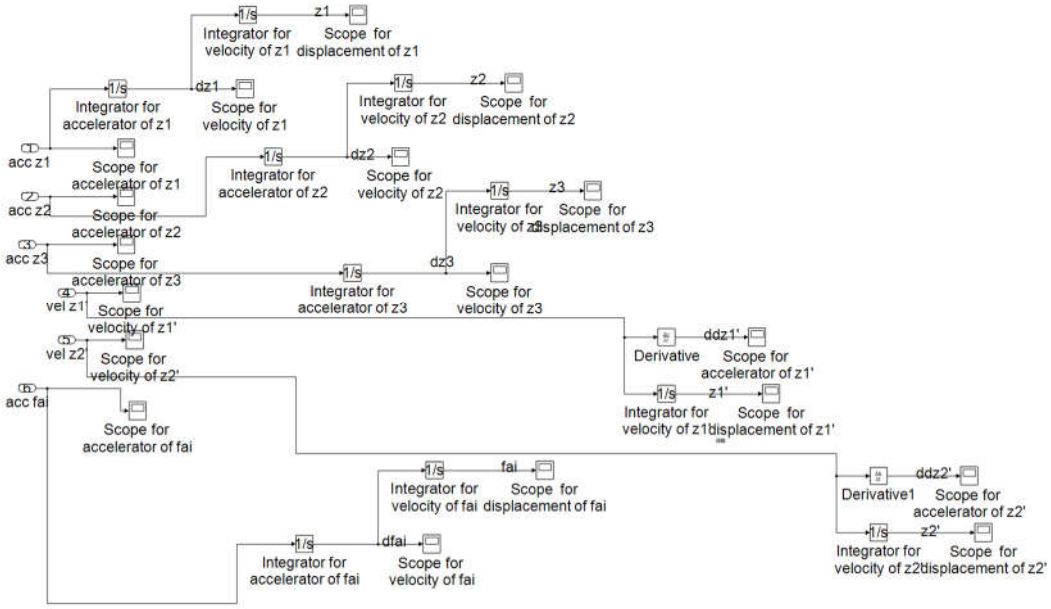
1/s
Integrator for velocity of z1
z1
Scope for displacement of z1
dz1
Integrator for accelerator of z1
Scope for velocity of z1
1/s
Integrator for velocity of z2
z2
Scope for displacement of z2
1
acc z1
Scope for accelerator of z1
1/s
Integrator for accelerator of z2
dz2
Scope for velocity of z2
2
acc z2
Scope for accelerator of z2
1/s
Integrator for velocity of z3
z3
Scope for displacement of z3
3
acc z3
Scope for accelerator of z3
dz3
1/s
Integrator for accelerator of z3
Scope for velocity of z3
4
vel z1
Scope for velocity of z1'
5
vel z2
Scope for velocity of z2'
6
acc fai
Scope for accelerator of fai
Derivative
ddz1'
Scope for accelerator of z1'
1/s
Integrator for velocity of z1'
z1'
Scope for displacement of z1'
1/s
Integrator for velocity of fai
fai
Scope for displacement of fai
Derivative1
ddz2'
Scope for accelerator of z2'
1/s
Integrator for velocity of z2'
z2'
Scope for displacement of z2'
1/s
Integrator for accelerator of fai
dfai
Scope for velocity of fai

(b)

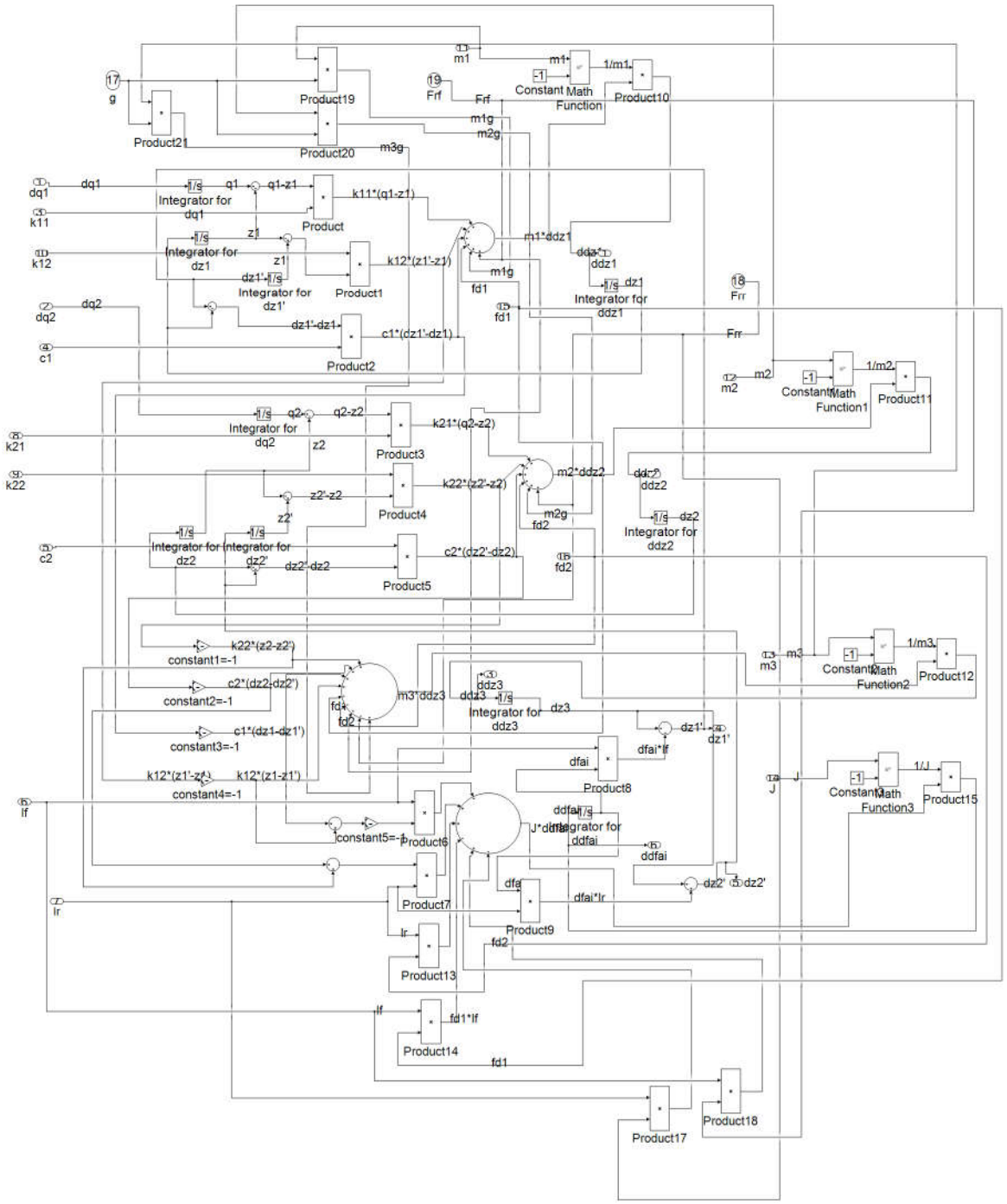

(c)

Figure 5-4 4-DOFs simulation model of suspension system of 1/2 vehicle in MATLAB/SIMULINK. (a) is the graphical block diagram, (b) shows the detail of the grey block of Figure (a), (c) shows the detail of the yellow block of Figure (a).

When the sine wave is used as the road input excitation:

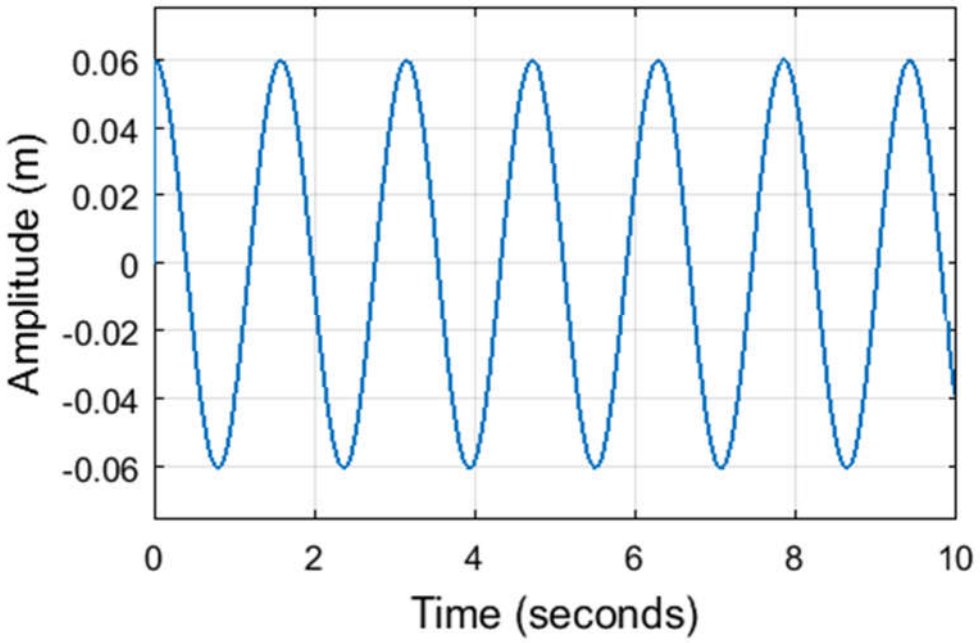

Figure 5-5 Use sin wave as the road input excitation

The vertical distance output signal is shown in Figure 5-6.

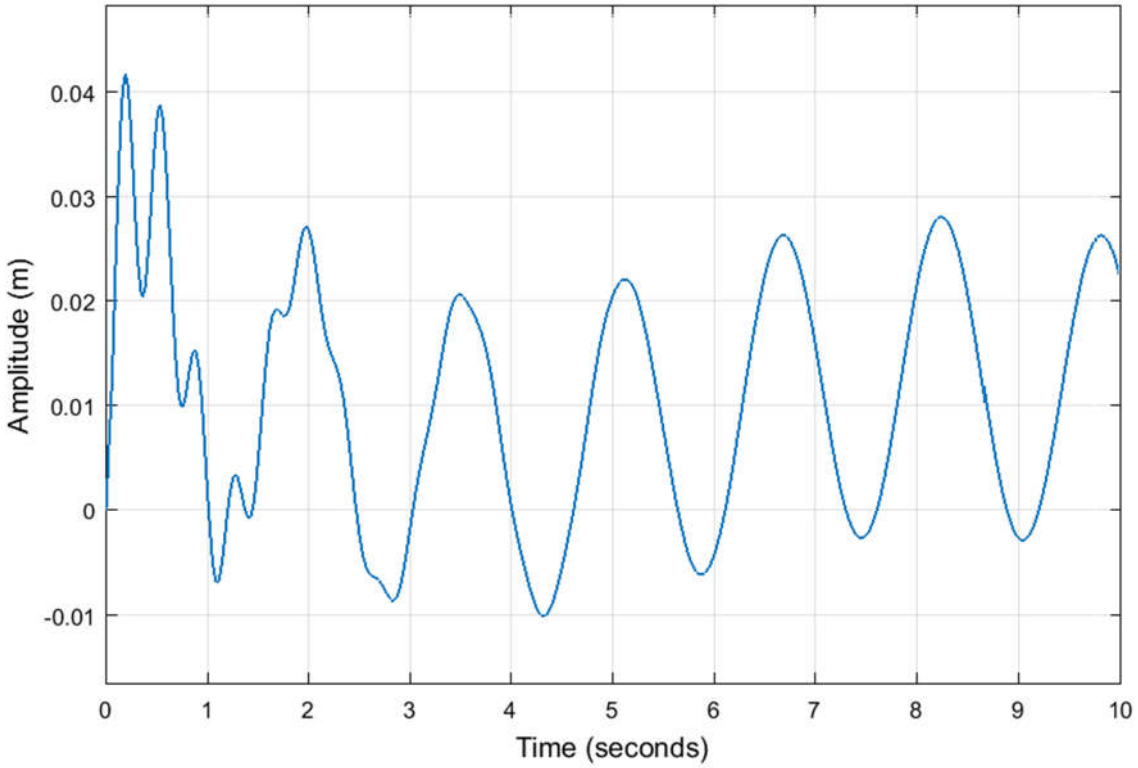

Figure 5-6 Vertical distance output wave of 4-DOF vehicle model

From Figure 5-6, it is known that the vibration of vehicle in vertical direction quickly stabilises to a fixed value.

5.1.3 7-DOFs suspension system of the whole vehicle

The system simulation model is established in MATLAB/Simulink:

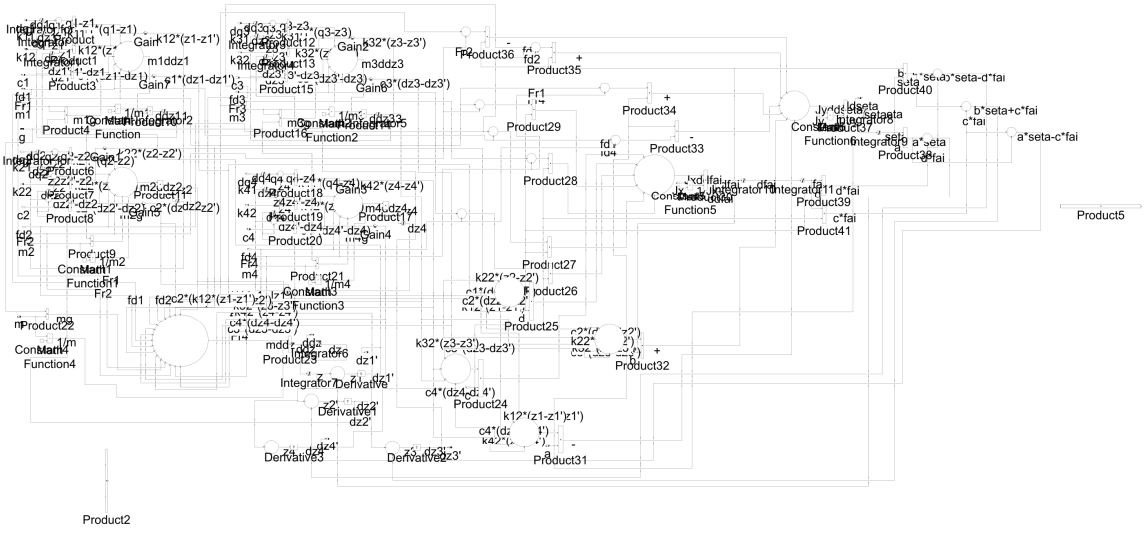

Figure 5-7 7-DOFs simulation model of suspension system of the whole vehicle in MATLAB/SIMULINK

The parameter subsystem is established as Figure 5-8 shows:

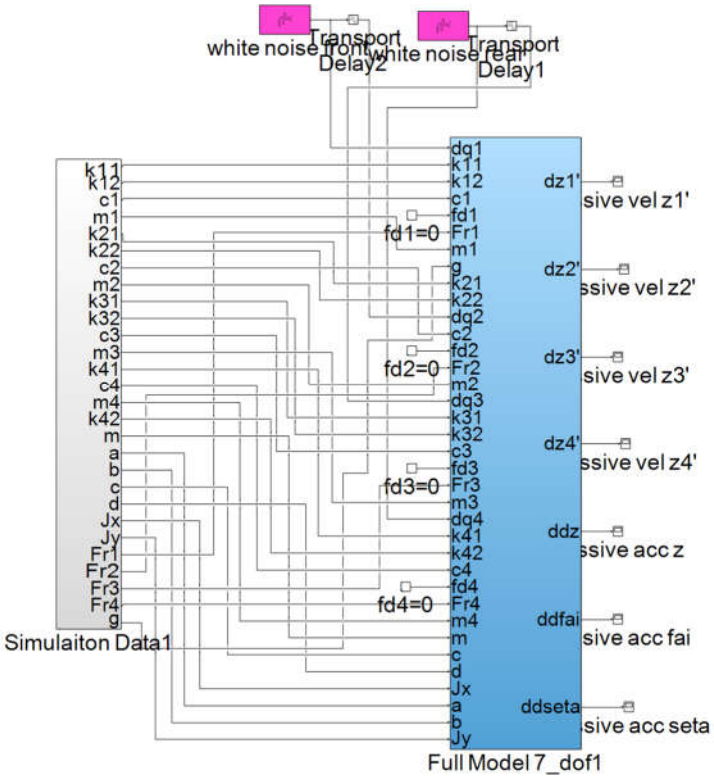

Figure 5-8 Parameter subsystem of 7-DOFs simulation model of suspension system of the

5.1.4 Simulate suspension using MATLAB/Simulink

Simdriveline is a new expansion of MATLAB Simulink, providing a complete set of analysis tool for mechanical modelling and simulation of transmission and driving system. It is an ideal tool for dynamic simulation of vehicle parts.

A sample suspension model designed in simulink using simdriveline is shown in Figure 5-9.

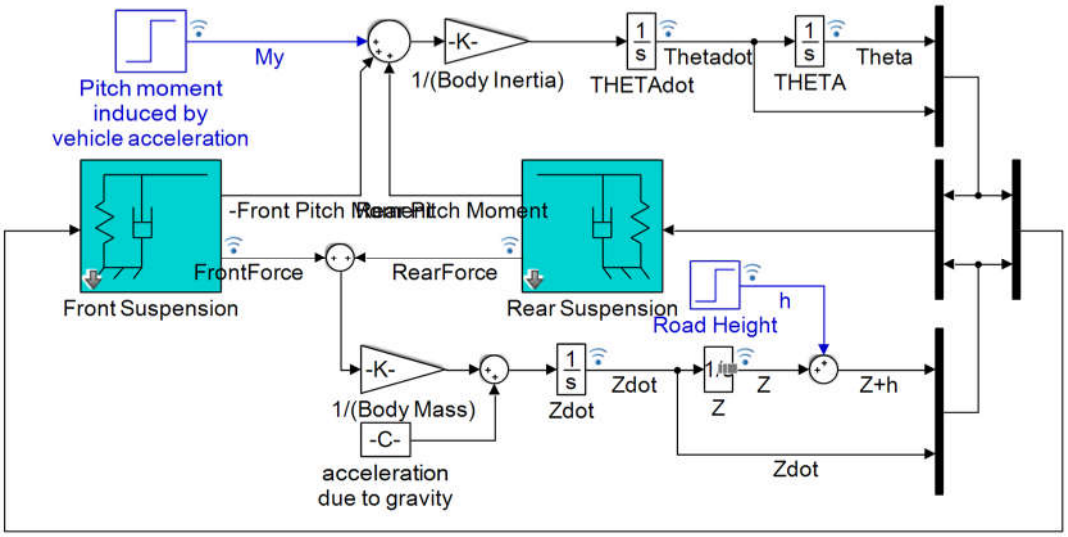

Figure 5-9 A sample suspension model designed in simulink using simdriveline

Figure 5-9 is the 1/2 vehicle model designed with simdriveline. Although this model has a concise form, it is also based on Figure 2-3 and Equation 2-2. As this model uses front suspension module and rear suspension module, which are encapsulated in simdriveline, it is impossible to open these two modules to see the detail. A module designed in this study based on the same theory is displayed in Figure 5-10.

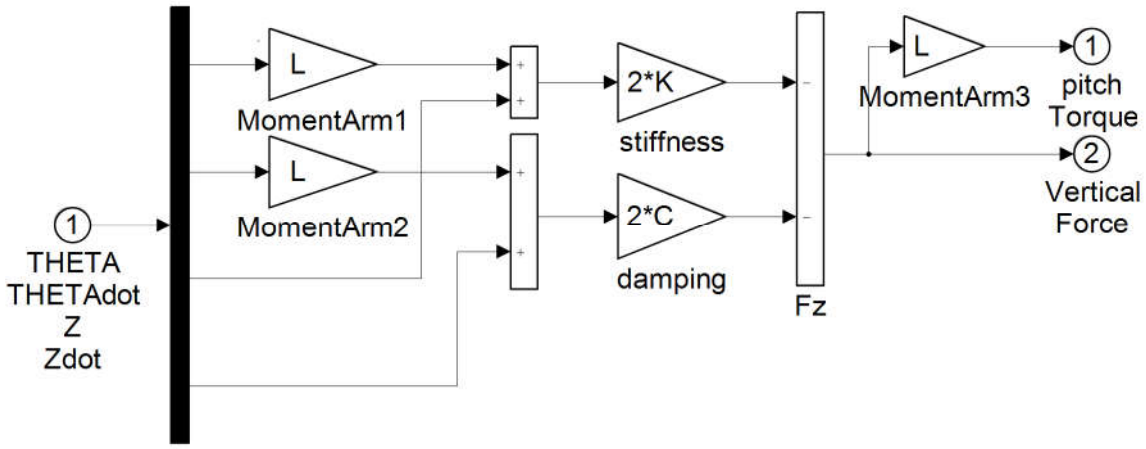

Figure 5-10 Sub-design of Figure 5-9, the front and rear suspension

According to parameters of general vehicles, default initial values are chosen as follows.

Lf = 0.9; % front hub displacement from body gravity centre (m)
Lr = 1.2; % rear hub displacement from body gravity centre (m)
Mb = 1200; % body mass (kg)
Iyy = 2100; % body moment of inertia about y-axis in (kg)
kf = 28000; % front suspension stiffness in (N/m)
kr = 21000; % rear suspension stiffness in (N/m)
cf = 2500; % front suspension damping in (N sec/m)
cr = 2000; % rear suspension damping in (N sec/m)

Focus on the Road Height input in Figure 5-11. Let it be a step input, as shown in Figure 5-11, which corresponds to vehicle driving over a road surface with a step change in height. Let the initial height of road is 0, then at time point7, the height changes to Height=0.01.

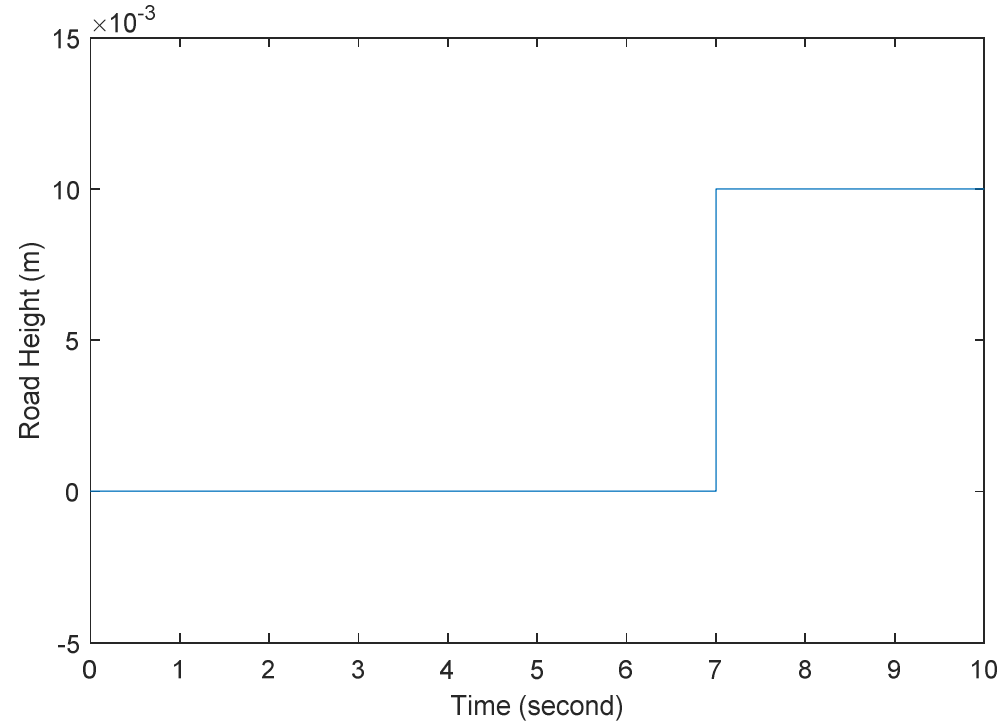

Figure 5-11 step input of road, height changes to 0.01 at time point 7

Run the designed suspension model, the vertical displacement of the vehicle body can be obtained, as Figure 5-12 shows.

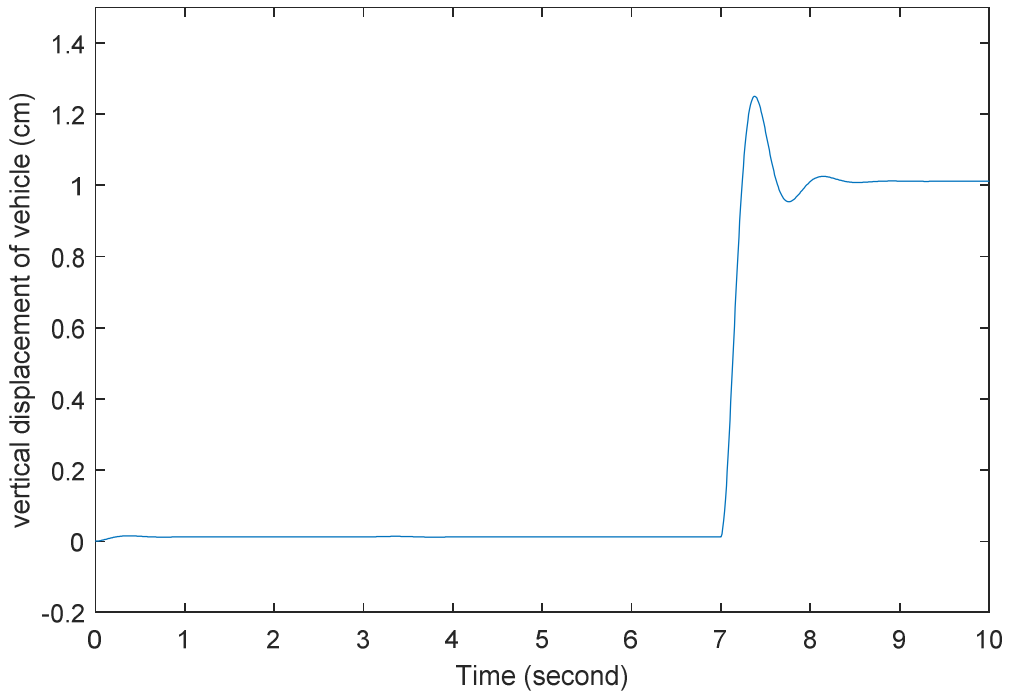

Figure 5-12 The vertical displacement of vehicle after it passes the step change of road. height=0.01m

The result shows that, the minimum value of vertical displacement is 0.12m, the maximum value is 0.1325m. Thus the vertical displacement with road height = 0.01m is 0.1325-0.12=0.0125m.

Similarly, the vertical displacement with road height of 0.02, 0.03, 0.05, 0.1 and same other starting conditions can be obtained, as shown in Table 5-1 (unit is m).

Table 5-1 vertical displacement of vehicle body with various step change of road (unit: m)

height of step change of road	minimum vertical displacement of vehicle body	maximum vertical displacement of vehicle body	displacement of vehicle body h=max-min
0.01	0.12	0.1325	0.0125
0.02	0.12	0.1449	0.0249
0.03	0.12	0.1573	0.0373
0.05	0.12	0.1821	0.0621
0.1	0.12	0.2440	0.1240

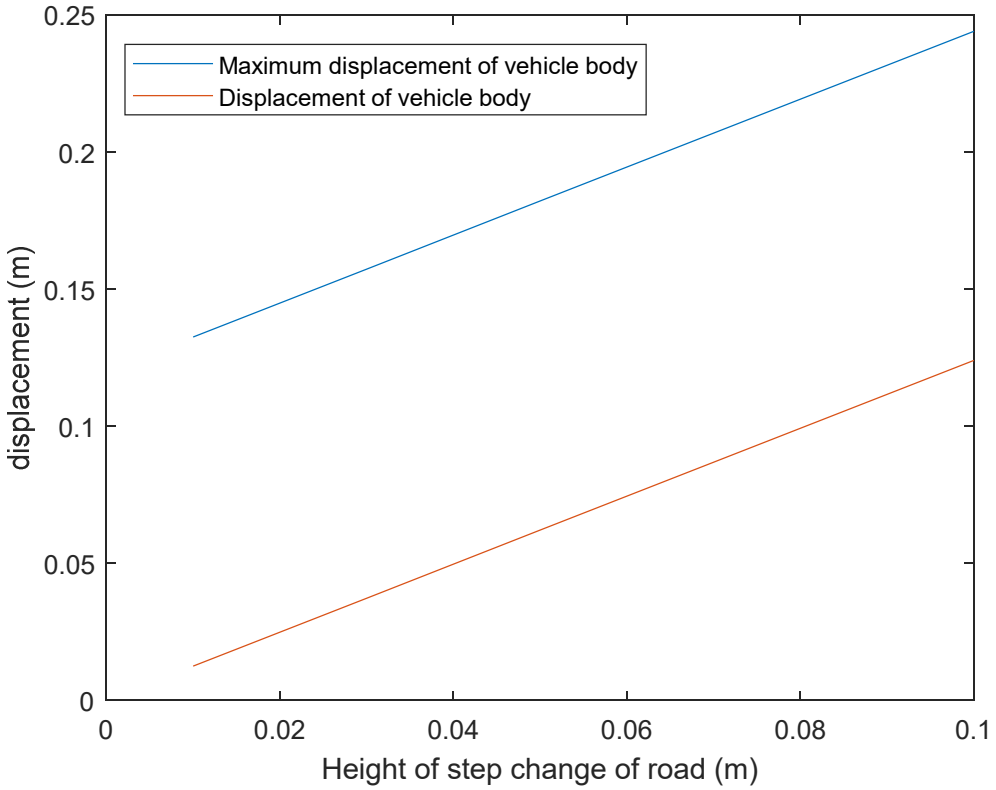

Figure 5-13 Relationship between height of step change of road, displacement of vehicle body and maximum displacement of vehicle body

From Table 5-1 and Figure 5-13 show that if we only consider the suspension system, the vertical displacement of vehicle body and the maximum displacement of vehicle body are proportional to the height of step change of road.

5.2 Tyre simulation

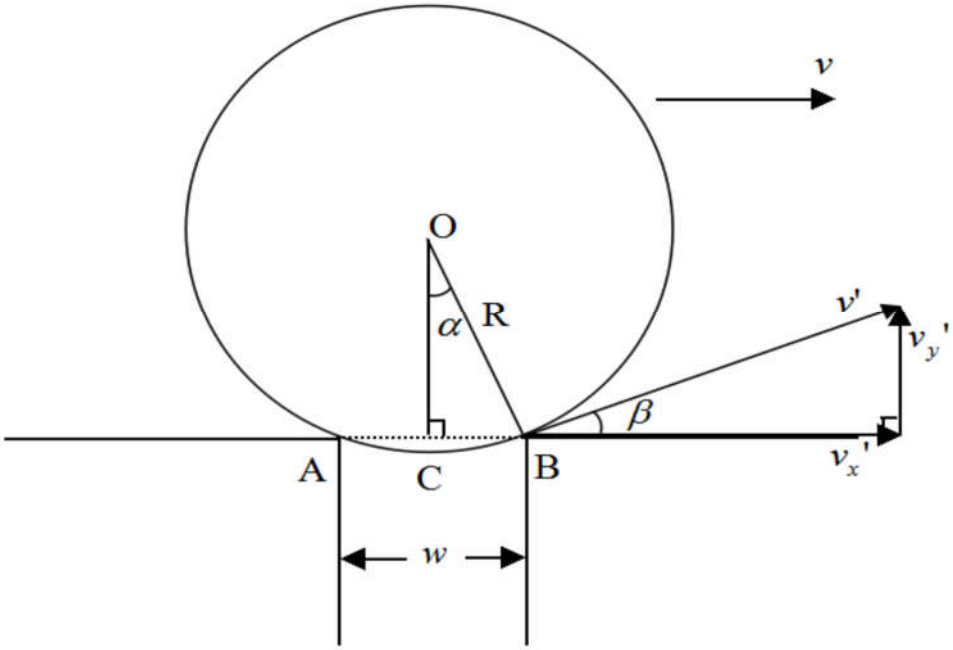

Figure 5-14 Tyre with center O passes pothole AB with width of w. The velocity of tyre before passing is v, the velocity after it bounces up from road is v' which can be decomposed to a component of v_x' horizontally, and a component of v_y' vertically.

As shown in the figure 5-13, assume the vehicle runs from left to right at the velocity of v with the tyre radius of R and the pothole width of w, when the rim of the tyre contacts the cutting edge A and trailing edge B of the pothole at the same time, collision occurs. That is to say, at this point, both A and B are on the circumference of the tyre. According to symmetry, it is known that by drawing a vertical line OC from the centre O to AB, the intersection C is located in the middle of A and B, i.e. AC=CB.

In case of taking no account of the energy loss (Wang et al., 2008), According to Appendix A, the bouncing height is

$$h = \frac{v^2 w^2}{8gR^2} \tag{5.1}$$

Based on the above formula, the gravitational acceleration g is constant, and assume the tyre radius R remains unchanged, the bouncing height is proportional to the square of velocity v, as well as to the square of the pothole width w.

Assume the vehicle running at 50mile/h, i.e. 22.35m/s, the pothole (bridge expansion joint) width w varies with the temperature change, and the width in winter and summer differs. The mean value 5cm, i.e. 0.05m is taken here; the gravitational acceleration is

taken as g=9.81; the specification of the tyre of Nissan Micra K11 used for this test, which manufactured in 1996 is 155/70R13, which means:

- 155 denotes the tyre width in mm;
- 70 denotes flatness ratio, i.e. the ratio of the tyre wall height to the tyre width and 70 representing 70%; generally, the flatness ratio ranges from 30% to 80%;
- R denotes the abbreviation of Radial, which means the tyre is of radiation layer structure;
- 13 denotes the nominal diameter of the wheel rim in inch.

The tyre's total outer diameter is the sum of the hub' outer diameter and the two tyres' wall height, therefore, the outer diameter is

$$13\times 0.0254 + 0.155\times 0.7\times 2 = 0.5472m$$

Then, the radius

$$R = \frac{0.5472}{2} = 0.2736m$$

Therefore

$$h = \frac{22.35^2\times 0.05^2}{8\times 9.81\times 0.2736^2} = 0.0582m$$

The formula above indicates that bouncing height of the tyre is approximately 5.8cm, when the vehicle contacts the pothole of 5cm in width at 50mile/h, if the loss of energy is not taken into account.

In fact, however, two principal losses should be taken into account: the energy-absorbing deformation of the tyre, and that of the vehicle caused by the shock and suspension, both of which, in essence, convert the mechanical energy into other forms of energy (such as heat energy) and then released. Therefore, the mechanical energy before and after the collision is no longer conserved.

Assume that the partial energy loss during the collision is converted into other forms of energy like heat energy, and define the consumed energy as k, and then

$$\frac{1}{2}mv_y'^2 = mgh + k \tag{5.2}$$

Namely

$$h = \frac{v^2w^2}{8gR^2} - \frac{k}{mg} \tag{5.3}$$

It is can be seen that the bouncing height is not only proportional to the square of speed and that of the width of the pothole, but also related to the mass of the vehicle and the consumed energy.

A further analysis of the process of collision is conducted as below: the collision can be divided into two steps from the tyre contacts the edge of pothole:

1. As the centre of the tyre approaches to the edge of the pothole, the tyre will deform due to depress, and in this process, the kinetic energy of the tyre converts into elastic potential energy. This process comes to its end and enters the next step after the pressure in question reaches its maximum.

2. The tyre centre starts to leave away from the pothole edge, namely, jump upward. The tyre begins to resume the deformation, and now the elastic potential energy formed by depressing in step 1 again converts into kinetic energy. The step ends with the deformation fully resumed and the separation from the pothole.

Set u' and v' as the velocities generated after the collision between ground and tyre separately, while u and v stand for that prior to the collision, then

$$C_r = \frac{u'-v'}{u-v} \tag{5.4}$$

in which Cr is Elastic Loss Coefficient of tyre. Due to the Elastic Hysteresis Loss, part of energy is lost (in the form of thermal energy) when the tyre deforms. Assume the ground is fixed, namely, the velocities before and after the collision are both 0, then,

$$C_r = \frac{u'-v'}{u-v} = \frac{v'}{v} \tag{5.5}$$

It can be see that, without energy loss, the mechanical energy is conserved and the velocities before and after the collision are equal, i.e.,

$$C_r = \frac{u'-v'}{u-v} = \frac{v'}{v} = 1 \tag{5.6}$$

Therefore

$$v' = v$$

This is the very matter of the conservation of mechanical energy without energy loss in question. Under this circumstance, the bouncing height of the tyre is proportional to the square of the velocity.

Actually, the coefficient of restitution is always smaller than 1, therefore,

$$C_r = \frac{u'-v'}{u-v} = \frac{v'}{v} < 1 \tag{5.7}$$

According to Appendix B,

$$h = \frac{v'^2 w^2}{8gR^2} = \frac{C_r^2 v^2 w^2}{8gR^2} \tag{5.8}$$

If the parameters of the vehicle and the width of the pothole are unchanged, then, w, g, R and C_r, in the formula are constants, therefore, the bouncing height h is still proportional to the square of velocity v.

The equation 5-8 shows the relationship between vehicle speed, pothole width and bounce height: when pothole width is constant, the vehicle bounce height is proportional to square of vehicle speed. When vehicle speed is constant, vehicle bounce height is proportional to square of width of pothole This shows that if vehicle bounce height and speed of vehicle are measured, the width of pothole can be calculated with Equation 5-8 (Note that "pothole" here represents a large enough pothole, on which the vehicle vibrates. That is to say, if the width of a pothole is too small, this pothole needs not to be detected, and should not be detected). In other words, to determine whether there exists a pothole, the detect vehicle bounce height needs to exceeds the threshold, the threshold setting should not be fixed, instead, it should be changed with the vehicle speed. The equation 5-8 reveals that, the threshold should be set proportional to the square of the vehicle speed. When the vehicle speed is slow then the threshold should be reduced, which can increase the detection accuracy; and when the vehicle speed is fast, the threshold increases, which can reduce the miscarriage of justice. In the previous literature, threshold values are fixed, so they got many miscarriages of justice. Equation 5-8 is used to generate speed-dependent dynamic thresholds, so the accuracy of the theoretical tests is much higher, which is proved in detection result shown in Chapter 7.

5.3 Conclusion

In this chapter, the factors of bounce height of vehicle and their relationship are studied. The suspension system and the tyre system were modelled and simulated in order to study the bounce height of vehicle. According to the equation of suspension system in Chapter2, 1/4, 1/2 and whole vehicle models are established, and then simulated by using Simulink. The conclusion is: if all other factors are unchanged, the bounce height of the vehicle has a linear relation with the height of the pothole.

Next, the corresponding formula of vehicle speed and the height of the bounce is established according to the law of conservation of energy in the simulation of tyre

system. The conclusion is: if all other factors are unchanged, vehicle bounce height has quadratic relationship with the speed of the vehicle. That leads to the conclusion that the amplitude threshold is proportional to the square of the speed of the vehicle. This conclusion will be verified in the experiments in Chapter 7.

Chapter 6. Data processing

6.1 Coordinate correction

There are three coordinate systems that are related to each other, they are mobile phone coordinate system (Figure 4-4), vehicle coordinate system (Figure 6-1) and global coordinate system (Figure 6-2), which is based on the starting point of the vehicle. In order to get the pothole data, mobile phone coordinate system need to be compared with global coordinate system. Since only the flat section is considered, vehicle coordinate system and global coordinate system are coincident. Therefore, when rotate the data in the mobile coordinate system, until it match the vehicle coordinate system, then the data can be converted into the global coordinate system, so that the position of the pothole can be obtained. This coordination transformation has nothing to do with the location information provided by GPS, but to derive the travel distance from acceleration data gathered by built-in sensor.

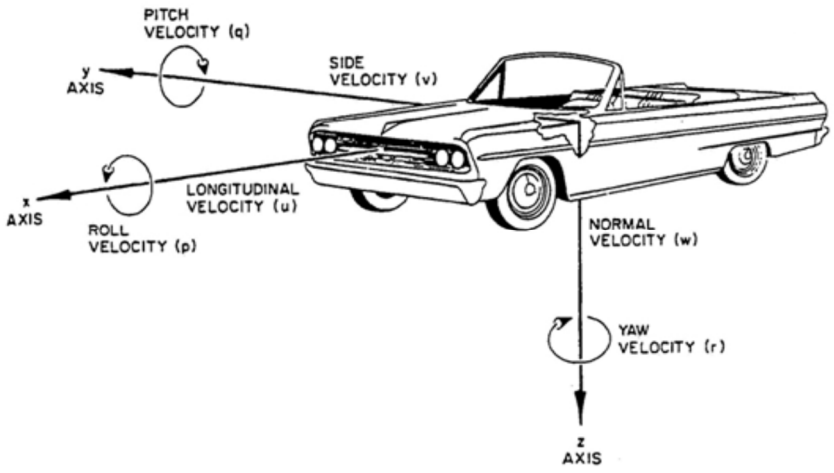

Figure 6-1 Vehicle coordinate system

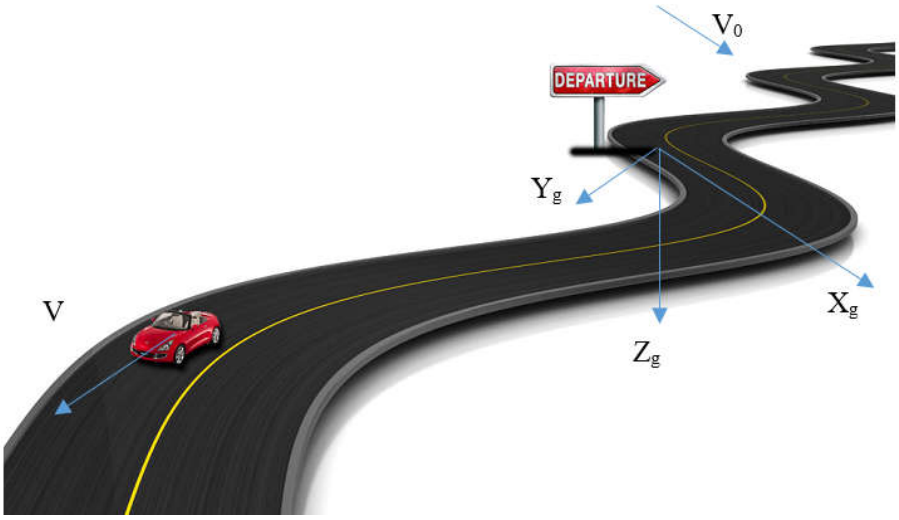

Figure 6-2 Nature coordinate system

The built-in sensors have their own three-dimensional coordinate system. The output data of sensor that has directions, such as acceleration, is represented in the sensor's own coordinate systems, which is called sensor coordinate system. The sensor coordinate system has X, Y and Z axis that are orthometric. The vehicle, on the other hand, has its own three-dimensional coordinate system: the X-axis is the direction of vehicle movement, Y-axis is the right-hand side of vehicle, and Z-axis is vertical to the chassis and pointing down. There is another (three-dimensional) coordinate system, which is called natural coordinate system. When vehicle is in uniform linear motion on a horizontal road, at one time point the vehicle coordinate system is considered as the natural coordinate system. Thus the X-axis of natural coordinate system is the direction of vehicle at the point it is set, the Y-axis is the right-hand side of vehicle, and Z-axis is the direction of gravity.

Note that:

1 The smartphone is fixed on the centre console, facing the rear window or the driver's seat and slightly upward sloping. Thus the sensor coordinate system cannot overlap with vehicle coordinate system;

2 Consider the smartphone and vehicle are rigid connected, the angle between sensor coordinate system and vehicle have can be considered as fixed;

3 Natural coordinate system never changes after it is set, while the vehicle coordinate system moves together with vehicle;

4 As in all my experiments, the vehicles are in uniform linear motion, the vehicle coordinate system is considered overlapped with natural coordinate system.

The pothole is in natural coordinate system, but the data from sensor is in sensor coordinate system. As the natural coordinate system is considered overlapped with vehicle coordinate system, the data from sensor should be rotated by the angle between sensor coordinate system and vehicle coordinate system.

The data can be processed according to the direction of gravity. Because no matter where is the smartphone is fixed or the angle, the direction of gravity is always the Z-axis of natural coordinate system. Hence the data from the acceleration sensor are added together in vector form, which is:

$$Z^2 = x^2 + y^2 + z^2 \tag{6.1}$$

In equation 6-1, Z is the vector of gravity (including its direction and size), on the same direction of Z-axis of natural coordinate system (vertical to the horizontal plane, pointing downward); x, y and z are the acceleration on X, Y and Z-axis of the sensor coordinate system. So:

$$Z = \sqrt{x^2 + y^2 + z^2} \tag{6.2}$$

But this transform method requires the vehicle to be in uniform linear motion. Once there is jolt (can be considered as noise in the field of Signal Process), there will be error in the value and direction of gravity.

So actually the data is transformed using principal component analysis (PCA). PCA is a processing method with linear transformation of multiple variables for data analysis and mathematical model establishment. It is invented by Karl Pearson in 1901. In the practical research, many relevant variables are chosen to be studied to comprehensively analyse the problem, in which each variable reflects information in some certain aspects of the result. The main function of PCA is to select important variables from multiple ones.

PCA gain the principle component by conducting eigen decomposition to the covariance matrix. The result of PCA is the eigen vector and eigen value. The mathematical definition of PCA is: an orthogonalization linear transformation in which the data is transformed from an old coordinate to a new coordinate system, making the variable with largest variance of any projection be on the first axis (also called as the first principle component) and the second variance on the second axis (also called as the second principle component), and so forth.

Define an n*m matrix, X^T is the average value (move to the original point from the centre of the average value), the row is data sample and the column is data category

(attention: the definition is for X^T not X). So the singular value decomposition of X is $X = W\Sigma V^T$, in which the matrix W with the size of m*m is the eigen vector matrix of XX^T, with the size of m*n is a nonnegative rectangle diagonal matrix, V with the size of n*n is the eigen vector matrix of X^TX. According to Appendix C,

$$XX^T = W\sum\sum{}^T W^T \tag{6.3}$$

Given a set of points in Euclidean space, the first principal component is corresponding to the line through equalization point of multi-dimensional space, ensuring the quadratic sum of the distance between each point and this line is minimal. After removing the first principle component, get the second one with the same manner, and so forth. Providing an effective method to reduce the dimension, PCA is often used to reduce the dimension of dataset and keep the largest contribution of dataset to the variance. This is achieved by keeping lower-dimensional components and ignoring higher-order components, thus the lower- dimensional components can keep the major aspects of the data.

As previously discussed, when the smartphone is fixed in the vehicle, the three axes of sensor coordinate system will form an angle with that of the vehicle coordinate system. When the vehicle stands still or is in uniform linear motion, because of the gravity, there is acceleration along Z-axis of the vehicle coordinate system with value of *g*, and in the X and Y axes the acceleration should be zero. However, in practice, the three axes are all affected by the vibration caused by the vehicle body, which is usually random noise signal. So on the Z-axis of vehicle coordinate system, the acceleration value is the sum of gravity *g* and noise signals. Generally, the acceleration of gravity is far more than that of the noise signals, while there is only noise signals on the other two axes. As the three axes are vertical to each other, they are not interrelated. On the other hand, because components of results of PCA are orthometric (which mean they do not related to each other), it can be used to do the coordinate correction of acceleration data. From the above discussion we can see that after PCA processing, the correlation between 3 data sets was eliminated. In the original data sets collected by the sensor, since the three axes of the sensor are not completely match with the nature coordinate system, data of the three axes collected by the sensor acquisition have some correlation. In other words, if there is a signal in the Z' axis direction of the nature coordinate system, then it will be shown in the X, Y, Z triaxial data of the sensor. Our aim is to rotate the coordinates so that in the final result, the signal is only shown on the Z axis, and the

other two axes have a signal amplitude of 0, that is, to eliminate the correlation between the three axes. PCA's function is through a conversion, transfer a group of coordinates to another group of coordinate system, but in the new coordinate system, X, Y, Z components are not related.

Generally, to make sure the minimum mean-squared error of approximate data is found, zero mean processing shall be done to the data before PCA. But in my study, the direction of gravity is the first principle component, and the mean value is necessary to find the direction of gravity. Therefore the zero mean pre-processing shall not be conducted, otherwise the result will be false.

As the vehicle is assumed to be in uniform linear motion, the vehicle coordinate system is overlapped with natural coordinate system. The vibration of vehicle should only happen on Z-axis and is irrelevant to X or Y axes (which are corresponding to the left-right steering and braking/accelerating respectively), only the first principle (the acceleration in Z-axis) is needed.

With the above methods, the data is transformed to the natural coordinate system, which makes subsequent process and analysis easier.

6.2 Convert Acceleration Data into Distance

The data obtained by the acceleration sensor is the acceleration of the smartphone, and because the smartphone is fixed on the vehicle, the acceleration can be considered as of vehicle as well. Because the displacement on the vertical direction (along or opposite the direction of Z-axis) happens on potholes, the position of each vertical displacement is the position of each pothole. Thus my aim is to obtain the displacement data of the vehicle, which is ΔZ. The sampling frequency (100 or 200Hz, which depends on the detection device) is fixed during the sampling process. Theoretically, speed value can be obtained through a single integration of acceleration data, and the displacement value can be obtained through a single integration of speed.

In practice these two integrations may be done in the time-domain or frequency-domain methods.

6.2.1 Time domain integral method

Time-domain integration is a way to obtain the displacement signal directly from acceleration signal by quadratic integral. Normally trapezoid formula or Simpson summation formula is used because of their intuitive form. However, the acceleration

signal measured in the experiment actually contains noise and DC component, so the result will contain trend term if the signal is integrated directly.

Let the acceleration signal be $a = f(t) + T$, in which T is the measurement error, then Simpson integral is used (See Appendix D for full details):

$$v = \frac{\Delta t}{6} \sum_{i=2}^{N} (a'_{i-2} + 4a'_{i-1} + a'_i) \tag{6.4}$$

In the equation 6.4, the symbol Δt means sampling interval, and the symbol v means the signal sequence obtained after a single integral.

6.2.2 Frequency domain integral method

According to Appendix E, Fourier transform of displacement can be obtained after the second integral:

$$S(n) = -\frac{1}{k^2} A = \sum_{k=0}^{N-1} \frac{1}{-(2\pi k \Delta f)^2} H(k) a_n e^{-i2\pi k \frac{n}{N}} \tag{6.5}$$

Where

$$H(k) = \begin{cases} 1, f_d \le kf \le f_u \\ 0, else \end{cases}$$

In equation 6.5, symbol Δf is frequency resolution, and f_d and f_u are the upper and lower limits of cut-off frequency respectively. N is number of points in data, and k is the frequency of Fourier component.

Velocity and displacement signal can be obtained by processing Fourier inverse transform to equation 6.4 and 6.5. This shows that, frequency-domain integral directly employs relationship (phase swap) of sine and cosine integrals in the frequency domain, which effectively avoids accumulation or amplifying effect on the small error of time-domain signal in the process of integral, and makes the results more accurate (Ribeiro et al., 2002). However, note that low-frequency signal has corresponding smaller k, and the denominator is larger in the equation 6.4 and 6.5. Considering the low precision of the acceleration sensor for the low frequency signal, small measurement error will cause large calculation deviation, so the low frequency signal is an important source of error of frequency- domain integral.

6.2.3 Discussion

In order to validate the method of the above two integral methods, assume that an acceleration signal is

$$a = 3\times\sin(2\pi\times30\times t)+2\times\sin(2\pi\times8\times t)+0.02 \tag{6.6}$$

The sampling rate is 260Hz and sampling time is 2.25 seconds.

In equation 6-15, constant value 0.02 is used to represent a small DC component. The curve of 6-15 is shown in Figure 6-3.

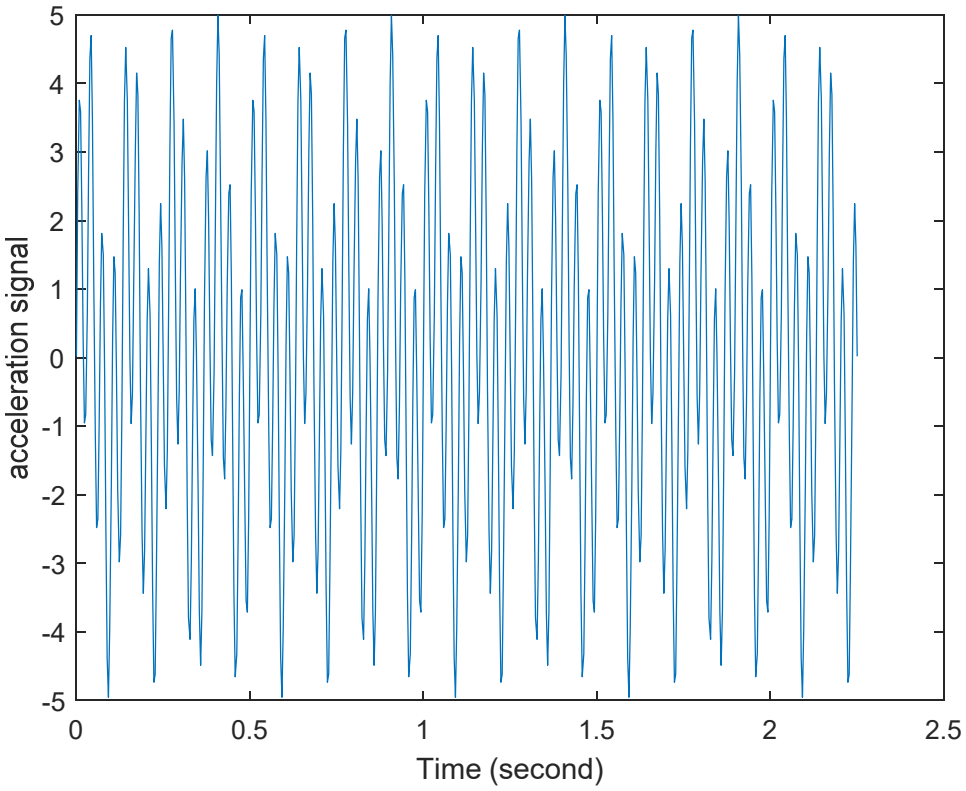

Figure 6-3 Image of equation 6-15

Integrate 6-15

$$\begin{aligned} A &= \int a\,dt \\ &= \int (3\times\sin(2\pi\times30\times t)+2\times\sin(2\pi\times8\times t)+0.02)\,dt \\ &= -\frac{\cos(60\times\pi\times t)}{20\times\pi}-\frac{\cos(16\times\pi\times t)}{8\times\pi}+\frac{t}{50}+C \end{aligned} \tag{6.7}$$

Let C=0, the result of single integration is shown in Figure 6-4.

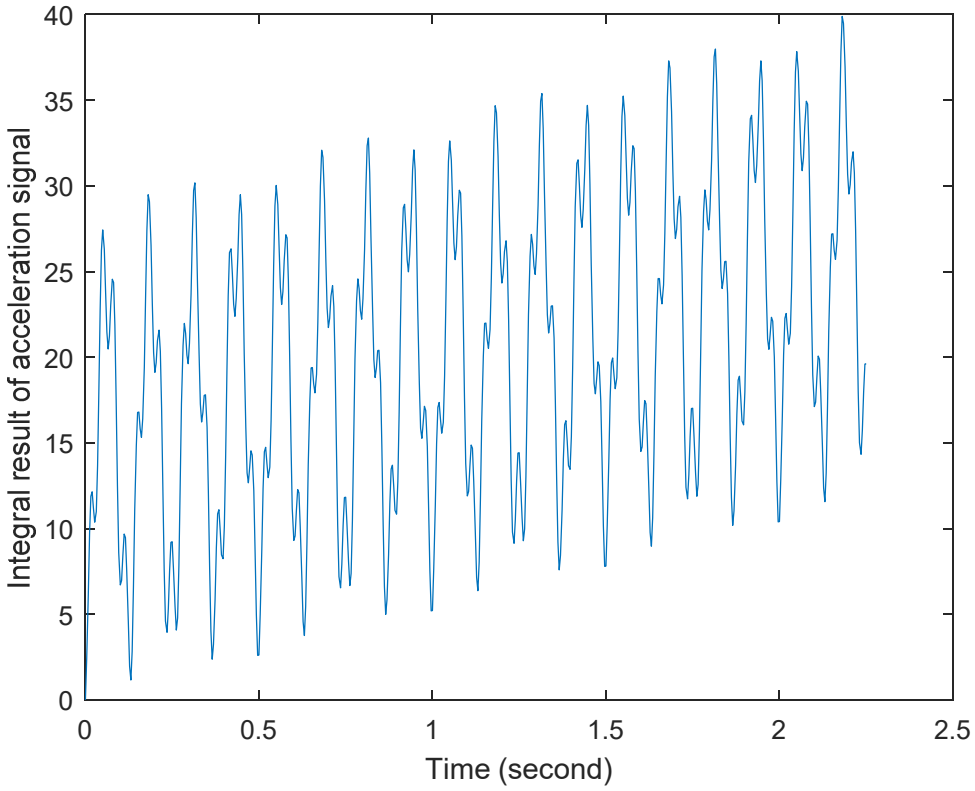

Figure 6-4 Integral result of equation 6-15

Figure 6-2 shows that, the constant value in original function results a linear component in the result of single integration, and the result has a positive offset.

Integrate 6-16 and the second integration is shown in equation 6-17

$$\begin{aligned} A' &= \int A dt \\ &= \int \left(-\frac{\cos(60\times\pi\times t)}{20\times\pi} - \frac{\cos(16\times\pi\times t)}{8\times\pi} + \frac{t}{50}\right) dt \\ &= -\frac{\sin(60\times\pi\times t)}{1200\times\pi^2} - \frac{\sin(16\times\pi\times t)}{128\times\pi^2} + \frac{t^2}{100} + C' \end{aligned} \tag{6.8}$$

Let $C = 0$, the result of second integration is shown in Figure 6-5.

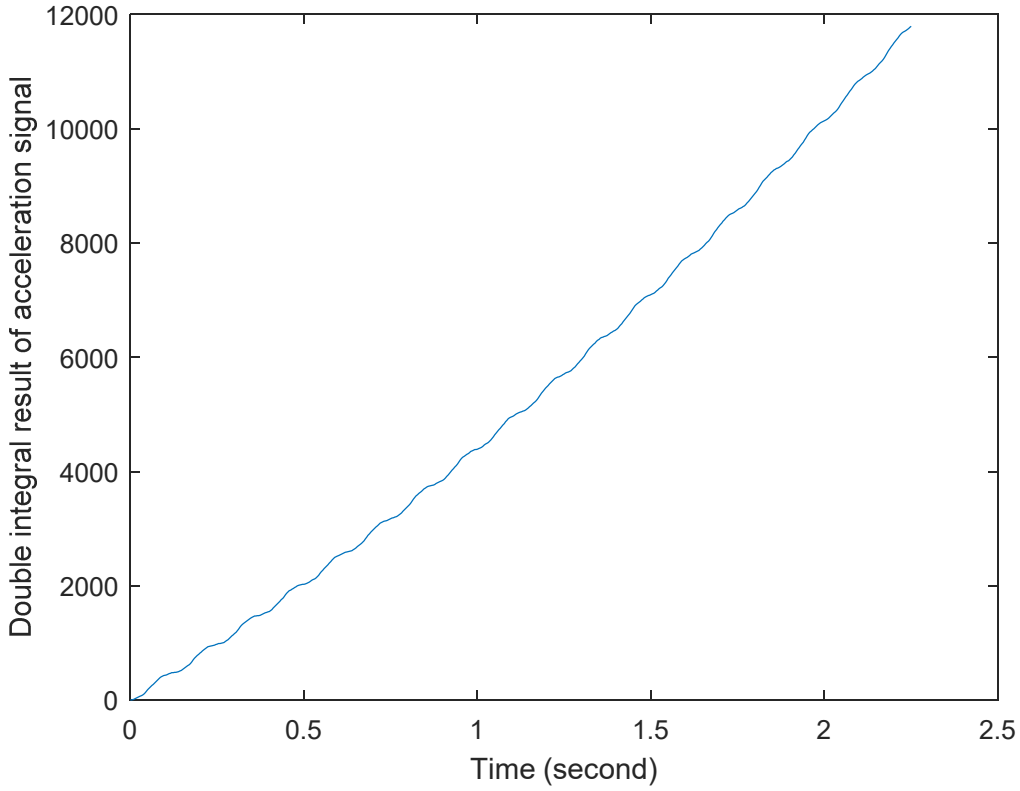

Figure 6-5 Double integral result of equation 6-15

Figure 6-5 shows that, the quadratic term adds a significant offset to the integration result. This significant offset is caused by the minor DC component in the original function. Without the DC component the result of single integration is shown in Figure 6-6.

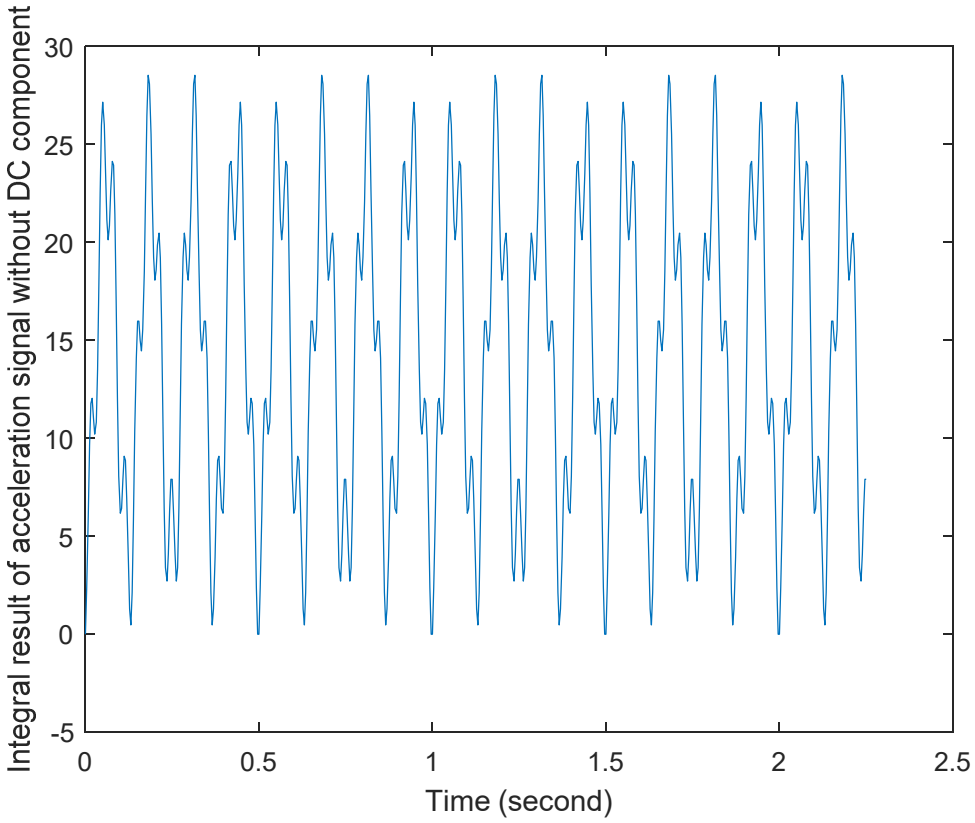

Figure 6-6 Integral result of equation 6-15 without DC component

The result of second integration is shown in Figure 6-7.

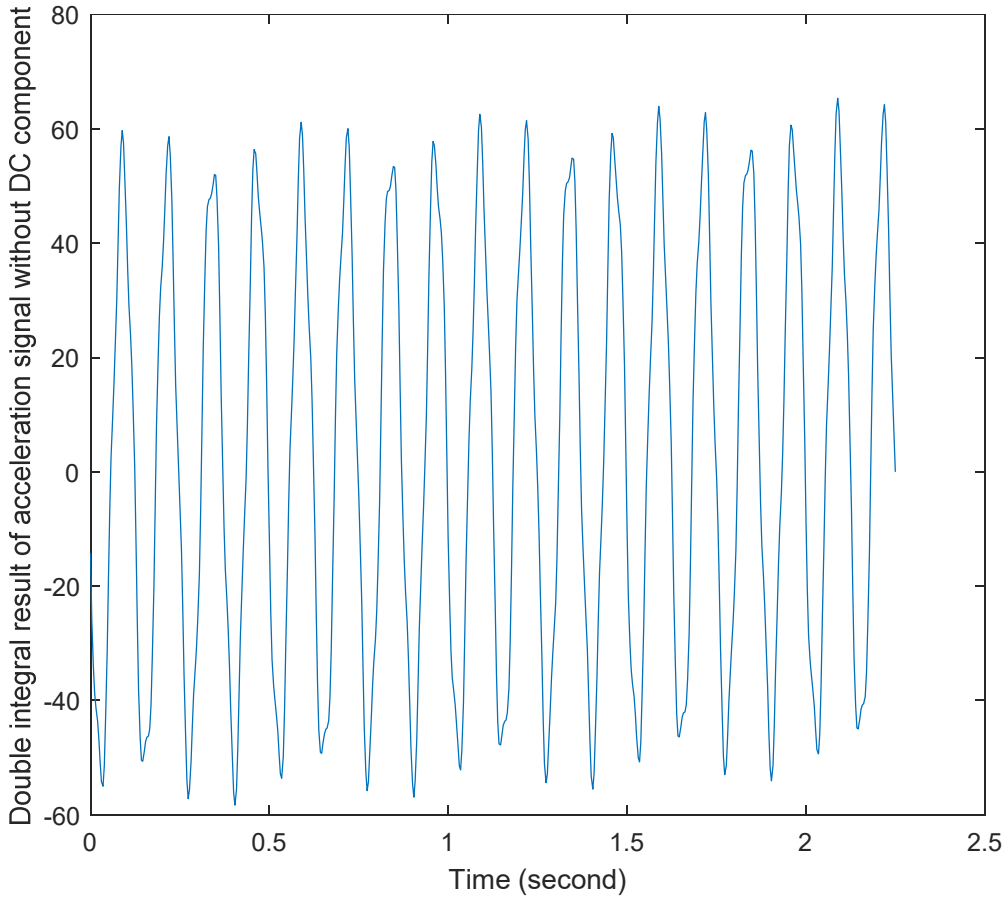

Figure 6-7 Second integral result of equation 6-15 without DC component

Both Figure 6-6 and 6-7 show a signal without offset, which is the type of result needed for this study. This case study shows the importance of DC component removal. Next, the single and second integration is done to the same signal in time-domain and frequency-domain. By comparing the result, it is known that which method is better. As shown in Figure 6-8, the result of single integration in frequency-domain does not contain offset.

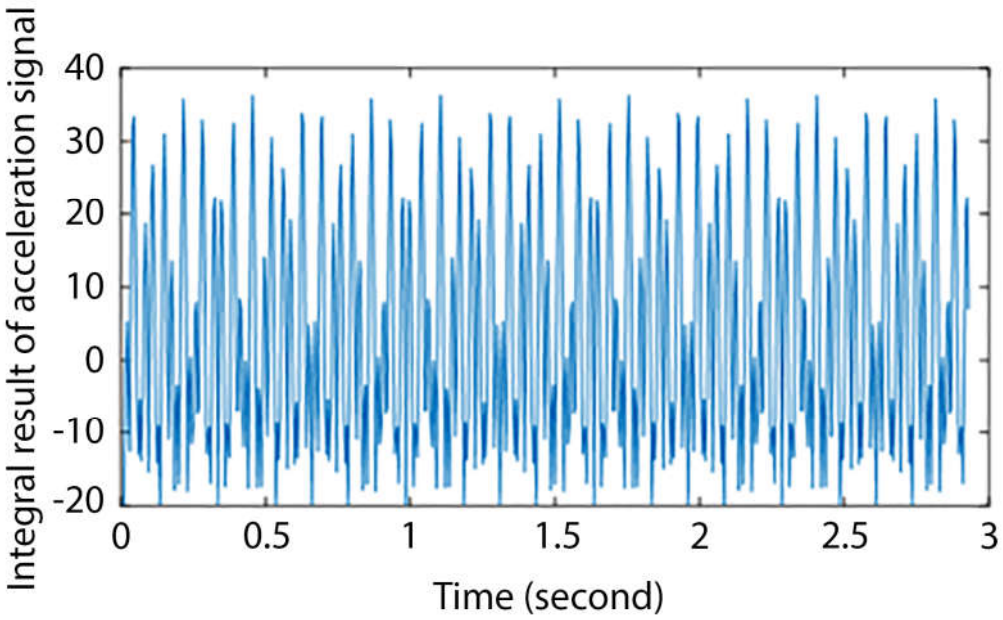

Figure 6-8 Integral result of equation 6-15 using frequency domain method

As shown in Figure 6-9, the result of second integration in frequency-domain does not contain offset either.

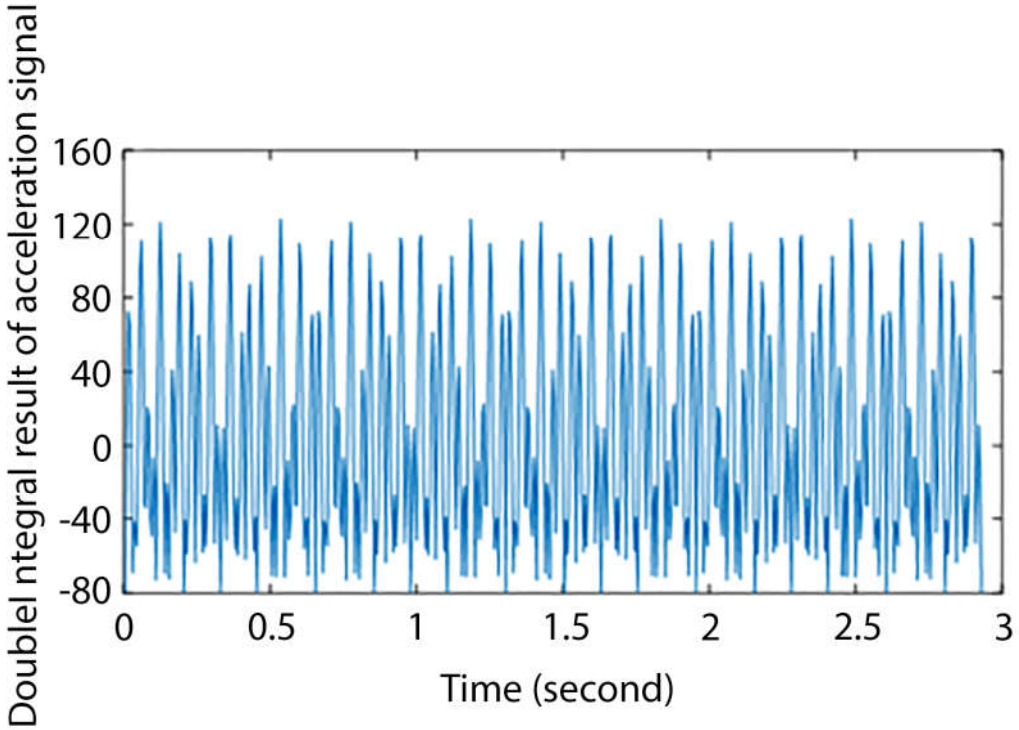

Figure 6-9 Second integral result of equation 6-15 using frequency domain method

Because the process of frequency-domain integration removes the DC component, it does not introduce offset even in second integration, which is good for the follow up processes of data.

In order to determine the accuracy of the two integration algorithms, we need to evaluate the error. In general, there are three kinds of error evaluation indicators (Jiang et al., 2009): average peak error, average maximum relative error and square sum error. The average peak error is the mean value of the positive and negative peaks of the integral displacement time course X(t) relation to the measured displacement time S(t) positive and negative peaks, respectively,

$$\mathrm{Erp} = \frac{1}{2} \times \left\{ \frac{|\max[X(t)] - \max[S(t)]|}{\max[S(t)]} + \frac{|\min[X(t)] - \min[S(t)]|}{\min[S(t)]} \right\} \tag{6.9}$$

The mean maximum relative error is the mean value of the positive and negative peaks of the relative error time course [X(t)-S(t)] relation to S(t) positive and negative peaks, respectively:

$$\mathrm{Err} = \frac{|\max[X(t) - S(t)]|}{\max[S(t)]} + \frac{|\min[X(t) - S(t)]|}{\min[S(t)]} \tag{6.10}$$

"Square and Error" describes the energy difference between the integral and the measured displacement:

$$\mathrm{Ersq} = \frac{\sum_{i=1}^{N}[x(i)]^2 - \sum_{i=1}^{N}[S(i)]^2}{\sum_{i=1}^{N}[S(i)]^2} \tag{6.11}$$

Where x(i) and S(i) are the displacement samples of X(t), S(t), and N is the number of sampling points of the signal.

The reason of the usage of the squard error is that, the peaks of two waveforms may not always appear at the same time. Thus the overall effect of the waveforms, i.e. the energy difference of the waveforms, should be examined.

There are 585 sample points in total. For each sample point, the integration is subtracted by theoretical estimation, the result is error. Error obtained by calculating two integral methods respectively as shown in the table 6-1:

Table 6-1 Error obtained by calculating two integral methods

	The average peak error (Erp) /%	The average maximum relative error (Err)/ %	quadratic sum error (Ersq) /%
An integral of time domain	23.18	113.46	180.33
An integral of frequency domain	0.12	0.41	1.01
Second integral of time domain	354.8	565.24	673.28
Second integral of frequency domain	0.01	0.12	0.43

According to Table 6-1, time domain integration introduces offset which becomes more obvious with the increase of time of integration. On the one hand, the estimation of DC component contains bias, because the signal is not integer-period sampled. On the other hand, constant term occurs after the time domain integral, which cause the offset in the result. In actual experiment, it is hard to conduct integral-period sampling, because the signal contains many frequency components. Although the error of the DC component estimation can be reduced by increasing sampling time, tiny error still can lead to a major offset. It can be seen from the Table 6-1, that result has been distorted in the second integral with time-domain integration, therefore the calculation is useless.

6.3 De-noising

Influenced by outside interference or artificial operation, the collected data inevitably contains large amounts of interference signal, and is deviated from the real value. An important task of digital signal processing is to reduce or eliminate the interference factors and remove the high-frequency noise in the collected data, so that the processed data is as close to its true value as possible.

The principles of de-noise are: (1) Smoothness: de-noised signal should have the same smoothness with the original signal; (2) Similarity: variance of de-noised signal and original signal should be as small as possible.

A model of a one-dimensional signal containing noise can be expressed as the following equation:

$$s(t) = f(t) + \sigma \cdot e(t) \qquad t = 0,...,n-1 \tag{6.12}$$

In the equation 6-18, $f(t)$ is the real signal, $e(t)$ is the noise, σ is the strength of noise, and $s(t)$ is the signal containing noise. De-noise of signal $s(t)$ is to eliminate the noise section in the signal and recover the real signal $f(t)$ from $s(t)$. In practical applications, the useful signals often manifest as low-frequency signals or stable signals, while the noise signal usually manifests as high-frequency signal. Therefore, the de-noise process can be done in accordance with the following methods: First, decompose into low-frequency part and high-frequency part. The noise is often included in the high-frequency part. Thus the high-frequency part is to decrease its amplitude. Finally, the signal is reconstructed. $\sigma \cdot e(t)$ is the noise section need to be eliminated in the signal and recover the real signal $f(t)$ from $s(t)$.

6.3.1 FFT

Fast Fourier transform (FFT) is a fast algorithm of discrete Fourier transform (DFT). Fast Fourier Transform (FFT) improves the computation efficiency by using the periodicity and symmetry of W_N factor. FFT algorithm can be basically divided into two categories: Decimation-in-time, (DIT) and Decimation-in-frequency (DIF). For full details please refer to Appendix F.

In the de-noise process of the signal, as Fourier analysis is a way to analyse signals in the frequency domain, any sudden change of the signal on the timeline will affect the entire spectrum of the signal, so that it cannot show the change of signal at a certain time point. In some cases, the target frequency exists not only in low frequency part of the raw data, but also in high frequency part. In these cases, if the original signal has high frequency in its initial stage, after being transformed by FFT, high-frequency components is filtered out when the low-pass filtering is added, , which means the useful signal is lost. This is the disadvantage of FFT as de-noise method.

A case-study is shown here, in which a cosine signal containing noise is de-noised by using FFT. The cosine signal (without noise) is:

$$x(t) = \cos(2\pi t)$$

Represented by MATLAB:

```
t=0:0.001:2;

x=cos(2*pi*t);
```

The waveform of this signal is shown in the Figure 6-12:

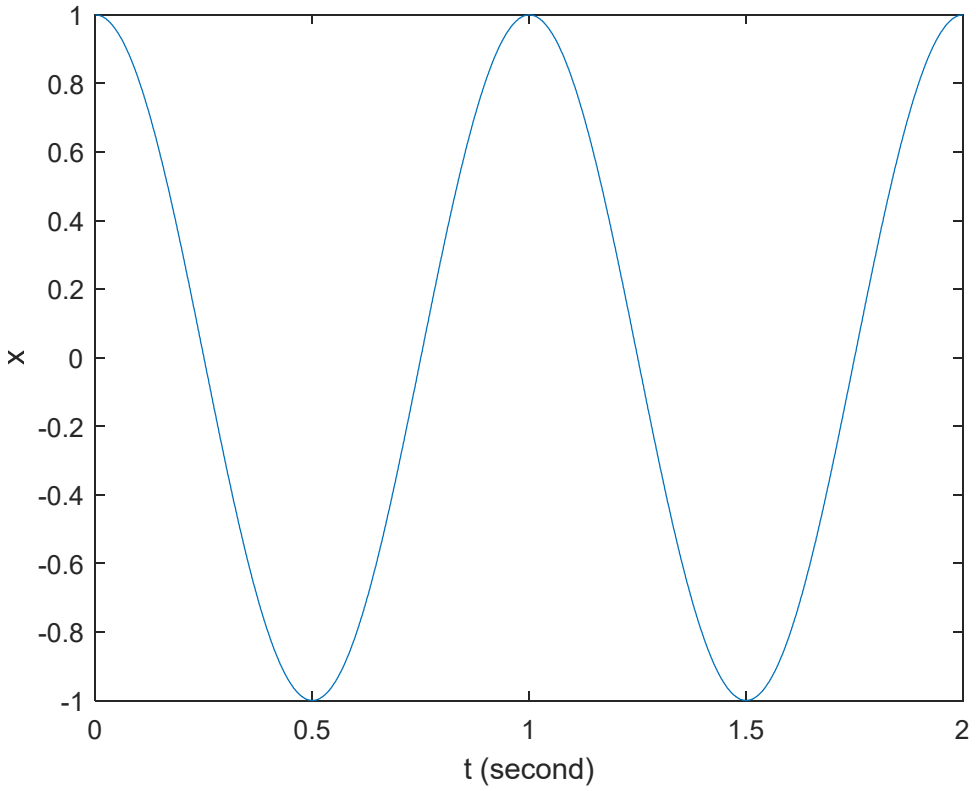

Figure 6-10 Original input signal

A random noise is added to the cosine signal:

f=x+0.25*randn(1,2001);

The waveform of signal with noise is shown in the Figure 6-13:

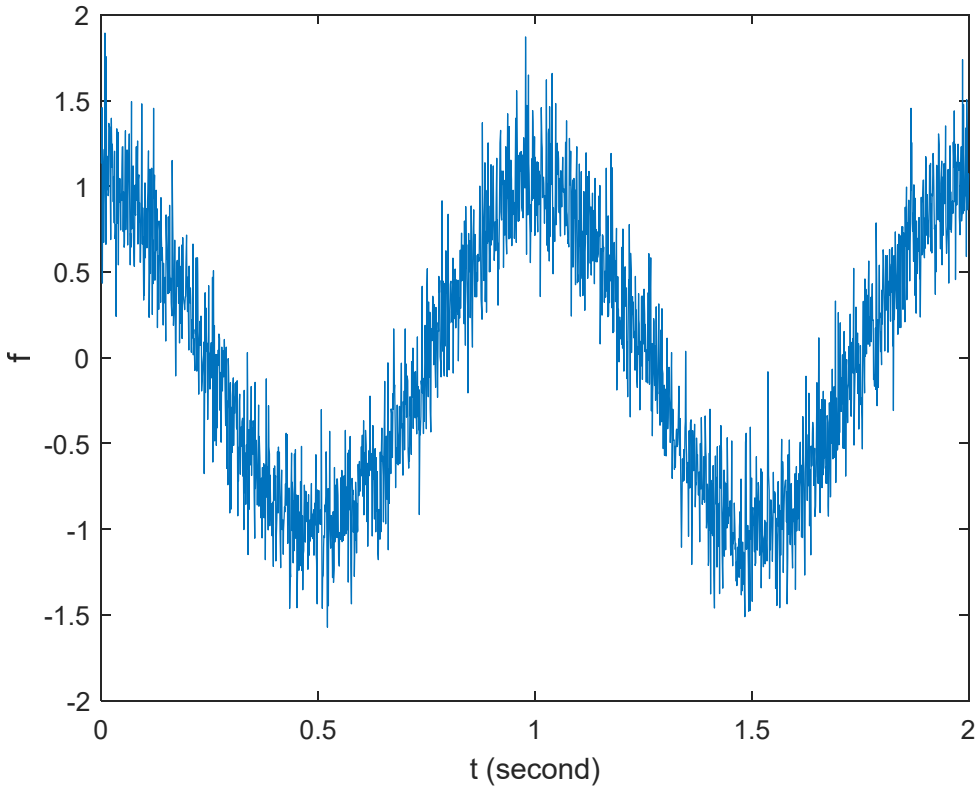

Figure 6-11 Input signal with random noise

The signal shown in Figure 6-13 is composed by low-frequency cosine signal and high-frequency random noise. The basic method of signal de-noise is to suppress the high-frequency section of signal and reserve the low-frequency signal.

The FFT process can be divided into the following steps:

1) Perform FFT computation on signal;

2) Suppress noise section of the signal according to the spectrum;

3) Obtain de-noised signal by implementing Fourier inverse transformation to the transformed spectrum.

In this signal, cosine signal is f(t), de-noised signal is g(t), the Fourier transform of f(t) is $F(\omega)$, similarly the Fourier transform of g(t) is $G(\omega)$. Then the process can be represented as:

$$G(\omega) = H(\omega) \cdot F(\omega)$$

$H(\omega)$ is the system frequency response of low-pass filter. When used to filter high frequency, typical $H(\omega)$ is in form of a step function in frequency domain. The value of step function $H(\omega)$ is 1 for all frequencies lower than the cutoff frequency, and it is 0 for all frequency higher than the cutoff frequency. When the Fourier

Transformation of input signal $F(\omega)$ is multiplied by $H(\omega)$, the high frequency part of $F(\omega)$ becomes 0. In this way the high frequency part of $F(\omega)$ is filtered, and $F(\omega)$ only contains low frequency part.

The FFT noise reduction processing procedure in MATLAB is as Appendix G. The result of FFT de-noise is shown in Figure 6-14:

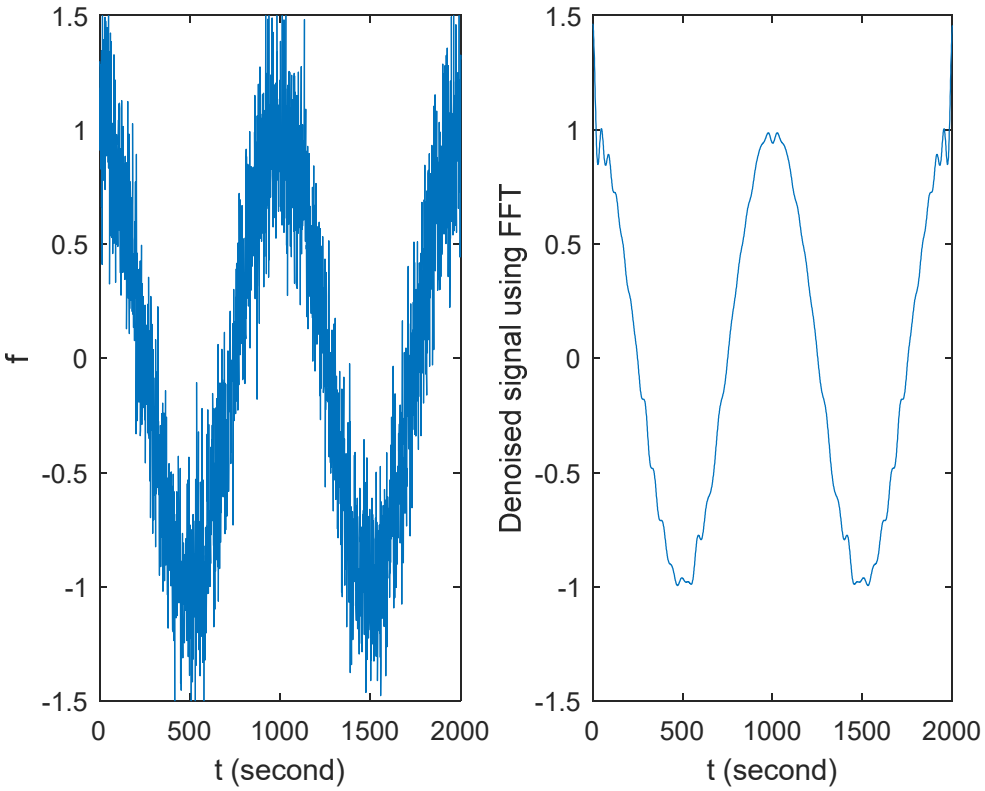

Figure 6-12 Noise reduction result

Figure 6-14 shows that the noise is significantly reduced, while the useful signal is kept. However there is still noise at peak and valley of cosine signal.

6.3.2 Wavelet de-noise

6.3.2.1 Application of wavelet

The deduction process of wavelet is in Appendix H.

6.3.2.2 Applying wavelets to reduce noise for signal.

Noise reduction is one of main applications of wavelets analysis in signal processing. Among orthogonal wavelet, as the selection of orthogonal basis is closer to practical signal itself than conventional approach, it is possible to separate noise easily through wavelets transform. The shortcoming of traditional noise-falling method is that it will

increase entropy deduced after signal transformation resulting in non-stationary property of signal can't be described.

Steps in the process of one-dimensional signal reduces noise by using wavelets are illustrated as shown below:

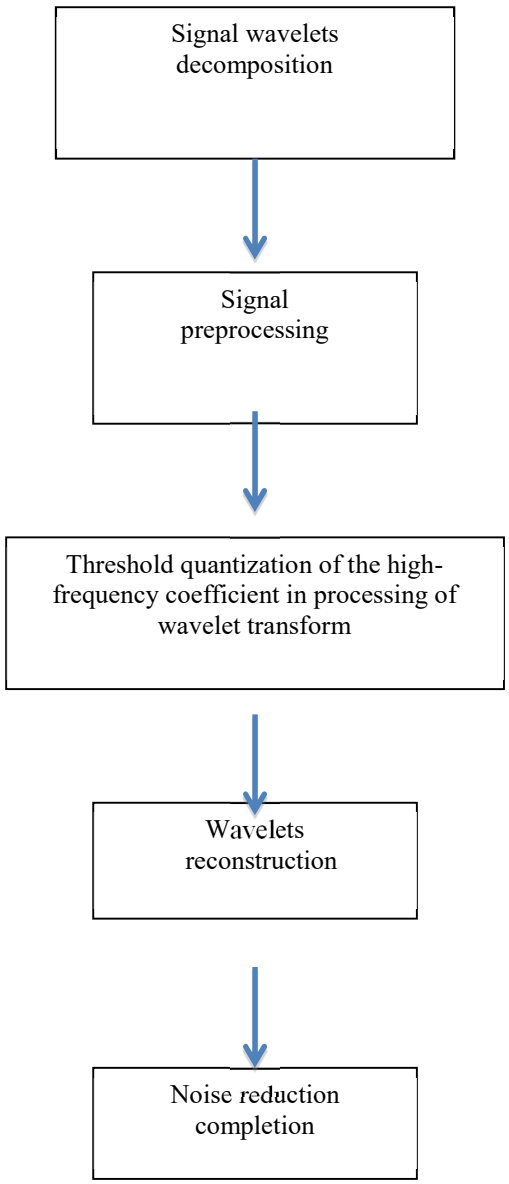

Figure 6-13 Steps in the process of one-dimensional signal reduces noise by using wavelets

Thus it can be seen that wavelets transform decomposes frequency band of signal into low-frequency and high-frequency components, and then decomposing low-frequency component into low-frequency and high-frequency components until reaching the number of layers needed to be decomposed. Wavelets tree is as shown below:

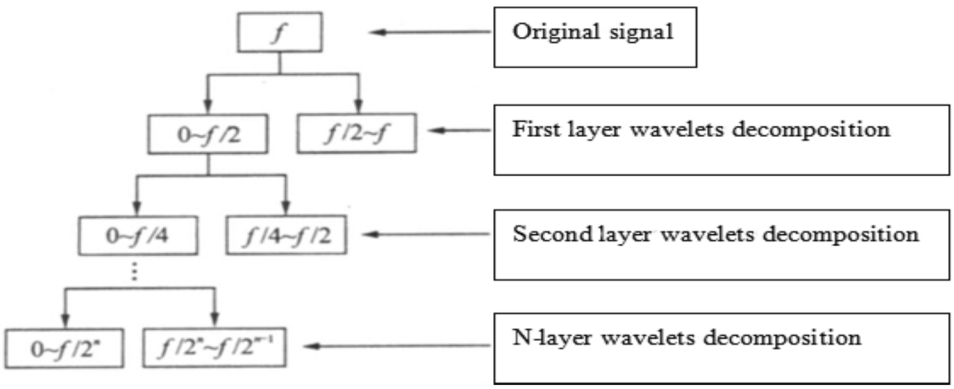

Figure 6-14 Signal decomposing using wavelet

Using the way of inhibiting detail coefficient with high frequency after the decomposition to zero to eliminate noise. In the process of wavelets decomposition, since approximation coefficient deduced from decomposition of each time is smoother than before, and the high-frequency noise eliminated be kept in detail coefficient. The goal of reducing noise can be reached as long as inhibiting detail coefficient to zero (it is also possible to use the method of zooming out detail coefficient on this layer).

Specific steps are as follows:

1). Decomposing noisy signal to eight layers by using dB10 wavelets.

2). Extracting approximation coefficients of 8_{th} layer as signal after noise reduction (if using the way of zooming out detail coefficient, it needs to reconstruct detail coefficient after inhibition and approximation coefficient on this layer to get signal after noise-falling). Here using the way of inhibiting detail coefficient to zero, the result is shown in Figure 6-17.

The wavemenu toolbox is the tool to process wavelet de-noise in MATLAB. When the raw signal is imported, parameters in wavemenu such as type of wavelet, order number of wavelet, and de-noise threshold can be setup, then the filter result can be pre-viewed.

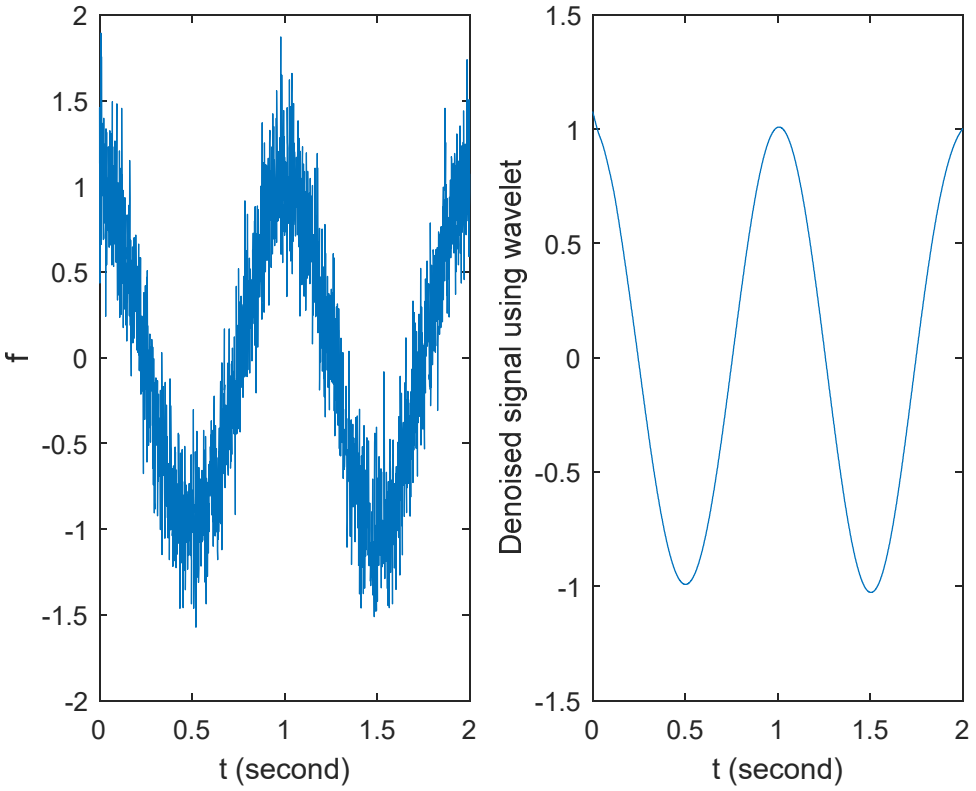

Figure 6-15 Noise reduction using wavelet decomposing

6.3.2.3 Discussion

Comparing Figure 6-14 and Figure 6-17 according to two principles of signal noise reduction (brought out at the beginning of Section 6.3), it can be seen that the de-noised curve from the wavelet is smoother. The standard deviation between noise-reduced signal and original cosine signal using wavelets transform method is 1.2755, while standard deviation using FFT transformation method is 2.5389. Therefore, from both two principles of noise reduction, wavelets transform method has obvious advantages over FFT transformation. Besides, wavelets transform method is more flexible, because different operations can be done on different layers.

6.4 Conclusion

The methods and steps of data processing is discussed in this chapter. Firstly PCA is used to correct coordinate. Then time-domain integration and frequency-domain integration are compared according to the result of two integral of acceleration signal. The result suggests that the frequency-domain integration is more efficient. At last two de-noise methods: FFT and wavelet are discussed, in which wavelet has better effect

than FFT. In Chapter 7, the data collected from my experiments will be processed with PCA, frequency-domain integration and wavelet de-noise.

Chapter 7. Data Processing and Discussion

In this chapter, I will perform analysis and processing to the acquired data of sensor and discuss the result.

7.1 Data processing

The Tayside Road Bridge was sampled for many times in the experiment. Five sets of data from the Tay Road Bridge were randomly chosen from all the data to be processed, analysed and discussed. The data processing procedure is discussed in this section. The result of Forth Road Bridge will be discussed in Section 7.4.

Data acquisition time: start from 20:59, January 3, 2013

File name: 20130103_205946.m

There are 893,314 points measured by acceleration sensor with the sampling rate of about 200Hz.

There are 893,318 points measured by gyroscope with the sampling rate of about 200Hz.

There are 4,379 points measured by GPS, with the sampling rate of about 1Hz.

The data from acceleration sensor is [0, 4,391.718]s.

The data from GPS is [0, 4,379]s.

All five sets of data are acquired when the vehicleis running on Tay Road Bridge, in which the second and fourth sets are acquired when the vehicle is running from north to south, the other three are acquired when the vehicle is running from south to north. There are about 30,000 points in each data set, including data of acceleration sensor and gyroscope, with the sampling rate of about 200Hz.

Due to the quality of road surface, the acquired data contains large noises. So the processing flow for the data is:

1. Select a proper piece of data generally with 30,000 or 35,000 points;
2. Conduct axis-correction to the data through PCA to make the sensor coordinate parallel to the natural coordinate system;
3. As the waveform of raw data is similar to dB wavelet, the dB wavelet can be used to de-noise data. Also from comparison experiments, it is known that dB wavelet is more effective than other typical wavelet. In summary, dB8 wavelet is chosen for the de-noise process;
4. The baseline of wavelet in the previous step is stored;
5. Get the baseline-drifted data by reducing the baseline from the de-noised data. This is for the pothole detection with threshold value;

6. Select a piece of GPS data and expand the data by interpolation so that the the length of GPS data equals to the length of acceleration and gyroscope data. Use this data as the x-axis for time (speed) correction;
7. Determine the pothole according to the threshold value.

The whole data process procedure can be divided to initialisation process, common process and pothole detection process, as shown in Figure 7-1, 7-2 and 7-3.

The initialization is shown in Figure 7-1. Firstly the sample rate of sensor is set as 100 Hz or 200 Hz with a pre-setting threshold. After 5 seconds, the speed of vehicle is detected: if it is between 50 and 70 miles/hour, the data collection is started; otherwise the vehicle speed is detected in 5 seconds. The next step is pre-process: as sensors may output bad points, this step is to remove those points. Next, a set of judgment rules are applied to detect weather the vehicle is on smooth road surface. If so, the process goes to a PCA (principle component analysis) to find vertical axis and calculate new threshold of time domain. If the vehicle is not on a smooth road surface, the process goes back to the second step, in which data collection restarts. The last step is wavelet. Because the road and vehicle condition various in each test, an initialization is required to obtain the value of parameters, which is shown in Figure 7-1. Firstly, data collected in the first five seconds is used to test vehicle speed and road straightness. If vehicle is between 50 and 70 miles per hour and road is straight and flat, the data is then processed by PCA and wavelet de-noise. In de-noise process, the 120% of maximum value of each level decomposed is used as new threshold.

The next step is the common process shown in Figure 7-2, in which the data is decomposed by wavelet. The threshold obtained in Figure 7-1 is used here to filter the data: all values smaller than threshold are set to zero. Then the rule of pothole detection is applied.

The rule of pothole detection is shown in Figure 7-3. When M number of sequential data points have value larger than the threshold, followed by N number of sequential data points have value smaller than the threshold, the last one of M number of sequential data points is considered as a pothole. Its position is recorded, and the threshold is updated at the same time. Then the common process repeats until all data is processed.

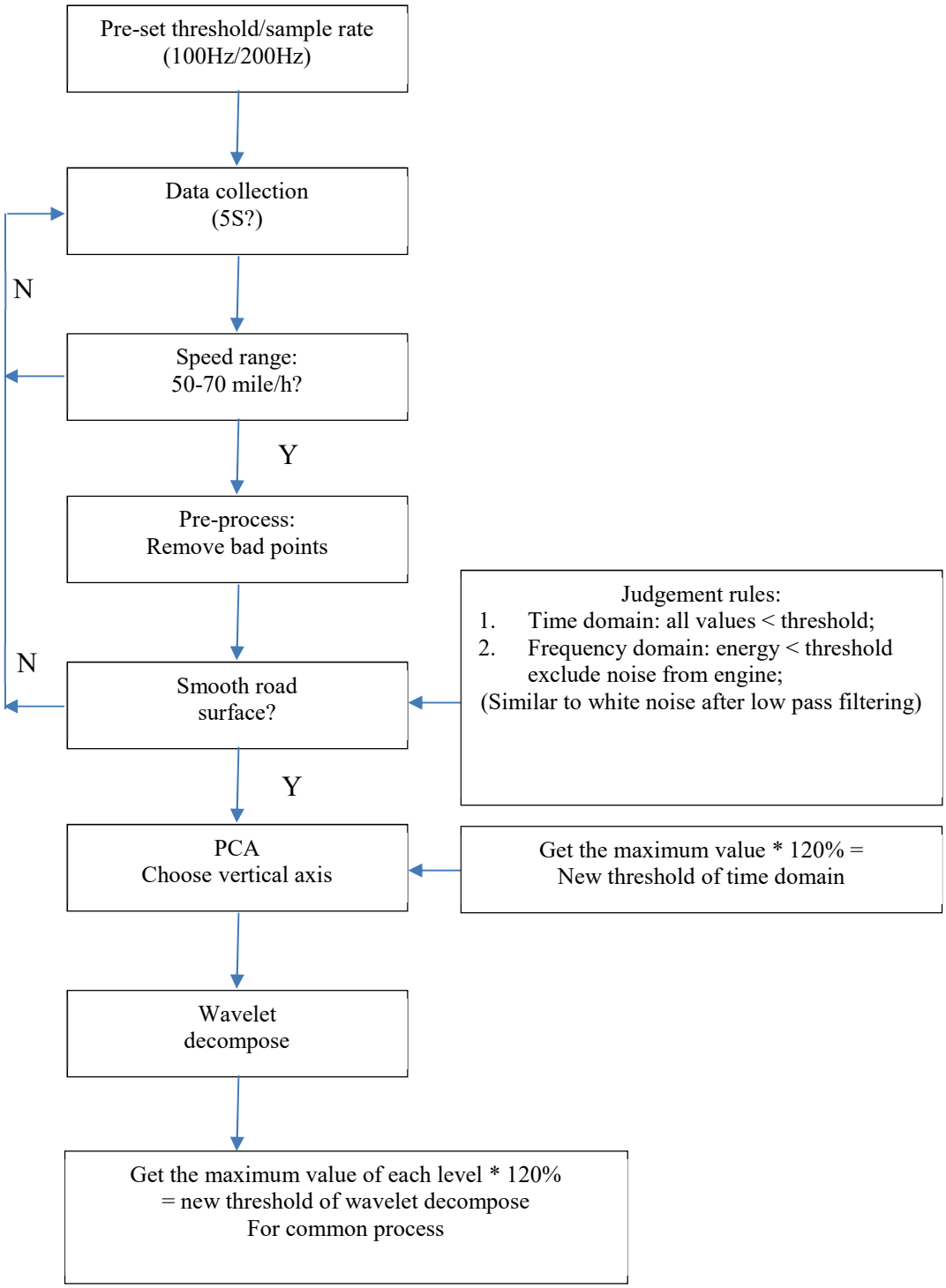

Figure 7-1 Initialisation process

In the initialisation process (shown in Figure 7-1), the sample rate is set as 100 or 200 Hz (depends on device), then the data is being collected for 5 seconds repeatedly until the speed of vehicle and condition of road satisfy experimental requirements: firstly the speed of vehicle is checked, which should be between 50 and 70 miles/hour; and then

the bad points from data are removed, then the data is used to check if the surface of road is smooth. When both the speed of vehicle and condition of road satisfy the experimental requirements, the initialisation process uses PCA to do axis-correction. Then the wavelet analysis is used (decompose then compose) to find the threshold of wavelet decompose which is then passed to common process, in which the data is collected and processed to detect the potholes. When all these are finished, the initialisation quits and the program switches to common process.

In the common process (shown in Figure 7-2), data is being collected and pre-processed to remove bad points. Then PCA is used for axis-correction, and the threshold of wavelet decompose passed from initialisation process is used by wavelet analysis for de-noise. Then the pothole detection algorithm is being operated to find potholes. If potholes are found, they are recorded with current GPS data. The common process runs until experiment ends.

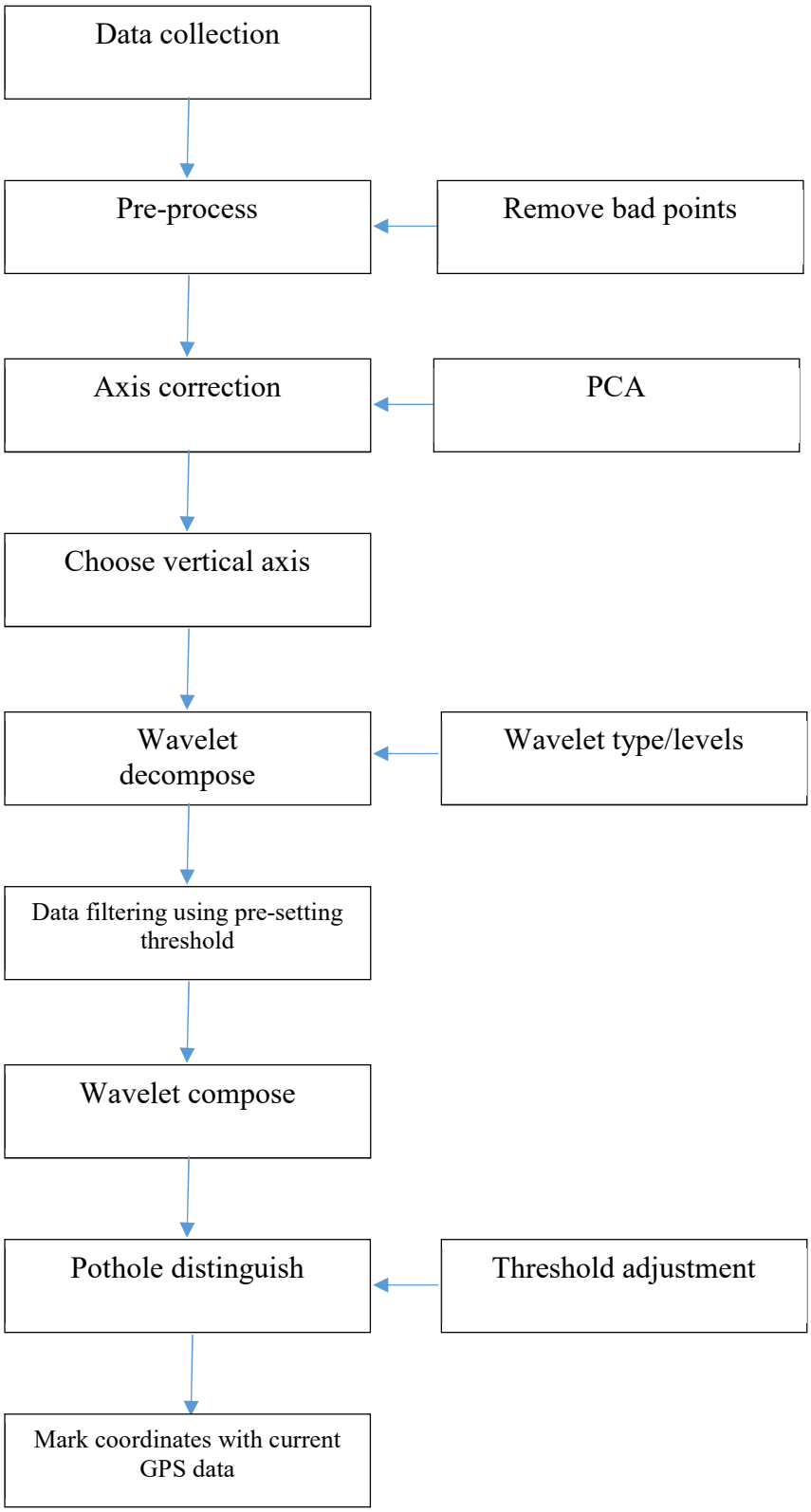

Figure 7-2 Common process

Pothole detection algorithm (shown in Figure 7-3)is called inside the common process, and is the core of whole pothole detection program. The pothole detection algorithm

firstly reads and scan a piece of data which is already filtered and de-noised by the common process. Then the data is compared with preset threshold which may be dynamically changed. If the data > threshold, then I consider a pothole is found. The position of this data is recorded. However if most of data is pothole according to the value of threshold, then it is known that the value of threshold is too low and then increased. After the value of threshold is changed, the current piece of data will be processed again.

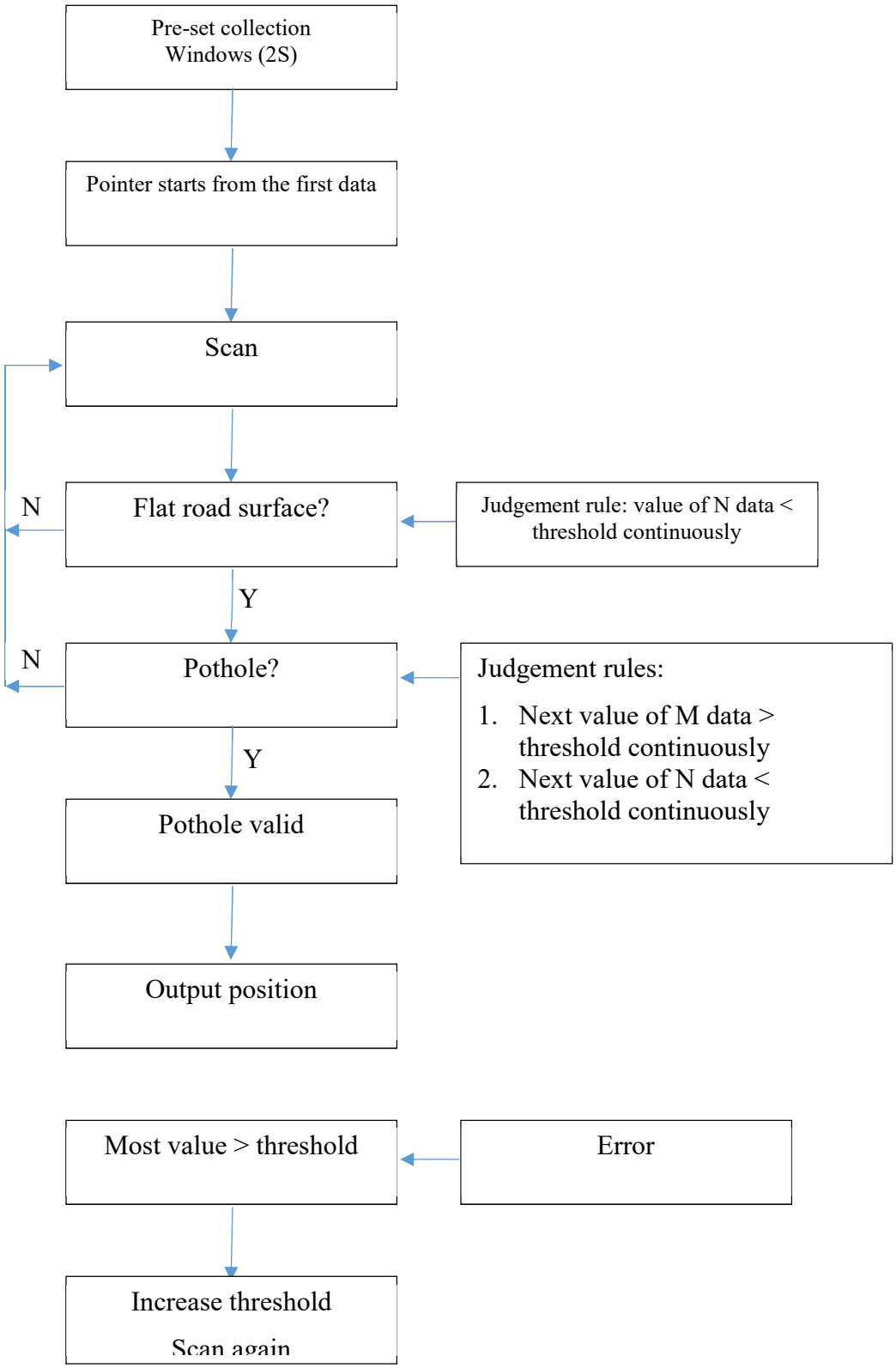

Figure 7-3 Pothole detect process

From the five sets of data being processed, one set is chosen as an example, which will be called Route 1 in the following part of the section the other four sets (Route 2-5) are attached in Appendix A.

The Route 1 data contains 30,000 points from point 105,001 to 135,000 of the raw data. The acceleration data is shown in Figure 7-4.

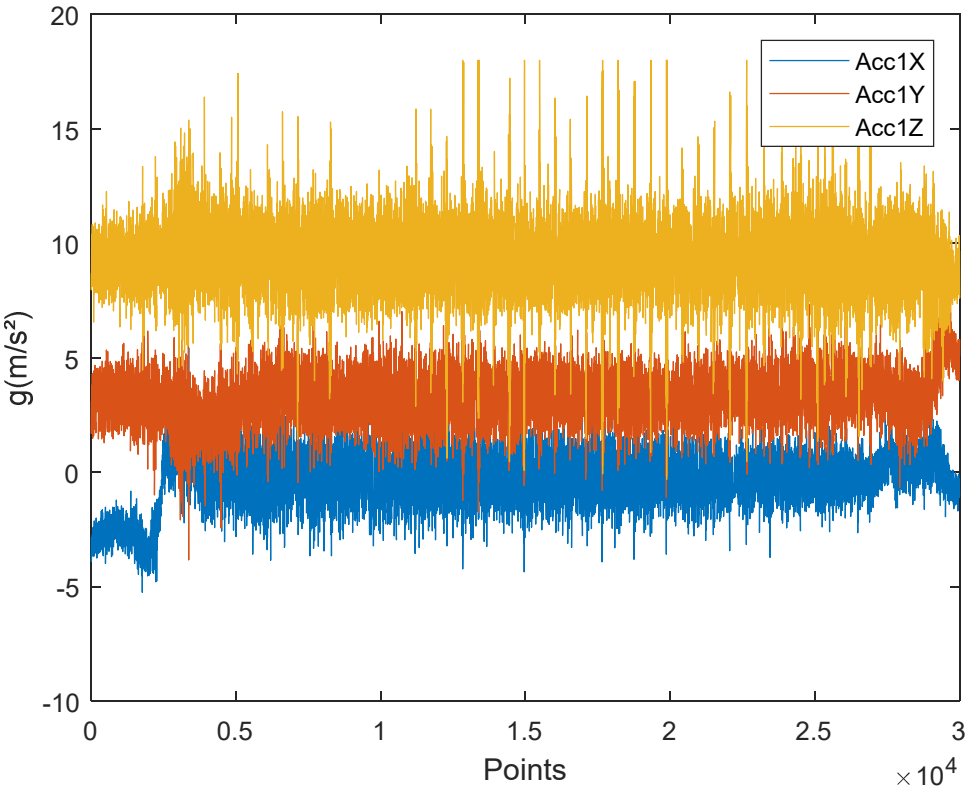

Figure 7-4 The acceleration data of Route 1

From the Figure 7-4, we can learn that the red part is Z-axis containing the measurement of gravity. But as the smartphone is not strictly parallel to the ground, part of the gravity is contained in the green part which means X-axis.

Axis-correction to the data with PCA:

[coeff,score,latent]=princomp(A);

'Pimcomp' is the function to process PCA in MATLAB. Its input is the original data that is correlated. The output consists of three parameters, 'coeff', 'score' and 'latent'. 'coeff' is a 3*3 matrix which contains all the eigenvectors of the covariance matrix corresponding to the original data set. This matrix is also called transformation matrix or projection matrix.

'score' contains three triaxial components, which are represented by three vectors arranged by the contribution rate from large to small. As discussed, these three components have no correlation. 'latent' is a one dimension column vector, in which each element represents the contribution rate of the corresponding data components. As there are three components in the data set, 'latent' has three elements, arranged from large to small. Therefore the the original data set A*coeff = score. By using Primcomp we can get the 'coeff':

coeff =

0.0395	-0.3348	0.9414
-0.7545	-0.6277	-0.1916
-0.6551	0.7027	0.2774

As shown in Figure 7-5, data of all three axes are de-noised with wavelet. In fact, only data on Z-axis is necessary to distinguish the pothole, but for clarity data on three axes are processed.

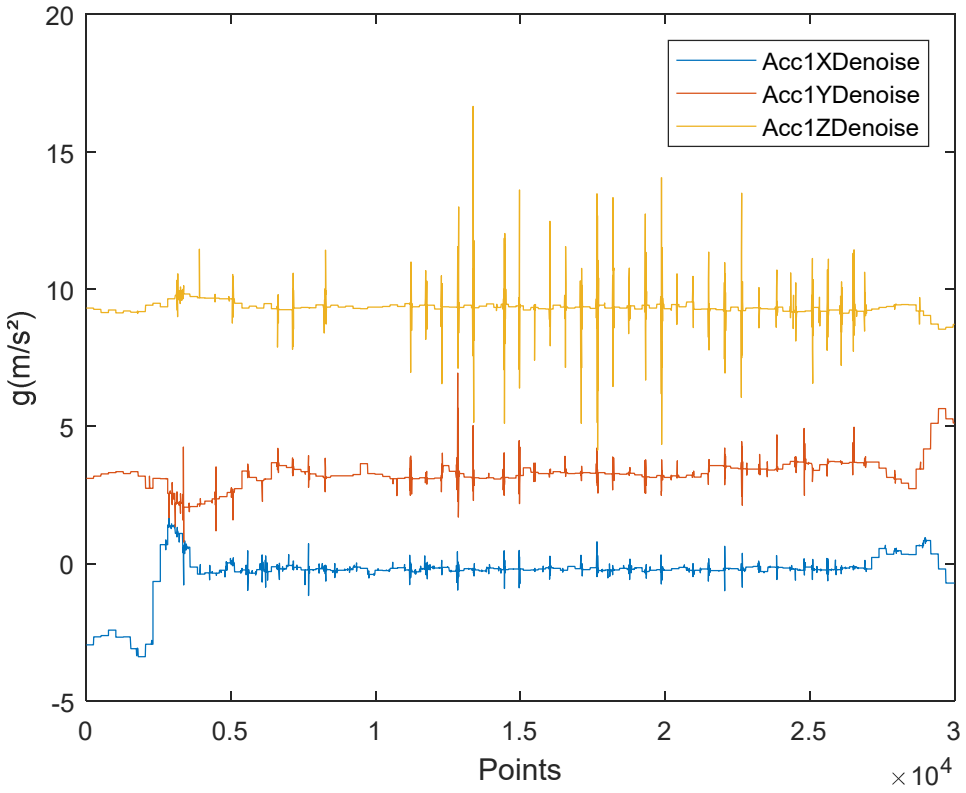

Figure 7-5 De-noise data on the three axes with wavelet of Route 1

From Figure 7-5, it is seen that due to the baseline drift, the threshold value is hard to be determined. Thus it is necessary to eliminate the baseline. Firstly the baseline is extracted from the result of wavelet decomposition, as shown in Figure 7-6.

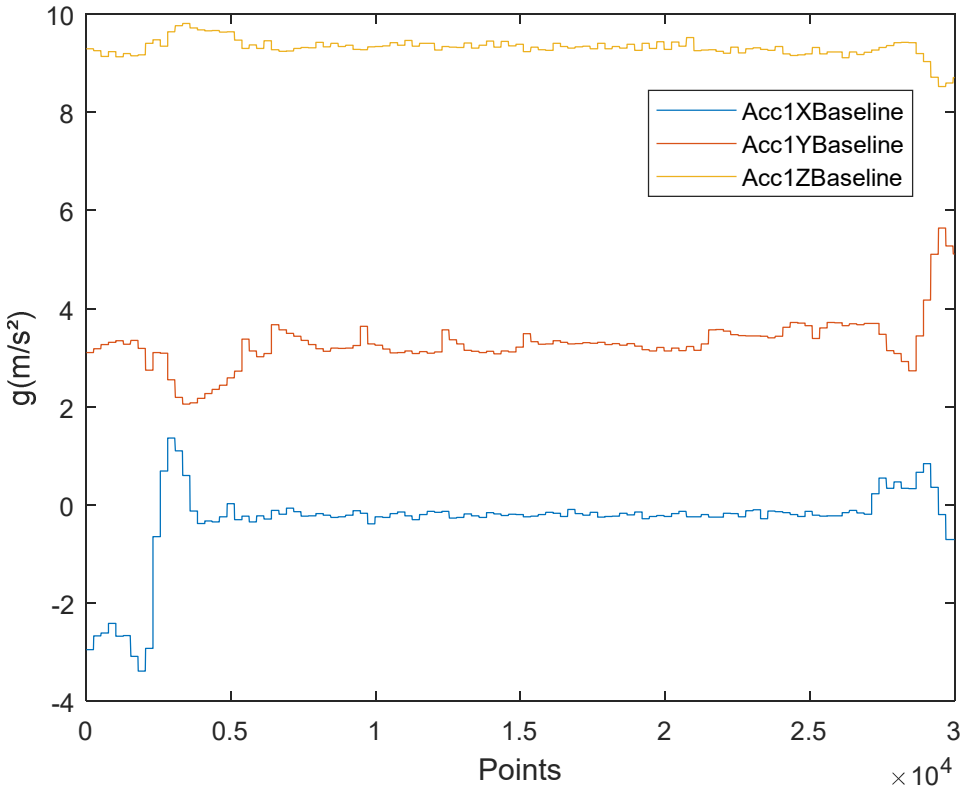

Figure 7-6 Baseline of acceleration data of Route 1

Then subtract the baseline from the de-noised data to get the result, as shown in Figure 7-7.

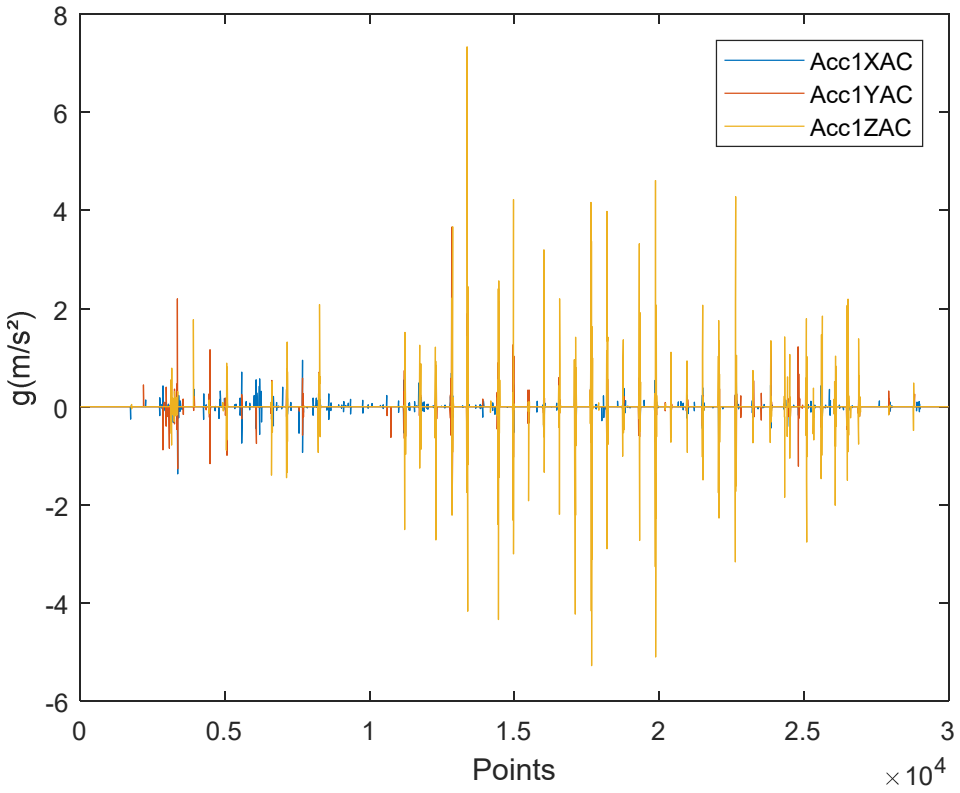

Figure 7-7 AC component of accelerometer data of Route 1

As can be seen from Figure 7-7 that, the red signal (Z-axis) is most sensitive to pothole, as it contains the largest amplitude, and in the experiment the detection vehicle is considered as in uniform linear motion and the largest vibration should be from the pothole. This conforms the assumption that axis Z is approximately vertical to the ground.

The next step is to calculate and store the position of potholes. The x-axis in Figure 7-7 means number of data, to obtain the position of each pothole, the x-axis needs to be transfer to distance. In order to calculate distance from number of data, the speed and sampling rate is needed. The sampling rate is fixed by smartphone setting. The speed of the vehicle, not as my assumption, is not exact constant, which explains vibrations on x and y axes in Figure 7-7. Thus to record the position of potholes, the data from GPS is used. The specific process is as follows:

Firstly time of beginning point and end point are found.

Acct(105001)=517.445 seconds;

Acct(135000)=665.296 seconds;

It is seen that this piece of data is from No. 517s to No. 665s. A piece of 150 seconds is selected from No. 517s to No. 666s, containing 150 seconds. The distance change in this period can be accurately read from the GPS data package.

```
GPSdist2=Location_GPS_dist(517:666);
```

Set 0 as the initial value of distance:

```
GPSdist2=GPSdist2-GPSdist2(1);
```

As the point frequency of GPS is one every second, there are totally 150 points. Interpolate the 150 points to 30,000.

```
xi=0.005:0.005:150;

x=0:149;

Dist2=interp1(x,GPSdist2,xi, 'spline');
```

Take the distance (0-2500m) as the abscissa:

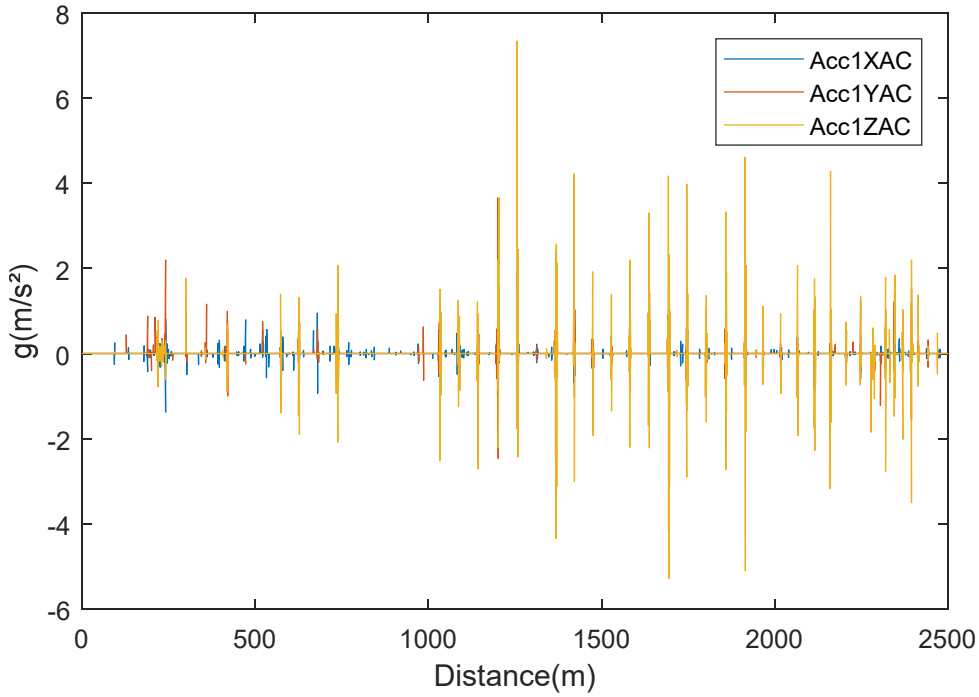

Figure 7-8 Use distance as the abscissa in Route 1

As seen from Figure 7-8, the processing result is very good with each pothole clear in the final result and the flat road surface free from noise.

As a contrast, process the gyroscope data of Route1 in the same way:

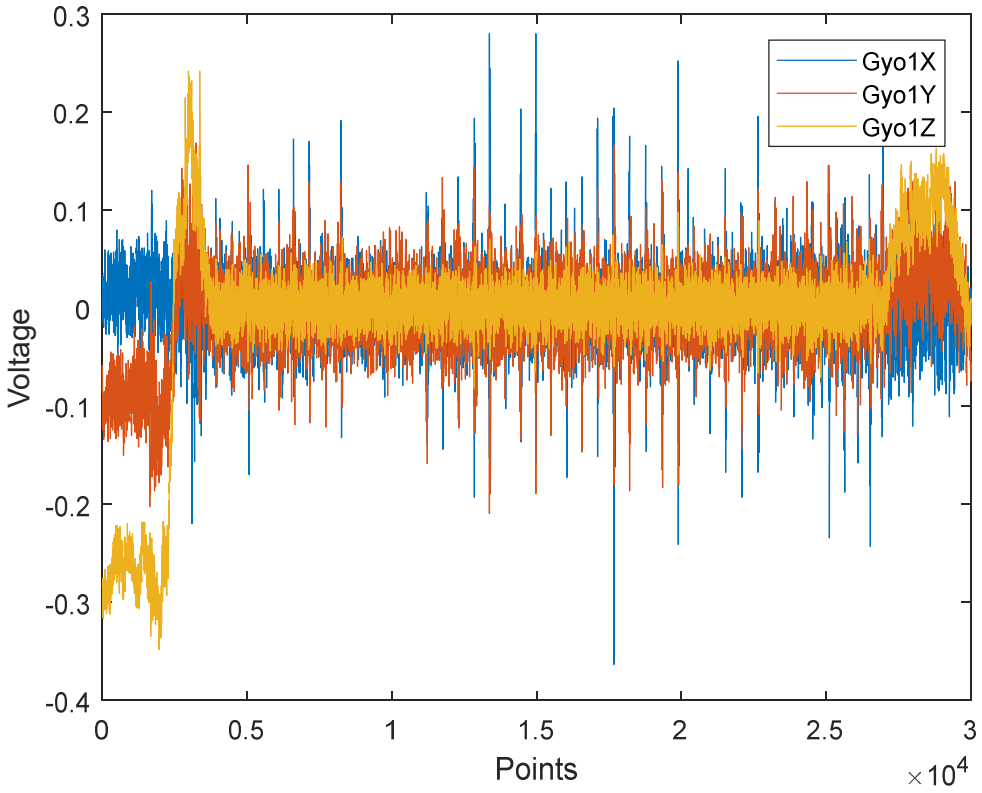

Figure 7-9 Gyroscope data of Route 1

It is seen that there is no DC component of gravity acceleration in gyroscope data and the data of three axes all fluctuates around zero.

Conduct PCA to the gyroscope:

[coeff,score,latent]=princomp(G);

coeff =

0.8657	-0.3956	0.3066
-0.2872	0.1090	0.9516
0.4099	0.9119	0.0193

Denoise the gyroscope data with dB8 wavelet:

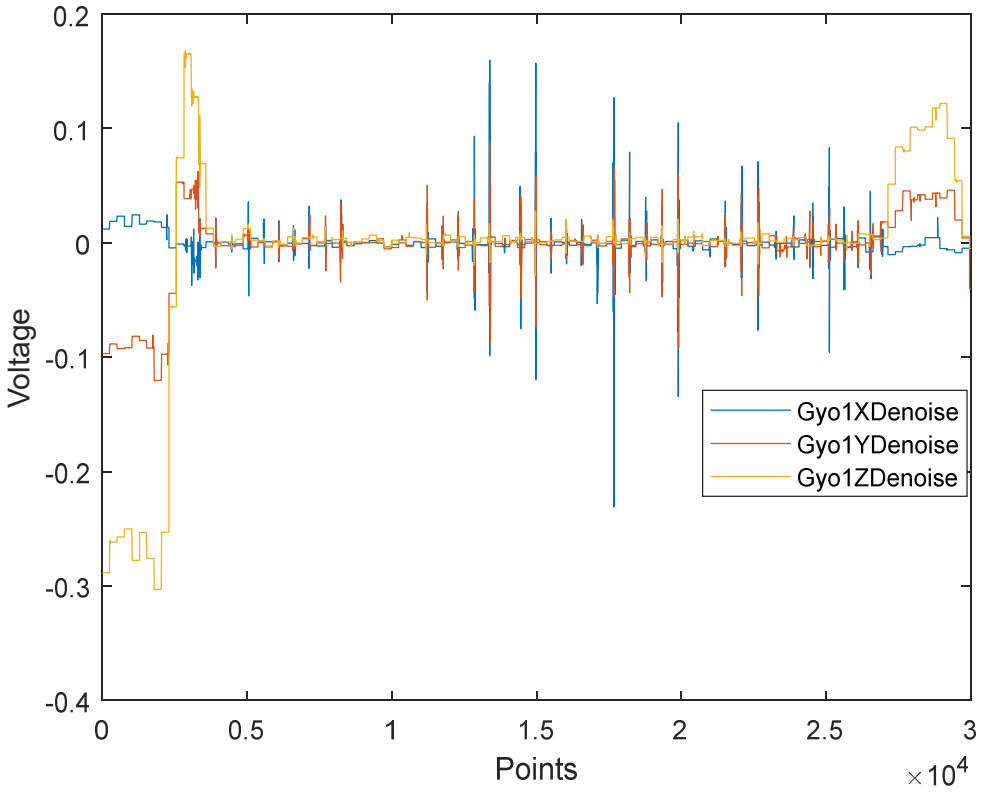

Figure 7-10 Denoise the gyroscope data of Route 1

It is seen that there is still fluctuation in some part, so extract the baseline from result of wavelet decomposition:

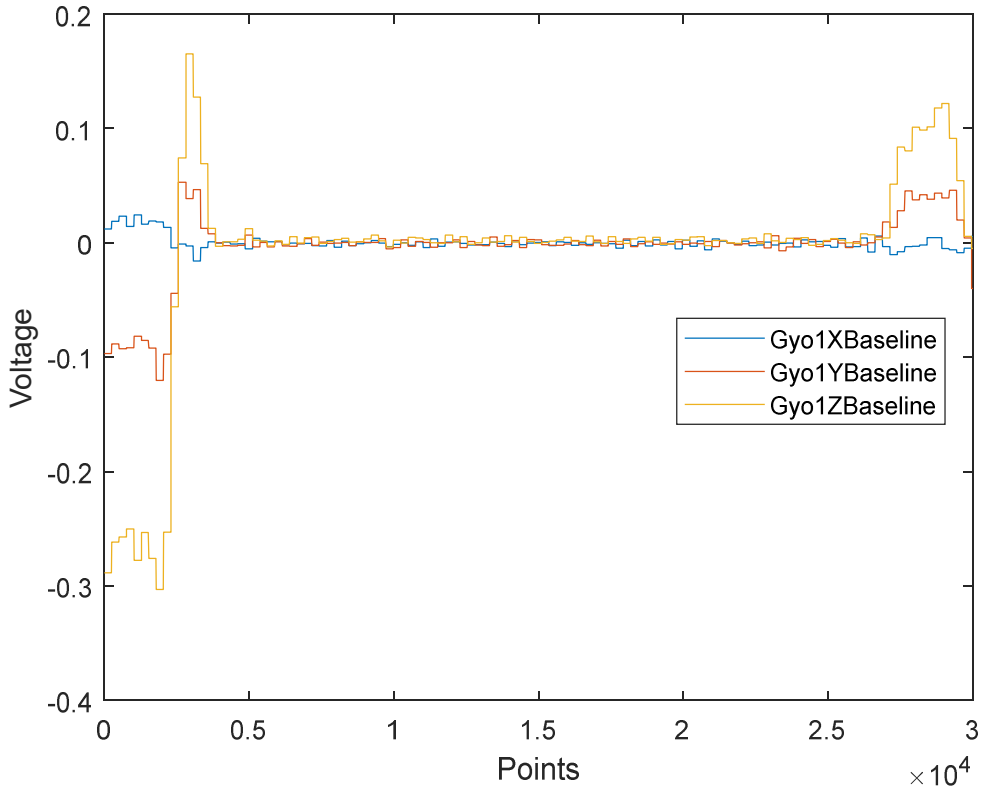

Figure 7-11 Baseline of gyroscope data of Route 1

Eliminate the baseline from the de-noised result:

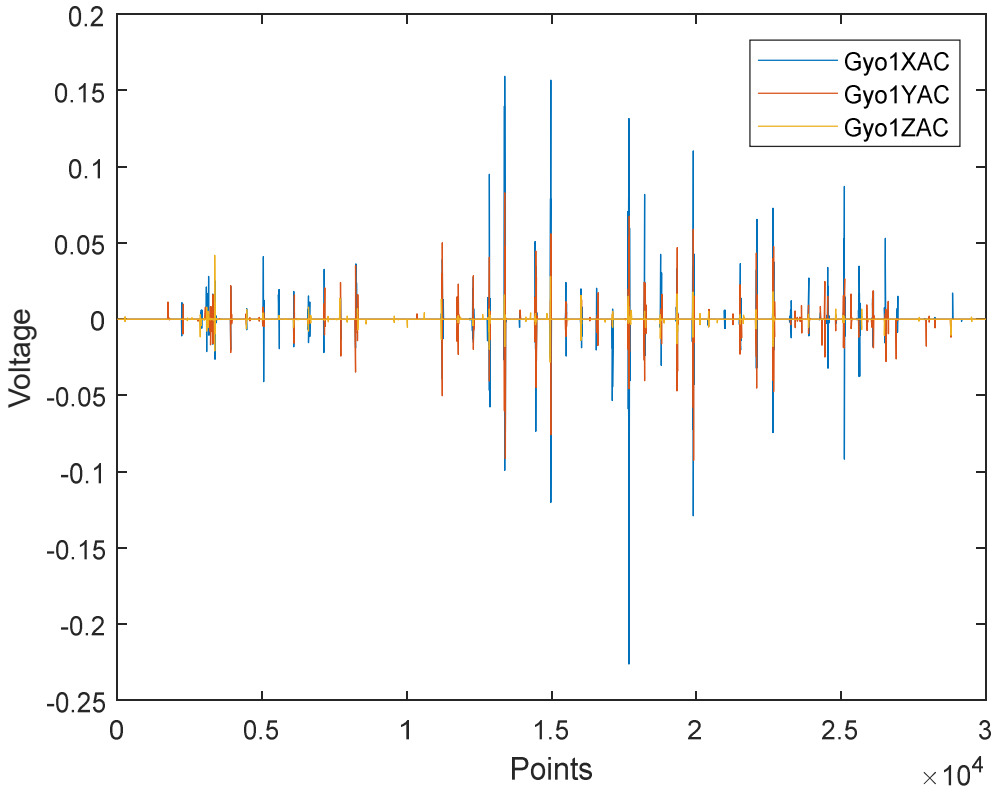

Figure 7-12 AC component of gyroscope data of Route 1

Conduct distance correction with Dist2 as the abscissa, the result is as follows:

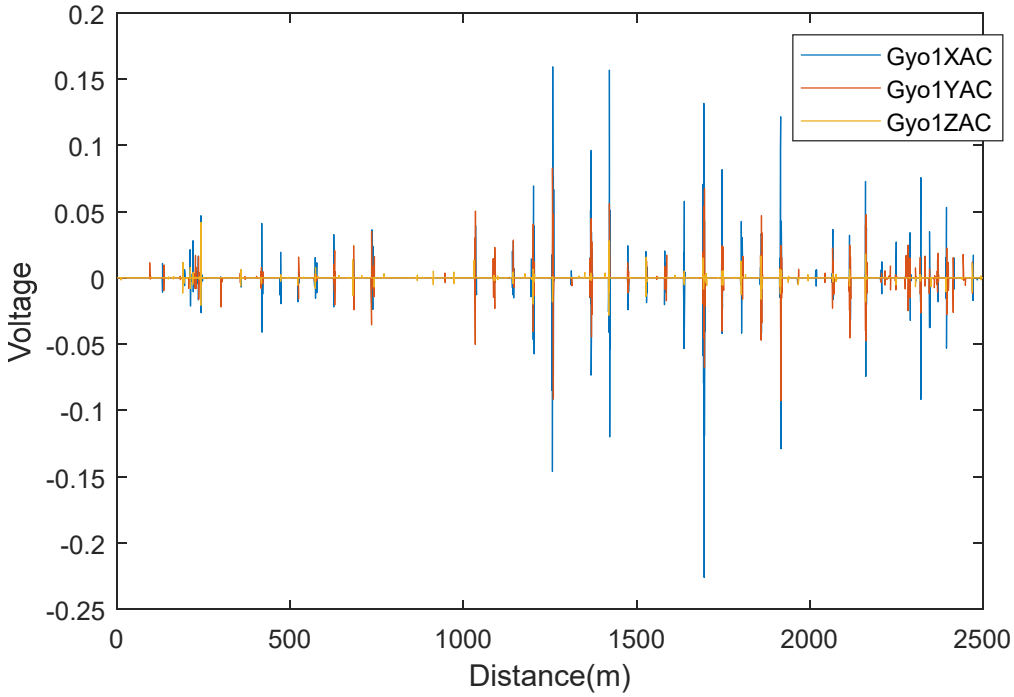

Figure 7-13 Conduct distance correction with Dist2 as the abscissa

It is seen that gyroscope data can represent most of pothole data, but its signal-to-noise ratio is not better than that of acceleration sensor.

Because Route 1 includes data points No. 105001 - No. 135000, from

Acct(105001)=517.445 seconds

Acct(135000)=665.296 seconds

It is known that Route 1 starts from 517th second of experiment, and ends at 666th second. Therefore the data from 517th second to 666th second of GPS data is taken for process:

Thd=Location_GPS_spd(517:666);

The GPS data can be drawn as Figure 7-14, in which x axis is time (measured by second) and y axis is velocity (measured by meter per second).

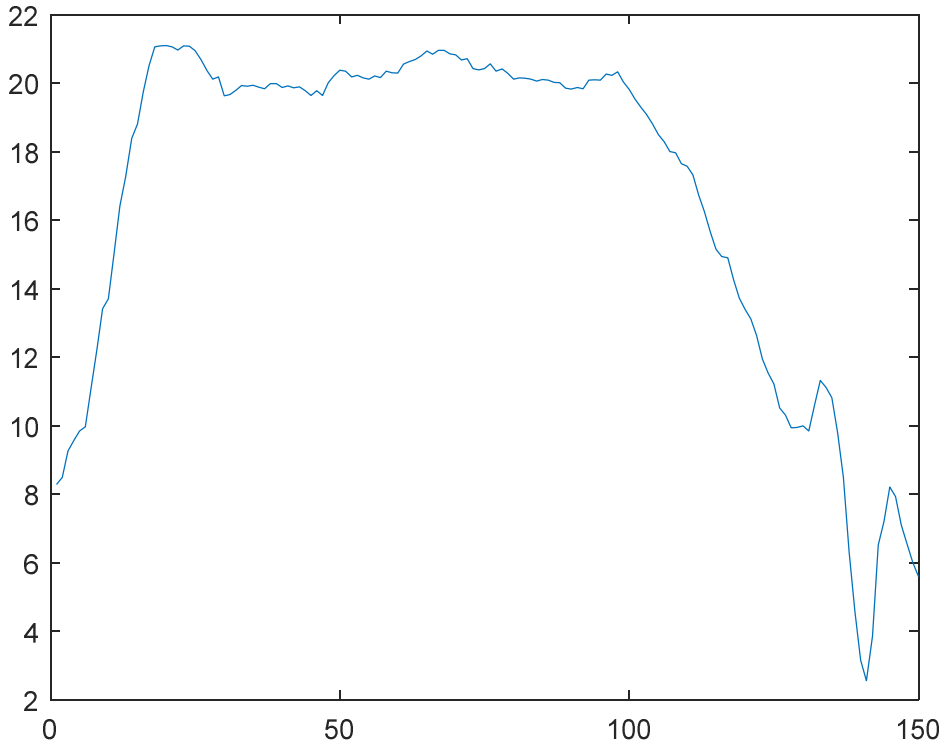

Figure 7-14 GPS speed data from 517th second to 666th second. X axis is time (second), y axis is velocity (m/s)

There are 150 data points in the figure. For convenience of calculation, these 150 data points are interpolated to 30,000 points. Because there are 30,000 data points for acceleration data, the speed and acceleration data is now one-to-one correspondence:

Thd2=interp1(x,Thd,xi, 'spline');

Based on the model discussed in Chapter 5, equation 5-8, the threshold of pothole judgment is proportional with square power of speed. Thus square calculation is applied to every point in Figure 7-14 GPS speed data from 517th second to 666th second. X axis is time (second), y axis is velocity (m/s):

Thd2=Thd2.^2;

A new curve is obtained through the square calculation, which is shown in Figure 7-15.

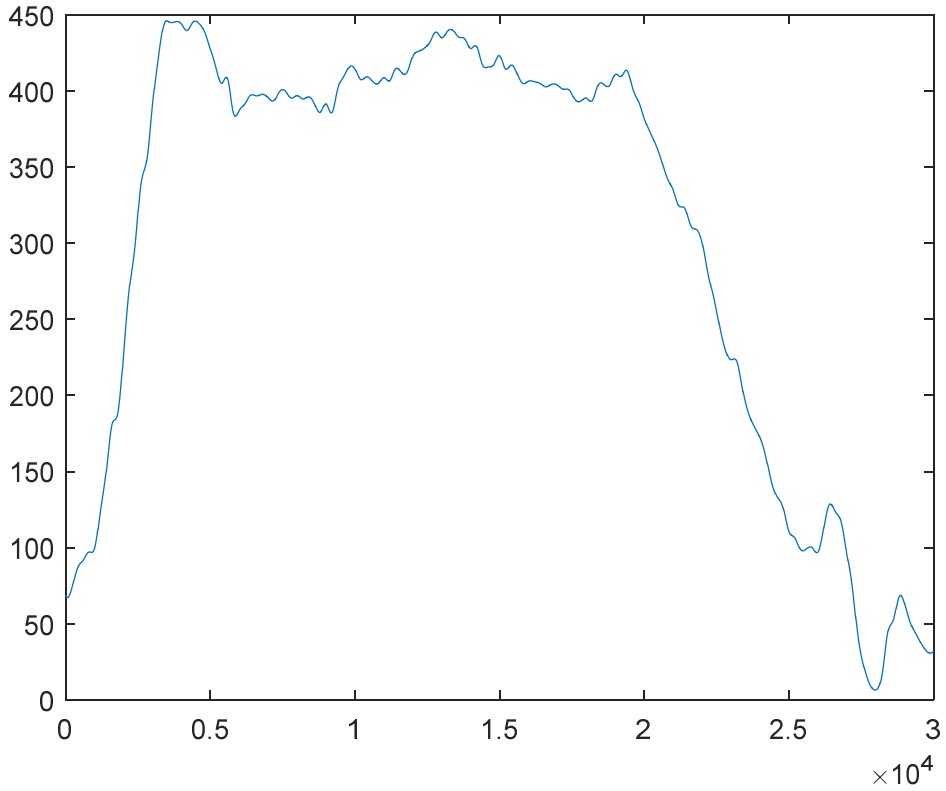

Figure 7-15 Square calculation applied to every point GPS speed data. X axis is points, y axis is square of velocity

The threshold is

Threshold=EmpCoef*Thd2;

In which EmpCoef is empirical coefficient. With tests, 1/600 is considered as a proper value of EmpCoef, with which the most potholes are found, at the same time, the non-pothole areas are not misjudged.

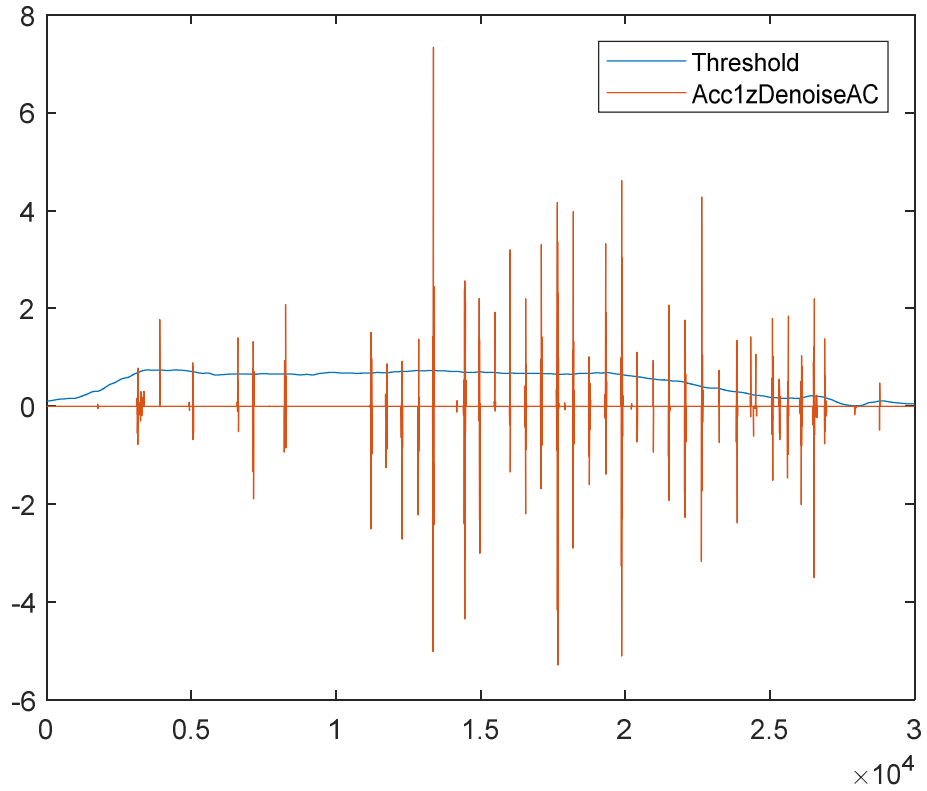

Figure 7-16 Threshold and Acc1zDenoiseAC. X axis is points, y axis is amplitude (m/s²)

In Figure 7-16, it is shown that the first value higher than threshold happens at about 27500th point, which happens before vehicle reaches the surface of bridge. This is because the speed of vehicle reduced to nearly zero when it passed the first expansion joint, and with the low speed, the expansion joint resulted a less obvious peak valued data (but it is still detected). Therefore the second peak valued data from right side (because the vehicle drives from right to left side) in Figure 7-16 is actually the first expansion joint on bridge.

From Figure 7-16, it is seen that an extra pothole is detected between the 4th and 5th expansion joint. Field survey proved that there is a crack on the road surface between the 4th and 5th expansion joint, which has similar effect of a real pothole. This result can partly prove the effeciency of the pothole detection method.

The 37th and 39th expansion joints are failed to be detected. The 30th, 31st, 32nd and 33rd expansion joints are also not detected. However the field survey proved that these four expansion joints did not exist on bridge. Therefore the detection result for these four expansion joints are correct.

To sum up, the detect rate is:

Misjudgment rate: 1/41=2.44%

Omission rate: 2/41=4.88%

Accuracy: 38/41=92.68%

Note that data has a very small value at the first expansion joint, at which the speed of vehicle is nearly zero. If the threshold is not proportional to the square of speed, either a large threshold value is used, in which case the first expansion joint is omitted; or a small threshold value is used, in which case, although the first expansion joint is detected, some noise may be misjudged as potholes. Therefore it is effective to set threshold as proportional to square of speed, and this increases the effeciency of detection method under relatively low speed.

Through above data processing, most potholes can be detected precisely. In total, 42 potholes can be detected. According to the sequence from north to south, the potholes are as follows:

Table 7-1 Tay Road Bridge pothole result

Pothole No.	Location(Unit 0.001m)	Value of Amplitude
1	479428	3.493479389617304
2	503359	12.282863975315701
3	562333	3.414440299183515
4	601293	10.426649739276137
5	647251	2.504766783280768
6	702528	13.162327754843496
7	758365	1.223170039320437
8	814388	23.958198894239505
9	869185	7.528773067211463
10	922705	13.943086050762023
11	977700	0.873244979196262
12	1033416	1.229766842508431
13	1085459	26.066322240274541
14	1140805	11.044496681966052
15	1192367	4.805444052843307
16	1247661	19.422785688228405
17	1301204	33.911657251870253
18	1361839	17.904420663242227
19	1411051	6.143552087759477
20	1471183	10.213872255771888
21	1525120	3.697307425589718
22	1579967	17.816857735391114
23	1632241	18.858027414966717
24	1682090	0.043926201928237
25	1741562	53.848259283426117
26	1791860	13.443920524897299
27	1848963	7.365587601658930
28	1904895	1.572325588118663
29	1953478	9.567219474089635
30		N/A

31			N/A
32			N/A
33			N/A
34	2244573	11.239200705316158	
35			
36	2353446	3.733065333508728	
37	2408206	4.101902478160083	
38			
39			
40	2568936	1.244674347299704	
41	2621007	0.311282845814263	
42	2669333	3.138815035002274	

7.2 Comparison between actual measurement of Tay Road Bridge pothole position and data processing result

In order to verify whether data processing result is right, writer conducts actual measure to Dundee Tay Road Bridge, measuring location of every pothole and taking pictures for width of every pothole. Measurement result is as follows.

Table 7-2 Pothole ID and the interval distance between potholes

Pothole ID	Interval distance (m)	Pothole ID	Interval distance (m)	Pothole ID	Interval distance (m)
D1	25.0	D15	54.0	D29	54.0
D2	26.0	D16	56.0	**D30**	?
D3	32.0	D17	54.0	**D31**	148.0
D4	38.0	D18	56.0	**D32**	?
D5	46.0	D19	54.0	**D33**	146.0
D6	56.0	D20	54.0	D34	56.0
D7	57.0	D21	56.0	D35	54.0
D8	54.0	D22	54.0	D36	54.0
D9	56.0	D23	54.0	D37	56.0
D10	54.0	D24	56.0	D38	54.0
D11	56.0	D25	54.0	D39	54.0
D12	54.0	D26	54.0	D40	56.0
D13	56.0	D27	56.0	D41	56.0
D14	54.0	D28	56.0	D42	

Figure 7-17 Normal expansion joint style of No. 1-29 and 34-42

Figure 7-18 Abnormal expansion joint style of No. 30, 31, 32, 33

According to actual measurement result, there are 42 expansion gaps totally. What should be noted here is that vehicles drive different lanes on the journeys from south to north and from north to south, thus there is difference of road surface condition, and it can't be regarded route1/3/5 as reverse order of route2/4. But location of pothole almost should be overlapped.

Among these 42 potholes, the last one (D42) routinely can't be detected because the last pothole locates in the end of bridge, and then roundabout. Vehicles have to slow down here to stop momentarily, and can't pass until confirm no vehicles passing on the right side of roundabout so that vehicles running speed has already been close to zero, resulting in the data of the last pothole has lost its value. Among the rest of 41 potholes, D30, D31, D32 and D33 has the lowest detectable rate. As we can see from actual photographs that these four potholes are very special. Actually they have been made asphalt perfusion treatment so that there almost is no difference between their surface and well-paved road surface, so observer can't find them unless he is very attentive. In fact, these three small wave crests can be seen among acceleration data, which evidences exactly the sensitivity of the algorithm is very high; they can't be seen when observing waveform in time domain. But it is possible to misjudge other well-paved road surface as pothole if detection threshold is set lowly, thus the three expansion gaps shouldn't be counted that pothole has already been detected. Actually, these three

expansion gaps with very small height shouldn't be judged as pothole, otherwise this algorithm will lost its meaning.

Except these four potholes, this algorithm has very high detectable rate for the rest of potholes, thus achieving purpose of design.

Compare the results with the 3D model of the bridge, we can find out that they match very well as expected. In Figure 7.19, the red lines are results from pothole detection, the black lines are the real position of potholes. It is shown that, the red lines appear at the same position of black lines, or appear near black lines, which means the potholes are detected, also the position of detected potholes are close to their real position.

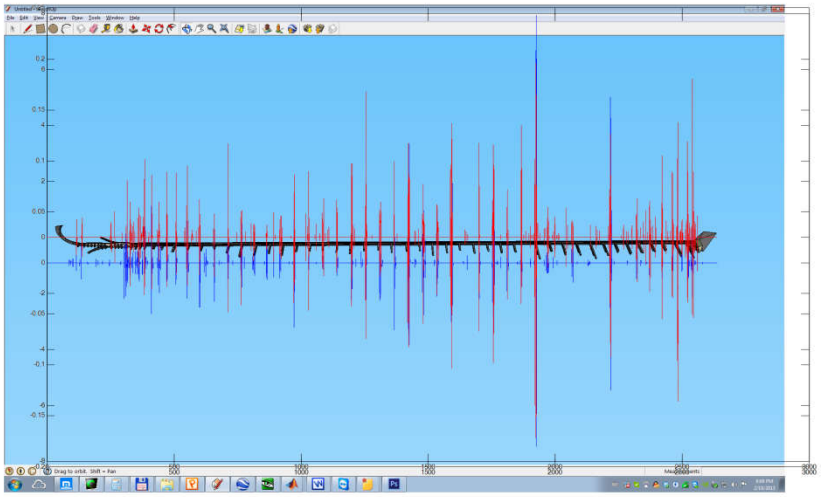

Figure 7-19 Tay Road Bridge result vs 3D model

7.3 Forth Road Bridge Data Processing result

The same method can be used with Forth Road Bridge, as shown in the following figure.

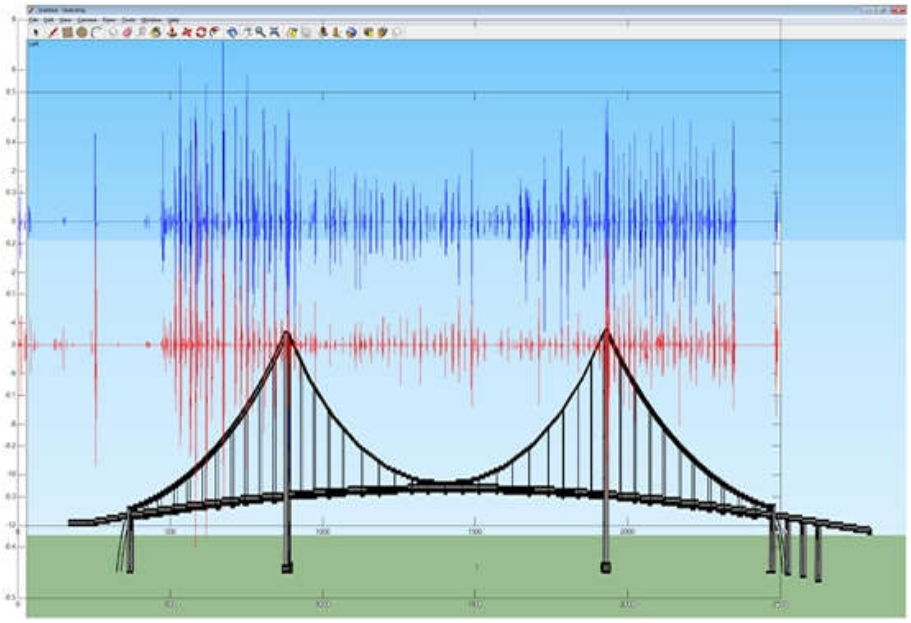

Figure 7-20 Forth Road Bridge result vs 3D model

The blue line is the accelerometer's data, and the red line is the gyroscope's data. As can be seen, most of these potholes can be identified out (more than 90 of these 100 potholes in total), but the S2 segment has several missing, which may be due to the expansion joint of Forth Road Bridge is relatively shallow and hard to be recognized well. on the other hand may be due to the arch style of the bridge which is not satisfied with the condition defined in chapter 5.

7.4 Real pothole detect test

A road in Camperdown Country park was chosen as the test road. There are some potholes on the road surface. The test date is 27/06/2016, and the test device is Samsung S4/GT-9505 (OS: Android 5.0.1) smart mobilephone. The software is Sensor Insider 3.1.2. Use a Vauxhall Astra 2001 1.6L automatic transmission car as the test vehicle.

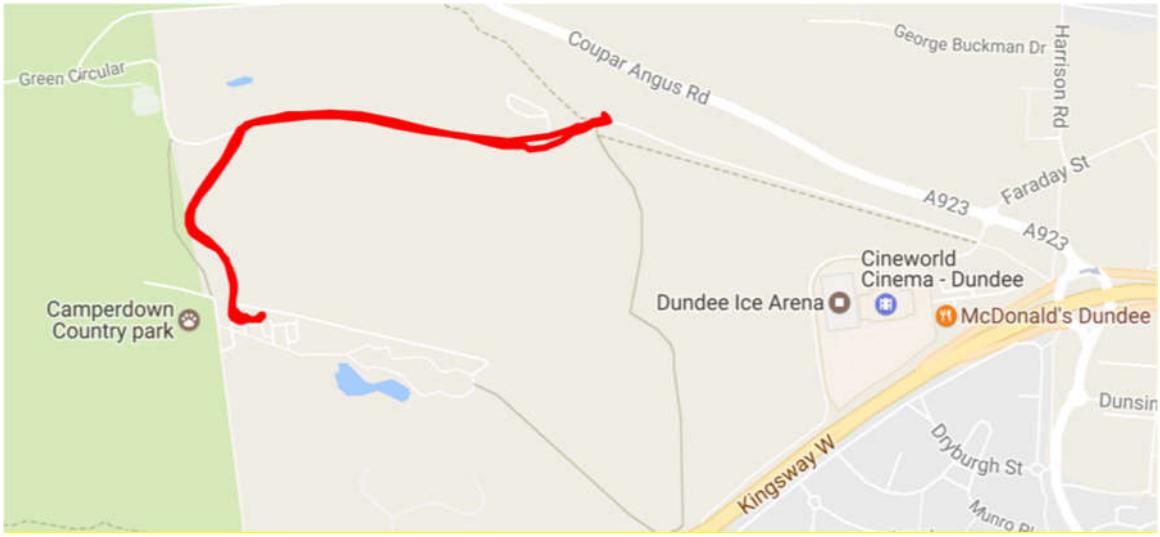

Figure 7-21 Road for test in Camperdown Country park (shown as the red route)

The testing road is shown as the red route in Figure 7-21. The car runs from the north side to the east side, and then return back to the start point.

Actual measurement result shows there are 11 potholes on the route. The distances between each pothole and the start point shows as Table 7-3.

Table 7-3 Distances between each pothole and the start point

ID	Distance to the start point (m)
1	770
2	813
3	875
4	1080
5	1103
6	1140
7	1180
8	1780
9	1877
10	1930
11	1960

The measurement repeated 4 times.

From the algorithm process we can see that, the final processed signal is the Z axis data after coordinate adjustment, so the X axis and Y axis data after coordinate adjustment do not need to be process further more. So in the data processing, after the three axes are corrected, only the z-axis data needs to be processed further more.

Some routes have two peaks at the beginning and end of the route, which are the vibrations caused by the start of the vehicle and the gear shift, and are removed when processing the data.

Those much closed data will be combined into one pothole.

Route1

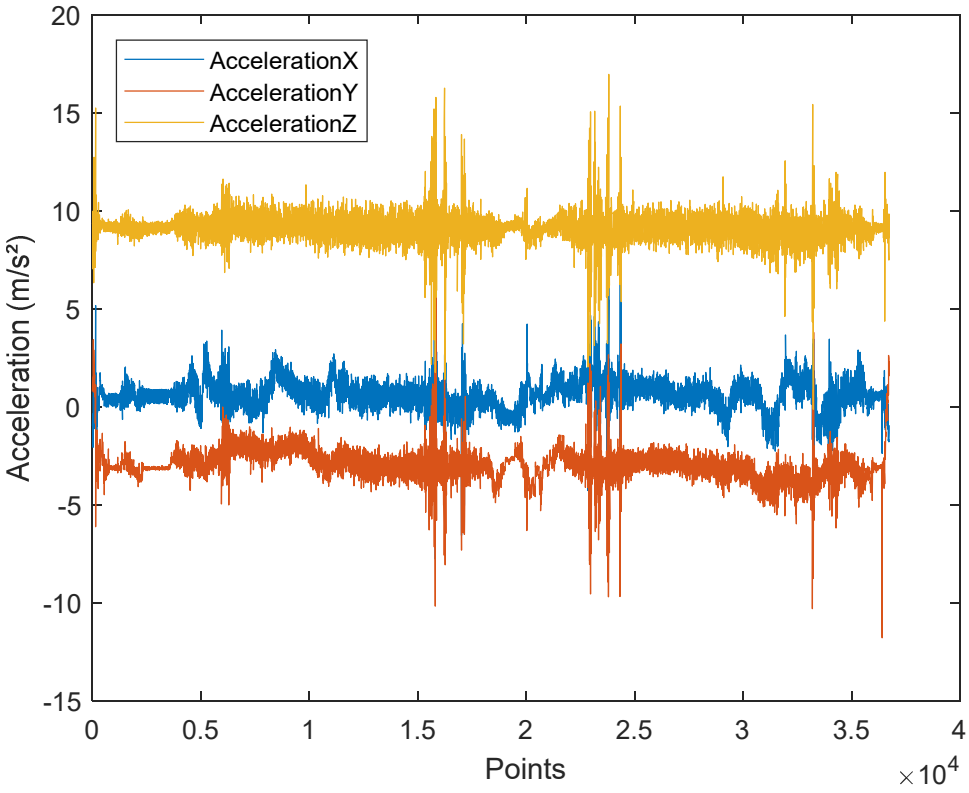

Figure 7-22 Three acceleration data of Route 1

The Route 1 data contains 36,700 points, 367 seconds. The maximum speed is 9.25m/s, the average speed is 5.40m/s.

Firstly process the axis-correction using PCA, then de-noise using wavelet.

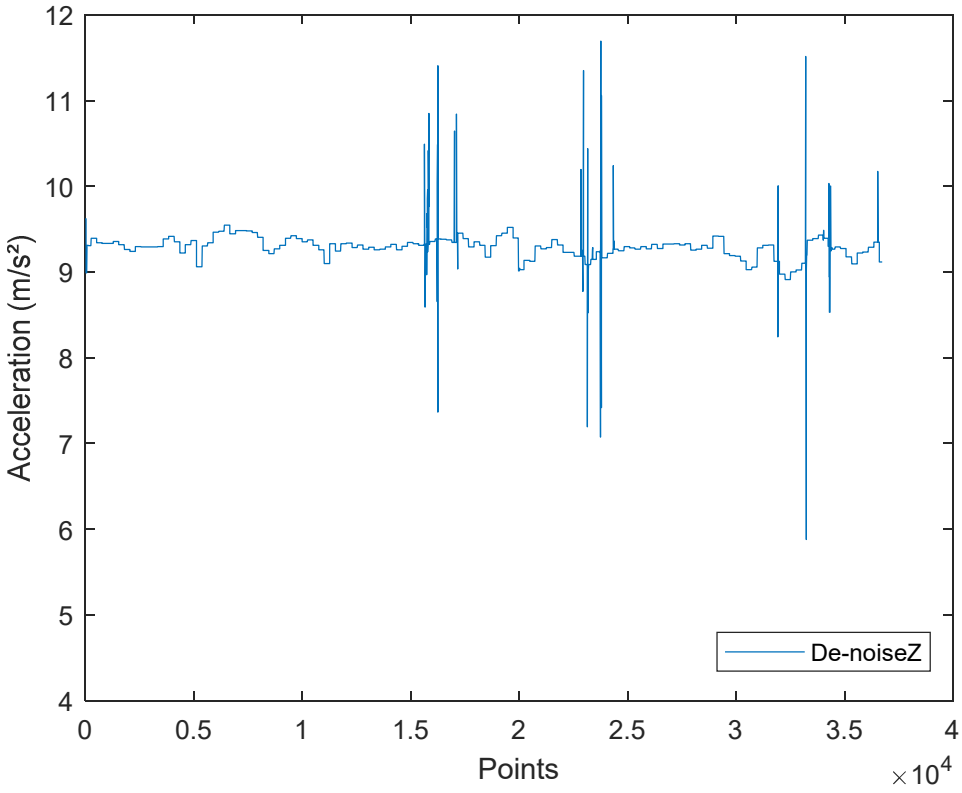

Figure 7-23 Wavelet de-noised result of Z axis of Route 1

Then the baseline of Z axis is extracted from the result of wavelet decomposition, as shown in Figure 7-24. So we get the Z axis without baseline drift as shown in Figure 7-25. Let the threadhold as:

Thd=speed.^2/100;

The coefficient is different from the expansion joint detection. That's because the test cars are different.

And using distance as the x axis, get the final result as shown in Figure 7-26.

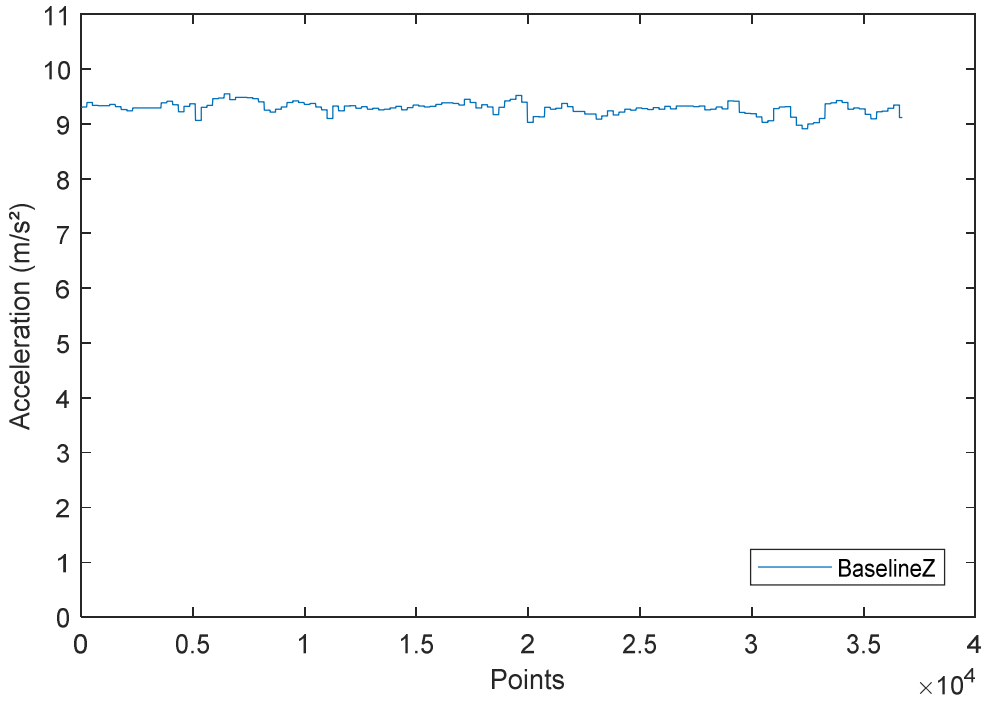

Figure 7-24 Baseline of Z axis of Route 1

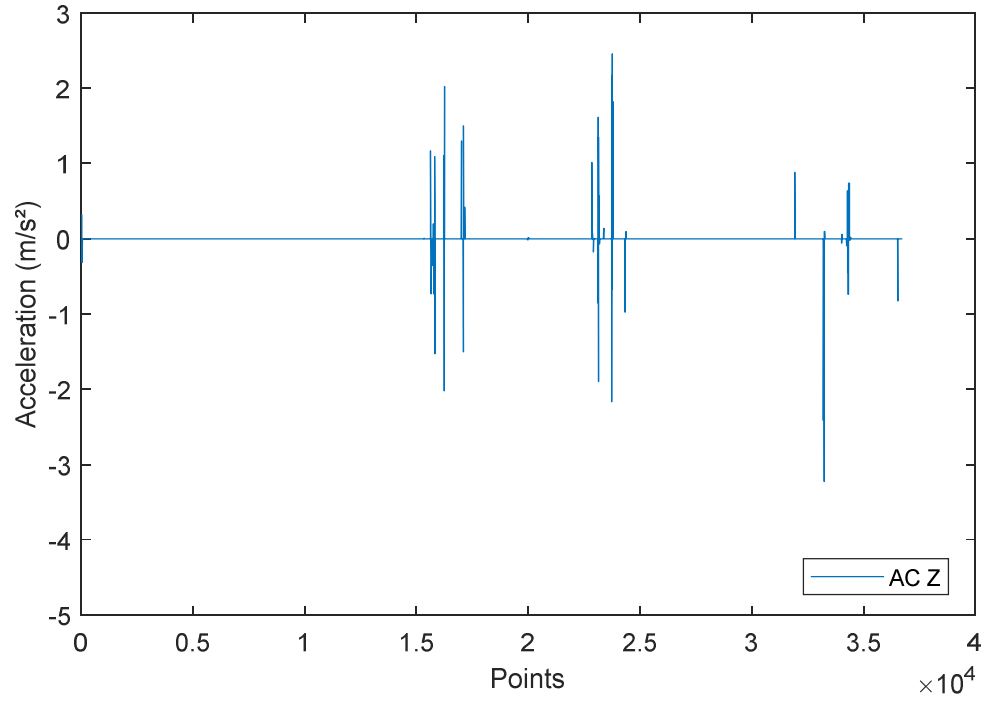

Figure 7-25 Z axis of Route without baseline

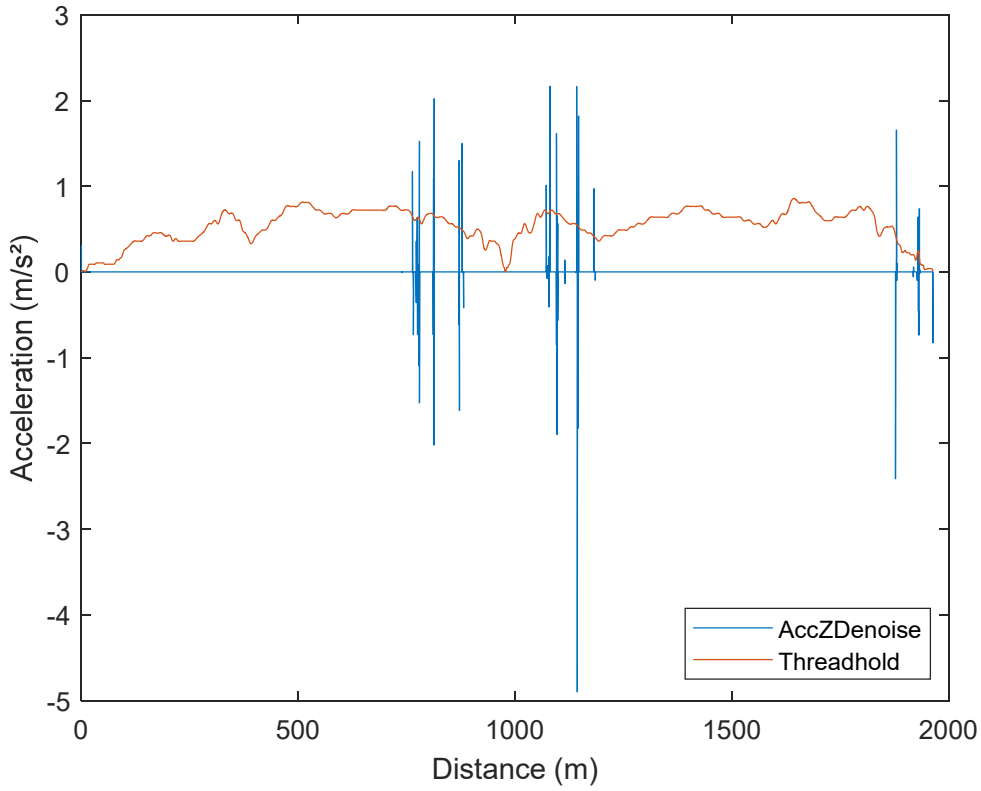

Figure 7-26 De-noised Z signal with threadhold. The x axis is distance

So we get the position of potholes.

Table 7-4 Detection result of Route 1

ID	Distance to the start point (m)
1	762.9
2	813
3	871
4	1072
5	Didn't check out
6	1143
7	1182
8	1779
9	1877
10	1928
11	1960

There is 1 pothole missed, the accuracy is 10/11=91%.

For full details of other 3 routes processing, please refer to Appendix .

To sum up, the detection result of all 4 routes shown as Table 7-5. We can see that there are 6 times missed, the total accuracy is 38/44=86.4%.

Table 7-5 The detection result of all 4 routes

ID	Distance to the start point (m)			
	Route 1	Route 2	Route 3	Route 4
1	762.9	758.6	762	755
2	813	Didn't check out	811	Didn't check out
3	871	869	873	863
4	1072	1078	1087	1086
5	Didn't check out	1102	1103	1103
6	1143	1149	1152	1152
7	1182	Didn't check out	1192	Didn't check out
8	1779	Didn't check out	1787	Didn't check out
9	1877	1882	1889	1887
10	1928	1930	1936	1923
11	1960	1958	1966	1935

7.5 Discussion

Seen from the above results of data processing, the original data is all with loud noise covering part or all of useful data. It is mainly because that when the vehicle is running, the sensor in the smartphone can not only detect signals of vibration from the vehicle caused by pothole but also noise from the road and noise caused by driver of the vehicle including engine and gearbox. The mix signals make it hard to detect the pothole signals in time domain. After wavelet denoising, the quality of signals becomes very good but with huge fluctuation in low frequency. The baseline drift may be caused by comprehensive reasons in many aspects in which the major possibility is the component of acceleration in the front-rear direction on axis Z of acceleration sensor during acceleration or deceleration. As three axes of the sensor in smartphone are not exactly parallel to that of the earth, it is hard to totally avoid the gentle baseline variation. This kind of baseline drift will make the threshold value used for detecting the pothole hard to be determined, so eliminating the baseline is very essential after denoising. In this experiment, the reusing of baseline after wavelet decomposition can not only achieve good result but also take advantage of the result in last step, which improves the processing efficiency. As the speed of vehicle is not a constant value in the experiment,

the accurate distance cannot be obtained by multiplying starting speed with experiment duration. The proper method is integral speed over time. Because GPS measures and stores the speed of vehicle up to once per second, the GPS data package is used in this study in order get accurate distance value from vehicle speed. The accurate distance value will help in obtaining accurate position of detected pothole. So here we use the speed provided by GPS data package. In the chapter for sensor, we have discussed it in detail and come to the conclusion: As the speed value directly adopts the calculation result of Doppler Effect, it is reliable with high accuracy and stability. Therefore the experimental result we get is accurate.

Chapter 8. Conclusion and Future Work

8.1 Conclusion and Prospects

8.1.1 Conclusion

In the Chapter 1, five questions are brought out:

1. In which way the traditional methods can be improved? Is there a new method that can exceed the traditional methods?
2. What equipments are required?
3. Which physical measurements should be kept?
4. What algorithm is required to analyse the data and obtain the result?
5. The new method should be proved to meet our goal.

With previous discussions in this thesis, all five questions can be answered:

1. In the Chapter 3 a new pothole detect method is carried out (for detail please refer to the following paragraph), comparing to the traditional methods, it is more efficient and has lower cost. Thus this new method is valuable and has good prospects;
2. As described in the Chapter 3, in this mew method a smart-phone with built-in acceleration sensor is required to be fixed in a vehicle. Especially, when a large number of vehicles have smart-phones with built-in acceleration sensors installed, the efficiency and accuracy of detection will be better than the traditional methods;
3. The new method will measure the acceleration of the vehicle while the vehicle is moving along the road;
4. The acceleration data is analysed by axis transformation, de-noise processing based on wavelet transform, please refer to the Chapter 3-6 for detailed description.
5. The smart-phone can read the acceleration data from its sensor do the analysis. In this way the pothole is detected. The whole process can be done by installing the app on smart-phone which is now very popular. In the Chapter 6, the new method is tested on the Tay Road Bridge. The result proved that, the new method can efficiently detect the potholes on the road. Therefore the new method does meet our goals.

In this paper, a dynamic threshold based on the instantaneous speed is proposed for the first time, which can improve the accuracy of detection, and experiments show high accuracy. The main problems encountered at this stage, is the need for a large number of experiments, through the acquisition and processing of different vehicles and

different traffic data, to obtain a large number of experimental data, to summarize the judgment threshold conditions under various conditions, in order to improve the detection of universality. In addition, it will be helpful to fuse the acceleration sensor data and the gyroscope data together to improve the stability and reliability of the pothole detection.

8.1.2 Future work and considerations

The following progresses are worthy of note.

1. Due to time constraints, app used herein is from the third party, it can only collect sensor data and stored in the phone's functions, we need to import data into the phone after post-processing of the data is pending completion of the experiment the computer to complete in the laboratory. So in the future a new app should be designed and implemented in order to achieve a full-fledged app all the features we need, these features include: collecting sensor data, process data and send the results to the server through wireless network (such as 3G/4G/Wi-Fi).
2. Design and implement server-side software functions, which should include: receiving mobile client app sent to deal with complete data and store in database, and compare with the road network data and uploaded data with other mobile phone to ensure the credibility of the data, and to notify the user by some easy ways.
3. Process the data in order to obtain a result of this step is completed either on the phone side, or can be placed on the server side, both have their advantages and disadvantages, from the care of the user's point of view, it should work to minimize the mobile phone amount, so the large amount of data processing work on the server side may be reasonable, but it should also take into account the load capacity of the server.
4. The threshold used in pothole detection should not be fixed, it should be related with the vehicle model. Therefore, the vehicle model should either can be input manually by the user, or mobile phone should be able to obtain these parameters through ODB-II port or some other vehicle communication interface automatically.

As discussed in Chapter 7, comparing the detection result with real pothole data of the Tay Road Bridge, it shows that the pothole detection on smartphone has good accuracy. Comparing with traditional detection methods in Chapter 2, this new method has advantage of high efficiency, high detection speed and low cost. In addition it is purely

automatic for the smartphone user. This method is suitable for promoting for large-scale application with proper operating design.

8.2 Design of Operating Mode

The design has two goals to achieve: 1.Covering road segment as much as possible (wherever there is road segment opened for vehicles, there is also data); 2. Refreshing data quickly (whenever there is new information of pothole, there should be reflected in the result in first time); the ideal situation would be that all the vehicles driving on the road is providing data for our system which means all vehicles is installed smartphone collecting and sending data. Of course, this is only an extreme ideal condition, the precondition must be there are enough vehicles as “inspection vehicle” if wanting the system run in high efficiency and get favorable effect. Thus, one issue that appears when considering the operating mode is: how to attract customers to use this software and make them willing to provide data for us?

First, what can be sure is that this software will not bring too much negative effects and burdens. Today, almost all OS of smartphone has the ability of running multitasks in parallel, therefore such software program without any running interface (start-up interface and control interface are certainly possible, but simplified control can be made completely) but only can be run in the background hardly causes any interference to the operation of the user, moreover for single driver, manipulating mobile phone in the process of driving originally should have been forbidden. The only thing may be affected is that the program will consume more power when running in the background, and invoke all sensor, control transmission of 3G module, receive power from data, increasing power consumption of mobile phone and shorting stand-by time. As for extent of affection, different result is from the different mobile phone. Further analysis is as follows:

1. CPU: nowadays, the CPU of the vast majority of smartphone, based on ARM kernel, has automatic power dissipation control functions and optimization function, and power dissipation of CPU can be adjusted while operating on the basis of load. This program, part of light load (sampling is only 100-150times per second, and there hardly is other treatments), has little effect on power dissipation; CPU of many new smartphone has two kernels, of which one is used for handling high performance computing and anther is used for bearing few calculations at very low power consumption. Since this

framework is able to further reduce power consumption, so it is very suitable for this program.

2. Transducer: today, almost power consumption of all acceleration sensor, gyroscope sensor is very low, which is mainly decided by their design proposal and processing technic.

3. Wireless communication module: this module is comparatively current consuming when working, and the current routinely is 6mA/12V. While since the data transmission speed of 3G/4G is so fast that we can store the collected data in memory as temporary storage and sends it out when accumulating to certain volume. With data volume of one hour, for example, saving 60X60X150 acceleration sensors, 60X60X150 gyroscopes, 60X60 GPS/speeds and data (4338000 data points totally) will takes space of 16MB totally on the basis of each data takes 4 bytes; it will takes 16000X8/200=640S (about 11 minutes) to complete uploading work on the basis of each data takes 4 bytes, with upload speed of 200kb, which needs to consume little power. If applying data compression technic or using 4G network to transmit in the future, the power consumption can be reduced further.

4. GPS receiver: generally, GPS is comparatively current consuming, while the power consumption of new GPS has already been improved.

But it is noticed that many users would make SATNAV by using smartphone in the long journey, which requires users to activate GPS module installed in smartphone itself, thus this program will not increase extra power consumption, and only needs GPS module to transmit measured data to STANAV software and itself.

In a word, when using smartphone, according to statistics, about 30%-40% power consumption can be displayed on screen, and about 30% power is consumed on connection of internet application, and the rest 1/3 is used for other software and processes.

Besides, most of the vehicles is equipped with vehicle-mounted charger (elicited by cigarette lighter or USB interface) so as to charge for mobile phone at any moments, and drivers also pay more attention when making SATNAV which is application with high power consumption by using mobile phone, so this is not a problem at all.

While just no harm is not enough. What need to do is to encourage users to install and use the software and make users benefit from use. The concrete implementation plan, of course, also need to be further planned, but since the system can achieve high-precision pothole maps, the driver should be informed of such information, from which

driver can benefit. When software, for example, perceives that the vehicle will soon cross a known area ahead where may have pothole, which can be broadcasted with the voice prompt. Software also can prompt the driver to pay attention to the road conditions and further broadcast the size or severity of the possible pothole so that the driver can take avoidance or deceleration measures timely. As long as the data is sufficient and valid and the rate of false alarm rate is low enough, I believe there will be a lot of users would use it. Meanwhile as the number of users increases, it will, in turn, promote the collected data further more detailed and timely, so the result will be more accurate. This will form a virtuous circulation.

Software can also add other functions to attract users, for example, voice broadcast warning information of an accident in front of the road, or the weather alerts, the wet and slippery road.

There is a type of important users who own moderate-load vehicles or heavy-load vehicles, and the most typical representative is the operating vehicle, including taxi, freight car, bus, etc. Running time of these vehicles on the road is much longer than that of general private cars, thus they can provide more data. Cooperation agreement can be reached with these vehicles' operating company to install this system on the vehicles, thus the efficiency of collecting data will be much higher. Certainly, the running time of taxi on the highway is less, and other vehicles mostly belonging to medium or large vehicles whose frequency responses are different from those of small cars. Proprietary software can be developed for specific models, and specific model parameters will be written fixedly to software in the future. Because vehicle models can match with collecting equipment, therefore, it is feasible to do so. Meanwhile, this method is provided with advantages of low costs but significant benefits.

This paper focus on the academic category such as technology and the algorithm of the project, while with respect to business model and operation mode the paper just conducted the preliminary design and discussion. Specific idea on this aspect can be cooperatively studied and implemented with relevant experts in the future.

So we can assume some future development trend:

1. Software will replace hardware;
2. Generality will replace specificity;
3. Service will replace purchase;
4. The cloud mode will replace local mode;

5. Big data integration will replace stand-alone device;
6. Free will replace payment (to the final customers);
7. Intelligent will replace non-intelligence.

8.3 Future works on real pothole detection methods

In this thesis, firstly the feasibility of pothole detection using smartphone is discussed. Then expansion joint is chosen as simplified pothole. The vehicle runs through expansion joint, and data is gathered by smartphone at the same time. Then various vehicle models are discussed, based on which data is analysed. The data analysis gives initial result. There are more work to be done in future, including:

1. Many parameters used in signal processing, including threshold of each order of wavelet filter and threshold of pothole judgment, are related to parameter of individual vehicle (such as suspension, tyre, etc.), which are obviously different for different vehicles. The algorithm should be able to calculate vehicle parameters by analysing sensor data, and then use these parameters to modify thresholds;
2. In this study, the smartphone is considered fixed on vehicle. However the smartphone may be anywhere in the vehicle, such as inside pocket, in real life. In addition, the smartphone may vibrate in different frequency from the vehicle if it is not properly fixed. To avoid the error, a better axis correction method needs to be considered;
3. Roads in real life are not all straight and flat. The accuracy of axes transformation is easily affected by turnings and slopes. In order to enable the detection method to deal with turnings and slopes, two improvements are required. One improvement is to continuously detect the direction of gravity to know whether the downward direction of vehicle is changed during driving. The other one is to calculate rotation of vehicle by integrate data gathered by gyroscope (which is angular velocity), so that change of the road direction including turnings and slopes can be mapped to three axes.
4. Some widely used wavelet basis and filter methods are used in this study due to limit of time. Although they are proved to be effective, a better result may be achieved with other wavelets. Also other filter methods may lead to higher signal-noise ratio or a decreased amount of calculation. More experiments are needed to get a balance between accuracy and calculation speed;
5. The data used in this study is gathered by third party applications, and processed by MATLAB. In future, an application should be designed to implement the data collection and processing functionality. The design and implementation of this

application should be carefully planned, including prephase investigation, requirement analysis, sub-system division, implementation, version control etc. Apart from that, in order to test and optimise the application, the value of parameters used in signal processing, including threshold of each order of wavelet filter and threshold of pothole judgment should be able to be modified during the running of application. Also the application should be able to display intermediate data to developers;

6. The data collection and processing application is part of whole pothole detection system. The result should be uploaded to a server, in which the data from all smartphone is stored and analysed, so that the wrong data can be filtered to provide more accurate result.

Reference

1. Aleksander Hać, Iljoong Youn. Optimal Semi-Active Suspension with Preview Based on a Quarter Car Model[J]. Journal of Vibration & Acoustics, 1992, 114(1):433 - 438.
2. Acosta, J. Adolfo, J. Ludwig Figueroa, and Robert L. Mullen. "Low-cost video image processing system for evaluating pavement surface distress." *Transportation research record* 1348 (1992).
3. Andrew, Andrew AS, and B. R. Colford. "Forth Road Bridge-maintenance challenges." In *Advances in Cable-Supported Bridges: Selected Papers, 5th International Cable-Supported Bridge Operator's Conference, New York City, 28-29 August, 2006*, p. 57. CRC Press, 2006.
4. Bakker, Egbert, Lars Nyborg, and Hans B. Pacejka. Tyre modelling for use in vehicle dynamics studies. No. 870421. SAE Technical Paper, 1987.
5. Barone, Martin R. *Impact vibrations of rolling tires*. No. 770612. SAE Technical Paper, 1977.
6. Bhoraskar, Ravi, Nagamanoj Vankadhara, Bhaskaran Raman, and Purushottam Kulkarni. "Wolverine: Traffic and road condition estimation using smartphone sensors." In *Communication Systems and Networks (COMSNETS), 2012 Fourth International Conference on*, pp. 1-6. IEEE, 2012.
7. Bujari, Armir, Bogdan Licar, and Claudio E. Palazzi. "Movement pattern recognition through smartphone's accelerometer." In *Consumer communications and networking conference (CCNC), 2012 IEEE*, pp. 502-506. IEEE, 2012.
8. Cadenas, Alejandro, José María González, and Oscar M. Solá. "Context-aware processing of mobile device sensor information: Car accident detection hosted service." In *Consumer Communications and Networking Conference, 2009. CCNC 2009. 6th IEEE*, pp. 1-5. IEEE, 2009.
9. Carter, Matt, Steve Kite, Naeem Hussain, Alan Seywright, Mike Glover, and Billy Minto. "Forth Replacement Crossing: Scheme design of the bridge." In*IABSE Symposium Report*, vol. 96, no. 6, pp. 107-116. International Association for Bridge and Structural Engineering, 2009.
10. Cheng, Heng-Da, and Mario Miyojim. "Automatic pavement distress detection system." *Information Sciences* 108, no. 1 (1998): 219-240.
11. Chen, Jia, et al. "Fatigue detection based on facial images processed by difference algorithm." *Biomedical Engineering (BioMed), 2017 13th IASTED International Conference on*. IEEE, 2017.
12. Chen Long, Zhang Xiaoliang, Nie Jiamei and Wang Ruochen. "Performance Analysis of Two-stage Series-connected Inerter-spring-damper Suspension Based on Half-car Model." *Journal of Mechanical Engineering*, no. 6 (2012):102-108.
13. Colford, Barry R. "Forth Road Bridge—maintenance and remedial works."*Proceedings of the ICE-Bridge Engineering* 161, no. 3 (2008): 125-132.
14. Dupont, Edmond M., Carl A. Moore, Emmanuel G. Collins Jr, and Eric Coyle. "Frequency response method for terrain classification in autonomous ground vehicles." *Autonomous Robots* 24, no. 4 (2008): 337-347.
15. ElMadany, Mohamed M. "Control and evaluation of slow-active suspensions with preview for a full car." *Mathematical Problems in Engineering* 2012 (2012).
16. Eriksson, Jakob, Lewis Girod, Bret Hull, Ryan Newton, Samuel Madden, and Hari Balakrishnan. "The pothole patrol: using a mobile sensor network for road surface monitoring." In *Proceedings of the 6th international conference on Mobile systems, applications, and services*, pp. 29-39. ACM, 2008.
17. Fan, ZHENG, YU Jiang, PEI Yi-jian, and Xiao Min. "The Co-simulation of mobile robot surmounting obstacles based on ADAMS-MATLAB."*Journal of Yunnan University (Natural Sciences Edition)* (2007): S2.
18. Fukuhara, Toshihiko, Keiji Terada, Makoto Nagao, Atsushi Kasahara, and Shigeki Ichihashi. "Automatic pavement-distress-survey system." *Journal of Transportation Engineering* 116, no. 3 (1990): 280-286.
19. Furuichi, Takahisa, and Hideo Sakai. *Dynamic cornering properties of tires*. No. 780169. SAE Technical Paper, 1978.
20. Gao, Wei, Nong Zhang, and H. P. Du. "A half-car model for dynamic analysis of vehicles with random parameters." In *5th Australasian Congress on Applied Mechanics (ACAM 2007)*, vol. 1, pp. 595-600. Engineers Australia, 2007.
21. GAO, Zhen-hai, Nan-ning ZHENG, and Hong Cheng. "Soft sensor of vehicle state based on vehicle dynamics and kalman filter." *Acta Simulata Systematica Sinica* 1 (2004): 007.
22. Georgopoulos, A., A. Loizos, and A. Flouda. "Digital image processing as a tool for pavement distress evaluation." *ISPRS Journal of Photogrammetry and Remote Sensing* 50, no. 1 (1995): 23-33.

23. GUAN, Xin, Su-min ZHANG, Zhen-hai GAO, and Jun ZHAN. "Vehicle State Estimation Using Automobile Dynamic Model with 7DOFs." *Science Technology and Engineering* 16 (2010): 017.
24. Guangqiang, Wu, and Fang Yuan. "T ime-domain simulation and analysis of vehicle ride comfort." *Automobile Technology* 2 (2007): 8-11.
25. Hesami, Reyhaneh, and Kerry J. McManus. "Signal processing approach to road roughness analysis and measurement." In *TENCON 2009-2009 IEEE Region 10 Conference*, pp. 1-6. IEEE, 2009.
26. Hou, Xiangshen, Hua Wang, Qi Wang, and Zheren Wang. "Development of automated inspection system for highway surface distress." In *Fundamental Problems of Optoelectronics and Microelectronics III*, pp. 65951Y-65951Y. International Society for Optics and Photonics, 2007.
27. Huan-yao, D. A. I. "Application and Study of Matlab on Time-frequency Analysis of Signal [J]." *Modern Machinery* 5 (2005): 000.
28. Hunt, H. E. M. "Modelling of road vehicles for calculation of traffic-induced ground vibration as a random process." *Journal of Sound and Vibration* 144, no. 1 (1991): 41-51.
29. Hunt, H. E. M. "Stochastic modelling of traffic-induced ground vibration." *Journal of Sound and Vibration* 144, no. 1 (1991): 53-70.
30. Huston, Dryver R., Noel V. Pelczarski, Brian Esser, and Kenneth R. Maser. "Damage detection in roadways with ground penetrating radar." In *8th International Conference on Ground Penetrating Radar*, pp. 91-94. International Society for Optics and Photonics, 2000.
31. Jiang Liangwei, Yao Lingkan, Wu Wei. "Study on Calculation of Dynamic Displacement from Time Integration of Acceleration in Shaking Table Model Tests of Side Slope." *Journal of Disaster Prevention and Mitigation Engineering*, 29 no. 3 (2009): 261-266.
32. Jiali, Wang, Jiang Li, and Liu Hong. "Auto static calibration of multi-axis force sensor based on triaxial accelerometer." *Chinese Journal of Scientific Instrument* 29, no. 2 (2008): 432.
33. LI, Wen-liang, Wei ZHOU, Zhi-ping GUO, and Kan ZHAO. "Safety Dynamic Simulation Study on Car Impact against the High Curb." *Tractor & Farm Transporter* 2 (2008): 010.
34. Lin, Jin, and Yayu Liu. "Potholes detection based on SVM in the pavement distress image." In *Distributed Computing and Applications to Business Engineering and Science (DCABES), 2010 Ninth International Symposium on*, pp. 544-547. IEEE, 2010.
35. Lin, Paul P., Maosheng Ye, and Kuo-Ming Lee. "Intelligent observer-based road surface condition detection and identification." In *Systems, Man and Cybernetics, 2008. SMC 2008. IEEE International Conference on*, pp. 2465-2470. IEEE, 2008.
36. LU, Zheng, Hai-lin YAO, and Zhi HU. "Dynamic response analysis of rough pavement under vehicle-road system coupled vibration." *Chinese Journal of Geotechnical Engineering* (2013): S1.
37. Mathur, Suhas, Tong Jin, Nikhil Kasturirangan, Janani Chandrasekaran, Wenzhi Xue, Marco Gruteser, and Wade Trappe. "Parknet: drive-by sensing of road-side parking statistics." In *Proceedings of the 8th international conference on Mobile systems, applications, and services*, pp. 123-136. ACM, 2010.
38. Mednis, Artis, Girts Strazdins, Reinholds Zviedris, Georgijs Kanonirs, and Leo Selavo. "Real time pothole detection using android smartphones with accelerometers." In *Distributed Computing in Sensor Systems and Workshops (DCOSS), 2011 International Conference on*, pp. 1-6. IEEE, 2011.
39. Mohajeri, M. Jerry H., and Patrick J. Manning. "ARIA (TRADEMARK): AN OPERATING SYSTEM OF PAVEMENT DISTRESS DIAGNOSIS BY IMAGE PROCESSING." *Transportation Research Record* 1311 (1991).
40. Mohan, Prashanth, Venkata N. Padmanabhan, and Ramachandran Ramjee. "Nericell: rich monitoring of road and traffic conditions using mobile smartphones." In *Proceedings of the 6th ACM conference on Embedded network sensor systems*, pp. 323-336. ACM, 2008.
41. Monti, Max. "Large-area laser scanner with holographic detector optics for real-time recognition of cracks in road surfaces." *Optical Engineering* 34, no. 7 (1995): 2017-2023.
42. Nejad, Fereidoon Moghadas, and Hamzeh Zakeri. "A comparison of multi-resolution methods for detection and isolation of pavement distress." *Expert Systems with Applications* 38, no. 3 (2011): 2857-2872.
43. Pacejka, Hans B. "Tyre factors and vehicle handling." *International journal of vehicle design* 1, no. 1 (1979): 1-23.
44. Perttunen, Mikko, Oleksiy Mazhelis, Fengyu Cong, Mikko Kauppila, Teemu Leppänen, Jouni Kantola, Jussi Collin et al. "Distributed road surface condition monitoring using mobile phones." In *Ubiquitous Intelligence and Computing*, pp. 64-78. Springer Berlin Heidelberg, 2011.
45. Promwongsa, Nattakorn, Pramookh Chaisatsilp, Supawat Supakwong, Chalermpol Saiprasert, Thunyasit Pholprasit, and Passakon Prathombutr. "Automatic accelerometer reorientation for driving event detection using smartphone." In *13th ITS Asia Pacific Forum, Auckland, New Zealand*. 2014.

46. Ravi, Nishkam, Nikhil Dandekar, Preetham Mysore, and Michael L. Littman. "Activity recognition from accelerometer data." In *AAAI*, vol. 5, pp. 1541-1546. 2005.
47. RIBEIRO, Josh GT, Jaime TP DE CASTRO, and Josh LF FREIRE. "Filtering in frequency domain to avoid time aliasing." In *SPIE proceedings series*. Society of Photo-Optical Instrumentation Engineers, 2002.
48. Sayers, Michael W. "The little book of profiling: basic information about measuring and interpreting road profiles." (1998).
49. Scavuzzo, Richard W., Timothy R. Richards, and L. T. Charek. "Tire vibration modes and effects on vehicle ride quality." *Tire Science and Technology* 21, no. 1 (1993): 23-39.
50. Strazdins, Girts, Artis Mednis, Georgijs Kanonirs, Reinholds Zviedris, and Leo Selavo. "Towards vehicular sensor networks with android smartphones for road surface monitoring." In *2nd international workshop on networks of cooperating objects, Chicago, USA*. 2011.
51. Tai, Yu-chin, Cheng-wei Chan, and Jane Yung-jen Hsu. "Automatic road anomaly detection using smart mobile device." In *conference on technologies and applications of artificial intelligence, Hsinchu, Taiwan*. 2010.
52. Takayama, Masahiro, and Koichi Yamagishi. "Simulation model of tire vibration." *Tire Science and Technology* 11, no. 1 (1983): 38-49.
53. Tao, Yin, et al. "Study of a new amblyopia diagnostic and therapeutic method along with the system implementation." *Biomedical Engineering (BioMed), 2017 13th IASTED International Conference on*. IEEE, 2017.
54. Wang, Kelvin CP, and Omar Smadi. "Automated imaging technologies for pavement distress surveys." *Transportation Research E-Circular* E-C156 (2011).
55. WANG, Qian-ting, Qi-zhong YI, and Yong-nan LIN. "Relation Between Off-road Terrain Unevenness and Wheel Jumping Estimation [J]." *Journal of System Simulation* 11 (2008): 061.
56. Wei, Liu, T. F. Fwa, and Zhao Zhe. "Pavement roughness analysis using wavelet theory." In *In Proceedings from the 6th International Conference on Managing Pavements. Queensland, Australia*. 2002.
57. Whiffin, A. C., and D. R. Leonard. *A survey of traffic induced vibrations*. No. Lr 418. 1971.
58. Wu, yanping, Dongyan Wu, Xu Xiem and Xu Zhang. "Response and vibration control of steel box-girder bridge when vehicles passing through the expansion joint [J]." Noise and Vibration Control. 2 (2013): 021.
59. Xiaoya, Chen Weizhen Wang Bingwen Hu. "Acceleration signal processing by aumerical integration [J]." *Journal of Huazhong University of Science and Technology (Nature Science Edition)* 1 (2010): 000.
60. XIE, Xu, Dong-yan WU, Jian-feng WANG, Shi-qi ZHANG, and Yong-jie ZHOU. "Dynamical behavior of steel box girder bridges due to vehicle-induced vibration at expansion joint [J]." *Journal of Zhejiang University (Engineering Science)* 10 (2009): 029.
61. Xu, Zhi, Kun Bai, and Sencun Zhu. "Taplogger: Inferring user inputs on smartphone touchscreens using on-board motion sensors." In *Proceedings of the fifth ACM conference on Security and Privacy in Wireless and Mobile Networks*, pp. 113-124. ACM, 2012.
62. Yan, A. Z., and H. Y. Zhou. "Mathematical model of the step road and analysis on the response of two DOF vehicle model." *Journal of Henan Polytechnic University(Natural Science)* 30, no. 1 (2011): 113-117.
63. Yang Xiaofeng, Yang, Li Peng, Zhang Xin, Bian Zhengzhong, and Wang Bo. "De-Noising of the doppler fetal heart rate signal with wavelet threshold filtering based on spatial correlation." In *Bioinformatics and Biomedical Engineering, 2007. ICBBE 2007. The 1st International Conference on*, pp. 928-931. IEEE, 2007.
64. ZHANG, Hong-liang, H. U. Chang-shun, and G. A. O. Jiang-ping f Education. "Parameters' Influence on Determination of Allowable Differential Settlement between Bridge and Approach Embankment." *Journal of Highway and Transportation Research and Development* 3 (2005): 012.
65. Zhang, Hong-Liang. "Determination of allowable differential settlement between bridge abutment and approach embankment with five-degree-of-freedom vehicle model." *International Journal of Pavement Research and Technology* 3, no. 6 (2010): 311-319.

Appendix A: Detailed deduction process of bounce height h without considering energy loss in tyre simulation

In Section 5.2, after the collision, the velocity has changed its direction form heading to the right horizontally to v', with the same magnitude, i.e. $|v| = |v'|$. At this point, the direction of v' is tangent to the circumference. That is to say, v' has a component of v'_x horizontally, and a component of v'_y vertically, vertically upward. Since v'_x and v'_y are perpendicular; the included angle β formed by v' with x axis is equal to $\angle AOB$, i.e. angle α. Therefore, the two triangles shown in the figure are similar. It can be concluded that

$$\frac{R}{\overline{CB}} = \frac{v'}{v_y'} \tag{A.1}$$

Since C is located in the middle of AB,

$$\overline{CB} = \frac{\overline{AB}}{2} = \frac{w}{2} \tag{A.2}$$

Put in the formulas above and the following can be obtained

$$v_y' = \frac{v'w}{2R} \tag{A.3}$$

Since only magnitude of v'_y is required and $|v| = |v'|$, therefore

$$v'_y = \frac{vw}{2R} \tag{A.4}$$

According to the law of conservation of energy, the gross energy before motion shall be equal to that after motion, that is to say, the sum of the kinetic energy and potential energy shall be conservative before and after motion:

$$\frac{1}{2}mv_1^2 + mgh_1 = \frac{1}{2}mv_2^2 + mgh_2 \tag{A.5}$$

In case of taking no account of the energy loss, before the tyre bounces vertically, it has an upward initial velocity equalling to v'_y and at the same time, the potential energy is assumed as 0. After the tyre bounces, the kinetic energy converts into potential energy; the vertical velocity at the highest point is 0, namely the kinetic energy is also 0, so that the kinetic energy fully converts into potential energy. Therefore,

$$\frac{1}{2}mv_y'^2 = mgh \tag{A.6}$$

So the bouncing height is

$$h = \frac{v_y'^2}{2g} \tag{A.7}$$

Therefore

$$h = \frac{v^2 w^2}{8gR^2} \tag{A.8}$$

Appendix B: Detailed deduction process of bounce height h with considering energy loss in tyre simulation

In Section 5.2, when considering energy loss, therefore

$$v' = C_r \cdot v < v \tag{B.1}$$

That is to say, the initial velocity is smaller than that of the incidence. Assume the kinetic energy of incidence is $\frac{1}{2}mv^2$, after rebounding, it is $\frac{1}{2}mv'^2$, and both the potential energy of incidence and bouncing are both 0, therefore, the kinetic energy is equal to the mechanical energy, and therefore, the energy lost is

$$k = \frac{1}{2}mv^2 - \frac{1}{2}mv'^2 = \frac{1}{2}m(1 - C_r{}^2)v^2 \tag{B.2}$$

After collision, along with the rising height of tyre, the vertical kinetic energy completely converts into potential energy after rebounding, therefore

$$h = \frac{v'^2\, w^2}{8gR^2} = \frac{C_r{}^2 v^2 w^2}{8gR^2} \tag{B.3}$$

Appendix C: Deduction process of PCA

In Section 6.1, let

$$\begin{aligned} Y^T &= X^T W \\ &= V \sum {}^T W^T W \\ &= V \sum {}^T \end{aligned} \tag{C.1}$$

When m<n-1, generally V is not uniquely defined but Y is. W is an orthogonal matrix, Y^T is the transposition of X^T, and the first row of which is made up of the first principle component, the second row is made up of the second principle component, and so forth. To obtain an effective method to reduce data dimension, we could map X to a low dimensional space only using the former L pieces of vectors.

$$\begin{aligned} Y = W_L^T X &= \sum\nolimits_L V^T \text{ where } \sum\nolimits_L \\ &= I_{L\times m} \sum \text{ with } I_{L\times m} \text{ the } L\times m \text{ rectangular identity matrix} \end{aligned} \tag{C.2}$$

W, as a single vector matrix of X, is also equivalent to the eigen vectors $C=XX^T$ of covariance matrix,

$$XX^T = W \sum \sum {}^T W^T \tag{C.3}$$

Appendix D: Time domain integral method

In Section 6.2.1, the velocity is obtained after the first single integration of acceleration data

$$v(t) = \int a(t)dt = \int (f(t) + T)dt = \int f(t)dt + T_t + X \tag{D.1}$$

The displacement is obtained in the second integral:

$$s(t) = \int v(t)dt = \int [\int f(t)dt]dt + 0.5T_t^2 + X_t + \lambda \tag{D.2}$$

The derivation of equations 6-6 and 6-7 shows that error term increases as time of integral increases, which cause large error in integral result. Therefore the acceleration signal needs to be de-noised and the DC component needs to be removed before acceleration signal is integrated in the time-domain. Generally, the DC component of the signal is estimated by mathematical expectation (mean value), i.e.

$$\overline{a} = \frac{1}{N}\sum_{i=0}^{X} a^i \tag{D.3}$$

After the DC component is removed, the acceleration signal turns to:

$$a' = a_i - \overline{a} \tag{D.4}$$

Then Simpson integral is used:

$$v = \frac{\Delta t}{6}\sum_{i=2}^{N}(a'_{i-2} + 4a'_{i-1} + a'_i) \tag{D.5}$$

Appendix E: Frequency domain integral method

In the process of frequency-domain integral, the signal is processed by Fourier transform before the integral. According to the integral feature of Fourier transform

$$F\left|\int_{-\infty}^{t} f(t)dt\right| = \frac{1}{ik}F[f(t)] \tag{E.1}$$

In which F means Fourier transform - Fourier transform should be processed when obtain speed signal and displacement signal from the integral of acceleration signal and then perform Fourier inverse transformation and take the real parts of results, thus can get time-domain speed signal and displacement signal. Taking Fourier transform of acceleration signal will get

$$A(k) = \sum_{n=0}^{N-1} a_n e^{-i2\pi k\frac{n}{N}} \tag{E.2}$$

Fourier transform of speed can be obtained after the first integral:

$$V(n) = \frac{A}{jk} = \sum_{k=0}^{N-1} \frac{1}{j2\pi k\Delta f} H(k) a_n e^{-j2\pi k\frac{n}{N}} \tag{E.3}$$

Fourier transform of displacement can be obtained after the second integral:

$$S(n) = -\frac{1}{k^2}A = \sum_{k=0}^{N-1} \frac{1}{-(2\pi k\Delta f)^2} H(k) a_n e^{-i2\pi k\frac{n}{N}} \tag{E.5}$$

Where

$$H(k) = \begin{cases} 1, f_d \le kf \le f_u \\ 0, else \end{cases} \tag{E.6}$$

In equation E.5, symbol Δf is frequency resolution, and f_d and f_u are the upper and lower limits of cut-off frequency respectively. N is number of points in data, and k is the frequency of Fourier component.

Appendix F: DFT and FFT

DFT of N point sequence $x(n)$ can be expressed as:

$$X(k) = \sum_{n=0}^{N-1} x(n) W_N^{\pi k} \tag{F.1}$$

In which

$$W_N = e^{-j\frac{2\pi}{N}}$$

The coefficient $\left\{W_N^{nk}\right\}$ is periodic

$$W_N^{nk} = W_N^{k(\pi+n)} = W_N^{(k+N)n} \tag{F.2}$$

Thus some items in DFT operation can be merged. Using $W_N^{k\pi+\frac{n}{2}} = -W_N^{kn}$ (symmetry) and periodicity, DFT of long sequences can be decomposed into DFT of short sequences.

Appendix G: MATLAB source code of FFT noise reduction processing procedure

. The FFT noise reduction processing procedure in MATLAB is as following:

```
t=0:0.001:2;
x=cos(2*pi*t);
y=x+0.25*randn(1,length(t));
subplot(1,2,1);
plot(y);
axis([0,2000,-1.5,1.5]);
Y=fft(y);Y=abs(Y);
index2=50:1950;
Y(index2)=zeros(size(index2));
X=ifft(Y);X=real(X);
subplot(1,2,2);
plot(X);
axis([0,2000,-1.5,1.5]);
```

Appendix H: Deduction process of wavelet

Definition of wavelets transform: assume $\psi(t) \in L(R) \cap L^2(R)$, $\hat{\psi}(\omega)$ means its Fourier transform, if $\hat{\psi}(\omega)$ satisfies the following conditions (Wei et al., 2002):

$$C_\psi = \int_K \frac{\left|\hat{\psi}(\omega)^2\right|}{\omega} d\omega < \infty \tag{H.1}$$

Then $\psi(t)$ is called basic wavelet. Through dimension scaling and translation, $\psi(t)$ generates the following function family:

$$\psi_{ab} = |a|^{-\frac{1}{2}} \psi\left|\frac{t-b}{a}\right| \qquad a \in R, a \neq 0, b \in R \tag{H.2}$$

It is called continuous wavelets generated by $\psi(t)$, of which a is called scale parameter, and b is translation parameter.

Under the discrete condition, wavelets sequence is:

$$\psi_{j,k}(t) = 2^{-j/2} \psi\left(2^{-j} t - k\right) \qquad j, k \in z \tag{H.3}$$

According to the allowable conditions, when $\omega = 0$, in order to ensure integrand as effective value, there must be $\hat{\psi}(0) = 0$, so equivalent condition obtained from equation above is

$$\hat{\psi}(0) = \int_{-\infty}^{\infty} \psi(t) dt = 0 \tag{H.4}$$

This equation shows that there is no direct component included in $\psi(t)$, in which only alternating component, namely unsteady , so it is called “wave”.

In order to make $\psi(t)$ has locality (namely attenuating quickly to zero outside of limited interval), it has to be added one attenuation condition

$$|\psi(t)| \leq \frac{c}{(1+|t|)^{1+\varepsilon}} \qquad \varepsilon > 0, c > 0 \tag{H.5}$$

The implication is: when $t \to \pm\infty$, attenuation speed of $|\psi(t)|$ is faster than that of $\frac{1}{|t|}$, attenuation condition urges wavelets must have locality. This locality is called “small” that “wavelets” derives its name from it. Wavelet transform is defined as:

$$w_f(a,b) = \int_R f(t) \overline{\psi_{a,b}(t)} dt = |a|^{-1/2} \int_R f(t) \overline{\psi\left(\frac{t-b}{a}\right)} dt \tag{H.6}$$

Reverse transform is:

$$f(t)=\frac{1}{C_{\psi}}\int_{R}\int_{R}\frac{1}{a^{2}}W_{f}(a,b)\psi\left(\frac{t-b}{a}\right)dadb \tag{H.7}$$

Among them, a is as scale factor, b reflects displacement.

Appendix I: Tay Road Bridge Data processing: Route 2 to 5

A, Data of Route 2

This piece of data is with 30,000 points from point 145,001 to 175,000. Firstly, process the acceleration data:

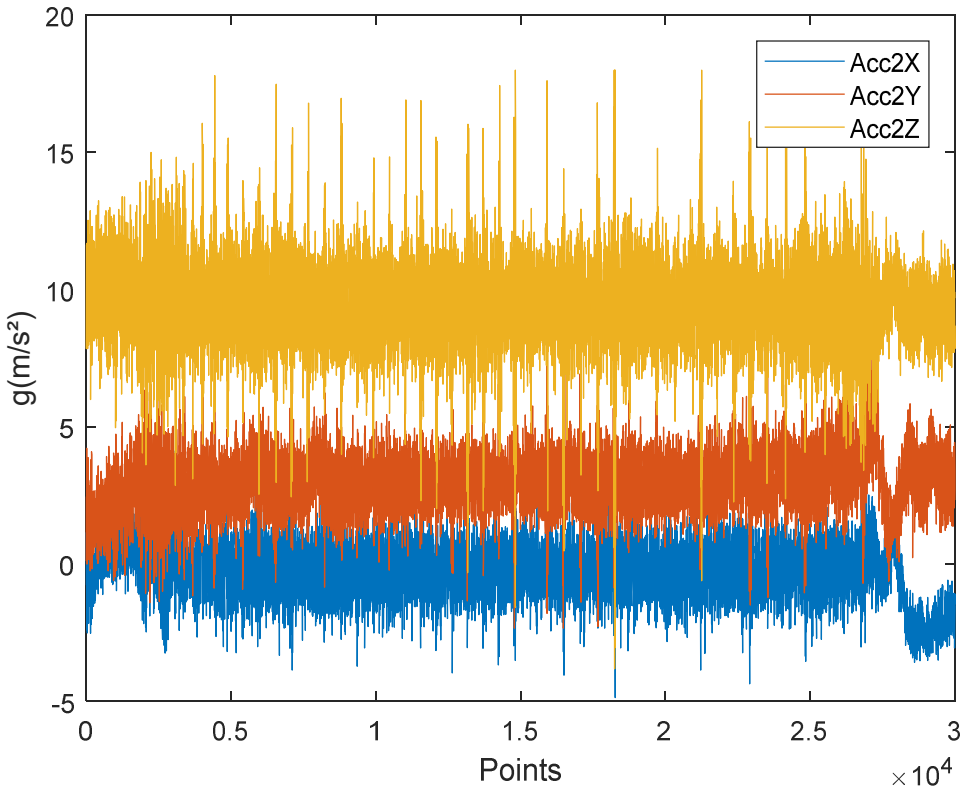

Denoise the data with dB8 wavelet:

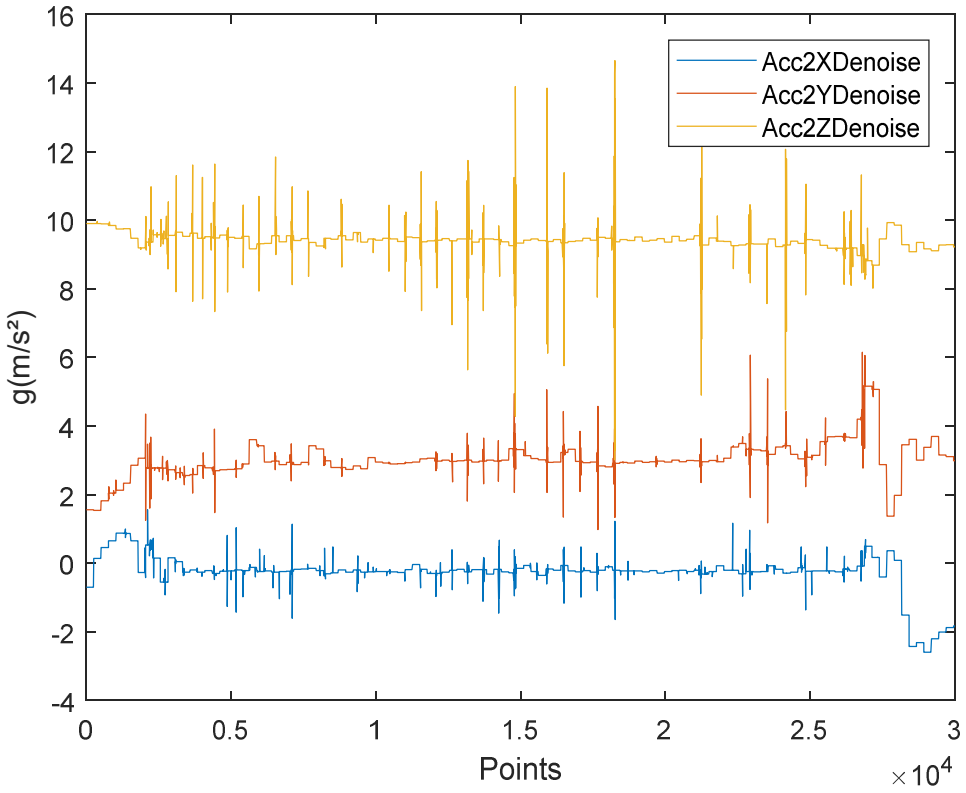

It is seen that the placement attitude of the smartphone is different from that in Route1. Extract the baseline from the data:

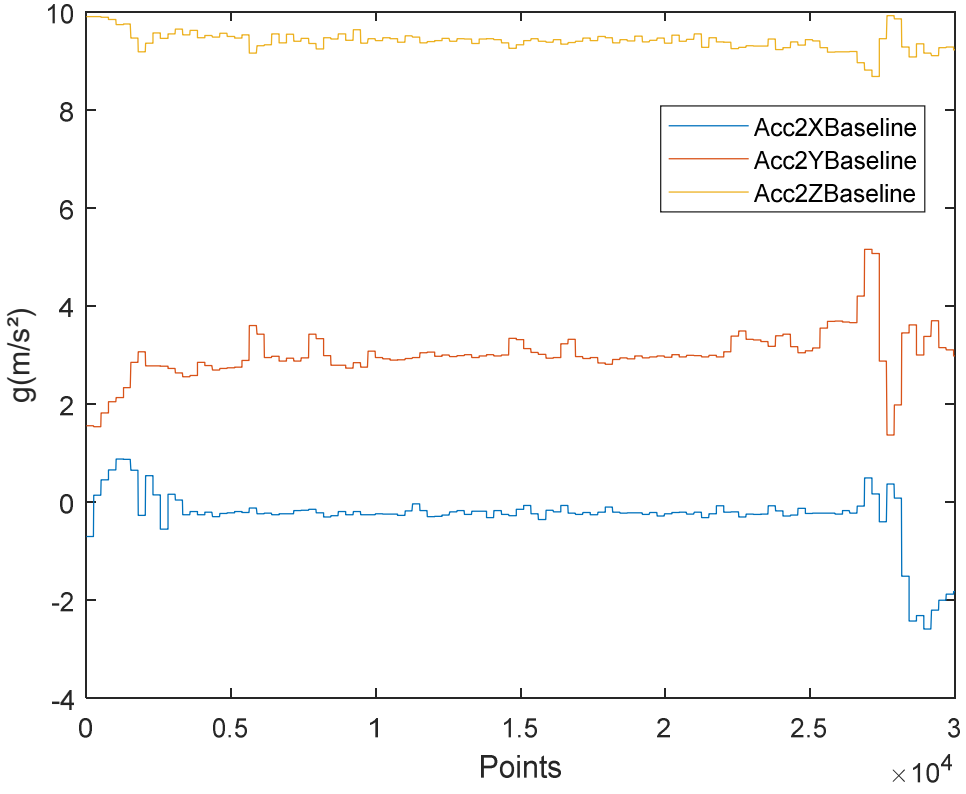

Eliminate the baseline by subtracting of last two results:

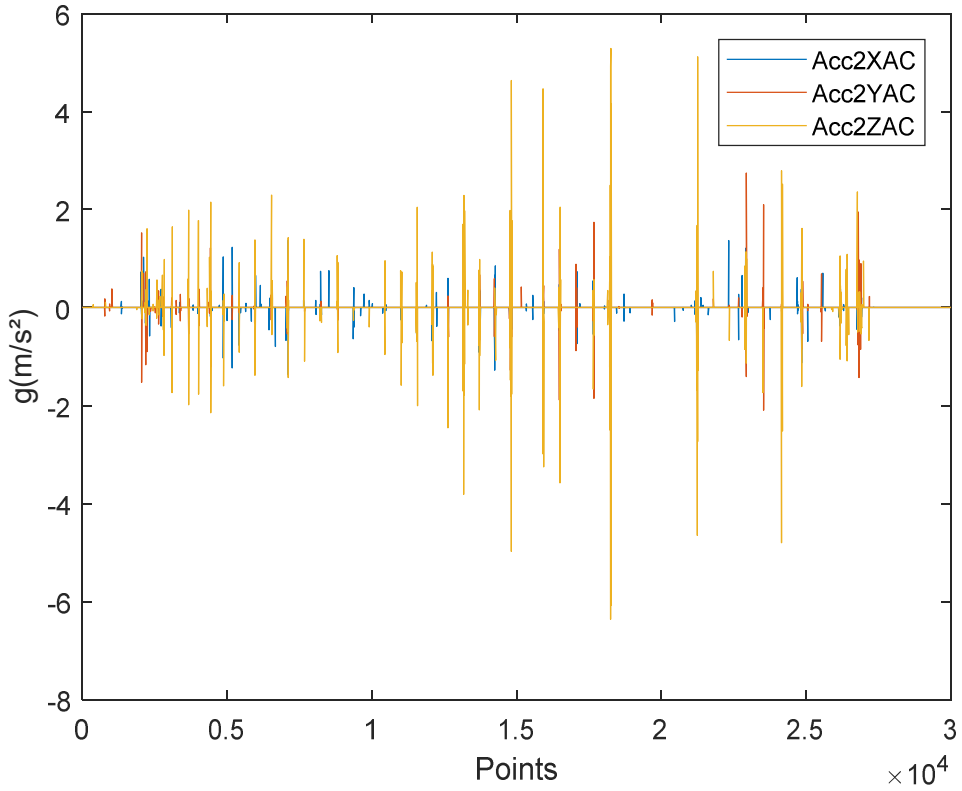

Conduct time correction with reference of GPS data:

Acct(145001)=714.559;

Acct(135000)=862.437;

The distance change in the 150 seconds selected from No. 714s to No. 863s is as follows:

GPSdist3=Location_GPS_dist(714:863);

Set 0 as the initial value of distance:

GPSdist3=GPSdist3-GPSdist3(1);

Interpolate the 150 points to 30,000:

xi=0.005:0.005:150;

x=0:149;

Dist3=interp1(x,GPSdist3,xi, 'spline');

Take the distance of 0-2500m as the abscissa:

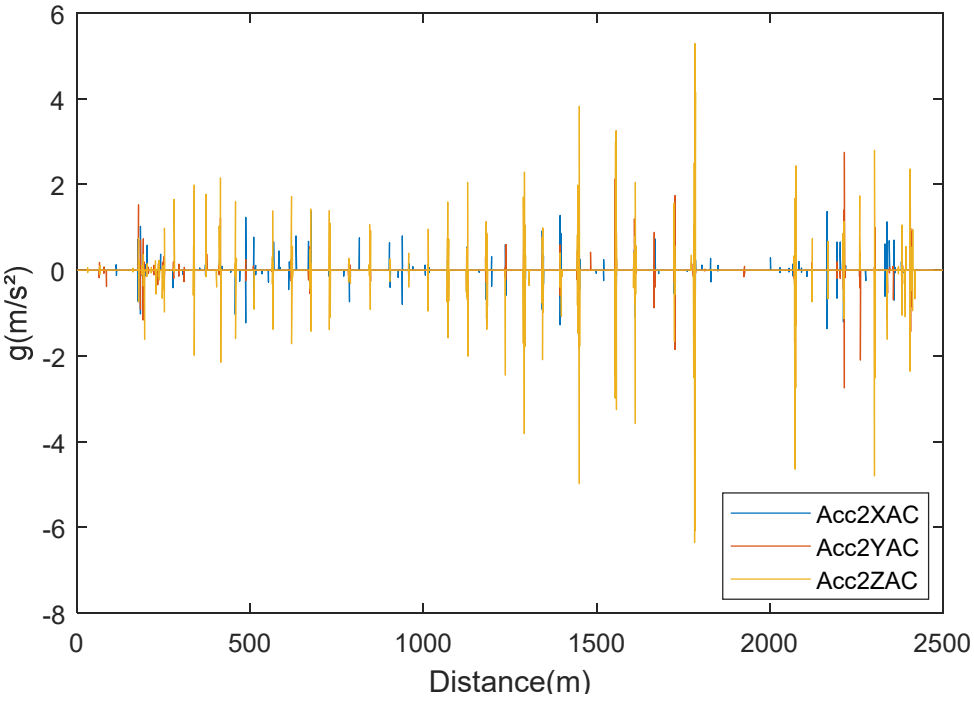

Process the gyroscope data as above:

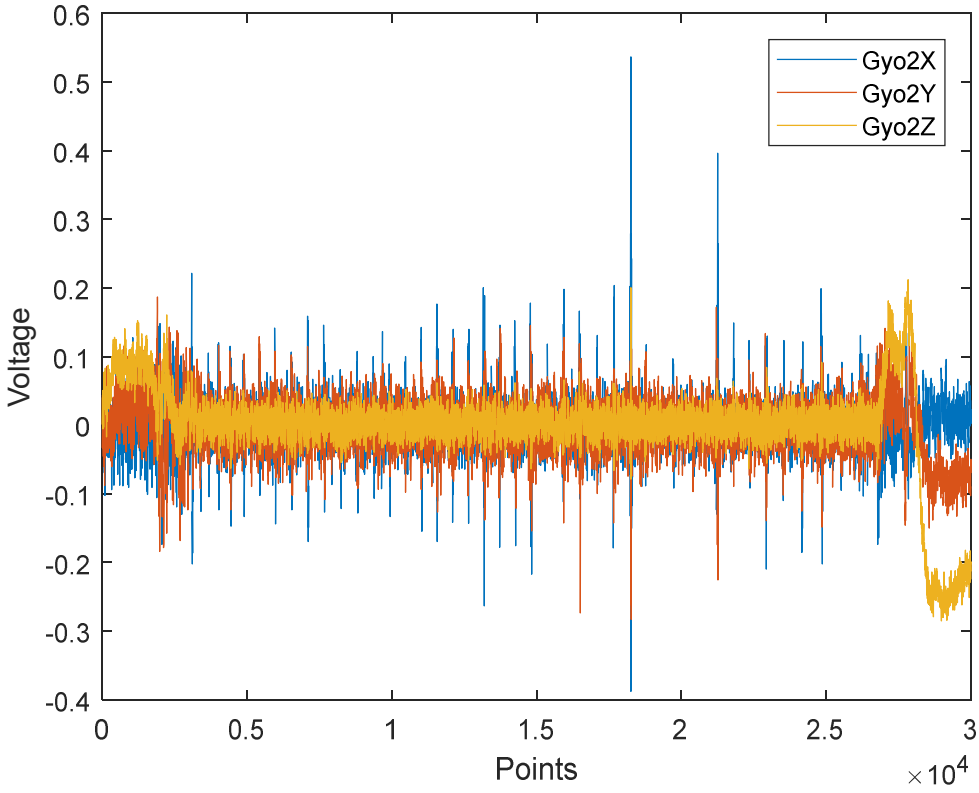

Denoise with dB8 wavelet:

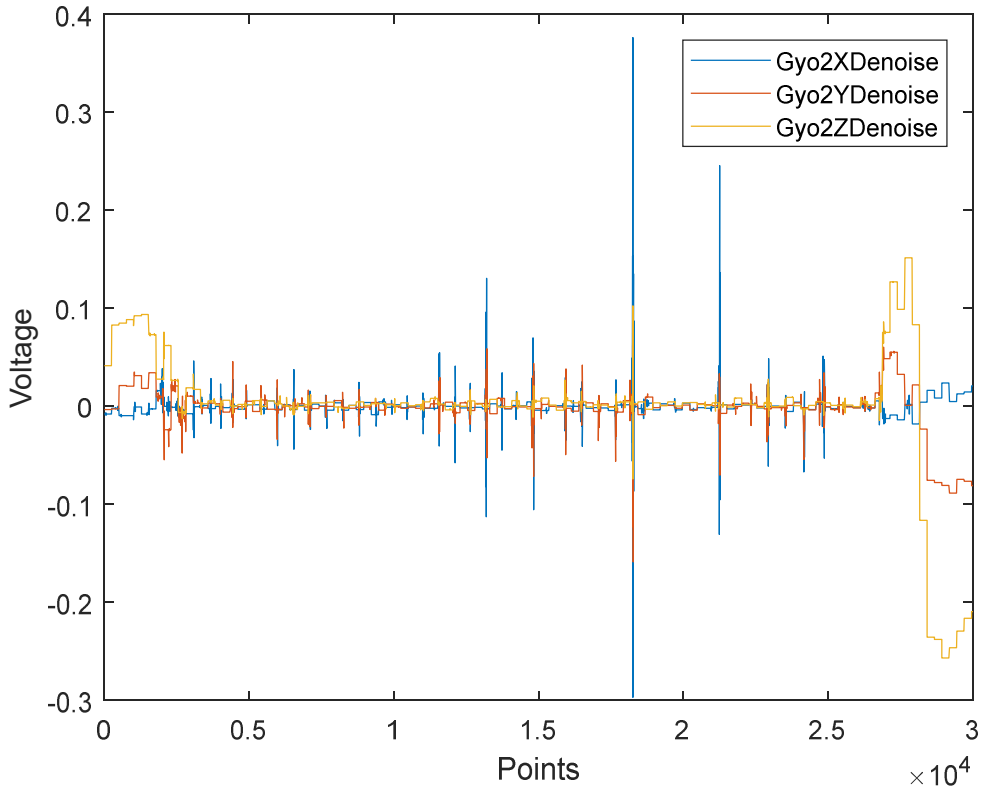

Extract the baseline from the result of wavelet decomposition in last step:

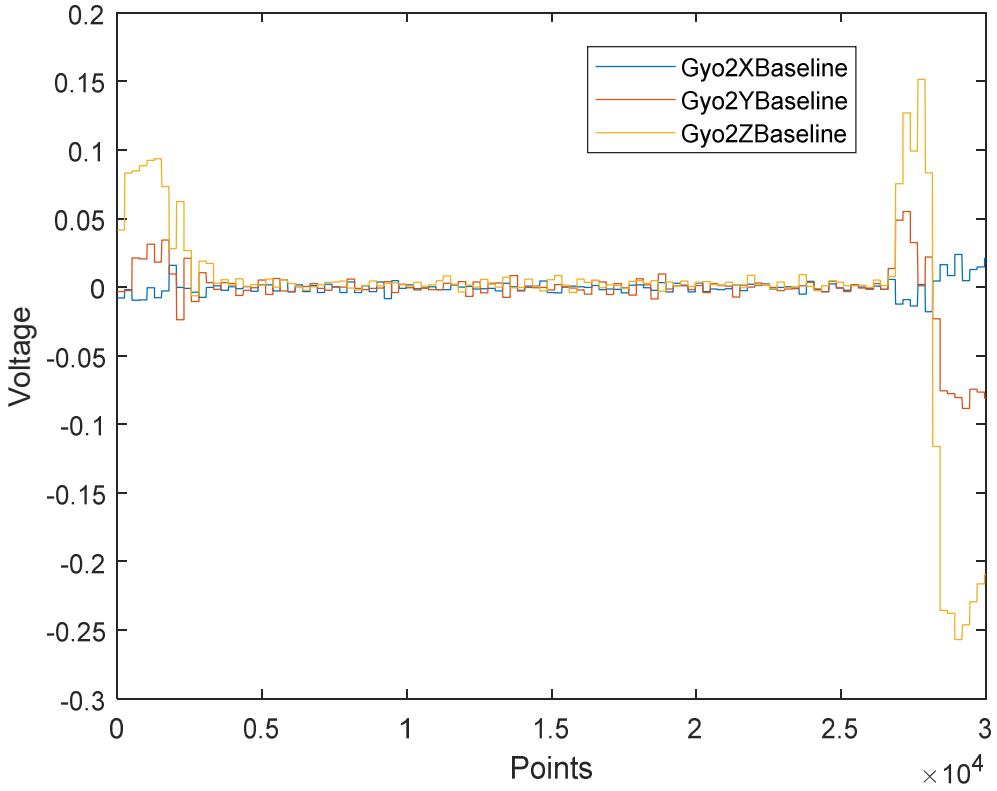

Eliminate the baseline by subtracting of the last two results:

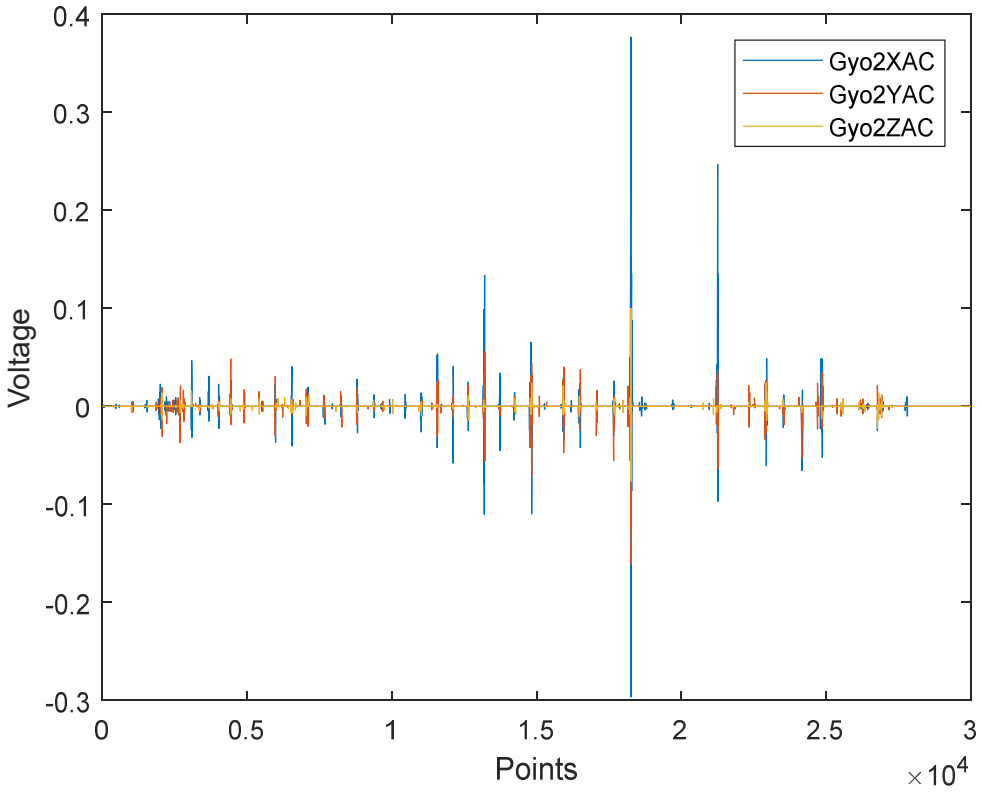

Take Dist2 as the abscissa:

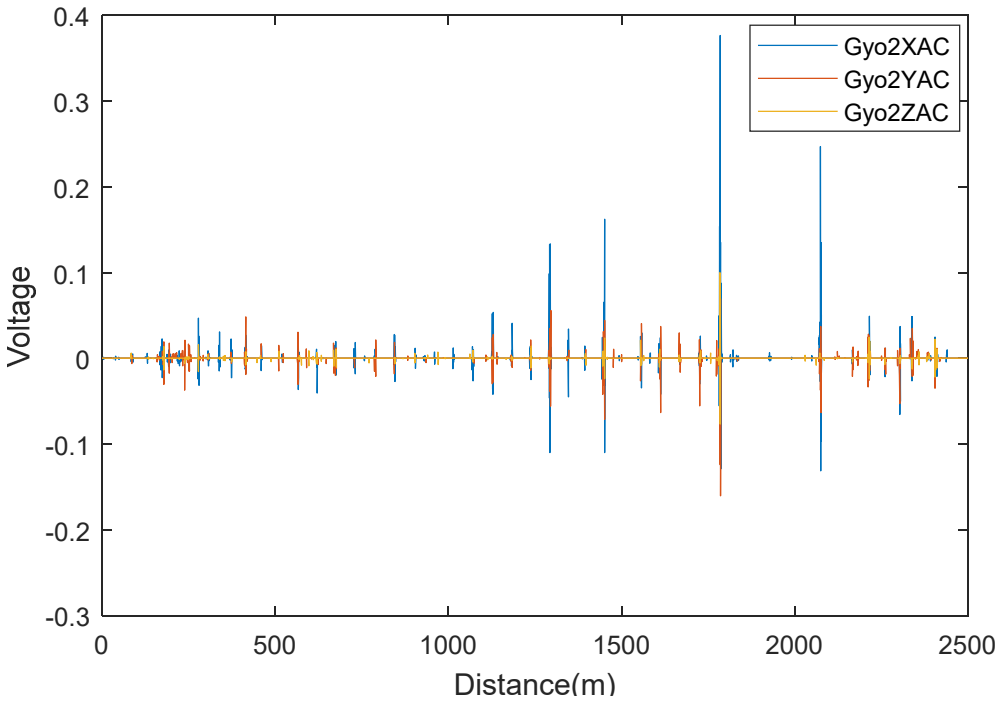

B, Data of Route 3

The piece of data contains 30,000 points from point 175,001 to 205,000. Firstly, process the acceleration data:

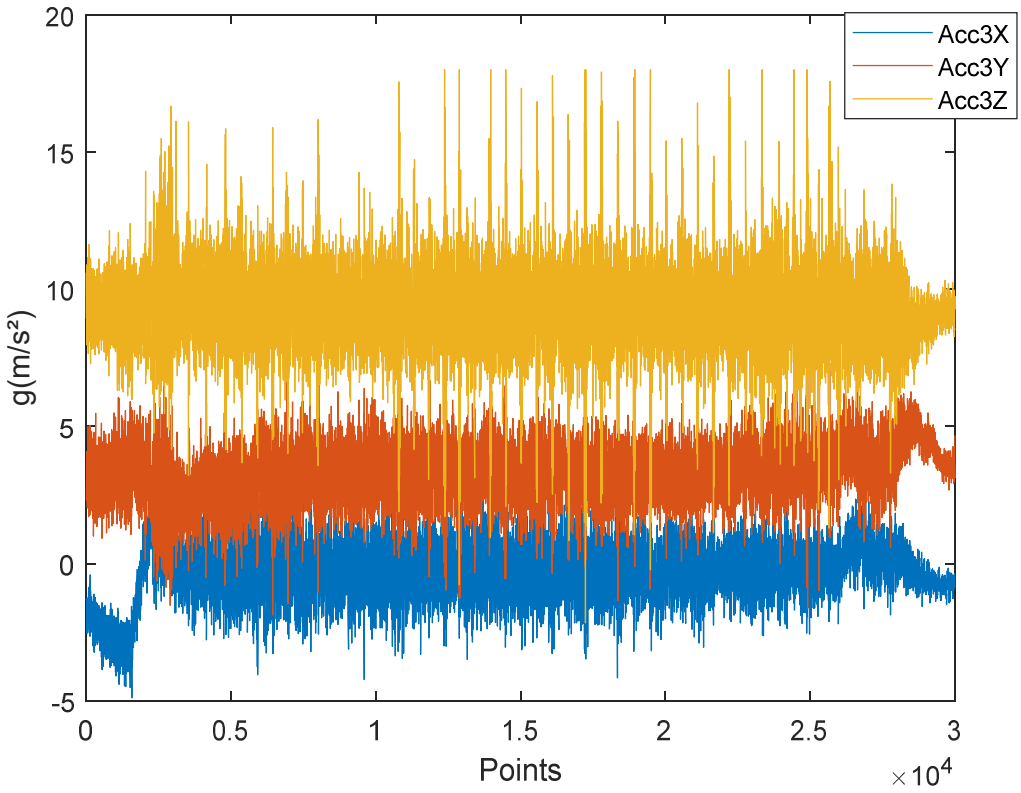

Denoise with dB8 wavelet:

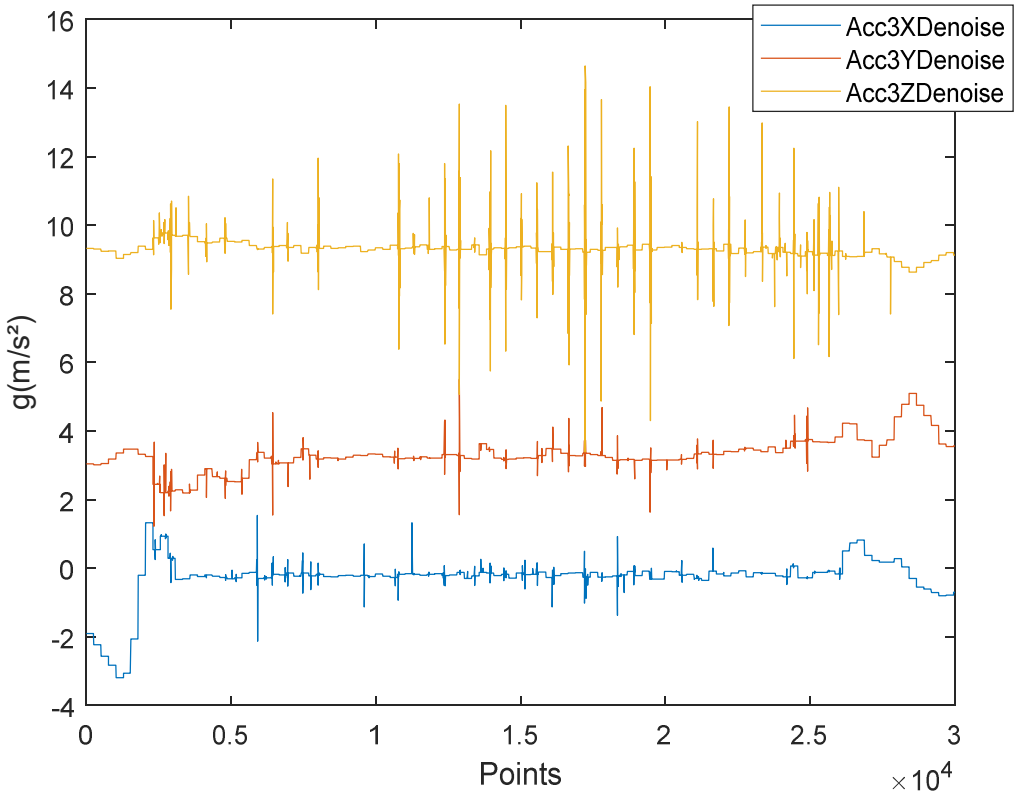

Extract the baseline from the result of wavelet decomposition:

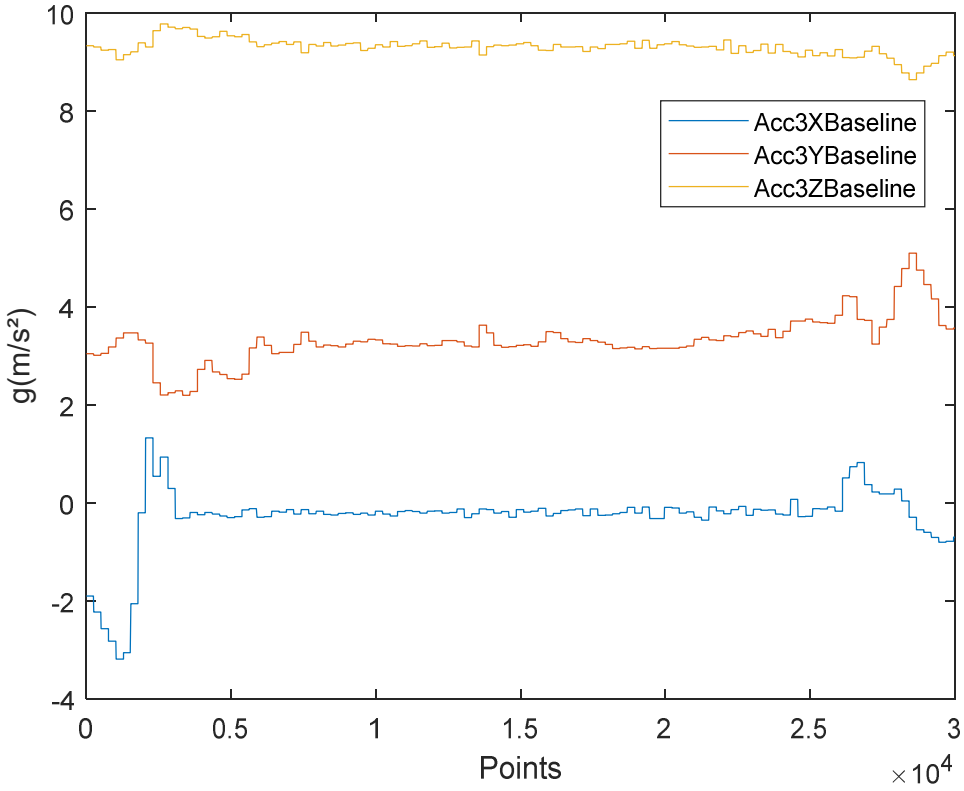

Eliminate the baseline by subtracting of last two results:

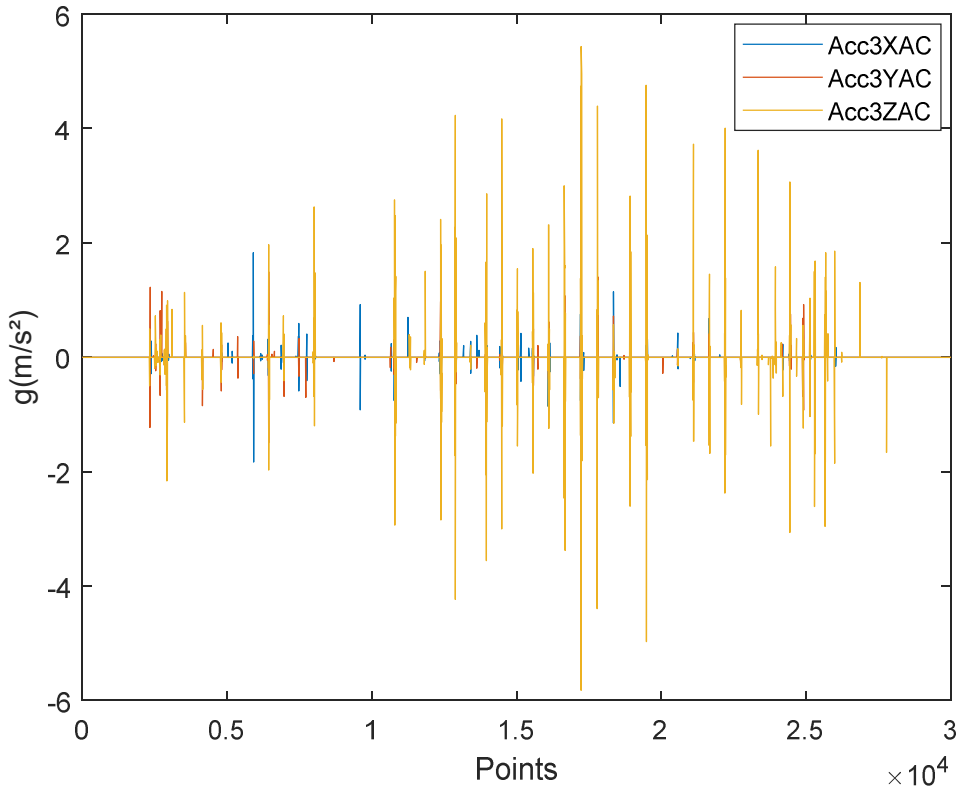

Time correction:

Acct(175001)=862.442;

Acct(205000)=1010.351;

The distance change in the 150 seconds from No. 862s to No. 1011s:

GPSdist4=Location_GPS_dist(863:1011);

Set 0 as the initial value of distance:

GPSdist4=GPSdist4-GPSdist4(1);

Interpolate the 150 points to 30,000:

xi=0.005:0.005:150;

x=0:149;

Dist4=interp1(x,GPSdist4,xi, 'spline');

Take the distance of 0-2500m as the abscissa:

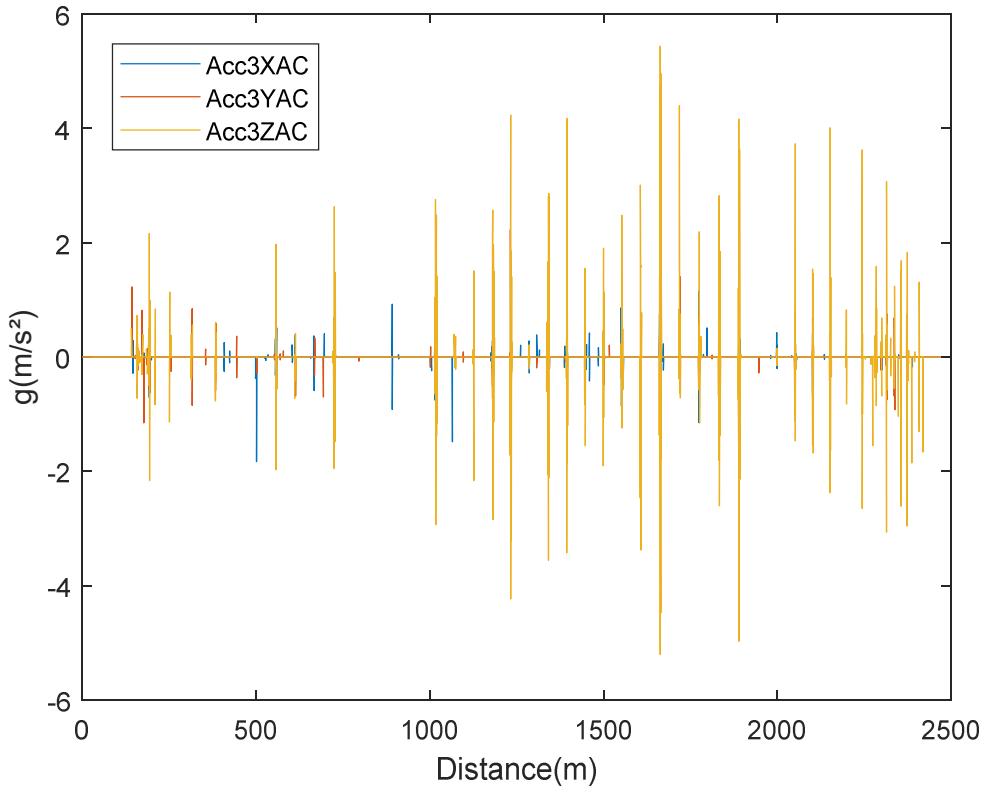

Process the gyroscope data as above:

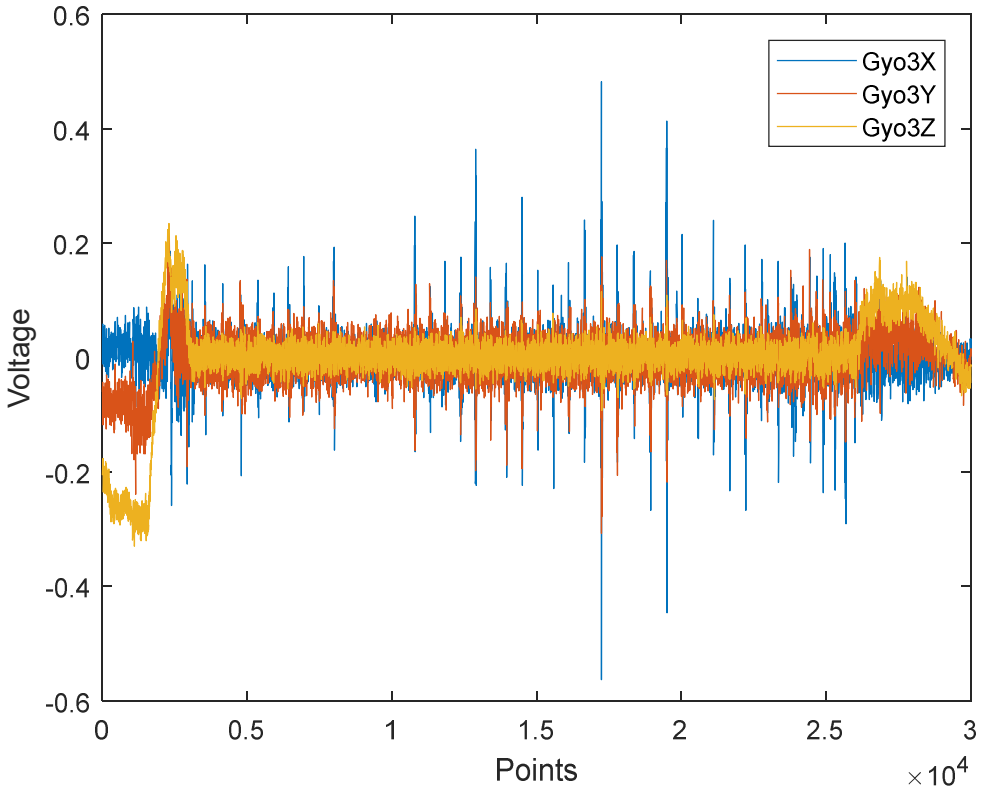

Denoise with dB8 wavelet:

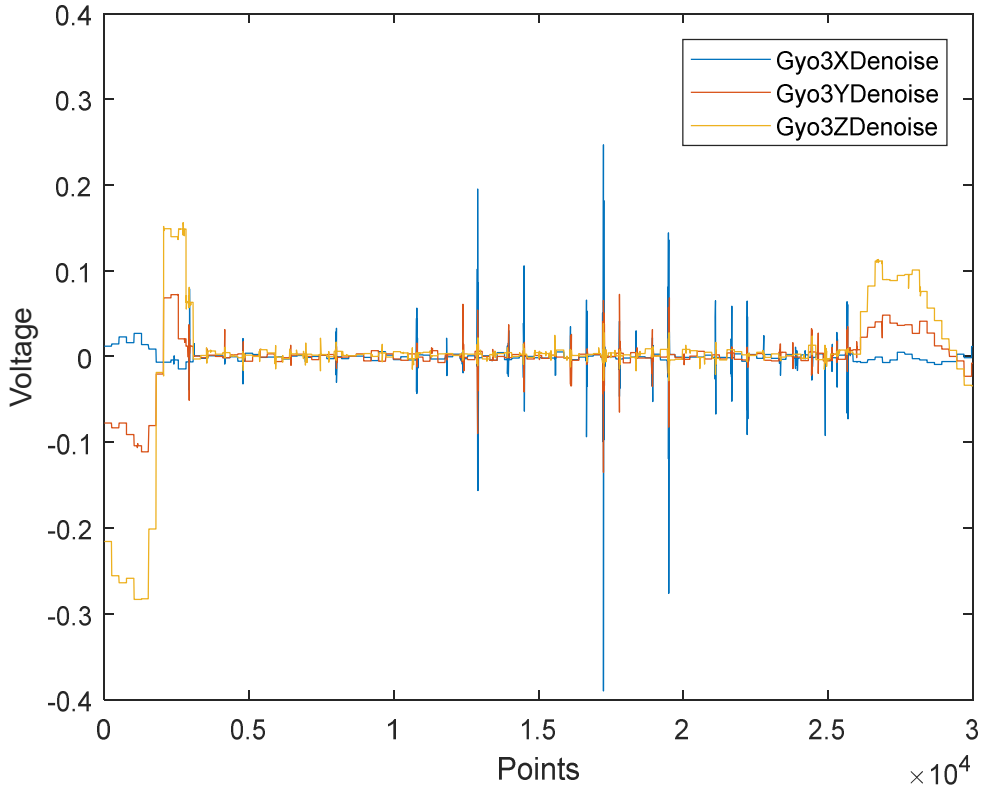

Extract the baseline from the result of wavelet decomposition:

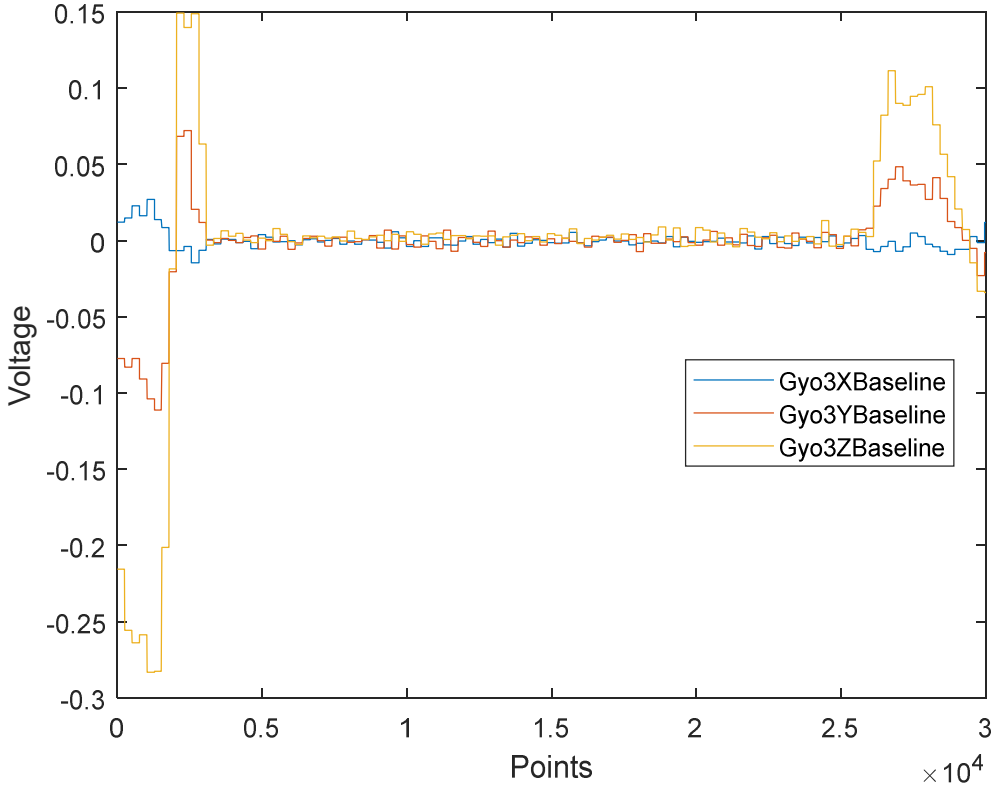

Eliminate the baseline:

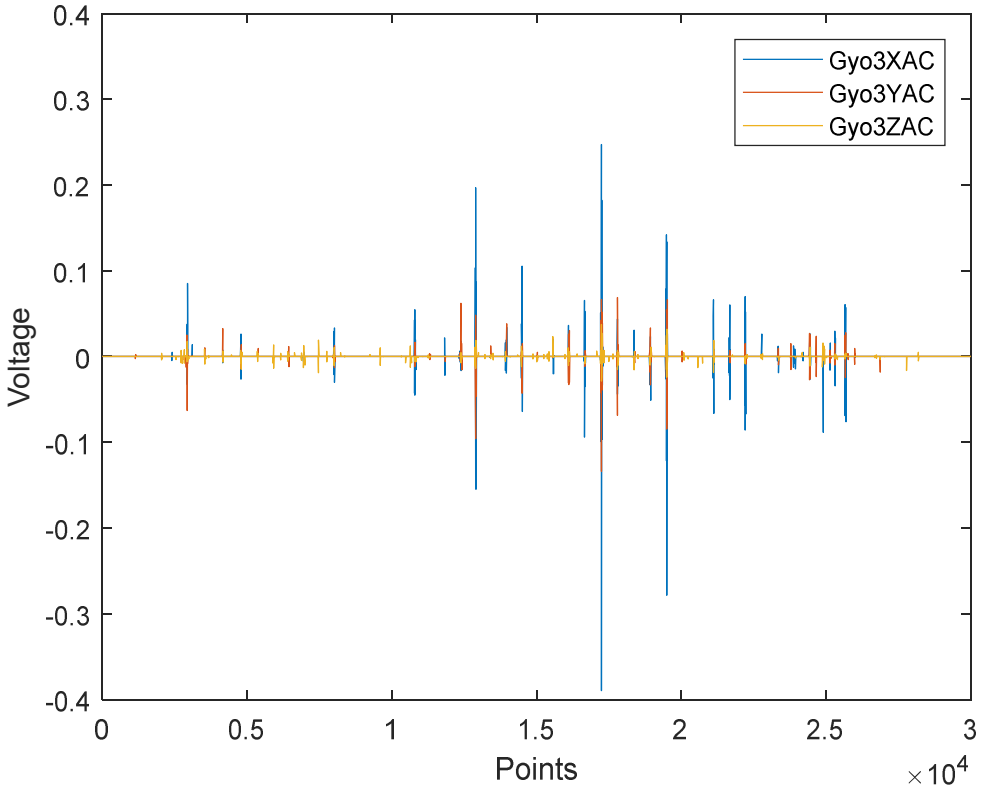

Take Dist4 as the abscissa:

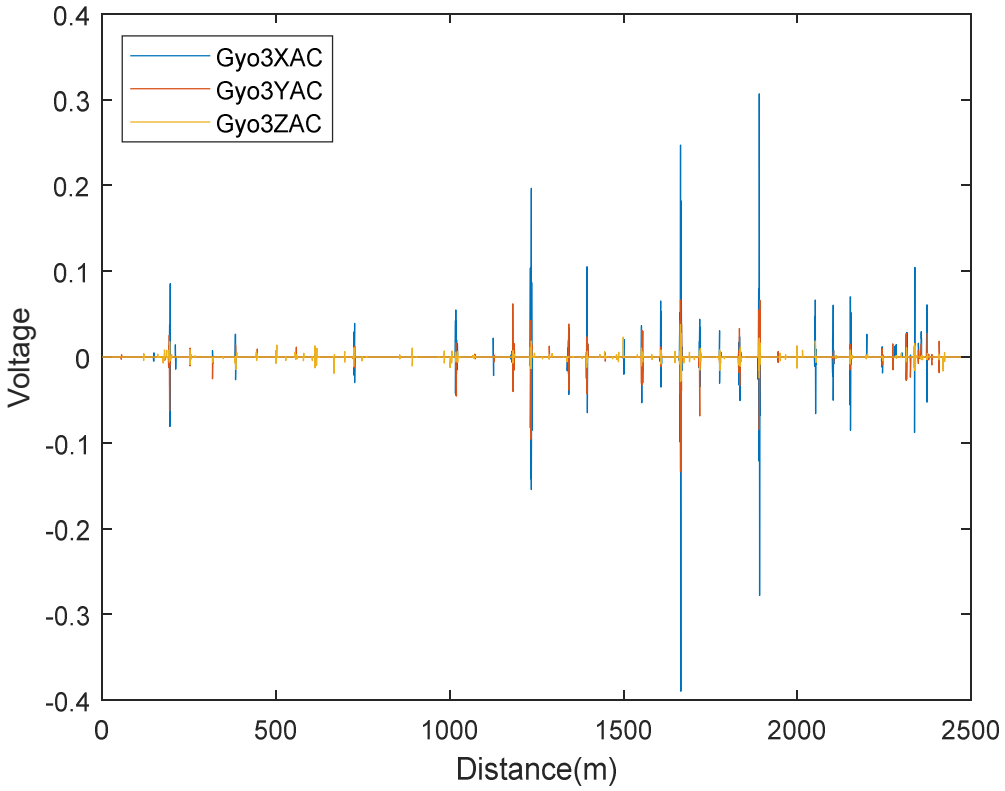

C, Data of Route 4

As the vehicle runs slower, in this piece there are 40,000 points from point 210,001 to 250,000.

Firstly process the acceleration data:

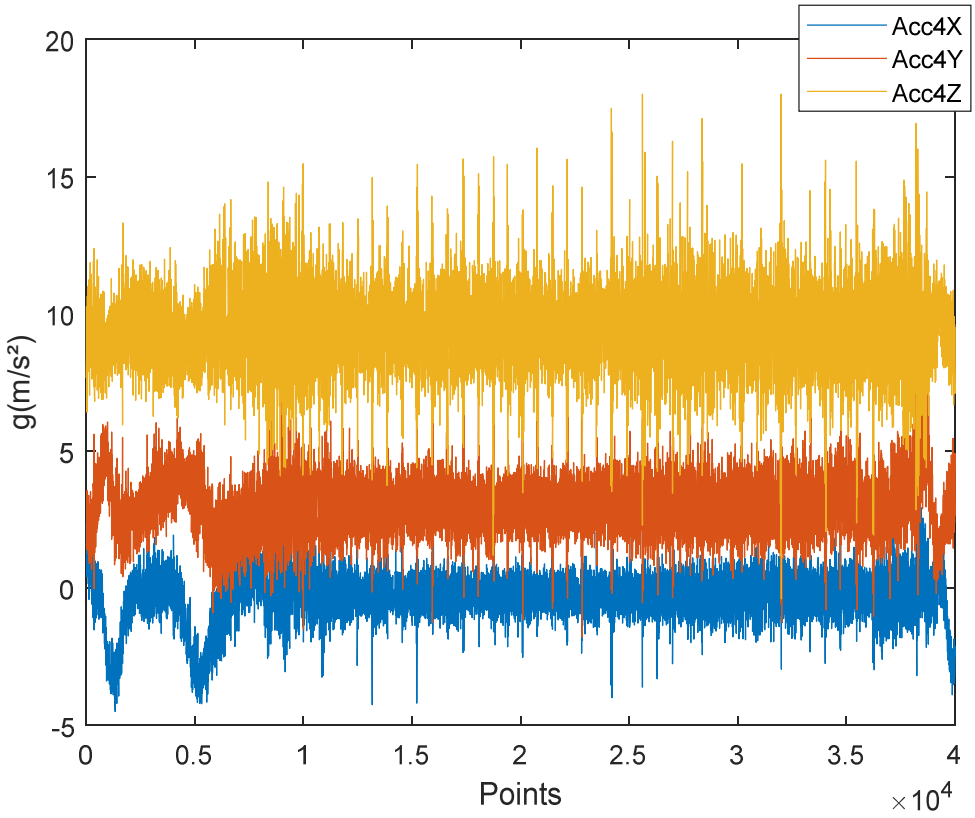

Denoise with wavelet:

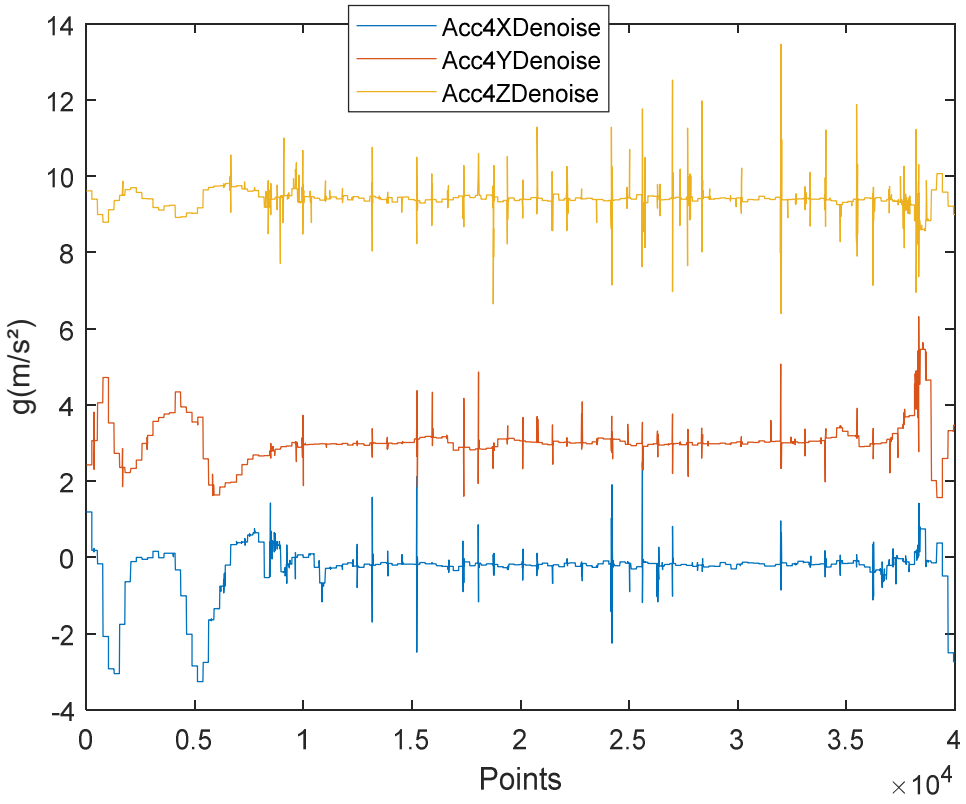

Extract the baseline:

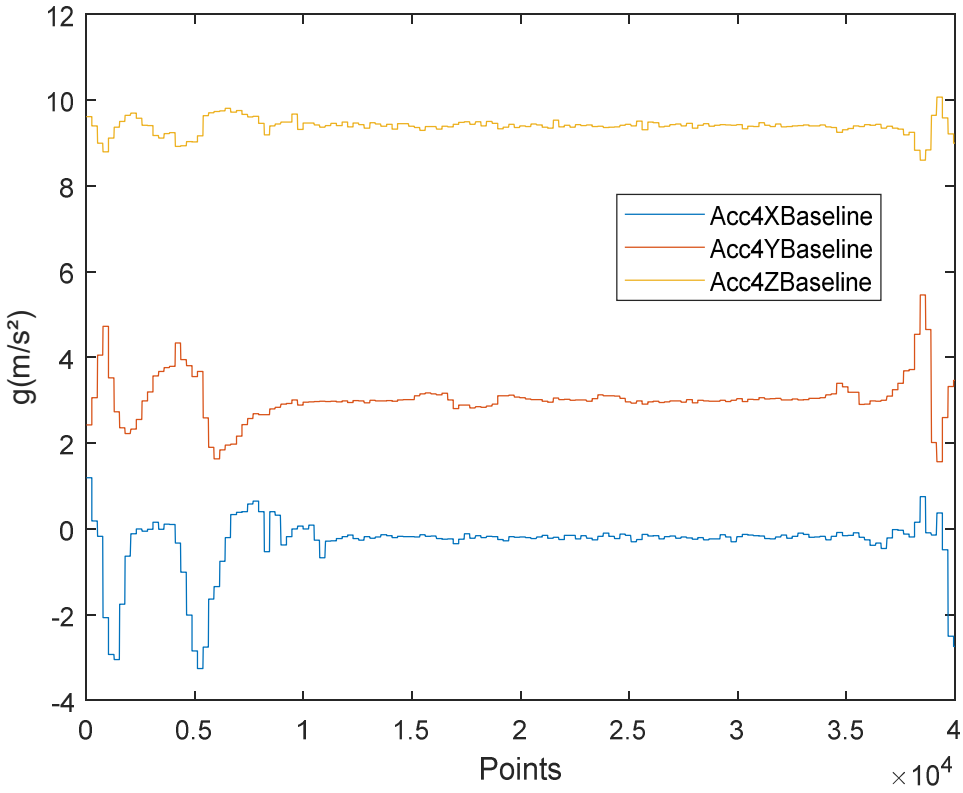

Eliminate the baseline:

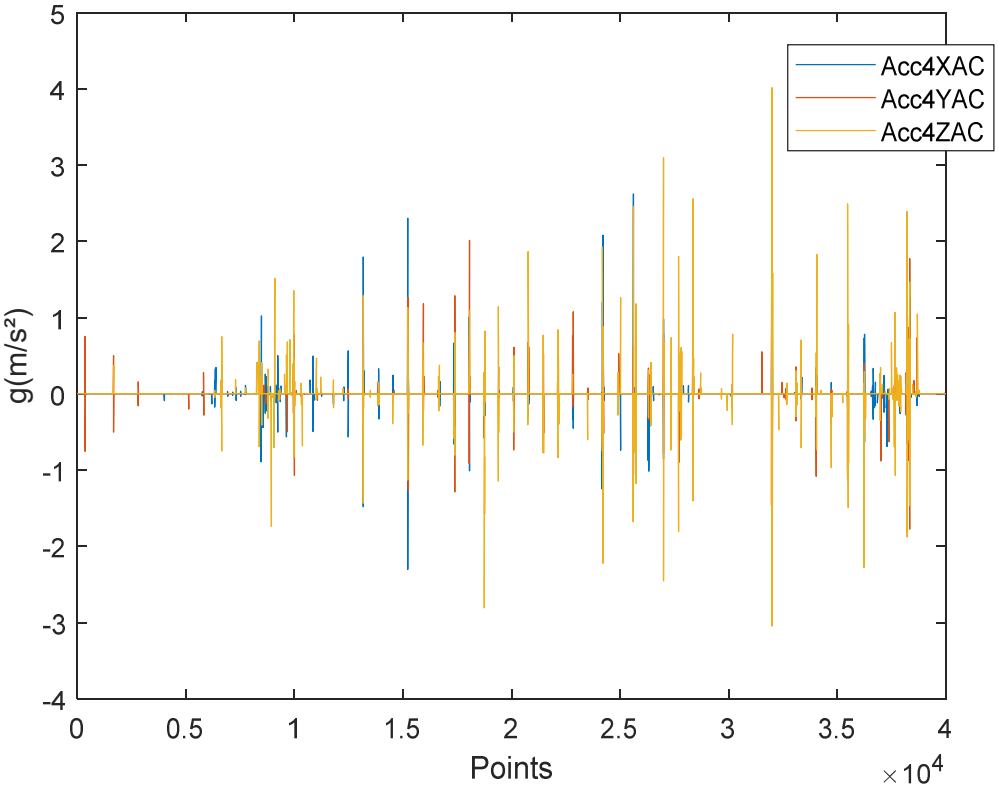

Time correction:

Acct(210001)=1035.024;

Acct(250000)=1232.24;

Select 200 seconds from No. 1034s to No. 1233s:

The distance change in the 200 seconds is as follows:

GPSdist5=Location_GPS_dist(1034:1233);

Set 0 as the initial value of distance:

GPSdist5=GPSdist5-GPSdist5(1);

Interpolate the 200 points to 40,000:

xi=0.005:0.005:200;

x=0:199;

Dist5=interp1(x,GPSdist5,xi, 'spline');

Take the distance of 0-3000m as the abscissa:

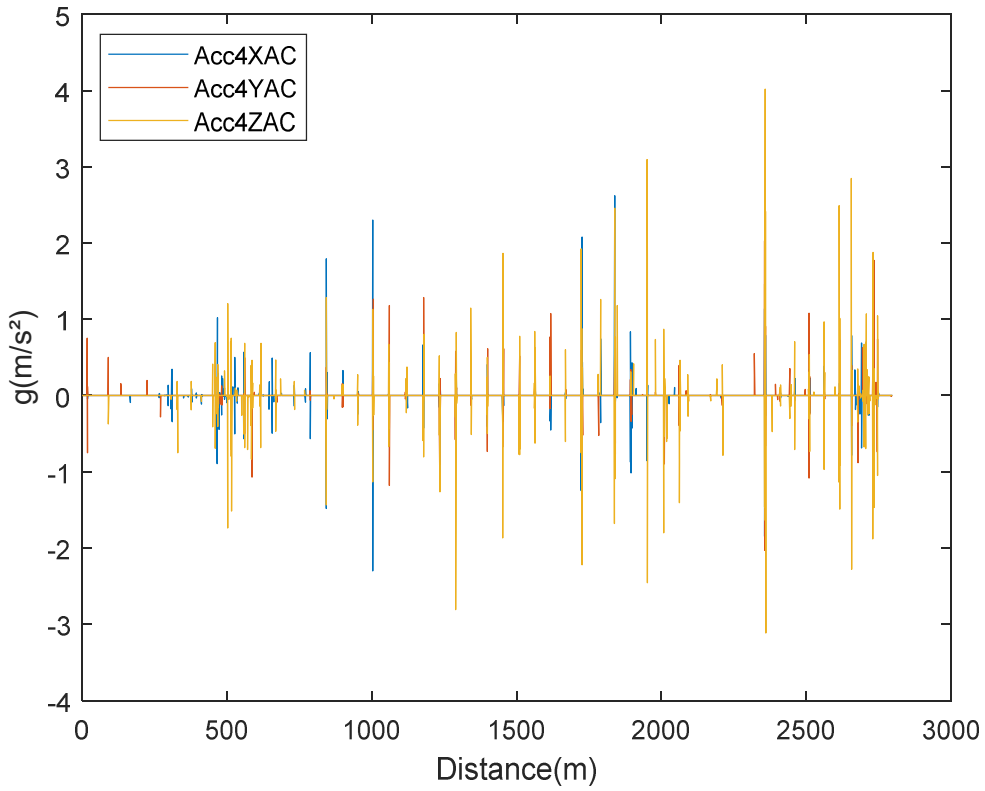

Then process the gyroscope data:

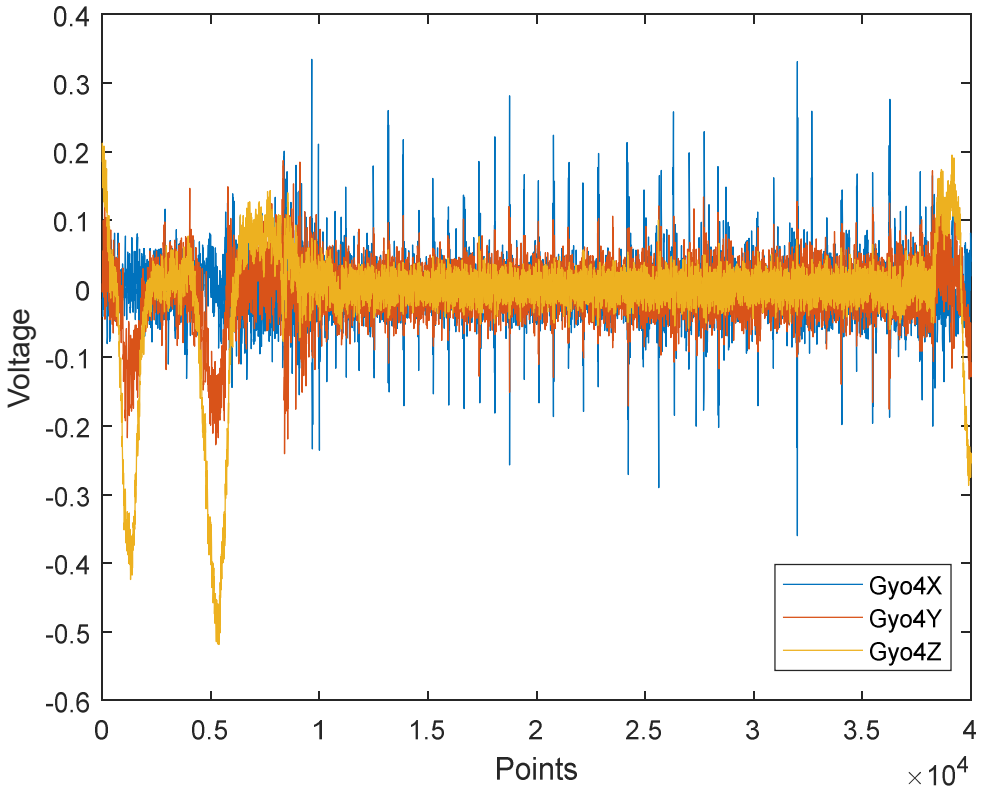

Denoise with wavelet:

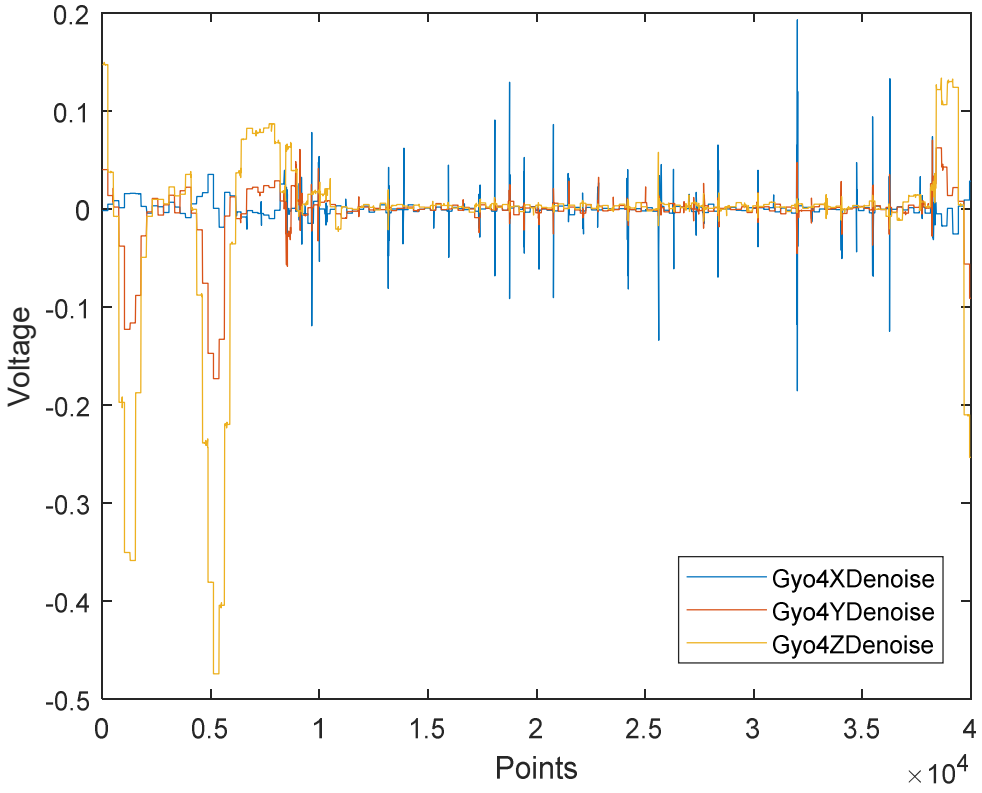

Extract the baseline:

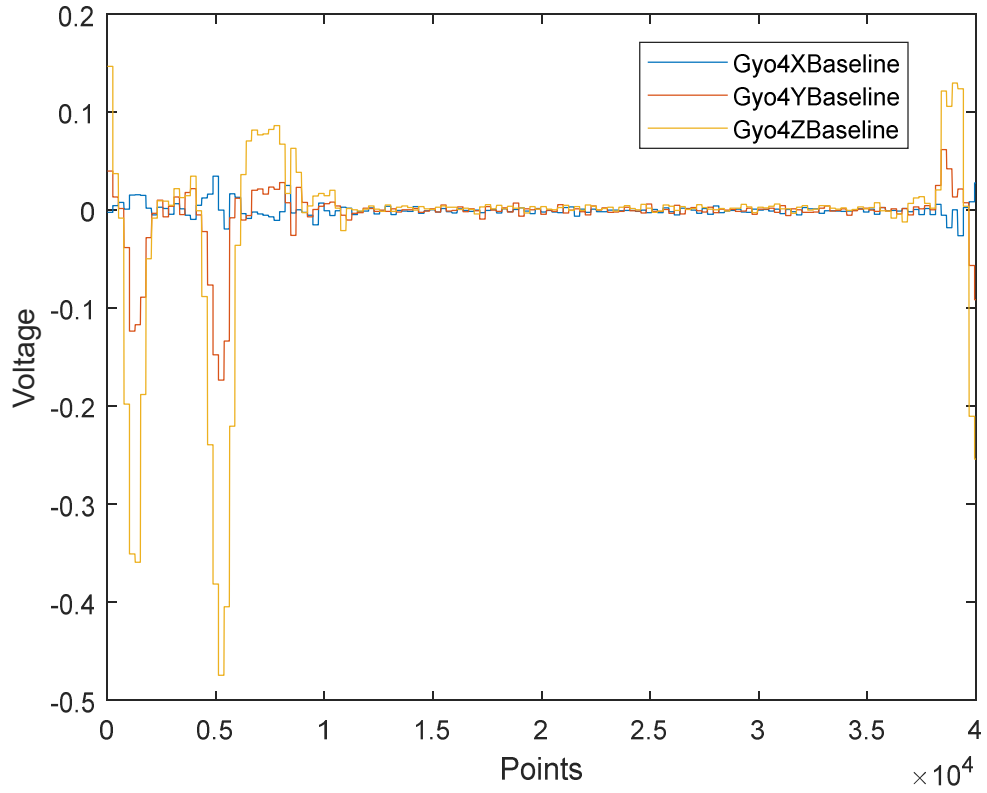

Eliminate the baseline:

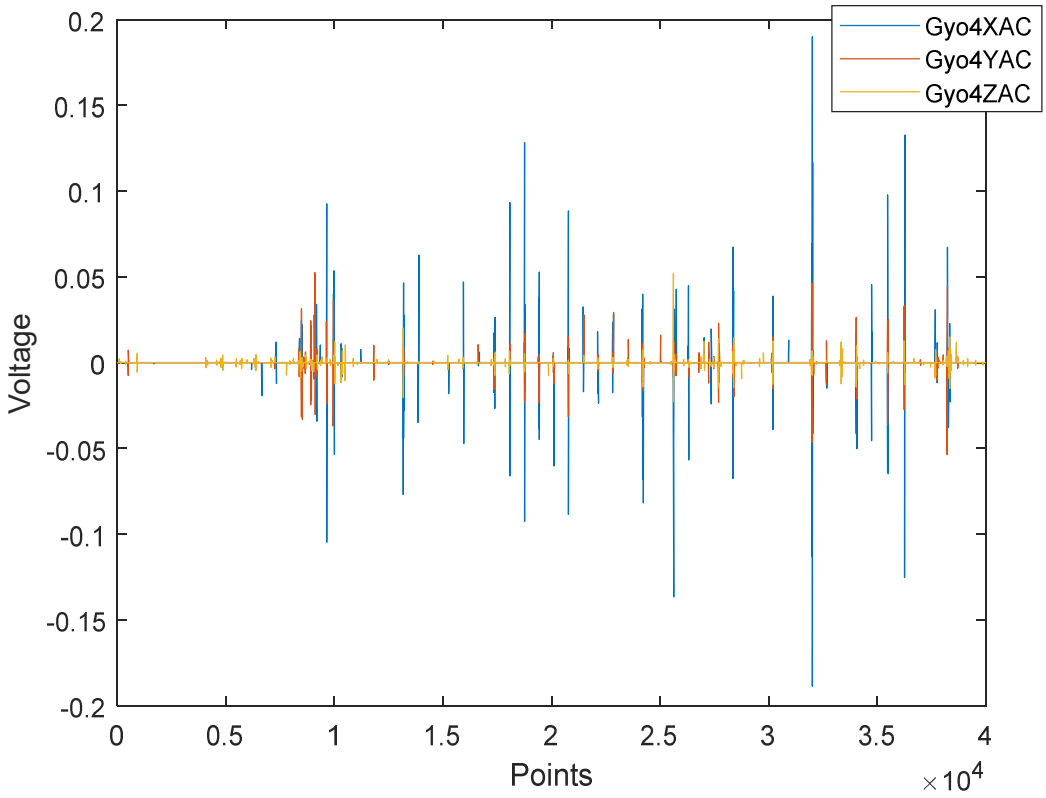

Take Dist5 as the abscissa:

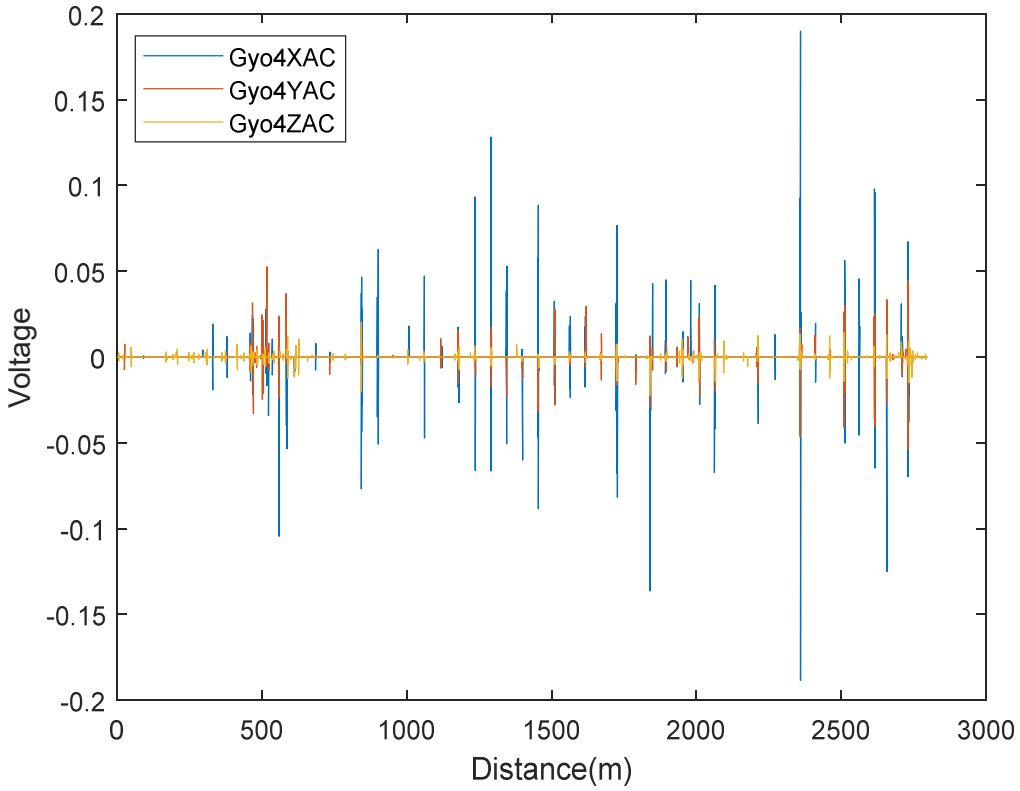

D, Data of Route 5

This piece of data contains 40,000 points from point 250,001 to 290,000.

Firstly process the acceleration data:

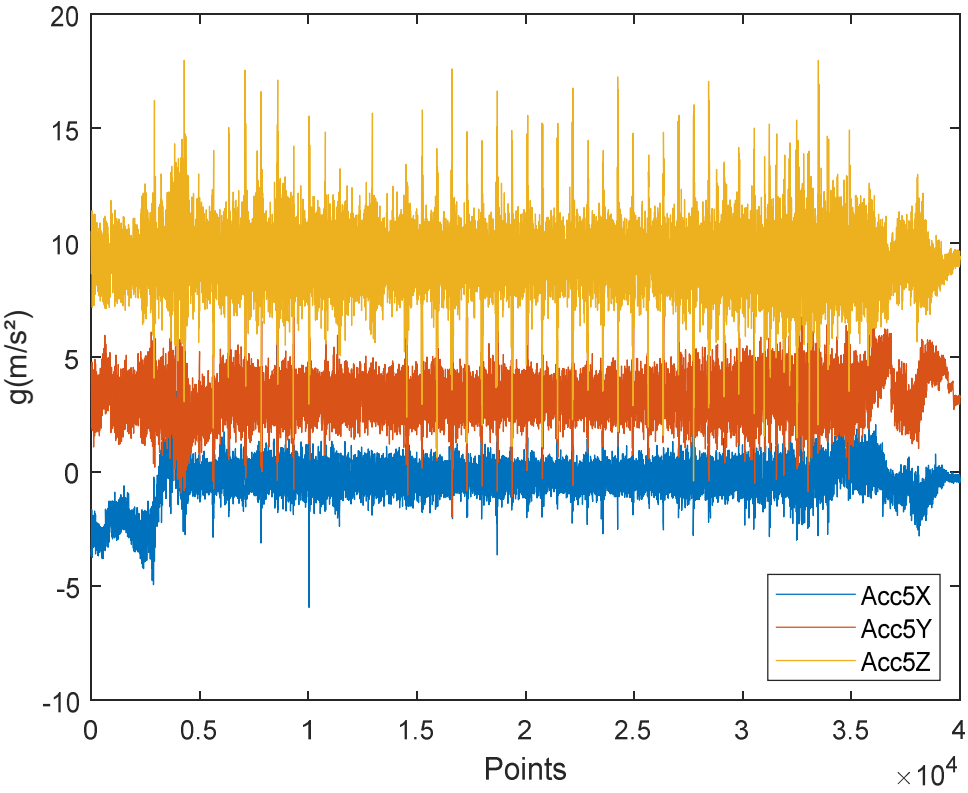

Denoise with wavelet:

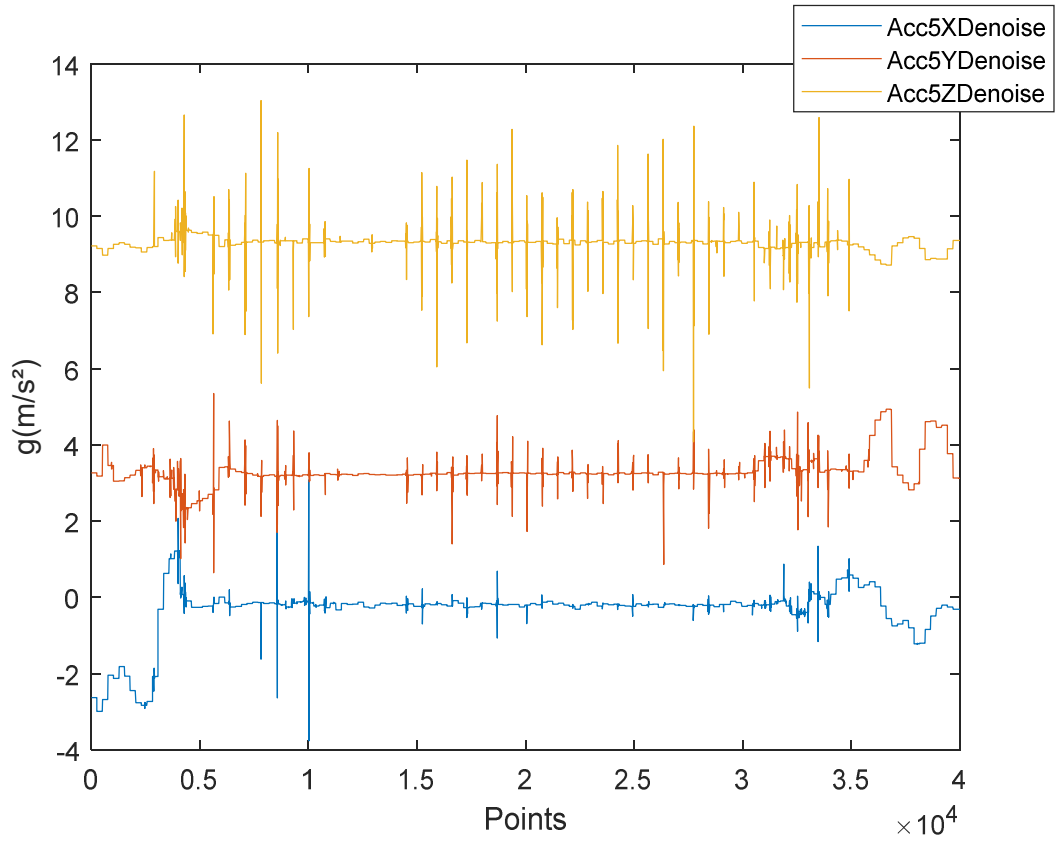

Extract the baseline:

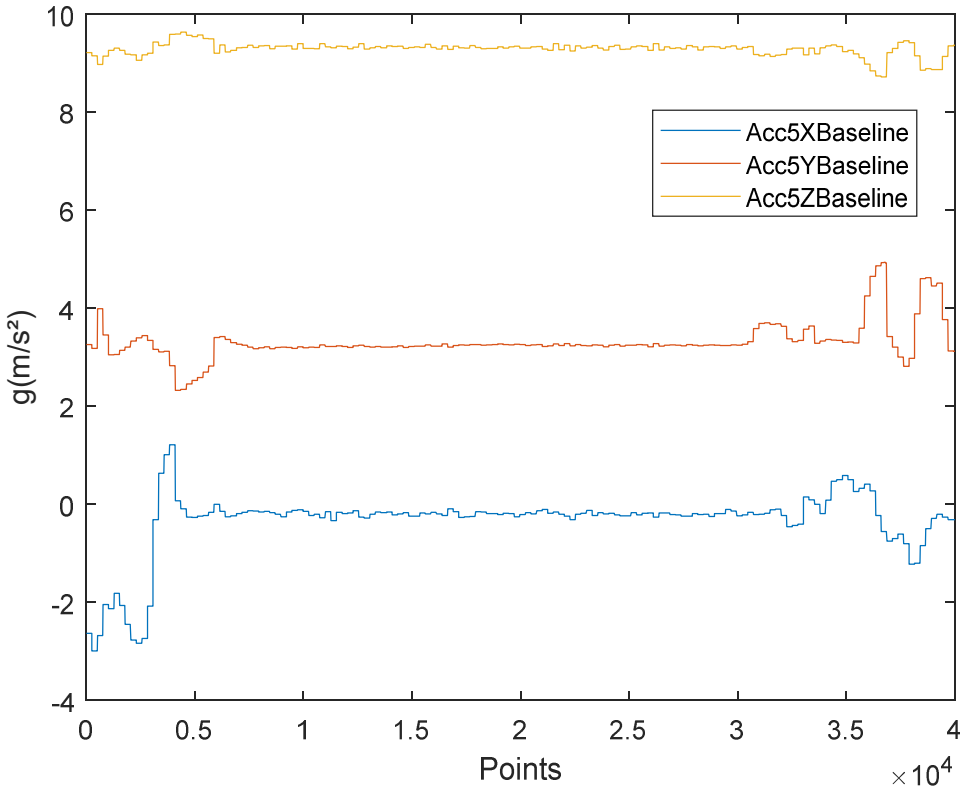

Eliminate the baseline:

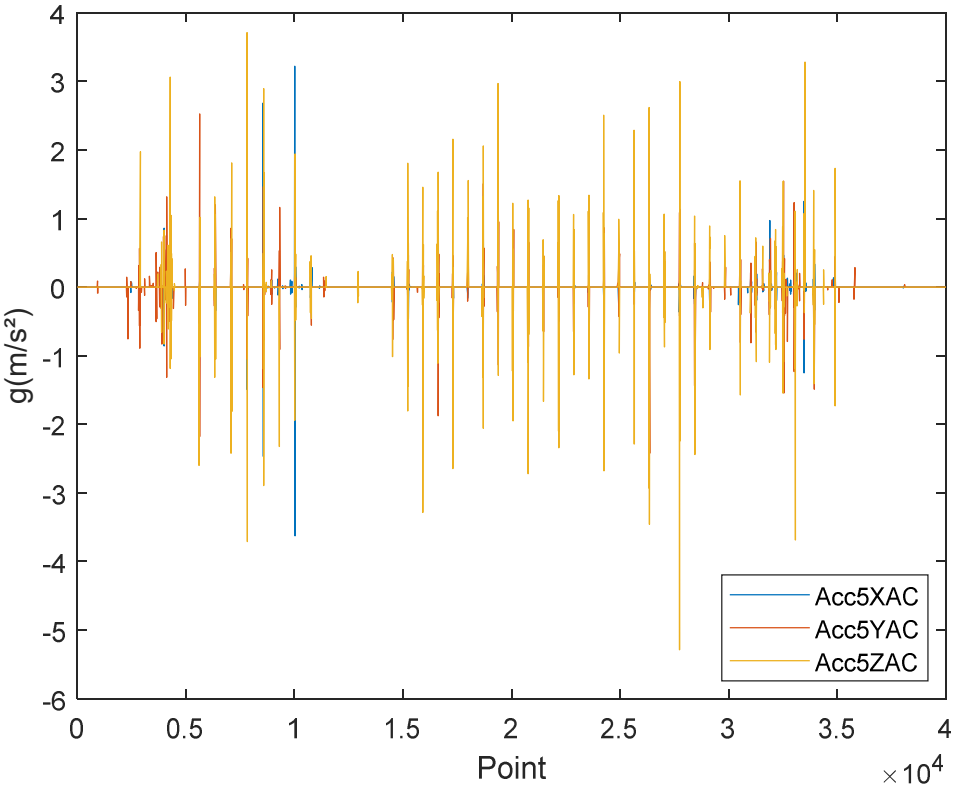

Time correction:

Acct(250001)=1232.245;

Acct(290000)=1429.52;

Select 200 seconds from No. 1231s to No. 1430s:

The distance change in the 200 seconds is as follows:

GPSdist6=Location_GPS_dist(1231:1430);

Set 0 as the initial value of distance:

GPSdist6=GPSdist6-GPSdist6(1);

Interpolate the 200 points to 40,000:

xi=0.005:0.005:200;

x=0:199;

Dist6=interp1(x,GPSdist6,xi, 'spline');

Take the distance of 0-2500m as the abscissa:

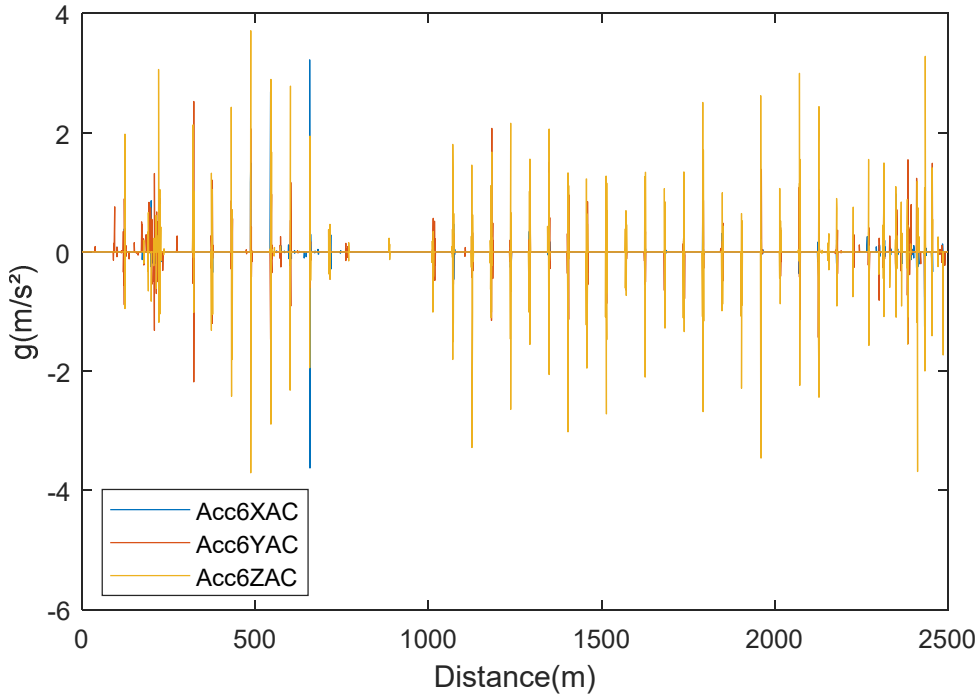

Then process the gyroscope data:

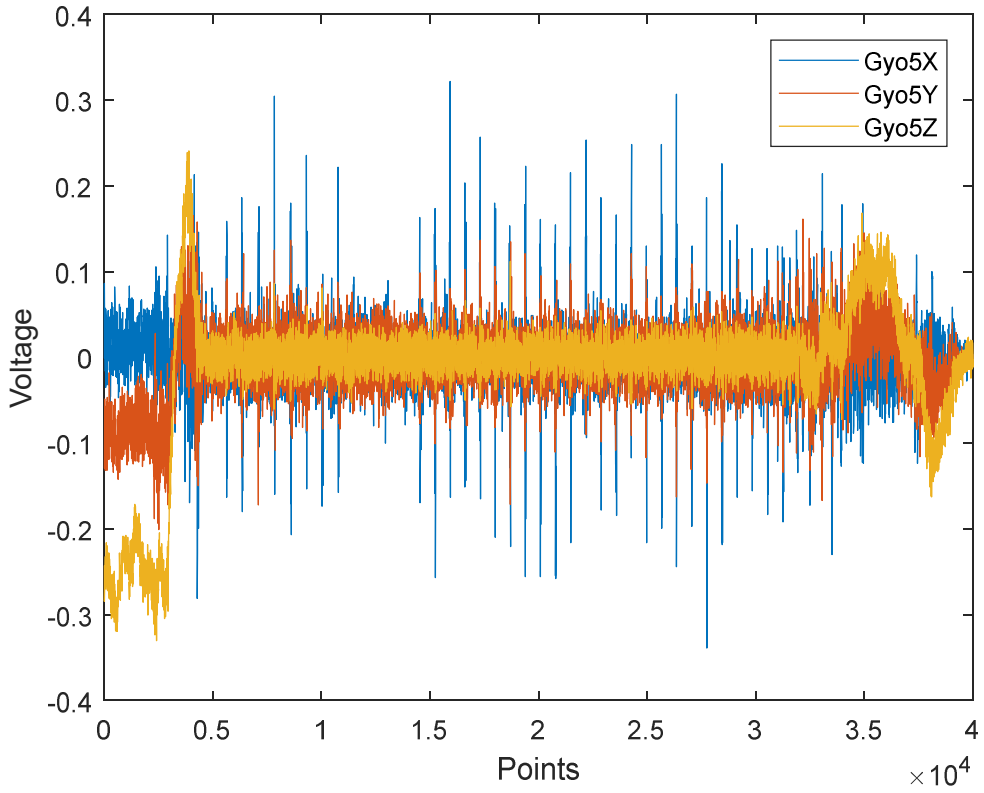

Denoise with wavelet:

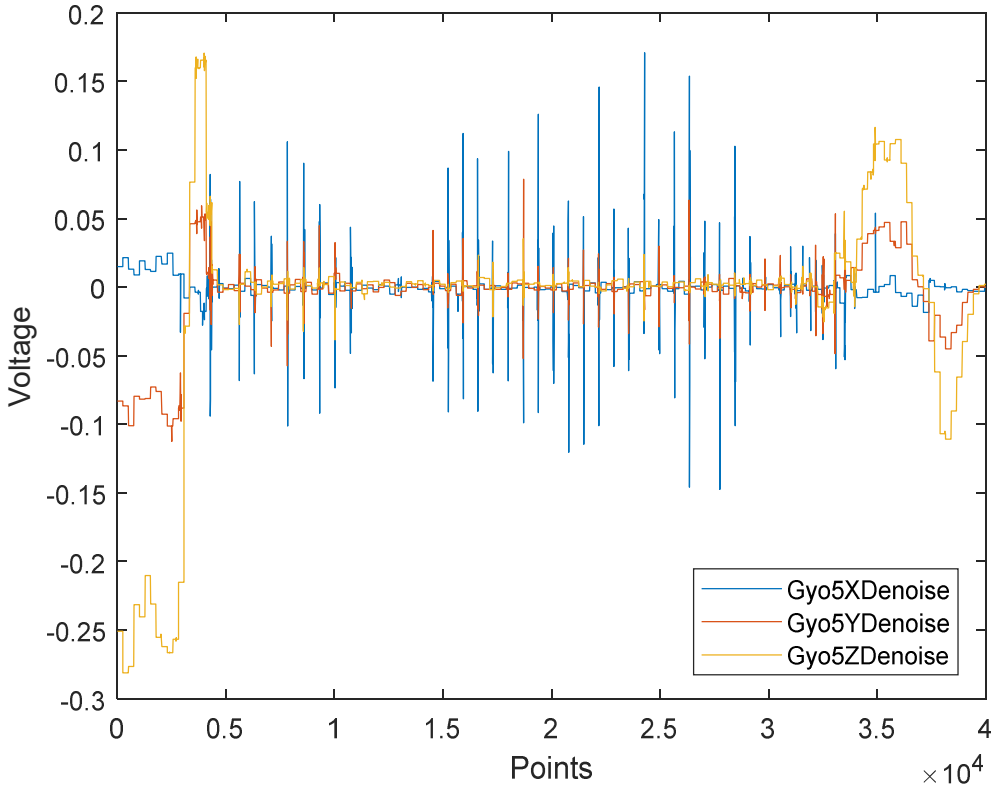

Extract the baseline:

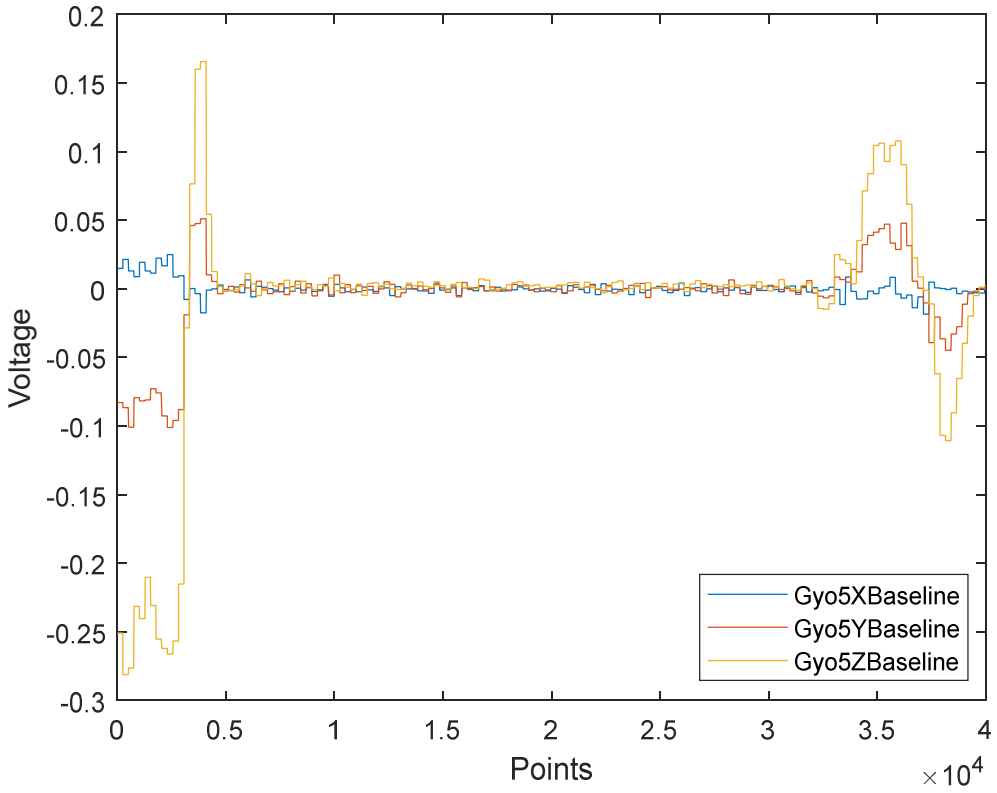

Eliminate the baseline:

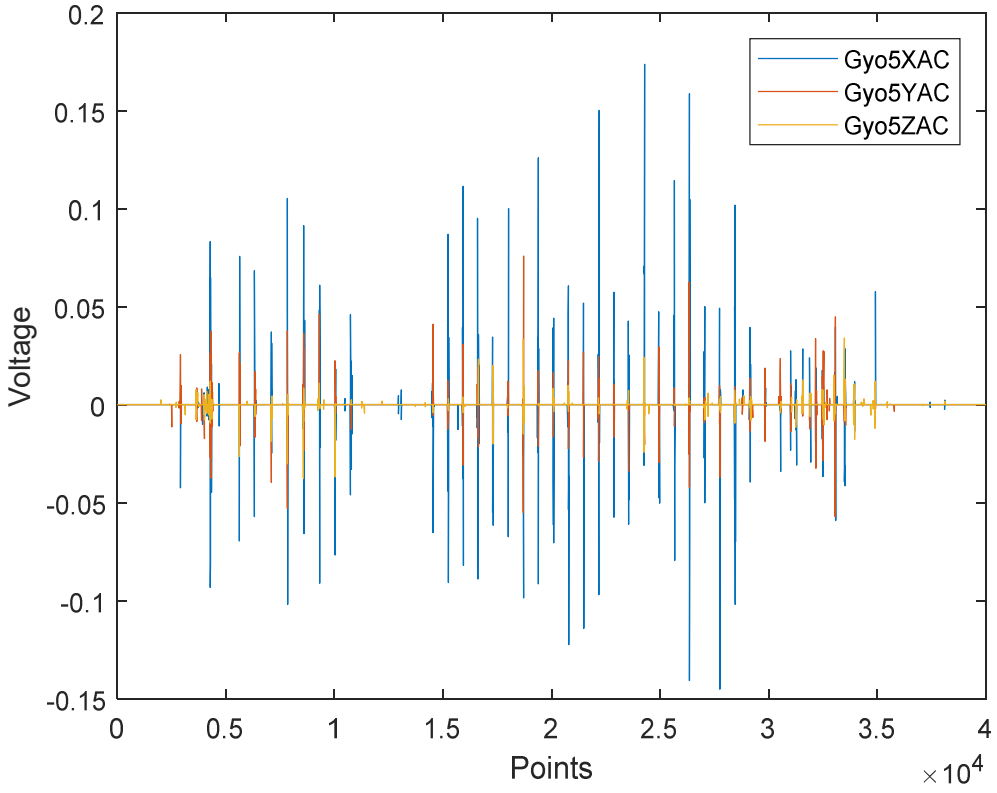

Take Dist6 as the abscissa:

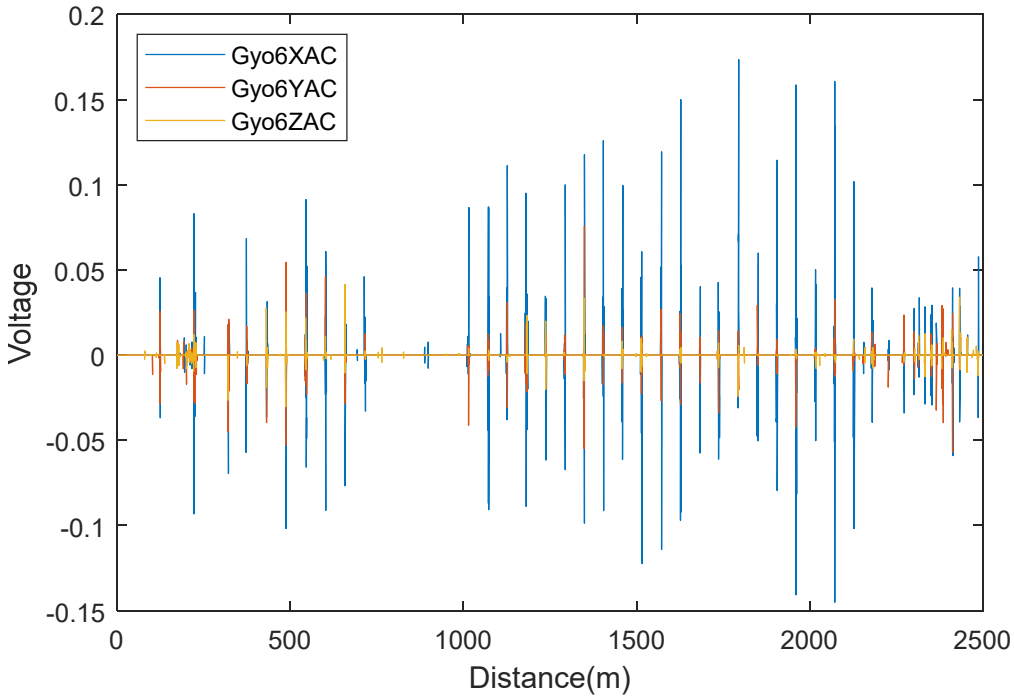
Gyo6XAC
Gyo6YAC
Gyo6ZAC
Voltage
Distance(m)
0.2
0.15
0.1
0.05
0
-0.05
-0.1
-0.15
0
500
1000
1500
2000
2500

Appendix J: Real road data process: Route 2 to Route 4

Route 2

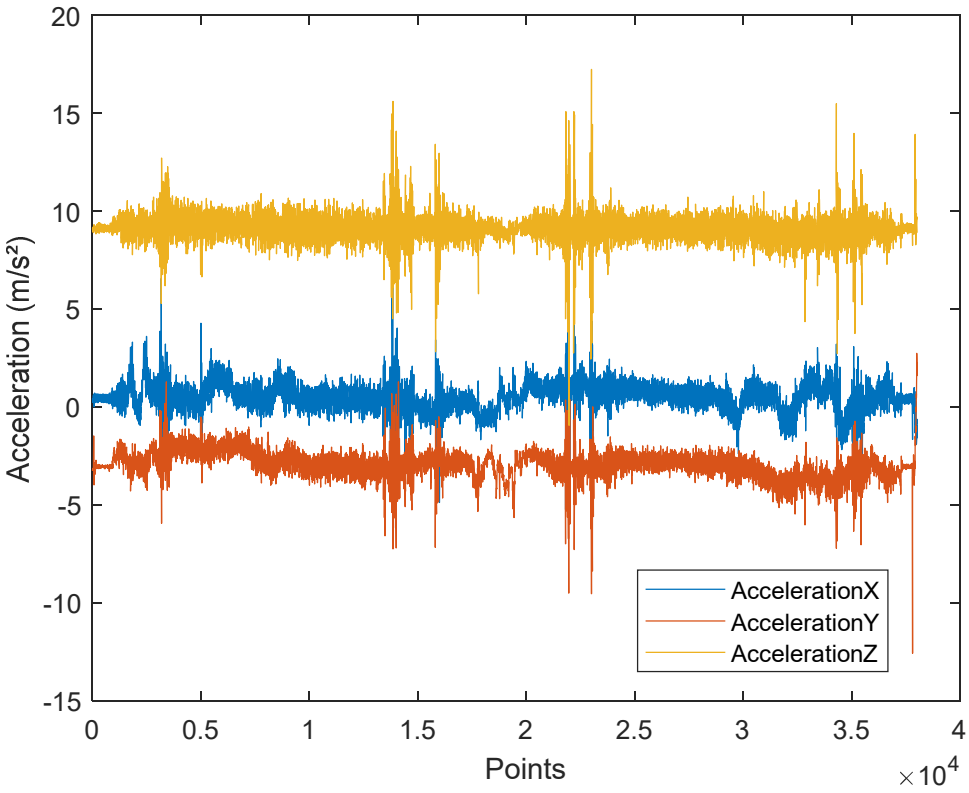

Figure J-1 Three acceleration data of Route 2

The Route 2 data contains 38,000 points, 380 seconds. The maximum speed is 7.75m/s, the average speed is 5.20m/s. Firstly process the axis-correction using PCA, then de-noise using wavelet.

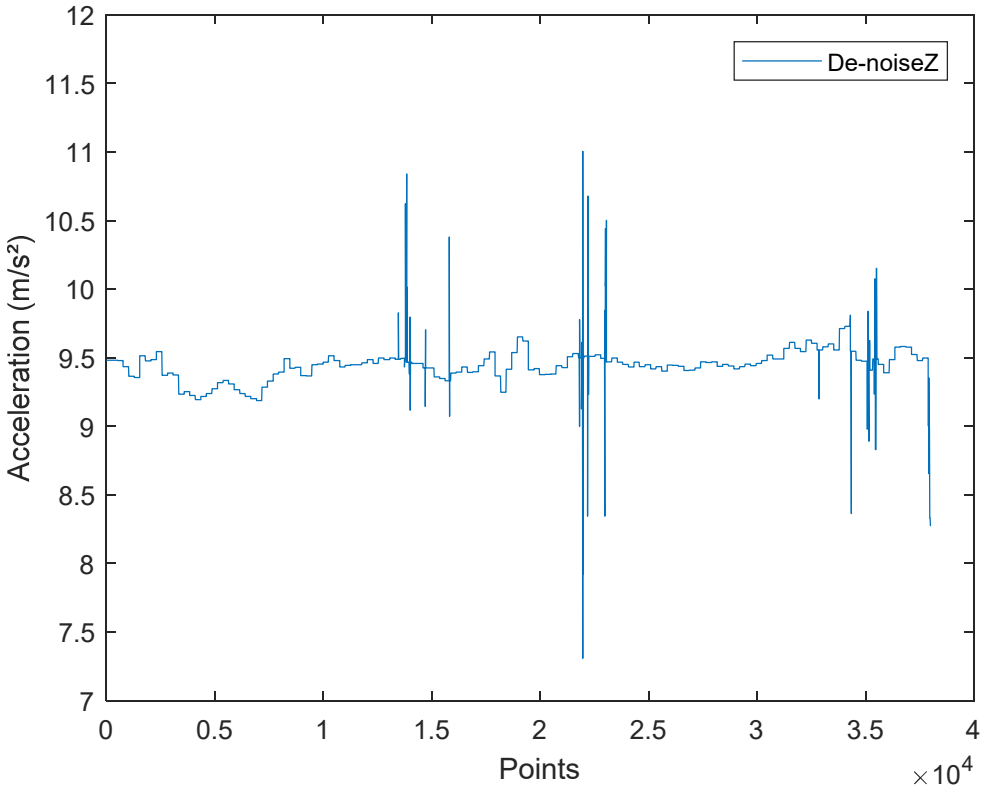

Figure J-2 Wavelet de-noised result of Z axis of Route 2

Then the baseline of Z axis is extracted from the result of wavelet decomposition, as shown in Figure J-3. So we get the Z axis without baseline drift as shown in Figure J-4. Let the threadhold as:

Thd=speed.^2/100;

And using distance as the x axis, get the final result as shown in Figure J-5.

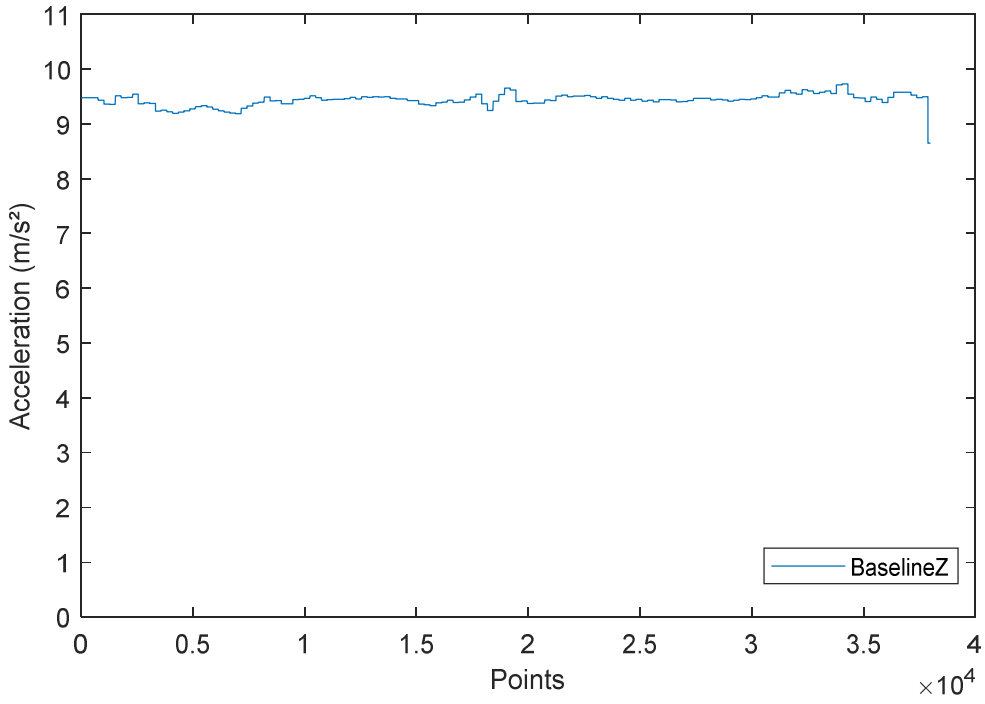

Figure J-3 Baseline of Z axis of Route 2

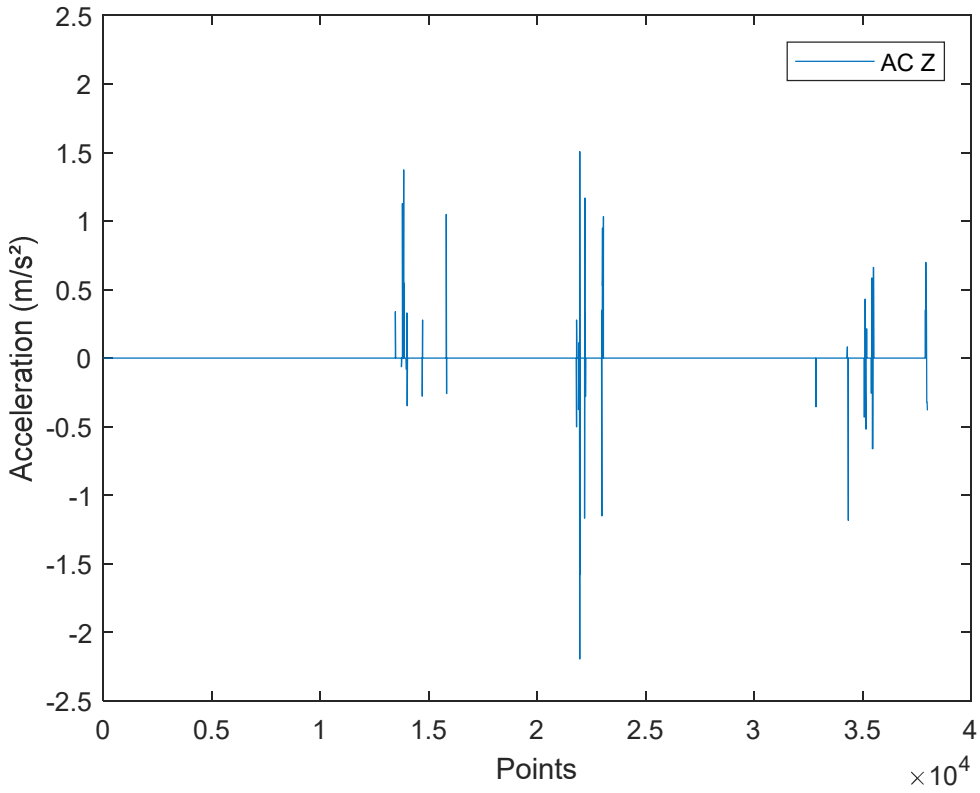

Figure J-4 Z axis of Route 2 without baseline

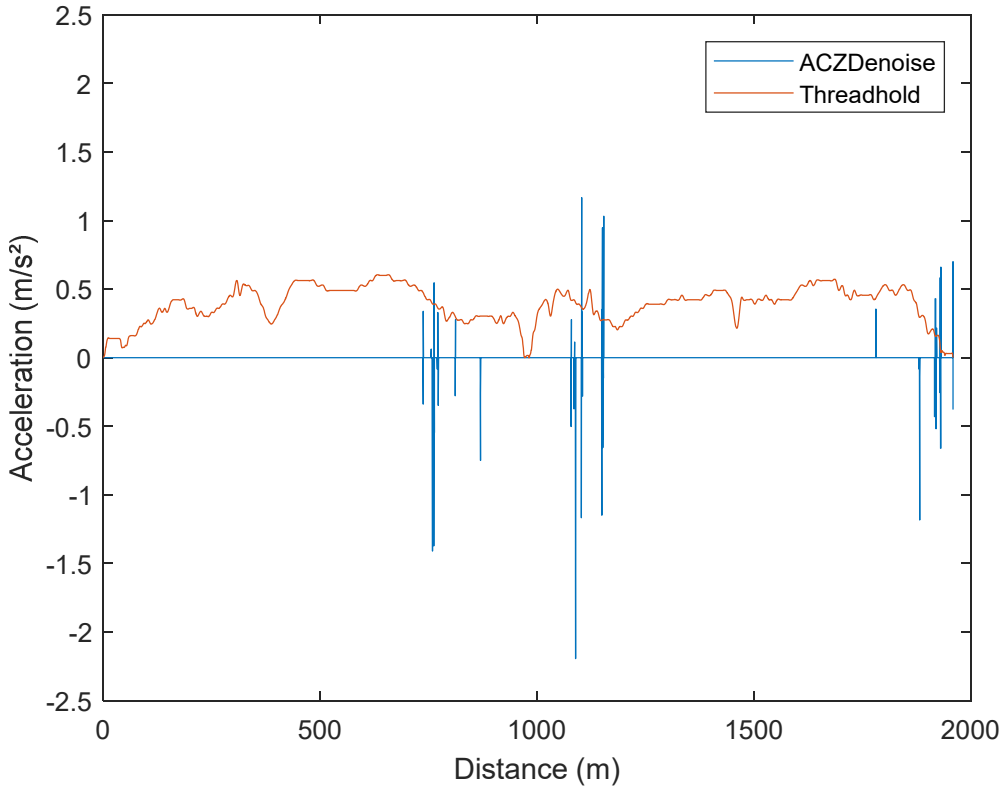

Figure J-5 De-noised Z signal with threadhold. The x axis is distance

So we get the position of potholes.

Table J-1 Detection result of Route 2

ID	Distance to the start point (m)
1	758.6
2	Didn’t check out
3	869
4	1078
5	1102
6	1149
7	Didn’t check out
8	Didn’t check out
9	1882
10	1930
11	1958

There are 3 potholes missed, the accuracy is 8/11=72.7%.

Route 3

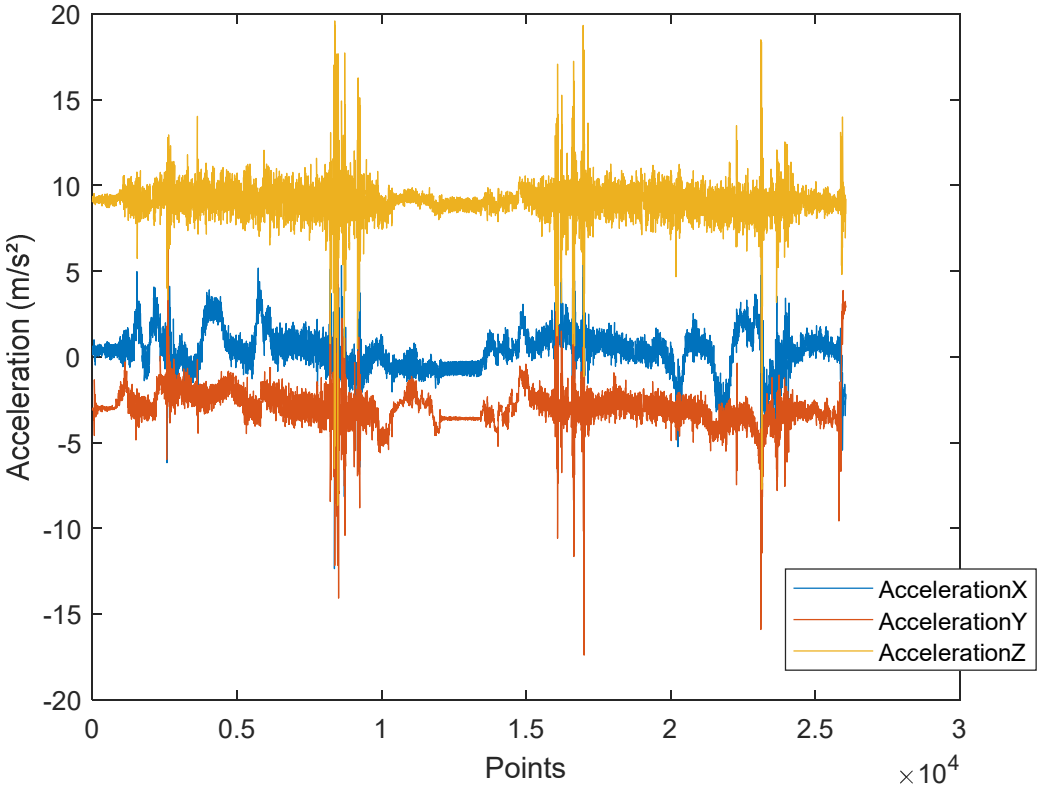

Figure J-6 Three acceleration data of Route 3

The Route 3 data contains 26,000 points, 260 seconds. The maximum speed is 15.75m/s, the average speed is 7.71m/s. Firstly process the axis-correction using PCA, then de-noise using wavelet.

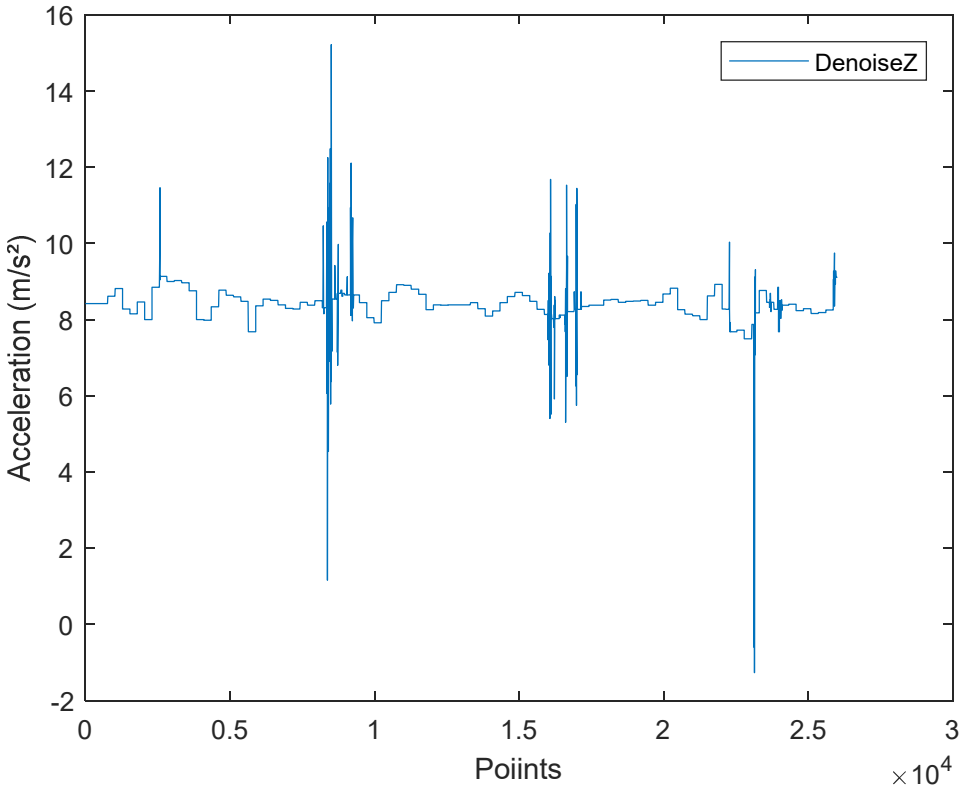

Figure J-7 Wavelet de-noised result of Z axis of Route 3

Then the baseline of Z axis is extracted from the result of wavelet decomposition, as shown in Figure J-8. So we get the Z axis without baseline drift as shown in Figure J-9. Let the threadhold as:

Thd=speed.^2/100;

And using distance as the x axis, get the final result as shown in Figure J-10.

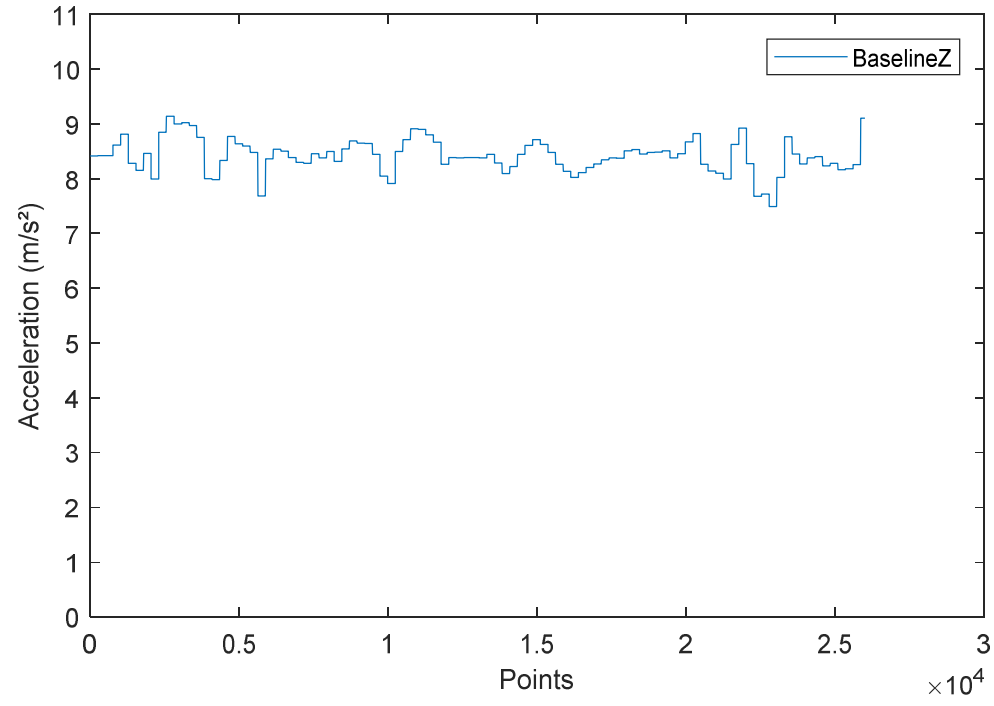

Figure J-8 Baseline of Z axis of Route 3

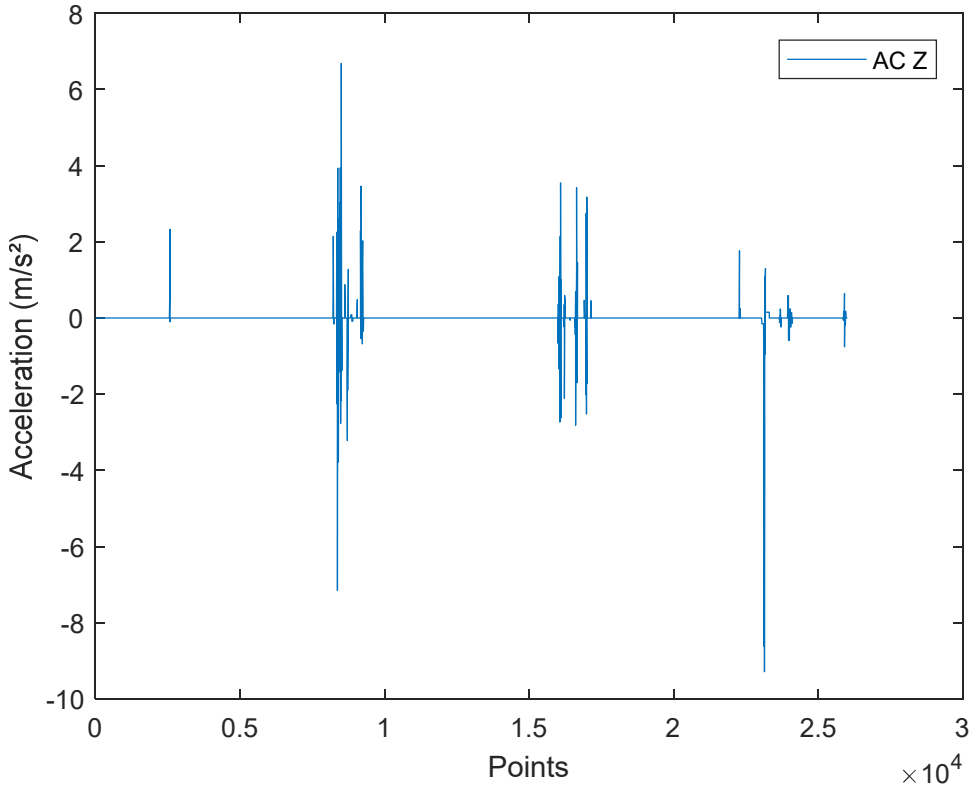

Figure J-9 Z axis of Route 3 without baseline

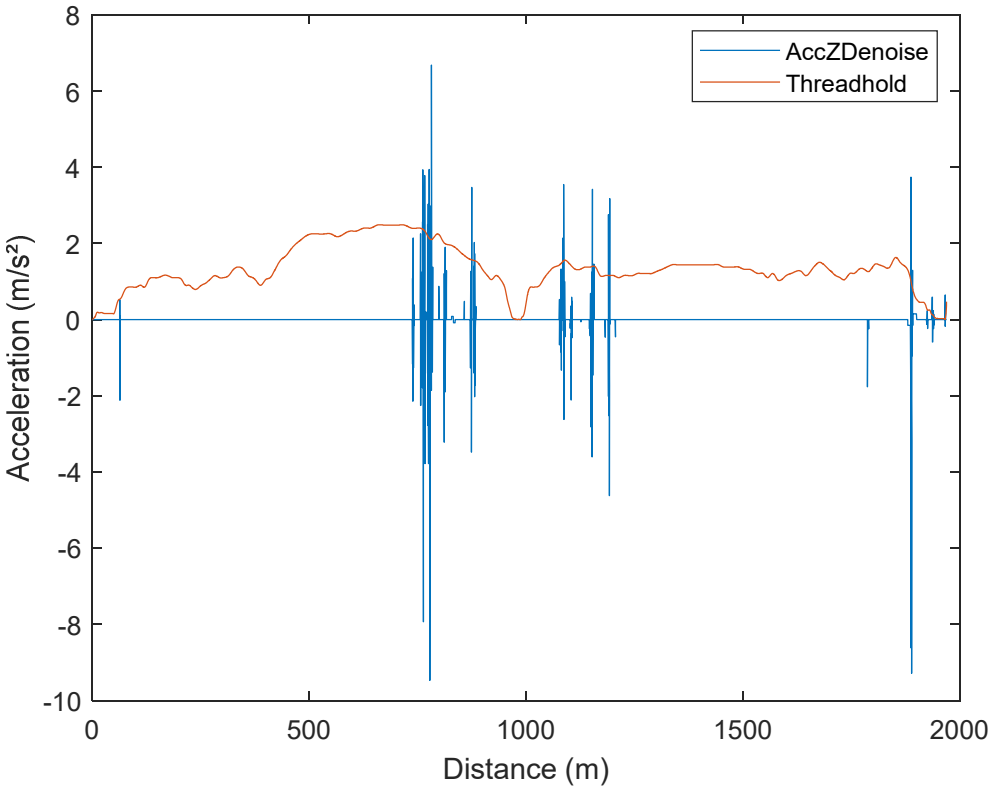

Figure J-10 De-noised Z signal with threadhold. The x axis is distance

So we get the position of potholes.

Table J-2 Detection result of Route 2

ID	Distance to the start point (m)
1	762
2	811
3	873
4	1087
5	1103
6	1152
7	1192
8	1787
9	1889
10	1936
11	1966

All the 11 potholes are detected out, the accuracy is 100%.

Route 4

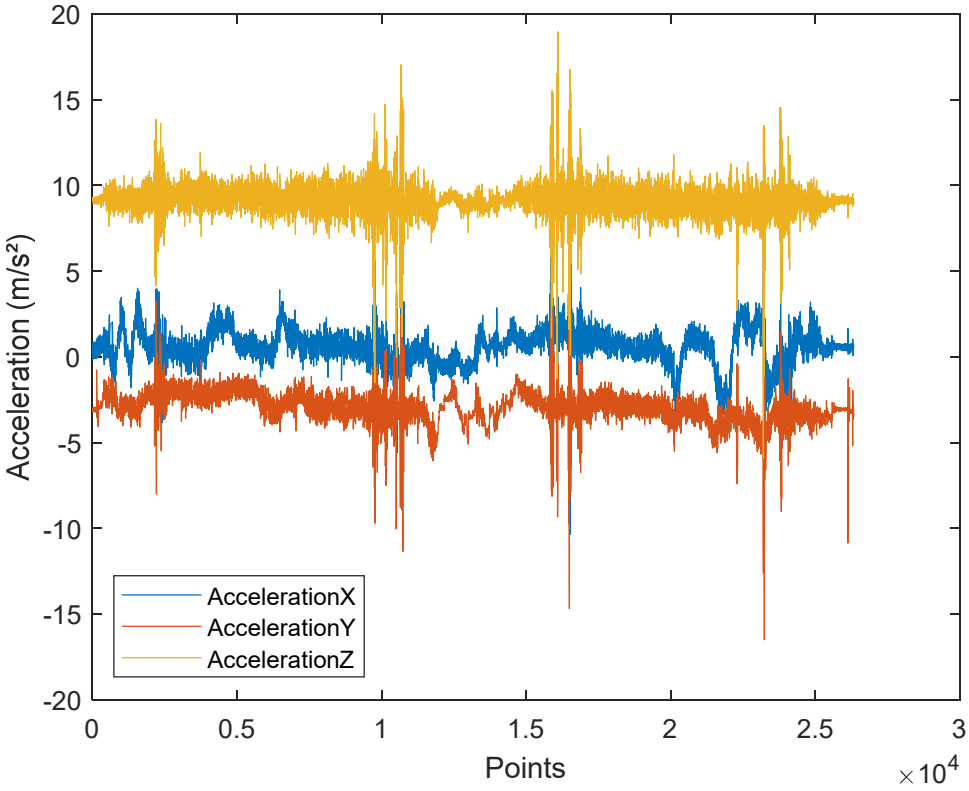

Figure J-11 Three acceleration data of Route 4

The Route 4 data contains 26,300 points, 263 seconds. The maximum speed is 14.00m/s, the average speed is 7.59m/s. Firstly process the axis-correction using PCA, then de-noise using wavelet.

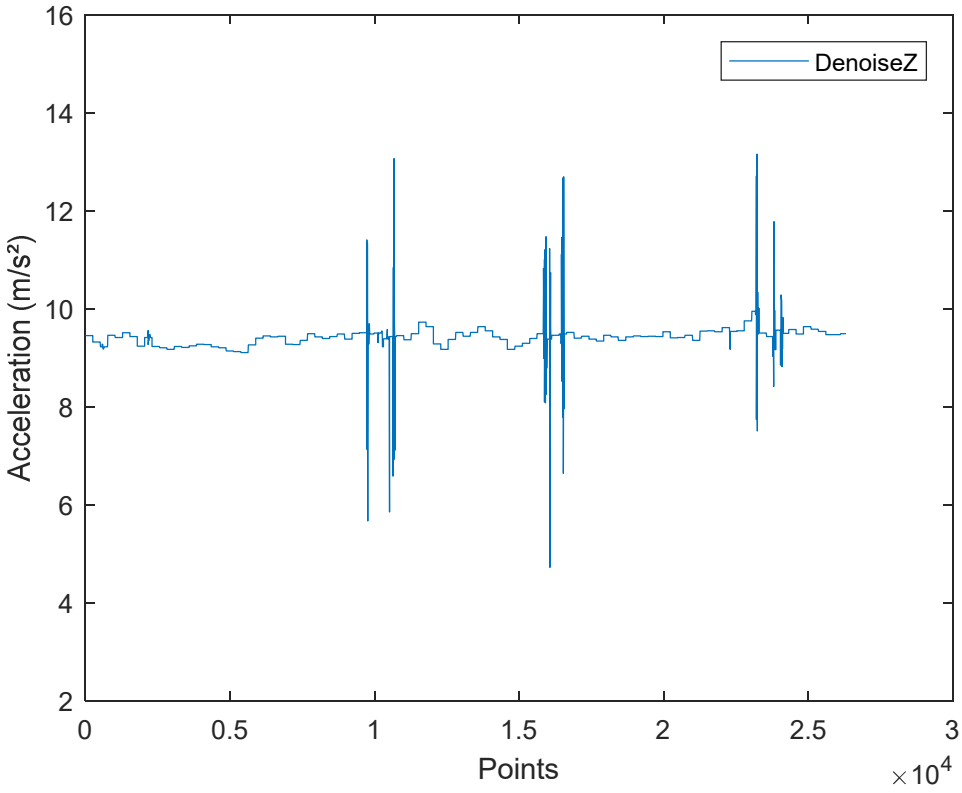

Figure J-12 Wavelet de-noised result of Z axis of Route 4

Then the baseline of Z axis is extracted from the result of wavelet decomposition, as shown in Figure J-13. So we get the Z axis without baseline drift as shown in Figure J-14. Let the threadhold as:

Thd=speed.^2/100;

And using distance as the x axis, get the final result as shown in Figure J-15.

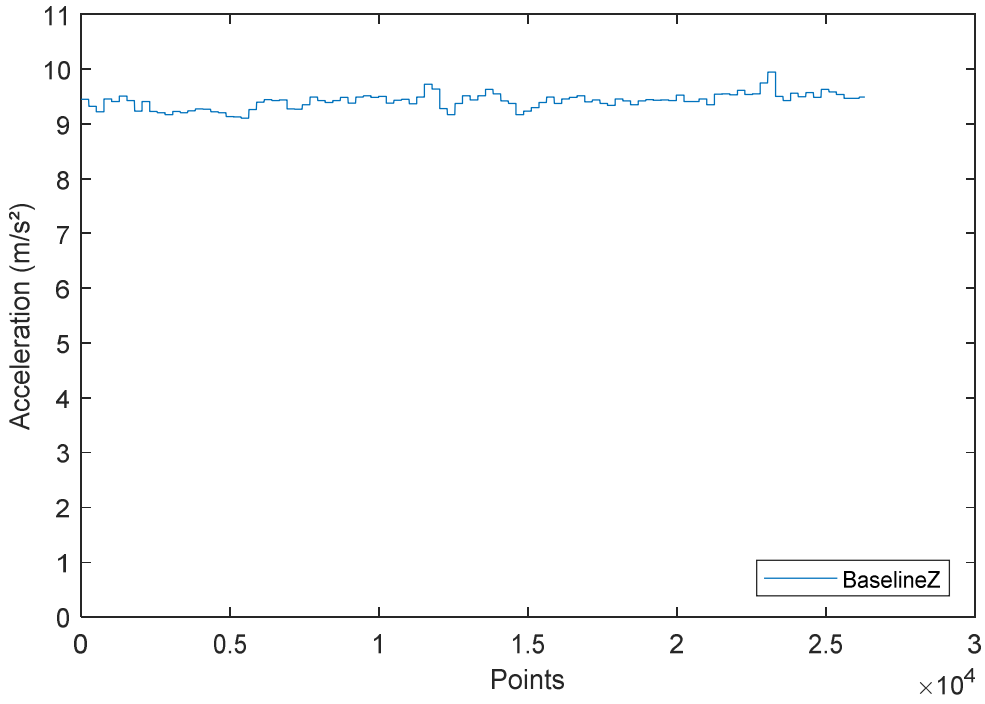

Figure J-13 Baseline of Z axis of Route 4

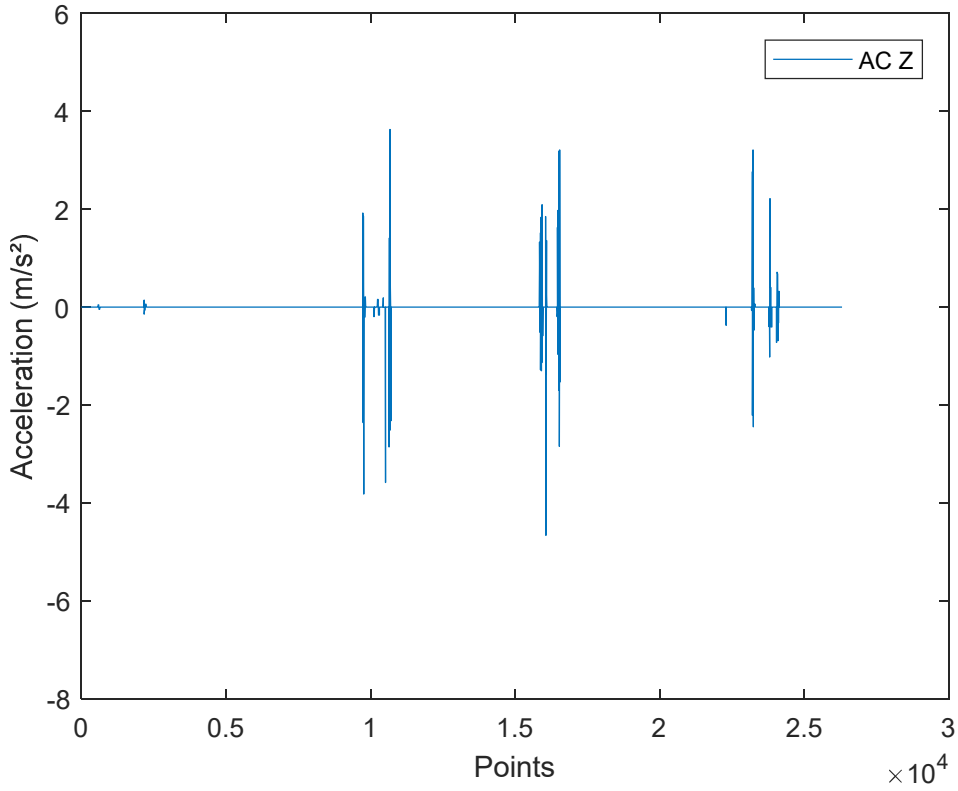

Figure J-14 Z axis of Route 4 without baseline

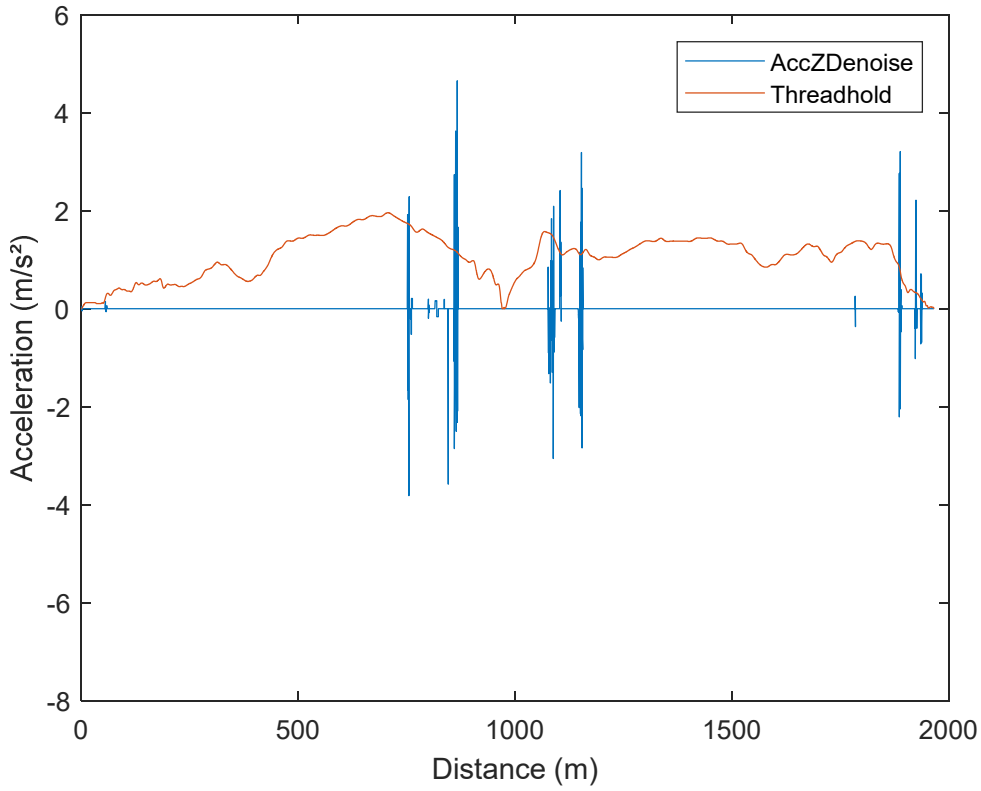

Figure J-15 De-noised Z signal with threadhold. The x axis is distance

So we get the position of potholes.

Table J-3 Detection result of Route 4

ID	Distance to the start point (m)
1	755
2	Didn’t check out
3	863
4	1086
5	1103
6	1152
7	Didn’t check out
8	Didn’t check out
9	1887
10	1923
11	1935

There are 3 potholes missed, the accuracy is 8/11=72.7%.

Appendix K: Publications

1. Chen, Jia, Yin Tao, Dalong Zhang, Xiaoli Liu, Zhen Fang, Qinwu Zhou, and Bo Zhang. "Fatigue detection based on facial images processed by difference algorithm." In *Biomedical Engineering (BioMed), 2017 13th IASTED International Conference on*, pp. 208-211. IEEE, 2017.
2. Tao, Yin, Jia Chen, Xiaoli Liu, Zhen Fang, Dalong Zhang, Qinwu Zhou, and Bo Zhang. "Study of a new amblyopia diagnostic and therapeutic method along with the system implementation." In *Biomedical Engineering (BioMed), 2017 13th IASTED International Conference on*, pp. 121-124. IEEE, 2017.
3. Dalong Zhang, Wei Wei, Qinwu Zhou, Bo Zhang, “Road Pothole Detection Using Built-in Accelerator in Smartphone.” In *Transactions on Internet and Information Journal Systems (TIIS)*. (Submitted)